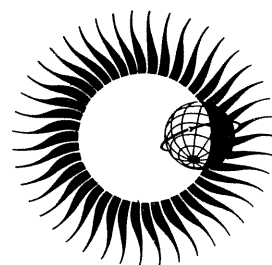


# WORLD DATA CENTER A

## Upper Atmosphere Geophysics



DATA ON SOLAR-GEOPHYSICAL ACTIVITY  
OCTOBER 24 - NOVEMBER 6, 1968



March 1970

# WORLD DATA CENTER A

National Academy of Sciences

2101 Constitution Avenue, N. W. Washington, D. C. U.S.A., 20418

---

World Data Center A consists of the Coordination Office  
and eight subcenters:

World Data Center A  
Coordination Office  
National Academy of Sciences  
2101 Constitution Avenue, N.W.  
Washington, D.C., U.S.A. 20418  
Telephone (202) 961-1404

Solar and Interplanetary Phenomena,  
Ionospheric Phenomena, Flare-Associated  
Events, Aurora, Cosmic Rays, Airglow:  
World Data Center A:  
Upper Atmosphere Geophysics  
Environmental Science Services  
Administration  
Boulder, Colorado, U.S.A. 80302  
Telephone (303) 447-1000 Ext. 3381

Geomagnetism, Seismology, Gravity and Tsunami:  
World Data Center A:  
Geomagnetism, Seismology, Gravity & Tsunami  
Environmental Data Service, ESSA  
Rockville, Maryland, U.S.A. 20852  
Telephone (301) 496-8160

Glaciology:  
World Data Center A:  
Glaciology  
American Geographical Society  
Broadway at 156th Syreet  
New York, New York, U.S.A. 10032  
Telephone (212) 234-8100

Longitude and Latitude:  
World Data Center A:  
Longitude & Latitude  
U.S. Naval Observatory  
Washington, D.C., U.S.A. 20390  
Telephone (202) 698-8422

Meteorology (and Nuclear Radiation):  
World Data Center A:  
Meteorology  
National Weather Records Center  
Asheville, North Carolina, U.S.A. 28801  
Telephone (704) 253-0481

Oceanography:  
World Data Center A:  
Oceanography  
Building 160  
Second and N Streets, S.E.  
Washington, D.C., U.S.A. 20390  
Telephone (202) 698-3753

Rockets and Satellites:  
World Data Center A:  
Rockets and Satellites  
National Academy of Sciences  
2101 Constitution Avenue, N.W.  
Washington, D.C., U.S.A. 20418  
Telephone (202) 961-1404

Upper Mantle Project:  
World Data Center A:  
Upper Mantle Project  
Lamont Geological Observatory  
Palisades, New York, U.S.A. 10964  
Telephone (914) 359-2900 Ext. 209

---

## Notes:

- (1) World Data Centers conduct international exchange of geophysical observations in accordance with the principles set forth by the International Council of Scientific Unions. WDC-A is established in the United States under the auspices of the National Academy of Sciences.
- (2) Communications regarding data interchange matters in general and World Data Center A as a whole should be addressed to: World Data Center A, Coordination Office (see address above).
- (3) Inquiries and communications concerning data in specific disciplines should be addressed to the appropriate subcenter listed above.

# WORLD DATA CENTER A

## Upper Atmosphere Geophysics



REPORT UAG-8 PART I

DATA ON SOLAR -GEOPHYSICAL ACTIVITY

OCTOBER 24 - NOVEMBER 6, 1968

compiled by

J. Virginia Lincoln

WDC-A, Upper Atmosphere Geophysics

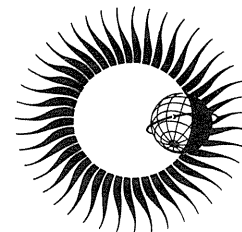
Boulder, Colorado

Prepared by Research Laboratories, ESSA, Boulder, Colorado  
and published by

U.S. DEPARTMENT OF COMMERCE  
ENVIRONMENTAL SCIENCE SERVICES ADMINISTRATION

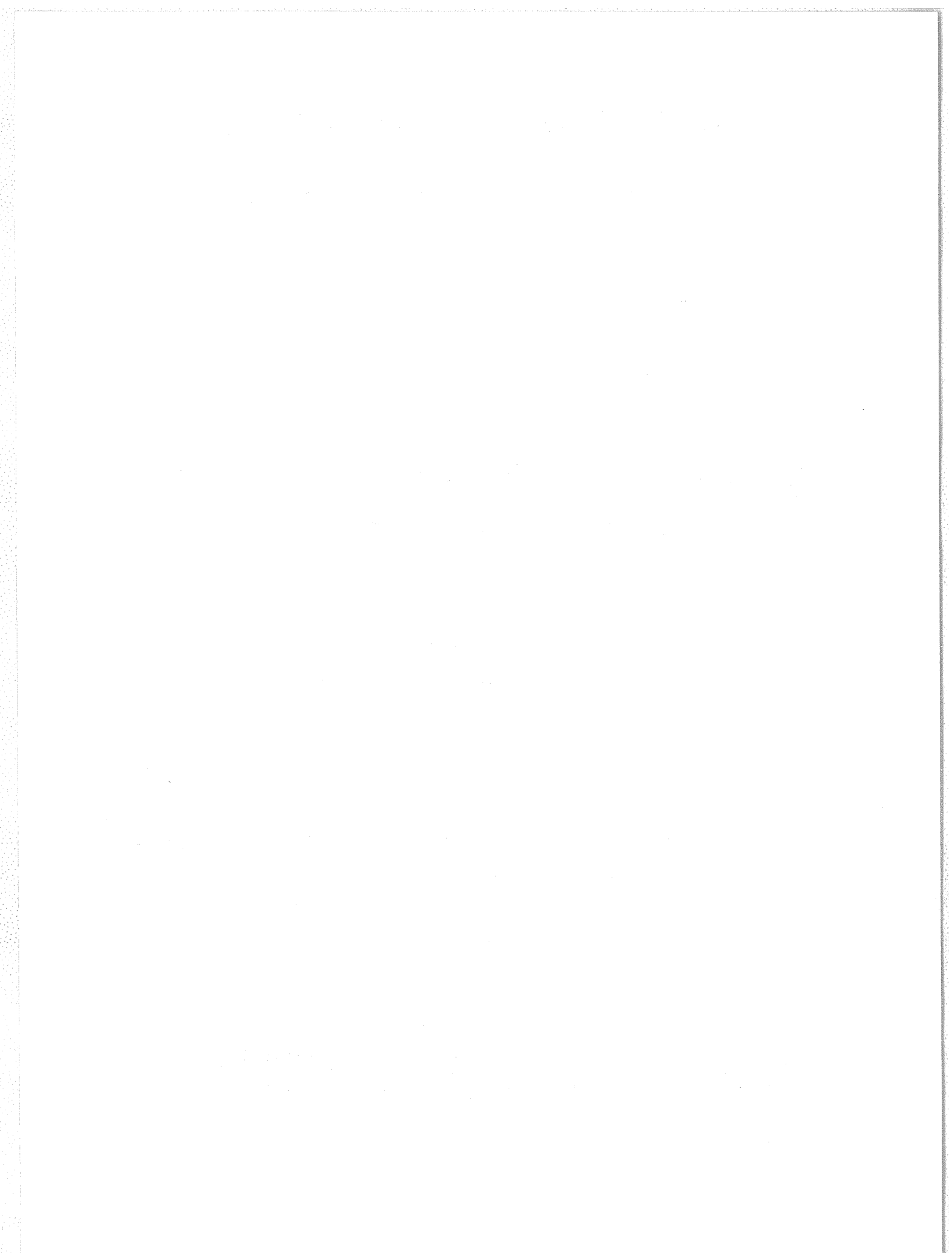
ENVIRONMENTAL DATA SERVICE  
ASHEVILLE, NORTH CAROLINA, USA 28801

March 1970



SUBSCRIPTION PRICE: \$9.00 a year; \$2.50 additional for foreign mailing; single copy price varies.\* Checks and money orders should be made payable to the Superintendent of Documents. Remittance and correspondence regarding subscriptions should be sent to the Superintendent of Documents, Government Printing Office, Washington, D.C. 20402.

\*Price of this issue \$1.75



## FOREWORD

One of the projects under the programs for cooperation in solar-terrestrial sciences since the IGY has been the selection through international mechanisms of intervals for special study, chosen on the basis of scientifically significant events or conditions which occurred. These "Retrospective World Intervals" have been chosen by the International Ursigram and World Days Service (IUWDS) and announced through suitable periodicals such as IQSY Notes or STP Notes. Their selection has tended to concentrate attention on these intervals which has resulted in intensified study and reports on observations and in research papers.

These selected intervals are, of course, coordinated with the scientific projects which are active in the solar-terrestrial scientific community and they are in fact a recognition of the interest and excitement of workers in the field. For example, the Proton Flare Project of July 1966 was one of these Retrospective World Intervals and resulted in a special scientific symposium which was published as IQSY Annals, Vol. 4. There have also been special meetings and publication on other intervals such as the solar-cosmic ray events of July 1959 and November 1960.

Another almost spontaneously selected interval was May 23, 1967 and this resulted in the compilation of many data details in a report issued by World Data Center A - Upper Atmosphere Geophysics, (UAG-5). This report which included many data which are normally not published but rather held in the WDC archives also included discussion, assessment and some interpretation of the data by many contributors. The report was well received in the scientific community and in fact the Inter-Union Commission on Solar-Terrestrial Physics (IUCSTP) made a recommendation at its January 1969 meeting in London:

"WORKING GROUP 12

Commends World Data Centre A (Upper Atmosphere Geophysics) for their efforts in producing the IER-FB Solar Geophysical Data reports and the UAG reports (particularly UAG 5 on the solar event of May 1967), and

Urges other Data Centres to adopt similar methods of data synthesis and dissemination."

The present report is a continuation of this effort in international cooperation. The period Oct. 24-Nov. 6, 1968 was again selected somewhat spontaneously by leading workers in the field as an outstanding example of major solar-terrestrial phenomena. In this case, an effort has been made to obtain contributions from all interested workers who might have significant observations, or other contributions to the study. Notices of the plan to compile these data volumes were sent to some 1500 active workers drawn from participants in the IUCSTP programs and contributors to the World Data Centers. Many replied that all that they had to offer was the data regularly sent to the WDCs. About 50 have sent more detailed data or discussions on the observations which are normally available.

These present reports therefore include the special contributions and in addition selections from the data normally available at WDCs which, in the opinion of the compiler, helped to round out the account of the solar-terrestrial phenomena under study.

These reports represent an effort to assemble data in a convenient form for elucidating the mysteries of solar-induced terrestrial phenomena. It is a truly international undertaking under the general auspices of Working Group 1 of IUCSTP. The acknowledgement of the many participants is implicit by the inclusion of their contributions in these reports. It is to be hoped that the reaction to these volumes will be a guide to what further data compilation projects of this kind should be attempted in the future.

A. H. Shapley, Chairman  
IUCSTP Working Group 1,  
Monitoring of the Solar-  
Terrestrial Environment

TABLE OF CONTENTS

	PAGE
PART I	
FOREWORD	
1. INTRODUCTION AND SUMMARY OF GENERAL ACTIVITY	2
2. HISTORY OF ACTIVE SOLAR REGION	11
3. OUTSTANDING SOLAR FLARES	30
4. SOLAR LIMB PHENOMENA	65
5. SOLAR RADIO EVENTS	68
PART II	
6. SOLAR X-RAYS	171
7. SUDDEN IONOSPHERIC DISTURBANCES	178
8. SPACE OBSERVATIONS - ELECTRONS, PROTONS, ALPHAS, INTERPLANETARY MAGNETIC FIELDS	190
9. COSMIC RAYS	225
10. GEOMAGNETIC DATA	229
11. AURORAL PHENOMENA	253
12. IONOSPHERIC PHENOMENA	256
ACKNOWLEDGEMENTS	310
INDEX	310

TABLE OF CONTENTS

PART I

	<u>Page</u>
FOREWORD	
A. H. Shapley	
1. INTRODUCTION AND SUMMARY OF GENERAL ACTIVITY	2
J. Virginia Lincoln	
2. HISTORY OF THE ACTIVE SOLAR REGION	
"Evolution of the Active Region (H $\alpha$ and K Faculae and Spots) of the Proton Events of October 29-early November 1968"	11
(G. Godoli, O. Morgante and M. L. Sturiale)	
"H $\alpha$ Disk Passage of the Active Region"	18
(M. McCabe)	
"On Some Aspects of the Early Evolution of the Region"	19
(T. Fortini and M. Torelli)	
"Sunspots Associated with the Proton Flares of Late October 1968"	22
(Patrick S. McIntosh)	
3. OUTSTANDING SOLAR FLARES	
"Eruptive Flare of October 24, 1968"	30
(H. Zirin)	
"Study of the Flares in the Active Region of the Proton Events of 1968 October 29 - Early November During its Transit October 21 - November 4"	34
(G. Godoli, O. Morgante and M. L. Sturiale)	
"Six Large Solar Events Recorded by the NASA Solar Particle Alert Network from October 27 to November 4, 1968"	40
(P. E. Lafferty, J. W. Snyder and J. H. Reid)	
"A Study of the Film Record of H $\alpha$ Flare of October 30-31, 1968"	48
(Richard A. Miller and Allan R. Trinidad)	
"Description of the H $\alpha$ Flares of November 1, 2 and 4, 1968"	54
(C. J. Macris and C. E. Alissandrakis)	
4. SOLAR LIMB PHENOMENA	
"Note on the Limb Passage of the Active Region November 2-4, 1968"	65
(Charles L. Hyder)	
"Eruptive Prominence Associated with the Solar X-ray Burst of 4 November 1968"	66
(Stephen Pinter)	
5. SOLAR RADIO EVENTS	
"Summary of Worldwide Outstanding Solar Radio Emission Events - Fixed Frequency and Spectral"	68
(Hope I. Leighton and J. Virginia Lincoln)	
"Millimeter Radio Emission of McMath Plage No. 9740"	97
(G. Feix)	
"Radio Burst Spectra Associated with Proton Flux Increases"	103
(D. S. Lund)	
"Solar Radio Activity in Plage #9740 22 October - 4 November 1968"	112
(John P. Castelli, Walter Clark, William O'Brien and Santimay Basu)	
"Solar Radio Bursts During the Period 27 October through 5 November 1968"	127
(Fred L. Wefer)	
"Report on the Solar Radio Events of the period 1968 October 27 - November 4"	136
(A. Böhme, F. Fürsternberg and A. Krüger)	
"Solar Activity at $\lambda = 1.6$ cm (19 GHz) During the Period 27 October - 4 November 1968 and its Relation to Proton Events"	145
(D. L. Croom and R. J. Powell)	
"Unusual 1 to 5 GHz Solar Radio Emission of 29 October 1968"	150
(R. A. Mennella and J. H. Reid)	
"Comments on Solar Circumstances at the Time of the Great Radio Frequency Burst, 1968 October 29, 1516 UT"	154
(Helen W. Dodson and E. Ruth Hedeman)	
"Movement and Structure in a Complex Solar Outburst at 80 MHz"	158
(N. R. Labrum)	
"Bursts of October 30-31 and November 4, 1968 at Toyokawa, Japan"	161
"Some Radio Bursts in the Period October 29-November 3, 1968 Observed at Metric Waves with High Temporal Resolution"	163
(A. Abrami)	
"Spectral Diagram of the Event of 1968 Nov. 2"	169
(K. J. van den Heuvel Rijnders)	

DATA ON SOLAR-GEOPHYSICAL ACTIVITY OCTOBER 24 - NOVEMBER 6, 1968

1. INTRODUCTION AND SUMMARY OF GENERAL ACTIVITY

by

J. Virginia Lincoln  
Space Disturbances Laboratory  
ESSA Research Laboratories, Boulder, Colorado

This report is the result of the response to the call for contributions for a data compilation on this period in late October to early November 1968 which included considerable solar flare activity and solar proton events followed by major geomagnetic and ionospheric disturbance. The contributions amounted to such volume it was decided to publish the report in two parts to permit easier handling. As with Report UAG-5, "Data on Solar Event of May 23, 1967 and its Geophysical Effects", issued February 1969, some of the data published in "Solar-Geophysical Data" are repeated here, and other reports routinely sent to World Data Center A - Upper Atmosphere Geophysics have been utilized. The value of this compilation, however, is because of the many contributions made by scientists throughout the world. It should be noted that each person's contribution has been prepared without the benefit of seeing the other contributions. Thus, there will be repetition but from different viewpoints.

The data are grouped into 13 sections. In a few cases the introductory text has been supplied by the compiler. Only minor editing, if any, has been made to the original contributions. The contributors are identified in detail in the various subsections, and without them this report would not have been possible. Their cooperation is gratefully acknowledged.

General Activity

To set the scene for the many contributions to follow some data first published in "Solar-Geophysical Data" or in "STP Notes" are presented. Casual examination of the Abbreviated Calendar Record for October 21 through November 4, 1968 reprinted on the following pages from STP Notes No. 7, indicates a sharp increase in solar activity on October 27 which continues through November 4, the date of west limb passage of McMath plage region 9740. The geophysical indices become disturbed on October 29. Statements concerning such geophysical activity appear on that date as well, and continue through November 2.

The solar activity history concerning McMath Region 9740, as such data are now presented in "Solar-Geophysical Data", appears in Table 1 below. The calcium plage data are from McMath-Hulbert Observatory; the sunspot magnetic field data from Mt. Wilson, Observatory; the area, count, and Zurich classification from Sacramento Peak Observatory; and the 9.1 cm data from Stanford University. See "Solar-Geophysical Data" Descriptive Text for units used.

TABLE 1

MCMATH REGION 9740 CMP DATE 28.4							RETURN OF REGION 9692				ROTATION 3								
CALCIUM PLAGE DATA							SUNSPOT DATA							9.1 CM					
YR	MO	DA	MC NO.	LAT	CMD	L	AREA	INT	MW NO.	LAT	CMD	L	MAG	H	AREA	CNT	C	INT	FLUX
68	10	21	9740	S14	E87	179	1200	2.5										9	4
68	10	22	9740	S13	E73	180	2500	3.0	17033	S15	E75	173	$\alpha\gamma$		130	6	D	25	11
68	10	23	9740	S15	E60	179	5700	3.0	17033	S17	E66	173	( $\beta\gamma$ )		420	15	D	29	12
68	10	24	9740						17033	S16	E49	175	( $\beta\gamma$ )	4	327	23	D	31	14
68	10	25	9740	S15	E33	178	6700	3.5							615	43	H	32	14
68	10	26	9740	S16	E20	180	7000	3.5	17033	S16	E25	173	( $\beta\gamma$ )	3	820	35	D	42	18
68	10	27	9740	S15	E10	176	7800	3.5	17033	S16	E13	173	( $\delta$ )	6	829	25	H	40	18
68	10	28	9740						17033	S15	W03	174	( $\delta$ )	5	759	58	H	50	22
68	10	29	9740	S15	W17	178	7700	4.0	17033	S14	W16	174	$\delta$		719	60	H	62	28
68	10	30	9740	S15	W32	180	7000	4.0		S15	W25				1014	40	H	46	21
68	10	31	9740	S16	W46	179	6500	3.5	17033	S16	W40	173	$\delta$		858	43	D	54	25
68	11	01	9740	S16	W60	181	5600	3.5	17033	S16	W53	172	( $\delta$ )	5	772	35	C	54	25
68	11	02	9740	S17	W72	180	5600	3.5	17033	S16	W69	172	( $\delta$ )	5	524	12	D	41	19
68	11	03	9740	S17	W83	177	3000	3.5		S15	W80				192	15	H	32	15
68	11	04	9740	S19	W94													20	9

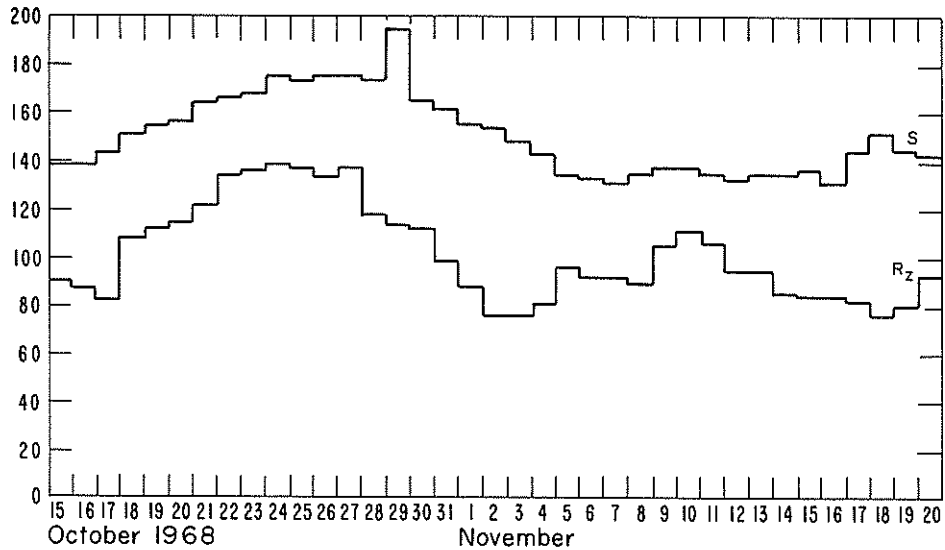
Following the Abbreviated Calendar Record pages will be found as Fig. 1 a reprint of the daily scout maps of solar phenomena for October 27, 1968 from "Solar-Geophysical Data" IER-FB 292 issued December 1968. The remaining days of the period of interest are not repeated in this form. The H $\alpha$ , sunspot and calcium plage histories are being discussed in later contributions to this report. However, to remind one of other general activity for the disk passage of the plage region, Fig. 2 presents the Stanford 9.1 cm maps, the Fleurs, Australia 21 cm maps and the Mt. Wilson magnetograms. Please see "Solar-Geophysical Data" IER-FB 292 and 293 of December 1968 and January 1969 for a larger reproduction size to permit reading of the numbers on the maps.

As another way of assessing the activity of this period the final R<sub>z</sub> and the 2800 MHz solar flux associated with the transit of this solar region are given below:

	<u>R<sub>z</sub></u>	<u>S</u>		<u>R<sub>z</sub></u>	<u>S</u>		<u>R<sub>z</sub></u>	<u>S</u>
Oct. 21	122	164.8	Oct. 26	133	174.6	Oct. 31	99	161.9
22	134	166.5*	27	138	175.1*	Nov. 1	89	155.7*
23	136	168.7	28	118	173.3	2	76	154.0*
24	139	175.2	29	114	193.8	3	76	148.5
25	138	173.8	30	112	166.2*	4	81	142.7

\*Adjusted for solar burst

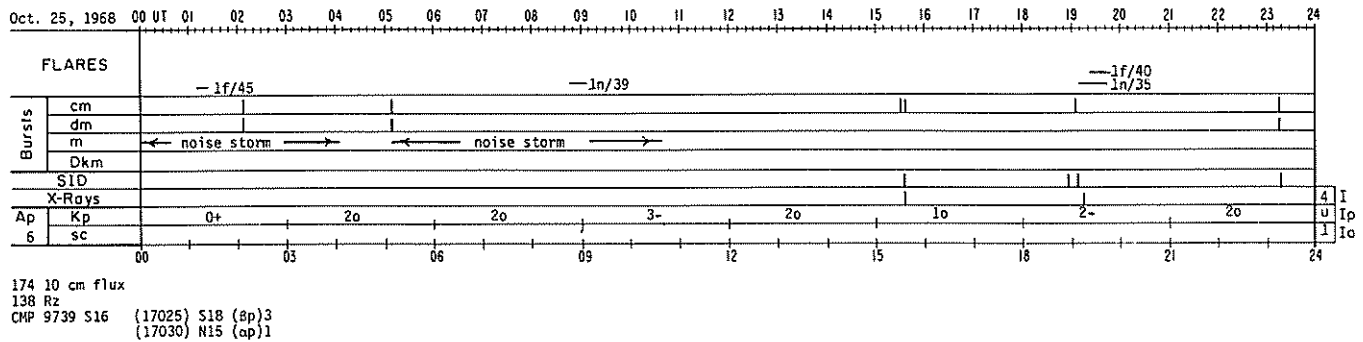
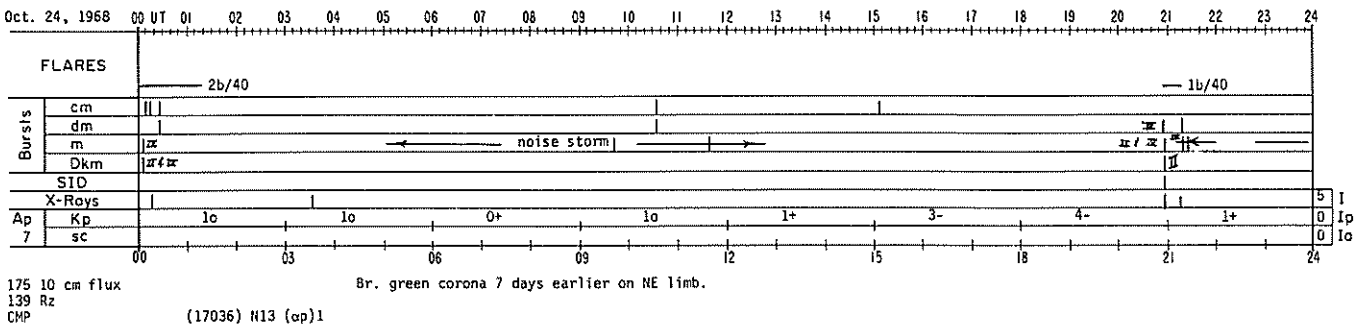
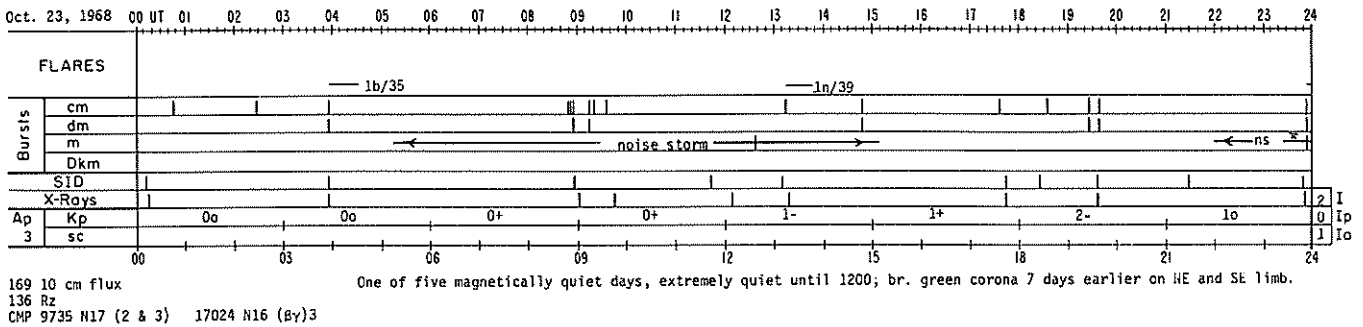
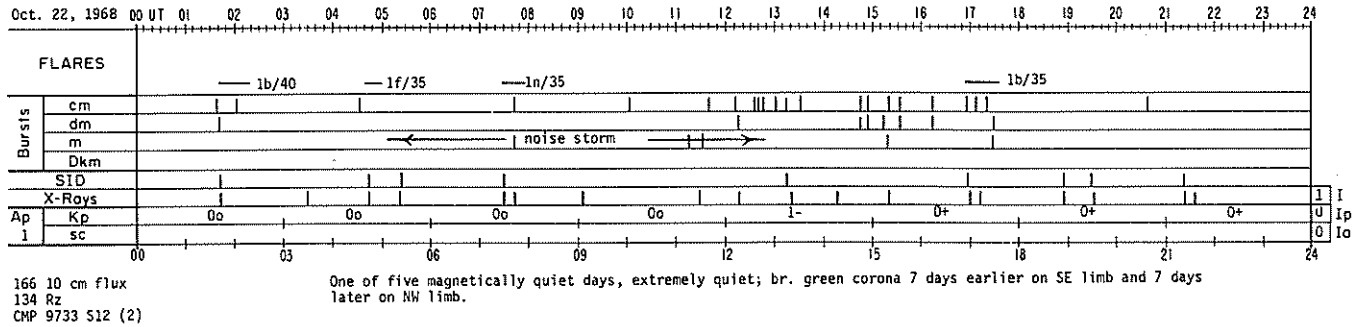
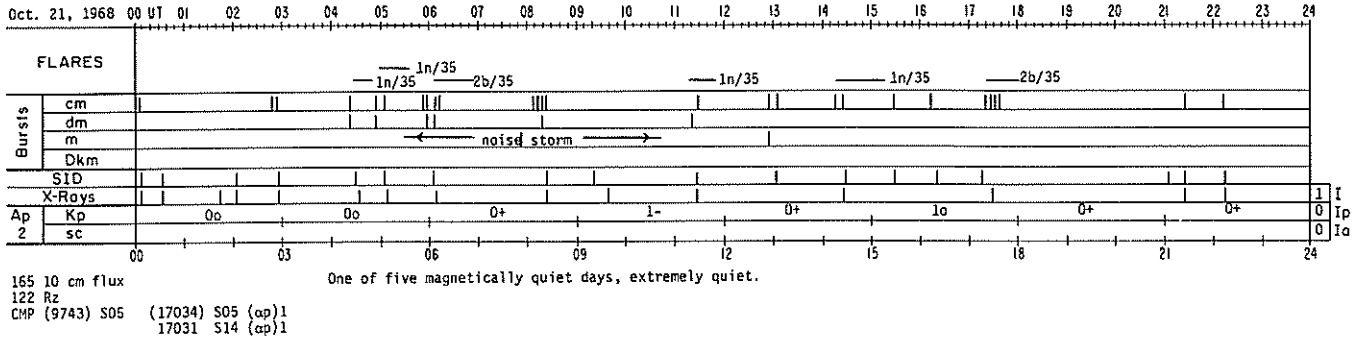
The histogram below depicts these same values in relation to several days either side to indicate the activity relative to the 27-day solar cycle at that time.



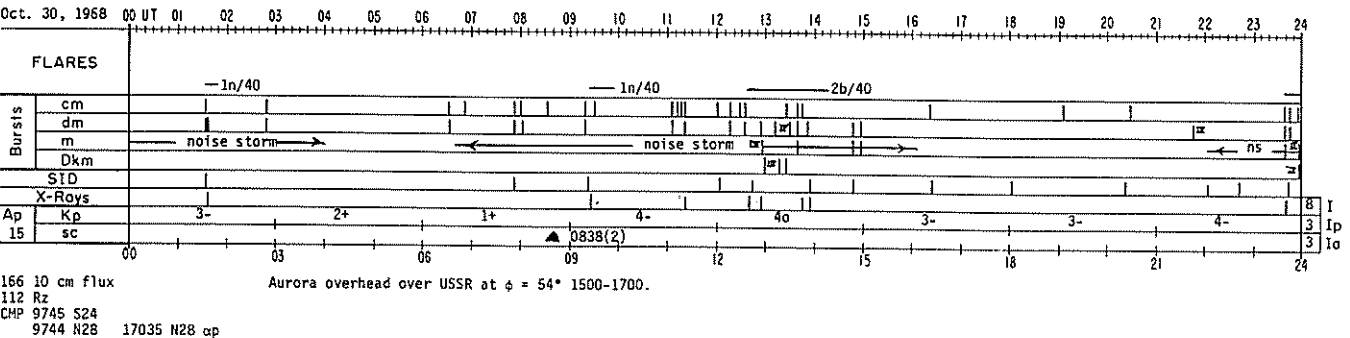
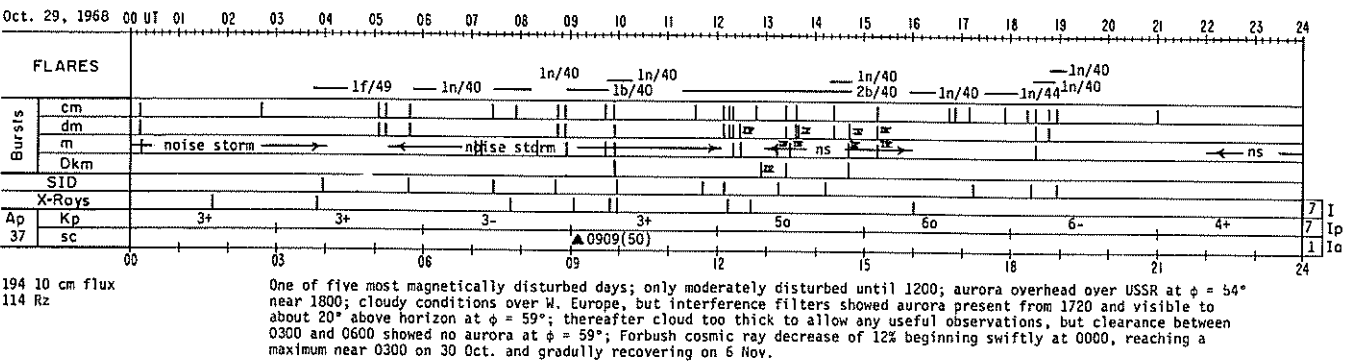
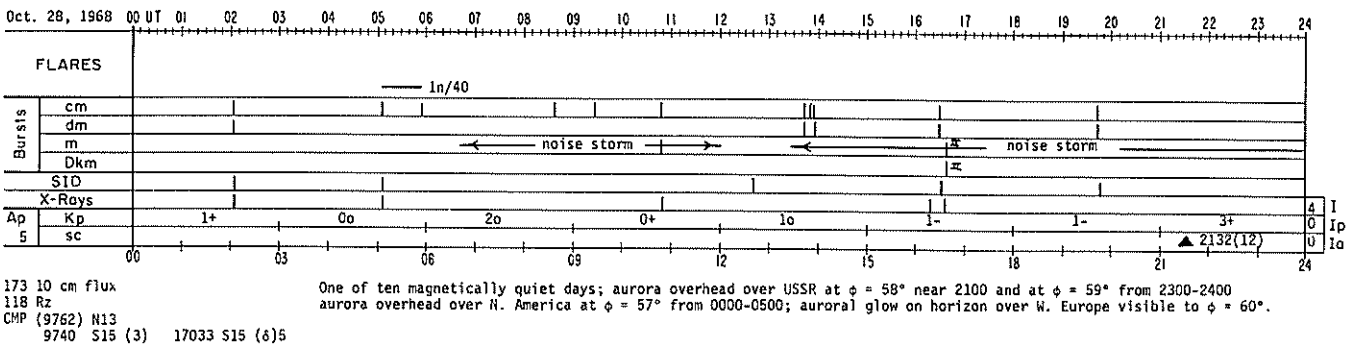
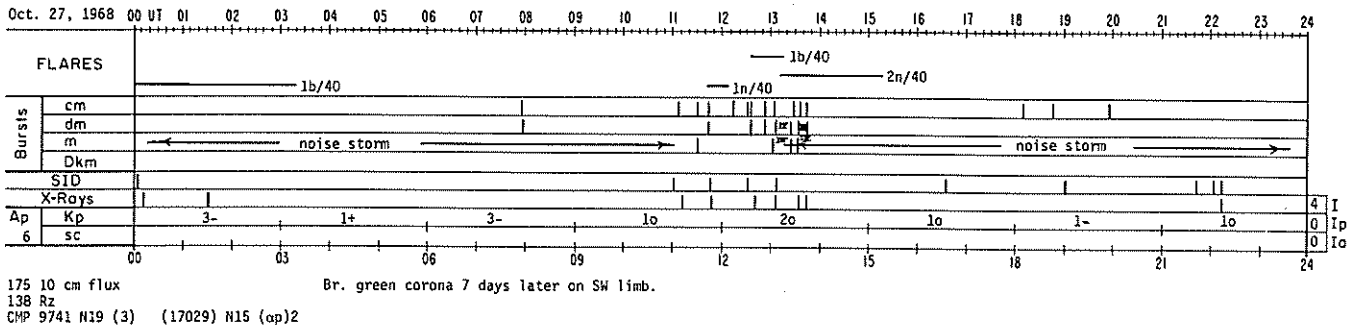
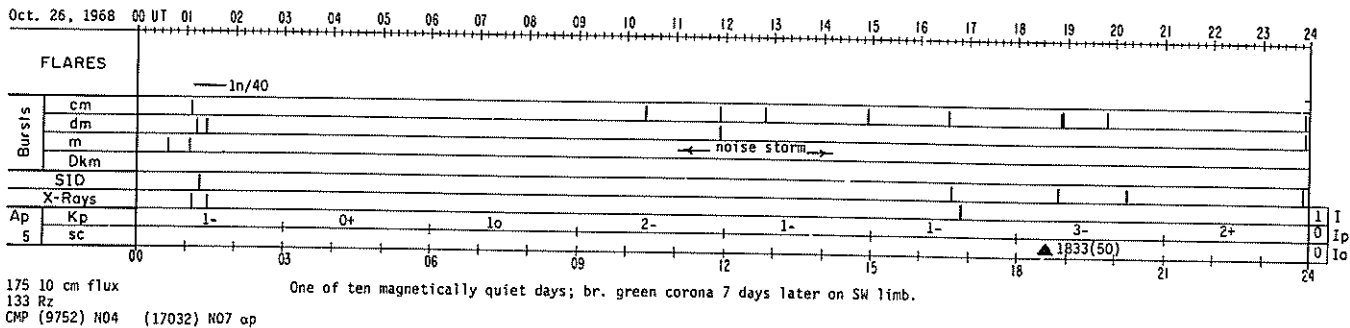
Daily solar flux at 2800 MHz, S, and relative sunspot numbers, R<sub>z</sub>, October 15 - November 20, 1968.

ABBREVIATED CALENDAR RECORD

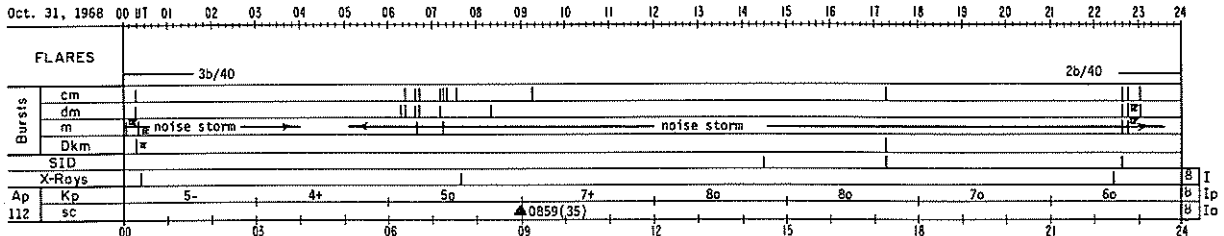
October 21 - November 4, 1968



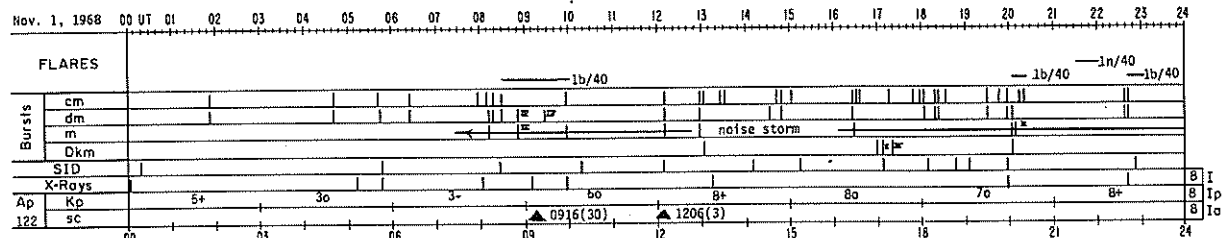
# ABBREVIATED CALENDAR RECORD (Continued)



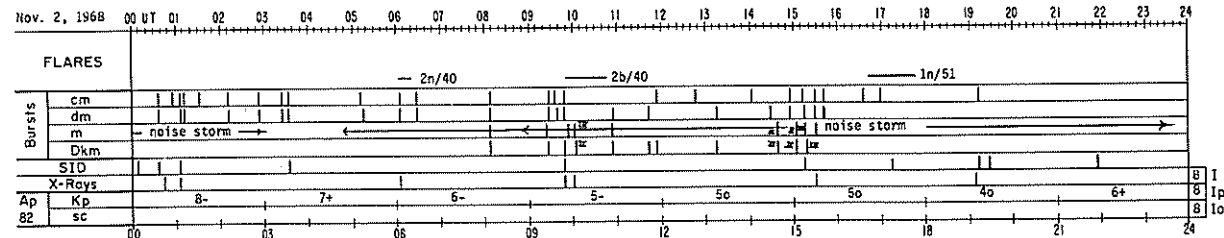
# ABBREVIATED CALENDAR RECORD (Continued)



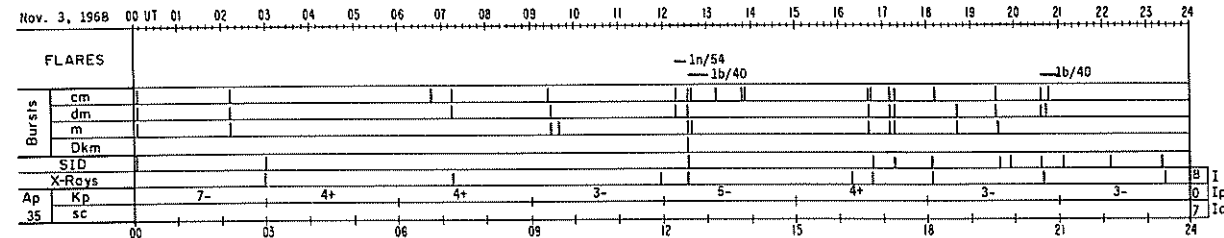
162 10 cm flux One of five most magnetically disturbed days, beginning of most disturbed period of year; aurora overhead over USSR at  $\phi = 54^\circ$  from 1500-2300; aurora overhead over N. America at  $\phi = 57^\circ$  from 0600-1100; active display of rayed arc and band visible over W. Atlantic at  $\phi = 57^\circ$  from 0100-0800; cloudy over W. Europe south of  $\phi = 60^\circ$ ; rayed arc, sometimes multiple and striated; base overhead over W. Europe at  $\phi = 64^\circ$  from sunset to 2140; pulsation occurred around 1900 and again from 2030-2115; a rayed arc with base overhead just north of Shetland after sunset, broke up about 1930 into several rayed bands, one showing striations, pulsation occurred just before the forms began to recede northwards about 2130 with the active phase of this display completed about 2200; large proton increase on  $>10$  Mev  $>30$  Mev and  $>60$  Mev counters on Explorer 34 peaks at 1800 and continues with another maximum on 1 Nov.



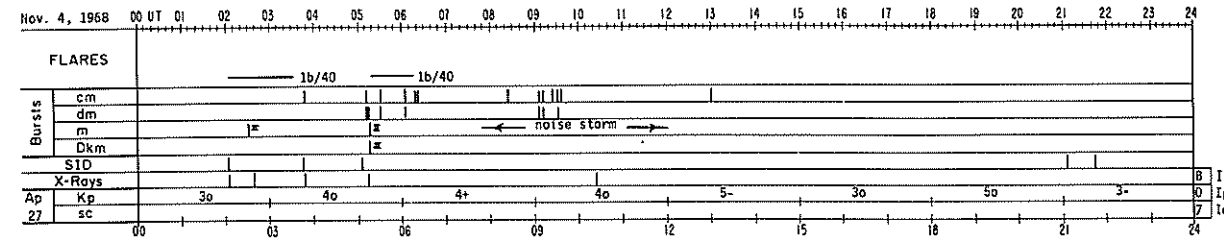
156 10 cm flux One of five most magnetically disturbed days; aurora overhead over USSR at  $\phi = 53^\circ$  near 0000, at  $\phi = 49^\circ$  near 1600, at  $\phi = 54^\circ$  from 1800-2200, at  $\phi = 51^\circ$  near 2300; brilliant auroral display over W. Europe and Atlantic lasting all night brighter and more active than the previous night, multiple rayed arcs and bands with patches, sometimes very bright with bases overhead between  $\phi = 60^\circ - 70^\circ$  in W. Europe and to lower  $\phi$ s over W. Atlantic, red coloration strongest from 2320-2340; overcast south of  $\phi = 60^\circ$  over W. Europe, intermittent pulsation flaring and flickering visible to  $\phi = 49^\circ$  over W. Atlantic; proton increase on  $>10$  Mev,  $>30$  Mev and  $>60$  Mev counters on Explorer 34 peaks 2100.



154 10 cm flux One of five most magnetically disturbed days; aurora overhead over USSR at  $\phi = 59^\circ$  0000-0200 and 1500; aurora visible overhead over N. America at  $\phi = 56^\circ$  from 0000-0500 and at  $\phi = 59^\circ$  from 0600-1100; moderately bright rayed arc over W. Europe, base overhead at  $\phi = 66^\circ$ , rays overhead at  $\phi = 63^\circ$  visible to  $\phi = 56^\circ$  at 0050.



148 10 cm flux One of five most magnetically disturbed days; aurora overhead over USSR at  $\phi = 59^\circ$  near 1500; br. green corona 7 days earlier on SE limb.



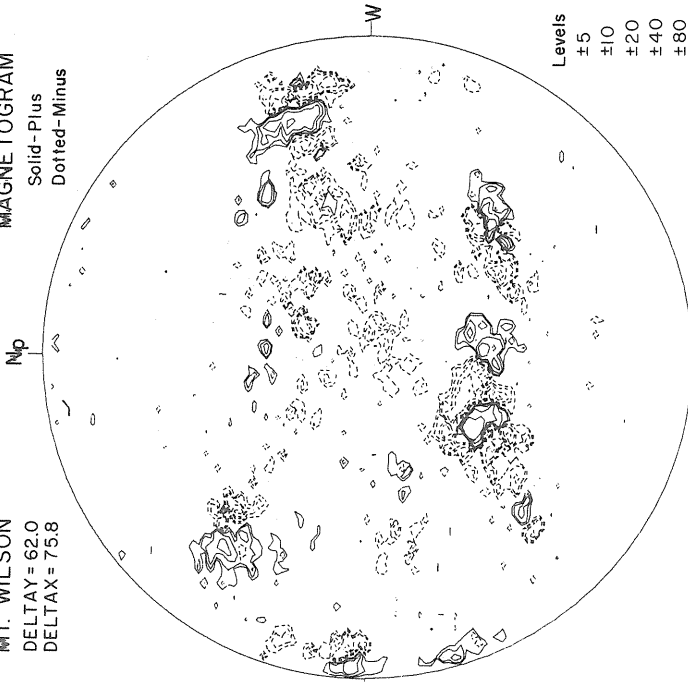
143 10 cm flux One of five most magnetically disturbed days; proton increase on  $>10$  Mev,  $>30$  Mev and  $>60$  Mev counters on Explorer 34, peaks 0800; br. green corona 7 days earlier on SE limb.

OCTOBER 27, 1968 (P = 25.28, B<sub>0</sub> = 4.81, L<sub>0</sub> = 194.56)

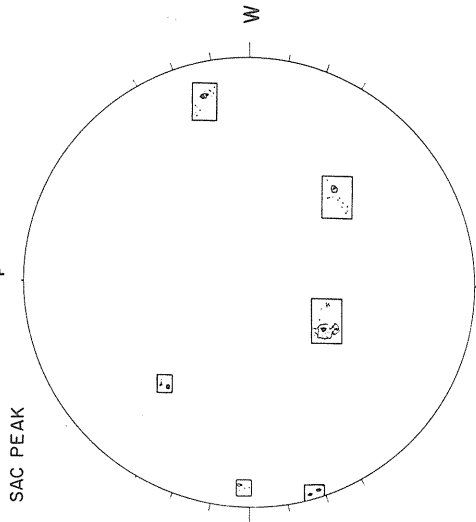
MT. WILSON  
DELTA TAY = 62.0  
DELTA TAX = 75.8

MAGNETOGRAM  
Solid-Plus  
Dotted-Minus

Levels  
±5  
±10  
±20  
±40  
±80



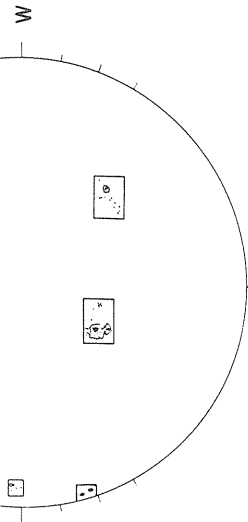
BOULDER  
H $\alpha$   
ESSA-BOULDER  
SUNSPOTS



SAC PEAK

Np

E



17.08-18.05 UT DATA INCOMPLETE

McMATH-HULBERT CALCIUM REPORT

35-82-3.5  
39-28-3.5  
40-78-3.5  
43-05-3.0  
44-21-2.5  
45-13-2.5  
47-26-2.5  
49-18-3.0

17.08-18.05 UT DATA INCOMPLETE

McMATH-HULBERT CALCIUM REPORT

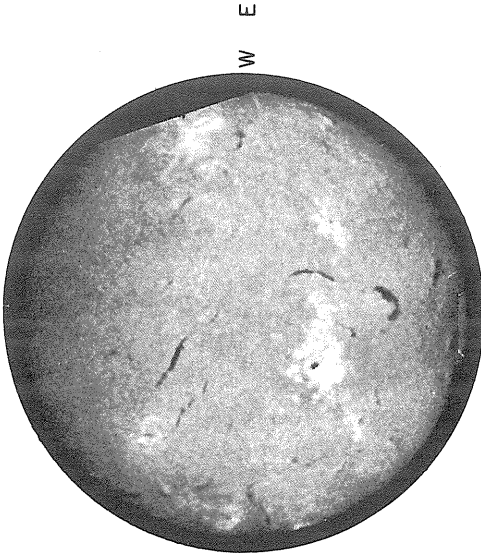
35-82-3.5  
39-28-3.5  
40-78-3.5  
43-05-3.0  
44-21-2.5  
45-13-2.5  
47-26-2.5  
49-18-3.0

7

BOULDER

H $\alpha$

Np



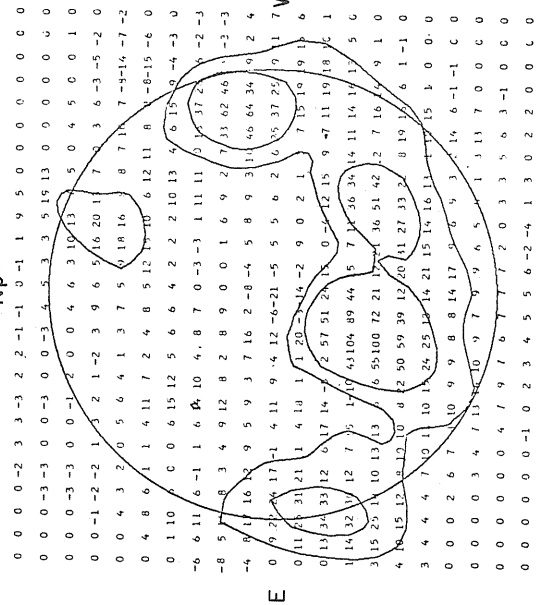
Np

E

1415 UT

STANFORD

9.1 cm.

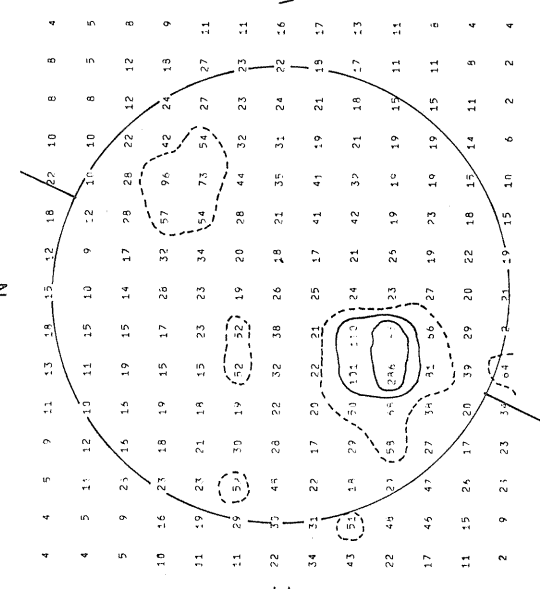


Brightness Unit 5000° K

20-21 UT

1528 UT

21 cm.



Brightness Unit 1700° K

02-03 UT

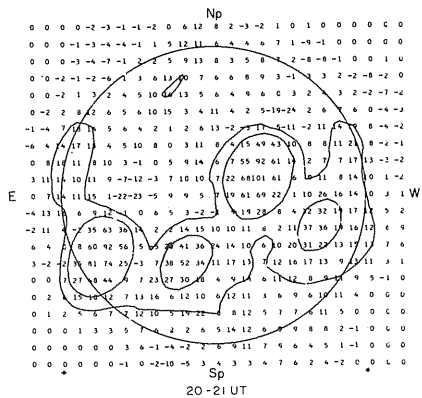
Resolution 3 Minutes of Arc

02-03 UT Brightness Unit 1700° K

Fig. 1 Daily scout maps of solar phenomena

STANFORD  
9.1 cm.

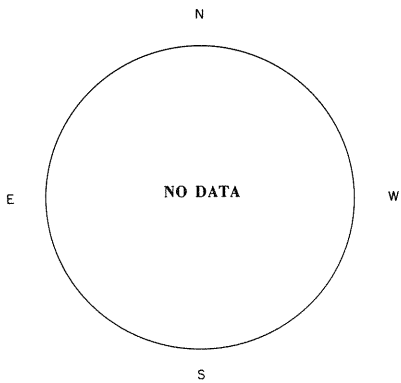
Brightness Unit 5000° K



20-21 UT

FLEURS, AUSTRALIA  
21 cm.

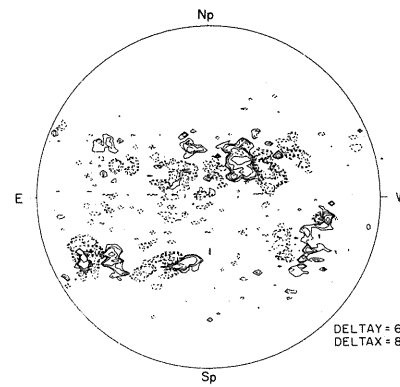
Resolution 3 Minutes of Arc  
Brightness Unit 1,700° K



24 OCTOBER 1968

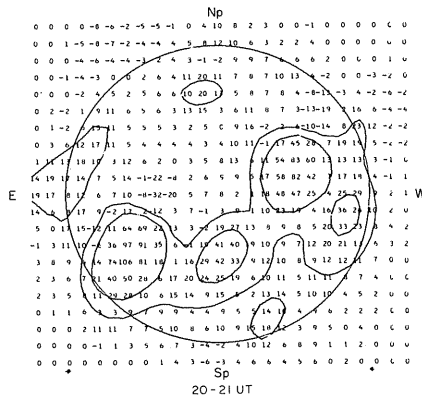
MT. WILSON  
MAGNETOGRAM

Solid-Plus  
Dotted-Minus

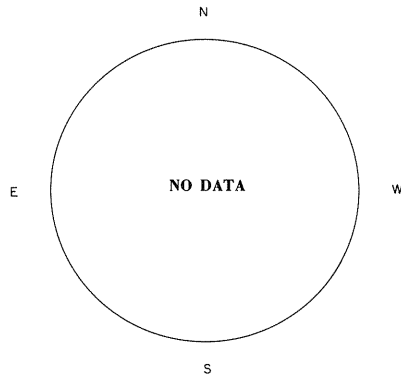


16:50-17:43 UT

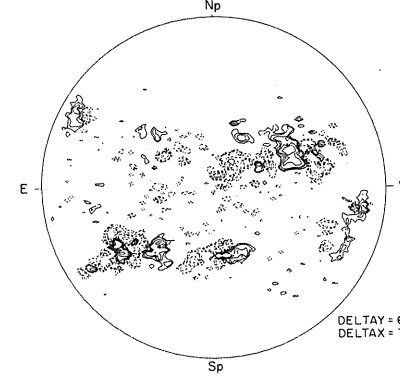
DELTA Y = 62  
DELTA X = 80



20-21 UT

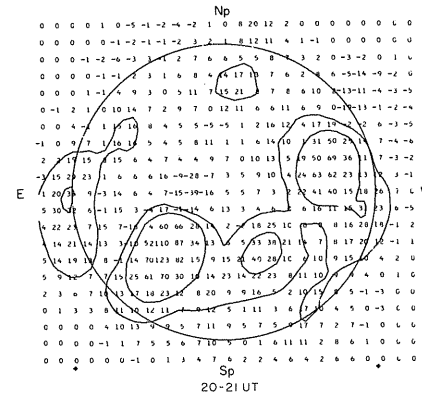


25 OCTOBER 1968

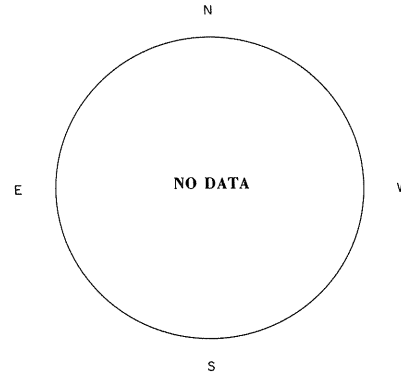


21:09-22:18 UT

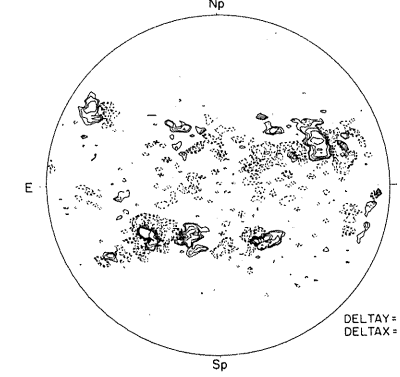
DELTA Y = 62  
DELTA X = 76



20-21 UT

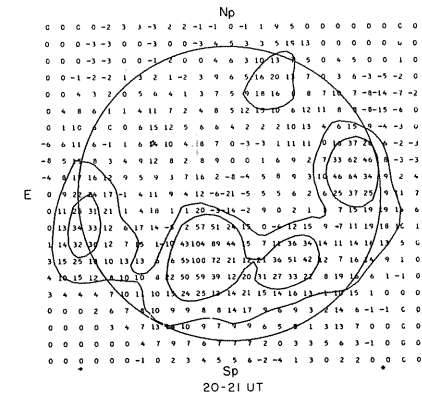


26 OCTOBER 1968

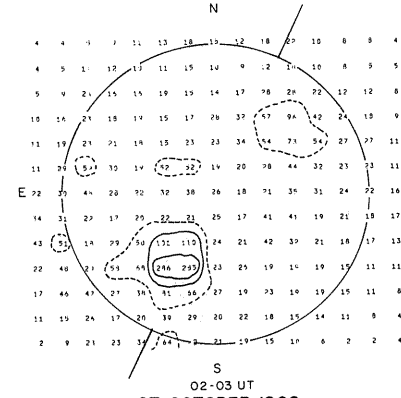


16:24-17:19 UT

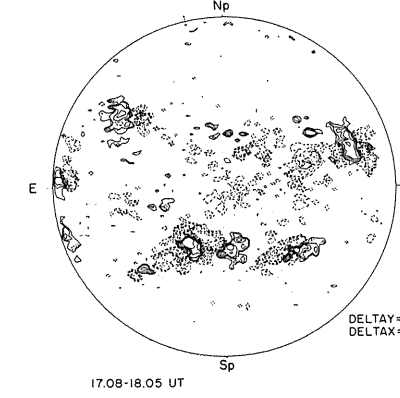
DELTA Y = 58.3  
DELTA X = 78.5



20-21 UT



02-03 UT  
27 OCTOBER 1968



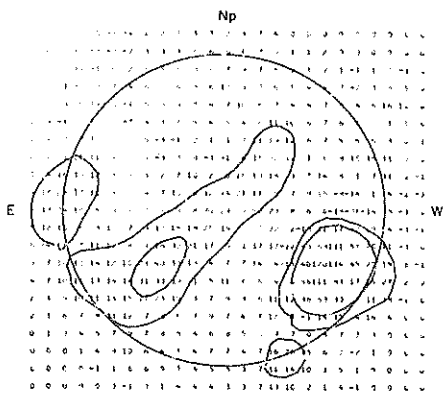
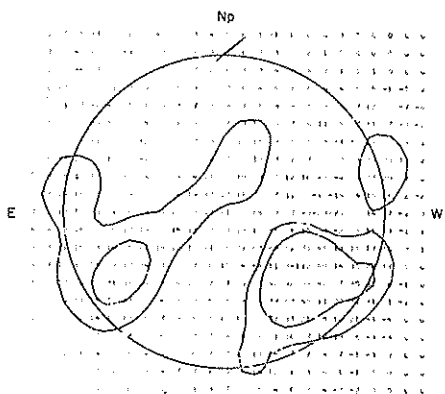
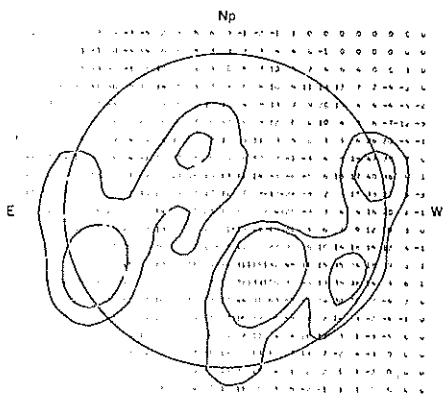
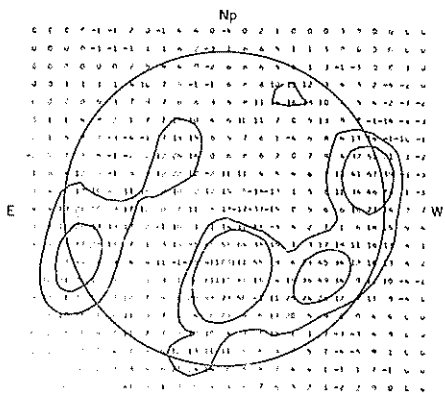
17:08-18:05 UT

DELTA Y = 62.0  
DELTA X = 75.8

Fig. 2. Stanford 9.1 cm maps, Fleurs 21 cm maps and Mt. Wilson magnetograms October 24 - November 4, 1968.

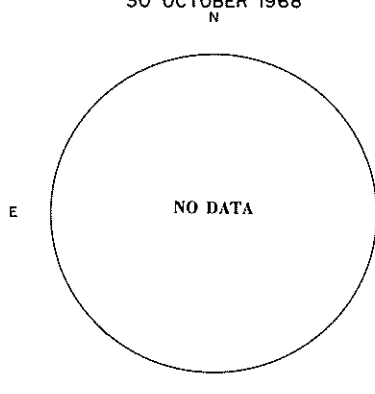
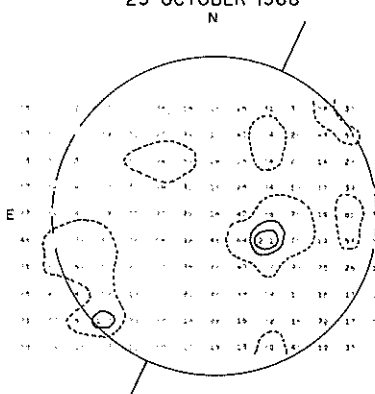
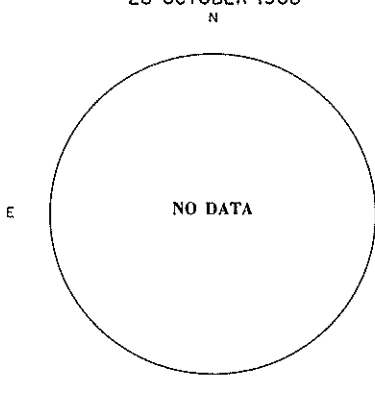
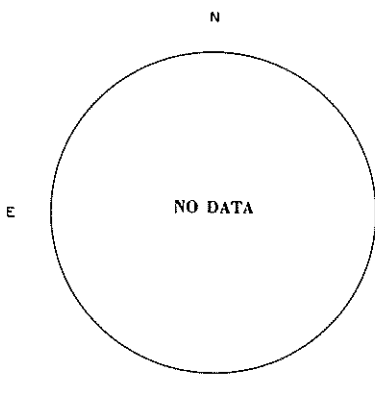
STANFORD  
9.1 cm.

Brightness Unit 5,000° K



FLEURS, AUSTRALIA  
21 cm.

Resolution 3 Minutes of Arc  
Brightness Unit 1,700° K



MT. WILSON  
MAGNETOGRAM

Solid-Plus  
Dotted-Minus

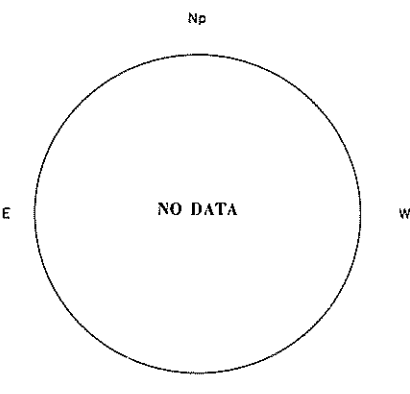
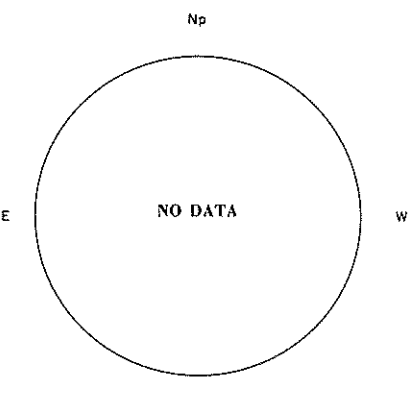
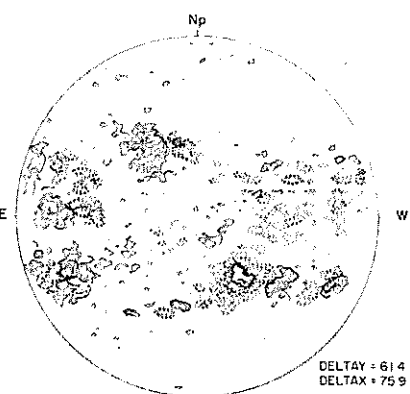
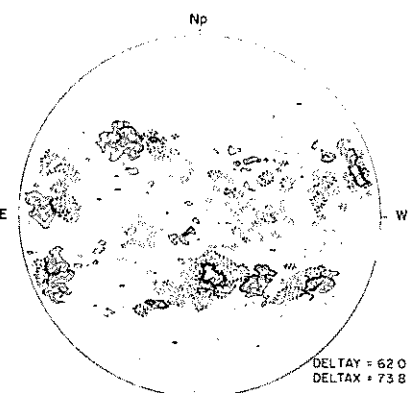


Fig. 2. (continued)

STANFORD  
9.1 cm.

Brightness Unit 5,000°K

FLEURS, AUSTRALIA  
21 cm.

Resolution 3 Minutes of Arc  
Brightness Unit 1,700°K

MT. WILSON  
MAGNETOGRAM

Solid-Plus  
Dotted-Minus

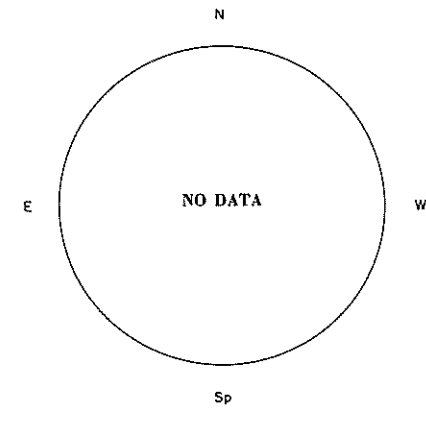
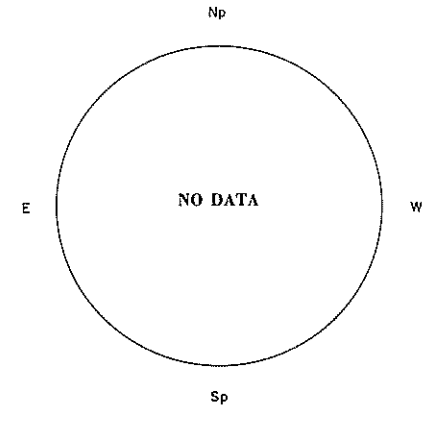
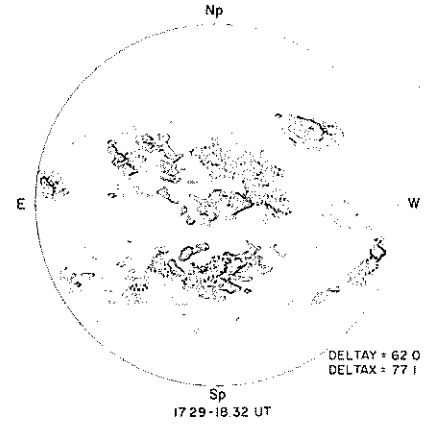
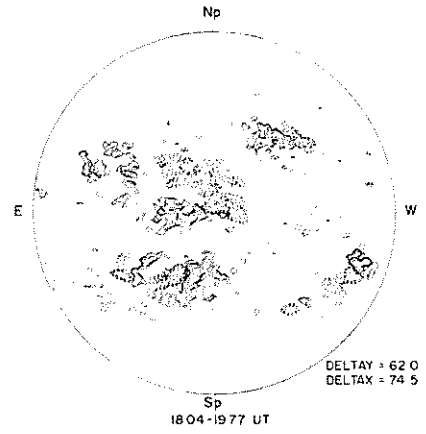
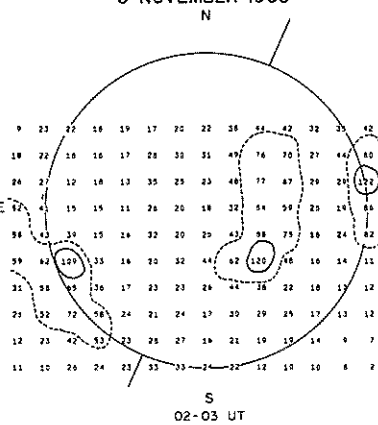
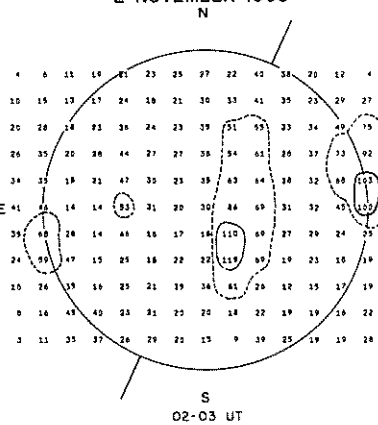
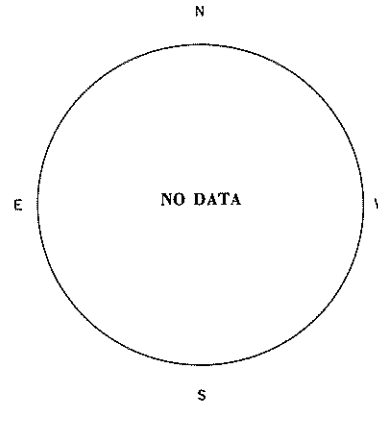
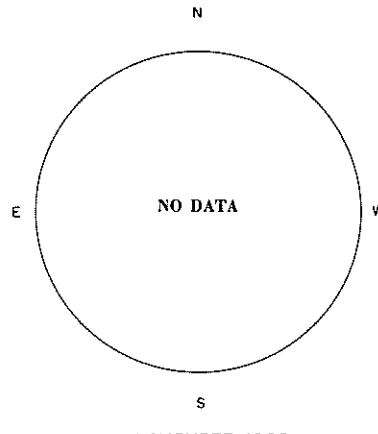
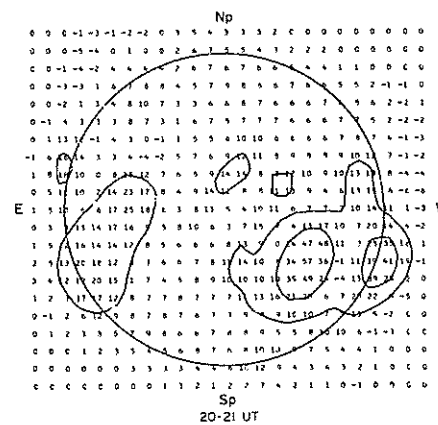
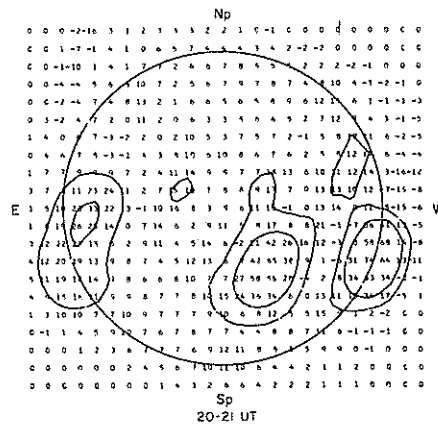
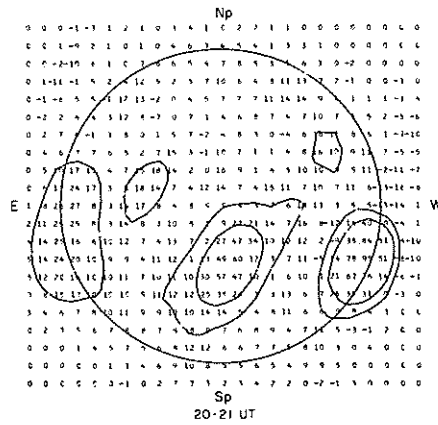
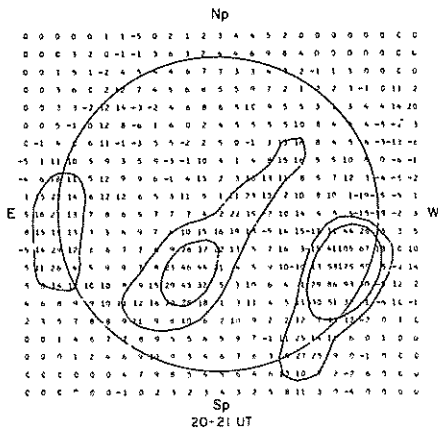


Fig. 2. (Continued)

## 2. HISTORY OF THE ACTIVE SOLAR REGION

"Evolution of the Active Region (H $\alpha$  and K Faculae and Spots) of the Proton Events of October 29-early November 1968"

by

G. Godoli, O. Morgante, and M. L. Sturiale  
Osservatorio Astrofisico di Catania  
Università di Catania, Consiglio Nazionale delle Ricerche

[The compiler has prepared the following paragraphs from the outline submitted by G. Godoli.]

The faculae and spot history of McMath region 9740 as observed at the Catania Observatory is presented in the figures to follow. The observations have been combined with data in the Fraunhofer daily maps and in "Solar-Geophysical Data". The active region at S15 and Carrington longitude L = 171 can be followed from August 29, 1968 to January 24, 1969. The region is born and dies on the invisible hemisphere. The sunspot group according to Mt. Wilson Observatory was  $\beta$ -type on its appearance September 1, 1968.

The H $\alpha$  and K faculae maps are shown in Fig. 1 a, b and c for the six transits of the active region. The four transits of the sunspot region are presented in Fig. 2. The H $\alpha$  faculae daily maps have been drawn using a 138s Durst projector from the heliograms of the Catania H $\alpha$  patrol. In this patrol one heliogram is made each five minutes (1 heliogram/5 min) with a Halle filter No. 78 fed by a single aspherical lens (15 cm/222 cm) from 75 minutes after sunrise to sunset. The filtergrams are 20.5-21 mm. in diameter. The maps were drawn at 150 mm. and reduced for printing.

The K faculae maps have been drawn using the same projector from the Catania K spectroheliograms. Daily K<sub>232</sub> spectroheliograms are taken at Catania with a small spectroheliograph fed by the Steinheil refractor (33 cm/347 cm). The spectroheliograms are 31.5-32 mm. in diameter and again the maps were drawn at 150 mm.

The sunspot daily maps have been drawn using a M35 Durst automatic projector from the heliograms of the Catania white light patrol. The Catania white light patrol is made hourly with a GH649 Kodak emulsion + a OG<sub>2</sub> Schott filter fed by the Cooke refractor (15 cm/223 cm) from 75 minutes after sunrise to sunset. The heliograms are 20.5-21 mm. in diameter and the maps have been drawn at 150 mm.

From the maps the evolution curves were deduced. These are presented in Fig. 3 a and b. The projected areas (Area<sub>p</sub>) are given in 10<sup>-4</sup> of the solar disk. The corrected areas (Area<sub>c</sub> = 1/2 Area<sub>p</sub> sec h) are given in 10<sup>-4</sup> of the solar hemisphere.

The following conclusions can be drawn from Figures 1, 2 and 3.

1. The H $\alpha$  and K faculae lasted six rotations;
2. The sunspot group lasted four rotations;
3. The sunspot group was born on the disk during the first transit of the faculae;
4. The sunspot group grows markedly during the period of occurrence of the proton events, and in general the sunspot group evolution curve is similar to that of proton emission as seen in the figures in "Solar-Geophysical Data" No. 298, p. 163 and No. 300, Part II, p. 91;
5. The area of the H $\alpha$  faculae is always smaller than the area of K faculae [Morgante 1968];
6. The maxima of H $\alpha$  and K faculae occurred on the same day November 1, 1968;
7. The decreasing portions of the evolution curves are unusually steep, as it was found for the K faculae evolution curve of proton flares of August 28 and September 2, 1966 [Godoli and Fossi 1968].

### REFERENCES

- GODOLI, G., and MONSIGNORI B. C. FOSSI 1968 Oss. Astrofis. Catania Pubbl. No. 122.
- MORGANTE, O. 1968 Mem. Soc. Astr. Ital., 39, 101.

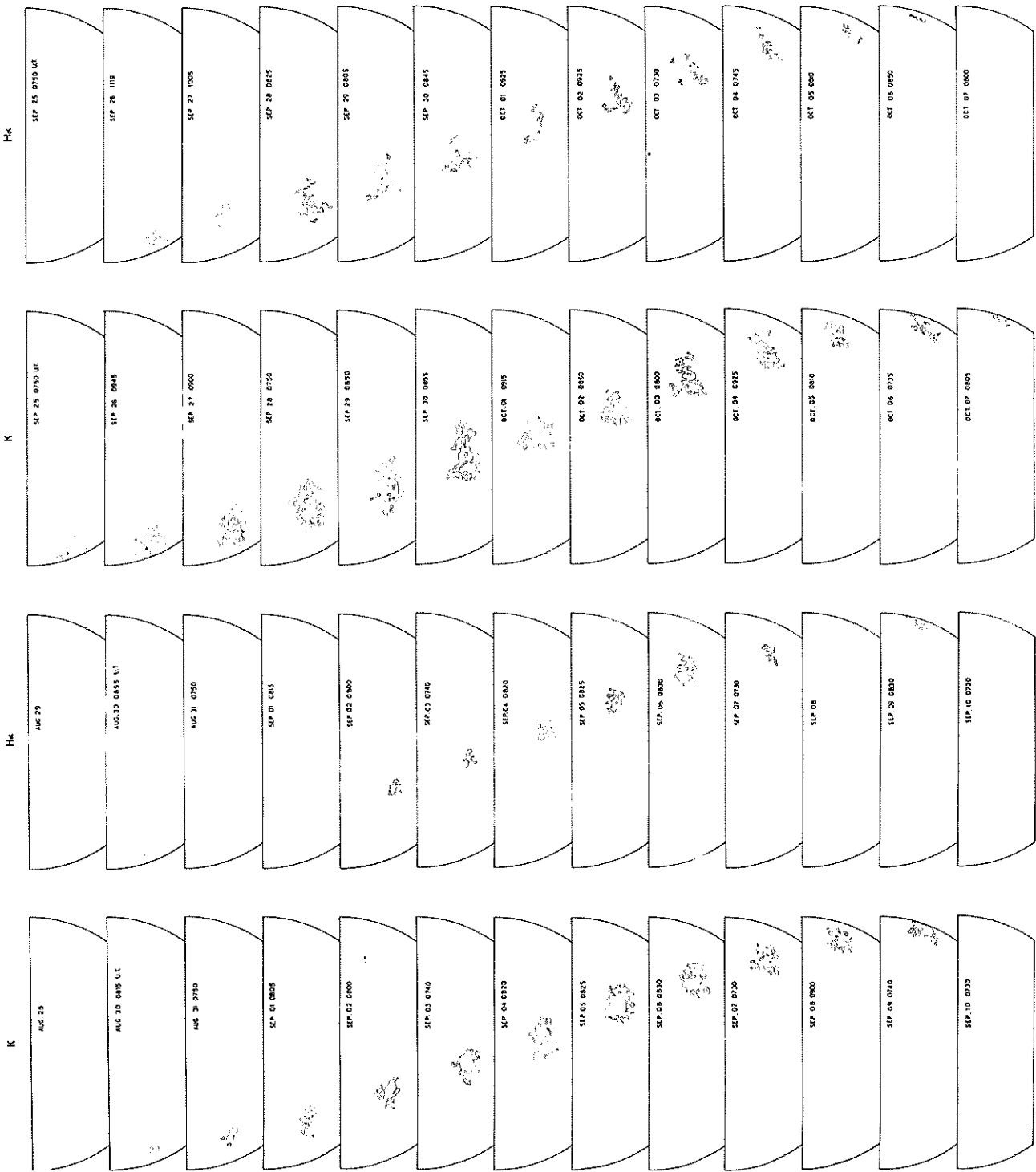


Fig. 1a. H $\alpha$  and K faculae maps for transits 1 and 2 of the active region.

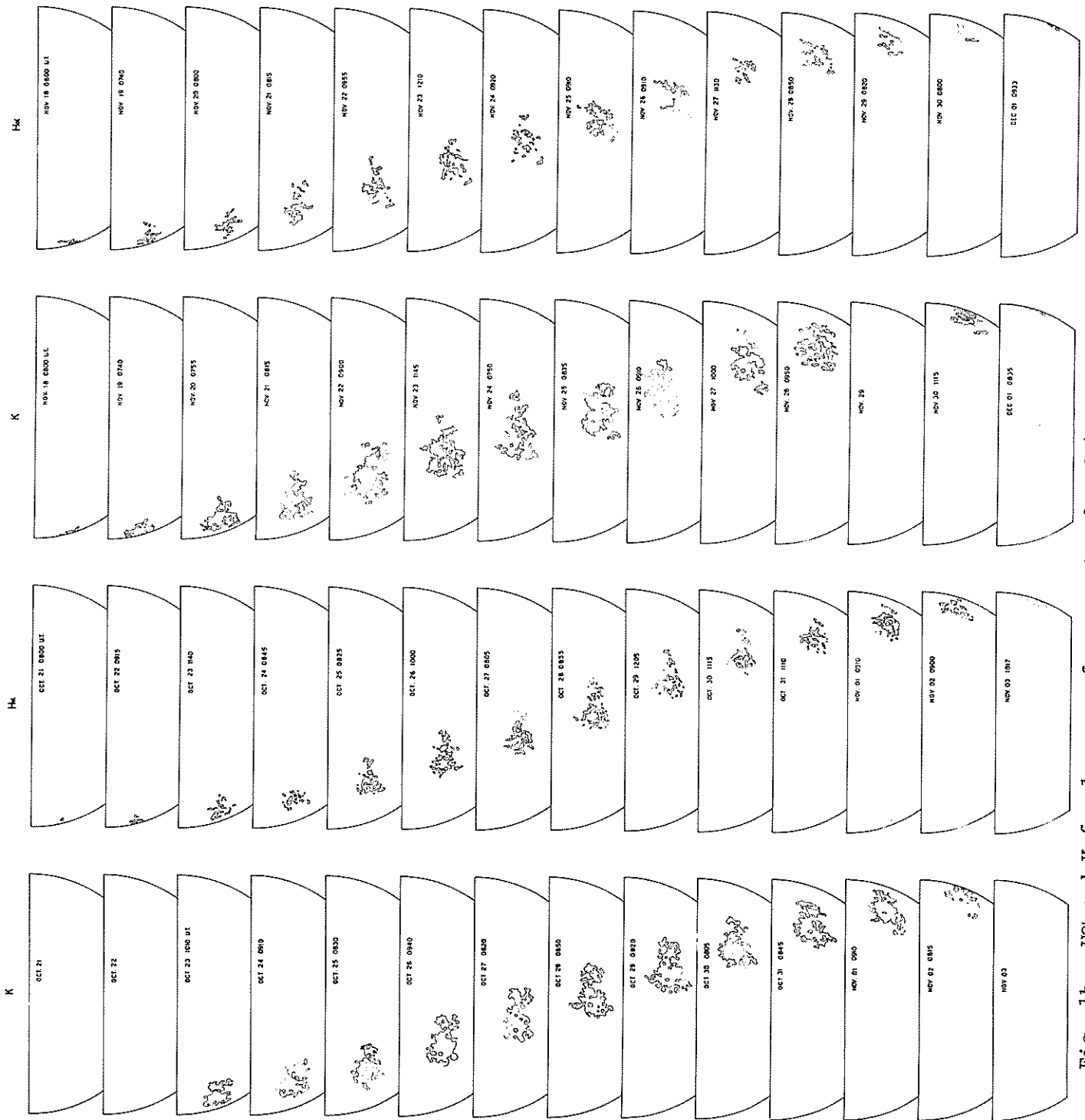


Fig. 1b. Hc and K faculae maps for transits 3 and 4 of the active region.



Fig. 1c. H<sub>K</sub> and K faculae maps for transits 5 and 6 of the active region.



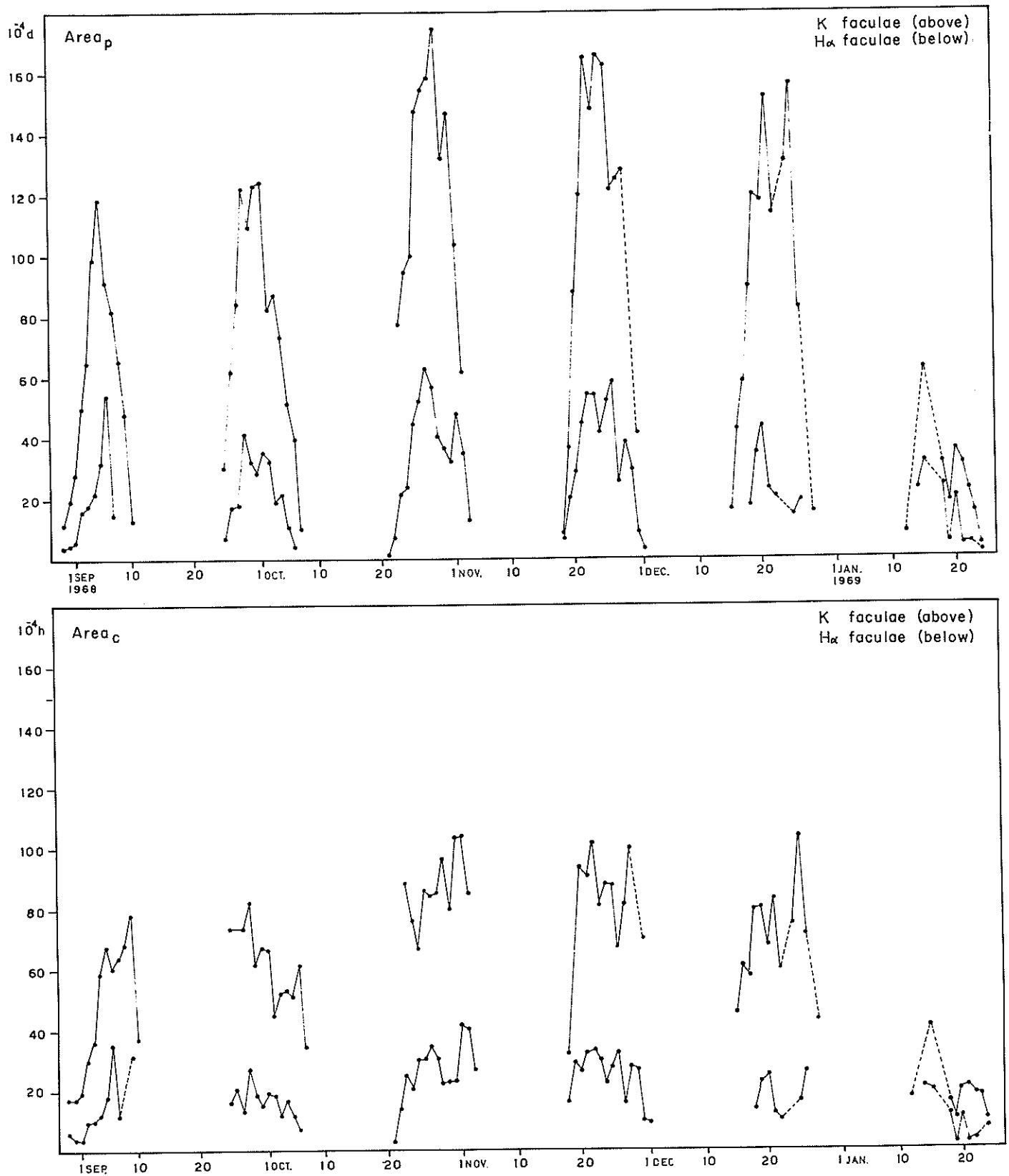


Fig. 3a. Daily projected area (Area<sub>p</sub>) and corrected area (Area<sub>c</sub>) of the H<sub>α</sub> and K faculae versus time.

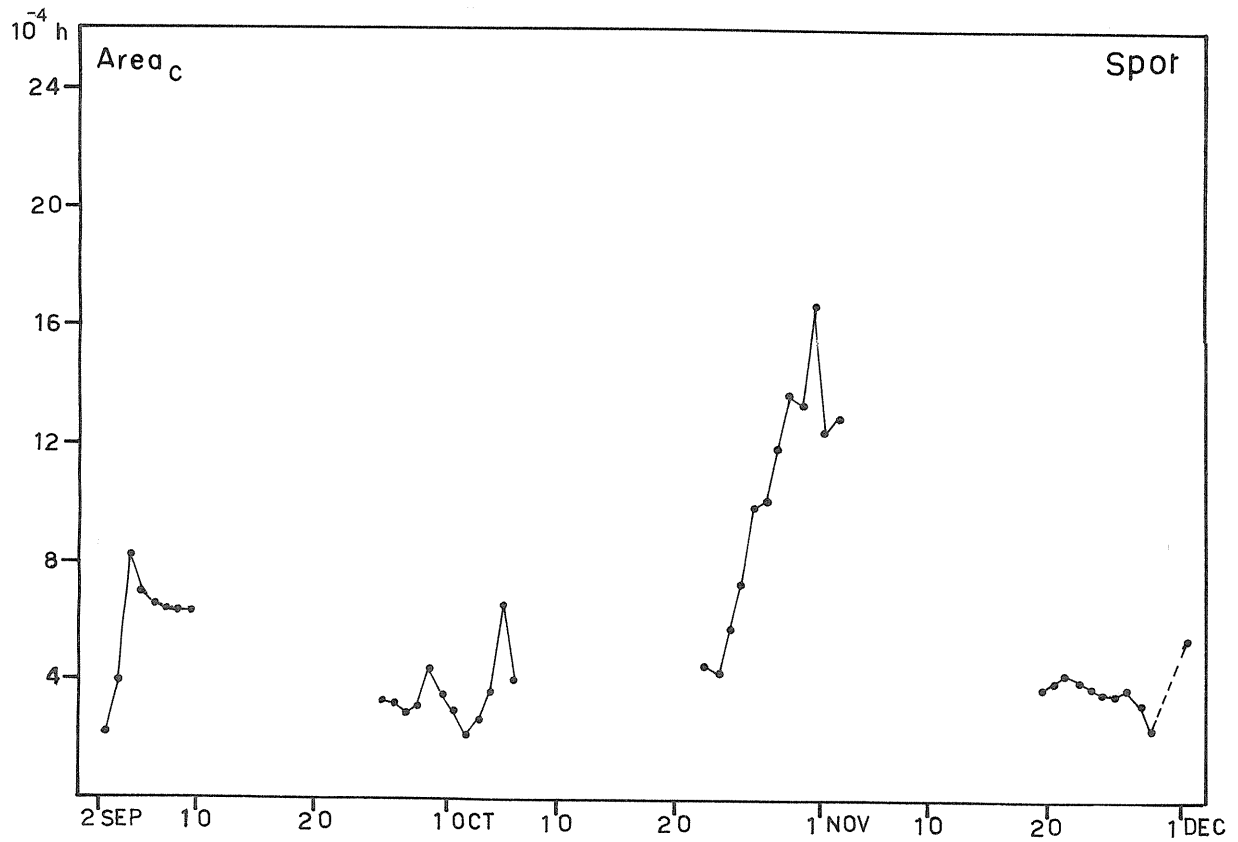
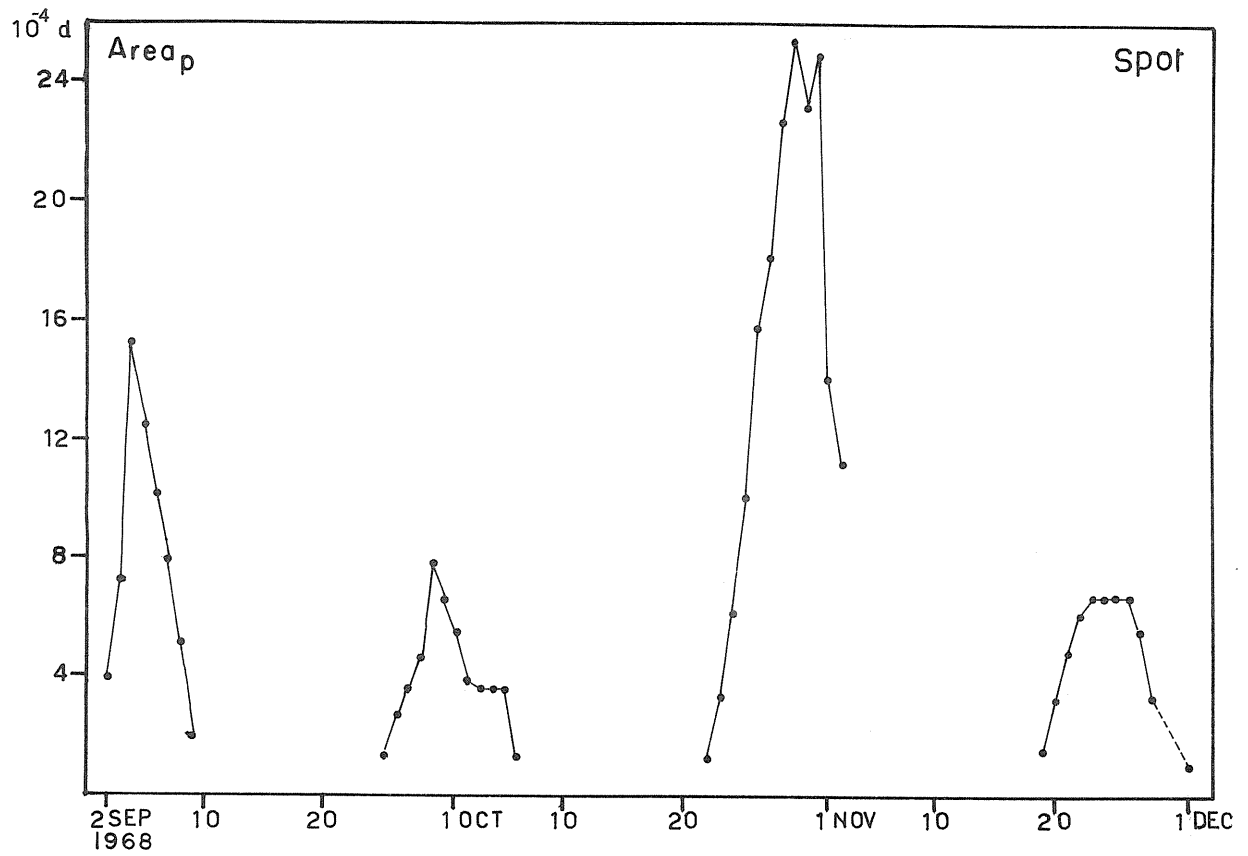


Fig. 3b. Daily projected area (Area<sub>p</sub>) and corrected area (Area<sub>c</sub>) of the sunspot group versus time.

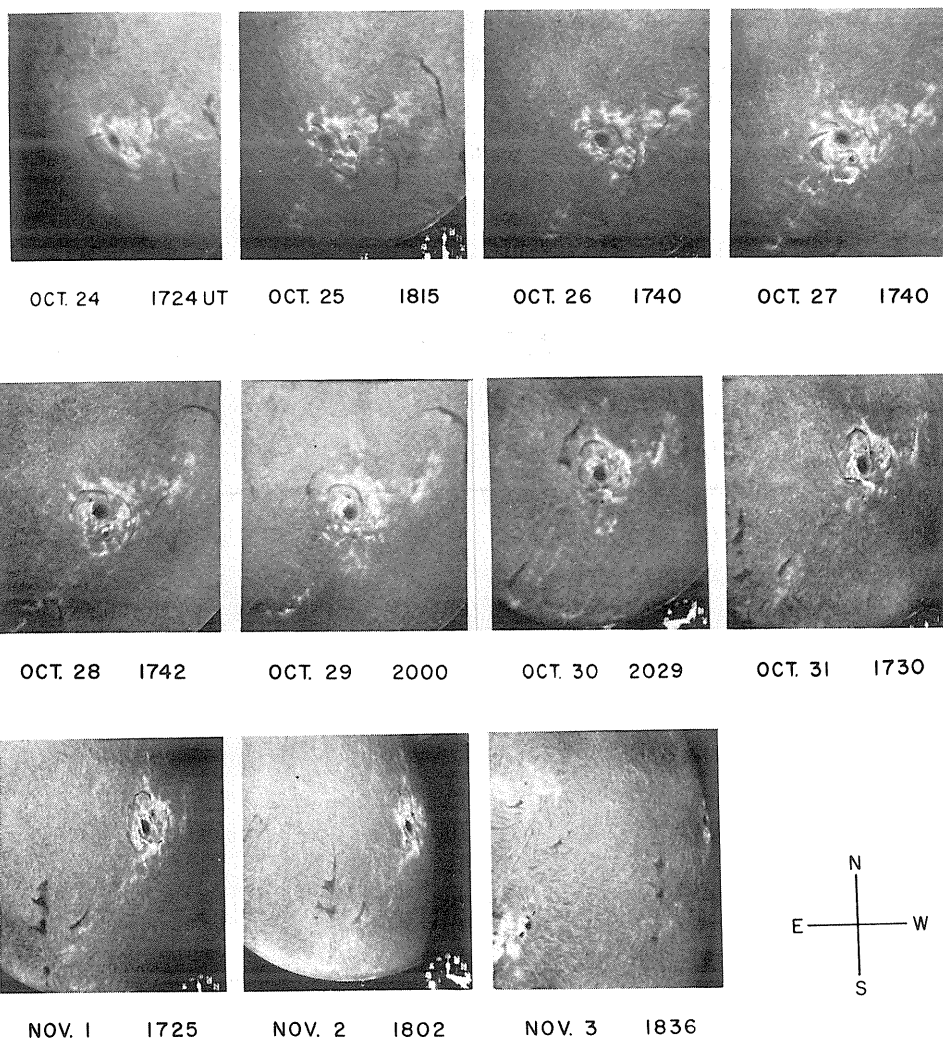
# "H $\alpha$ Disk Passage of the Active Region"

by

Marie McCabe  
Institute for Astronomy  
University of Hawaii

[The compiler has prepared the following paragraph from information furnished by Miss McCabe.]

In Fig. 1 is shown the disk passage of the active region McMath plage number 9740 from October 24 through November 3, 1968. These H $\alpha$  pictures were taken at the Haleakala Observatory on the large scale system with image diameter approximately 5.0 cm. Such pictures were taken for approximately two hours each day during this period, with the usual flare patrol program operating the rest of the time.



## DISK PASSAGE OF ACTIVE REGION (LARGE SCALE SYSTEM—IMAGE DIAM. $\approx$ 5.0 cms.)

Fig. 1 Large scale observations at the Haleakala Observatory

# "On Some Aspects of the Early Evolution of the Region"

by

T. Fortini and M. Torelli  
Osservatorio Astronomico di Roma

The McMath 9740 region during its transit on the disk from October 21 through November 3, 1968 could be morphologically classified as a B configuration [Avignon, Martres and Pick, 1964], i.e. a large unipolar spot encircled by a field of opposite polarity. It was the third return of the McMath 9634 region, born on the disk early in September. Its main character was established before the west limb passage of the disk transit in September and it is perhaps of significance to recall a few of the circumstances which outlined the birth and early evolution of the center. The center was born on September 1 at the south-east end of a filament that during the next day was destroyed, probably due to this new disturbance reaching the solar surface. The development of the plage and particularly of the spots was steep, as shown in Fig. 1, and accompanied by the fast separation of the two polarities, the reduction of the following spots and the establishment of a large and intense western spot (or leader). At this stage, September 6, the leader spot presented the activity characteristic of other centers with a fast evolution [Fortini and Torelli, 1968], i.e. the production for many hours of numerous surges and flare-puffs around the western edge as in Fig. 2. This activity seemed to start the decay of the center before a second active phase was initiated on September 8 with the interaction of the large spot with a newly born sunspot group shown in Fig. 3. Unlike other cases in which the interaction is between the eastern spot of the first center with the western component of the following center, in this case it was the following component of the second center interacting with the leader of the old center. The interaction was highlighted by fairly new activity before the western transit. The interaction of the two centers resulted in a high gradient of the longitudinal magnetic field and moderate activity. There was a 2B flare on September 28 shown in Fig. 4, on the east edge of the large spot, that on this second transit from September 25 through October 8 was the only remnant of the sunspot group.

The high activity of the region in its third return was very probably excited by a new center born on its west on the opposite hemisphere and by many new disturbances reaching the solar surface during the October 21 to November 3 transit. However, the magnetic configuration initiated in the first rotation was still very stable, and at this very site the activity of the region was particularly frequent.

## REFERENCES

- |  |      |   |
|--|------|---|
| AVIGNON, Y.,<br>M. J. MARTRES and<br>M. PICK | 1964 | "Identification de classes d'éruptions chromosphériques associées aux émissions de rayons cosmiques et à l'activité radioélectrique", <u>Annales d'Astrophysique</u> , <u>27</u> , 23-28. |
| FORTINI, T.,<br>M. TORELLI                   | 1968 | "Ejections of matter from the main component of fast growing sunspot-groups", <u>Nobel Symposium</u> , <u>9</u> , 173-170.  |

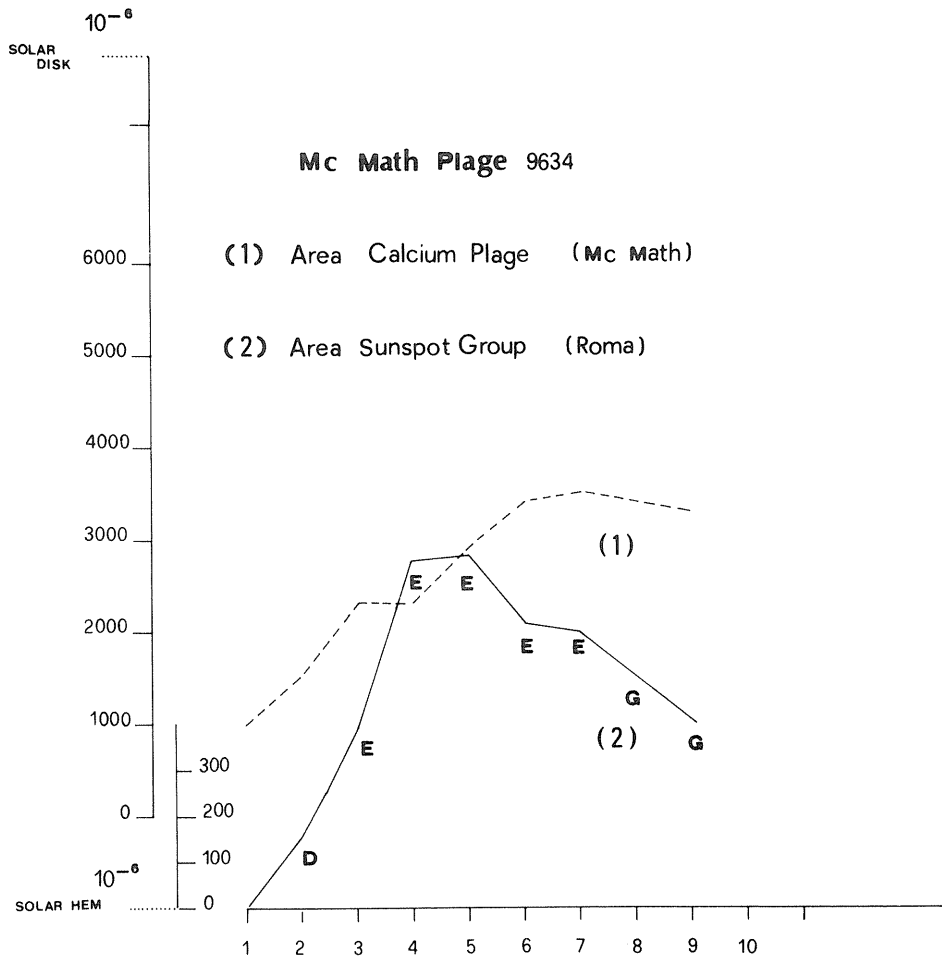


Fig. 1a. Development of the calcium plage and sunspot areas of the McMath center 9634, September 1968.

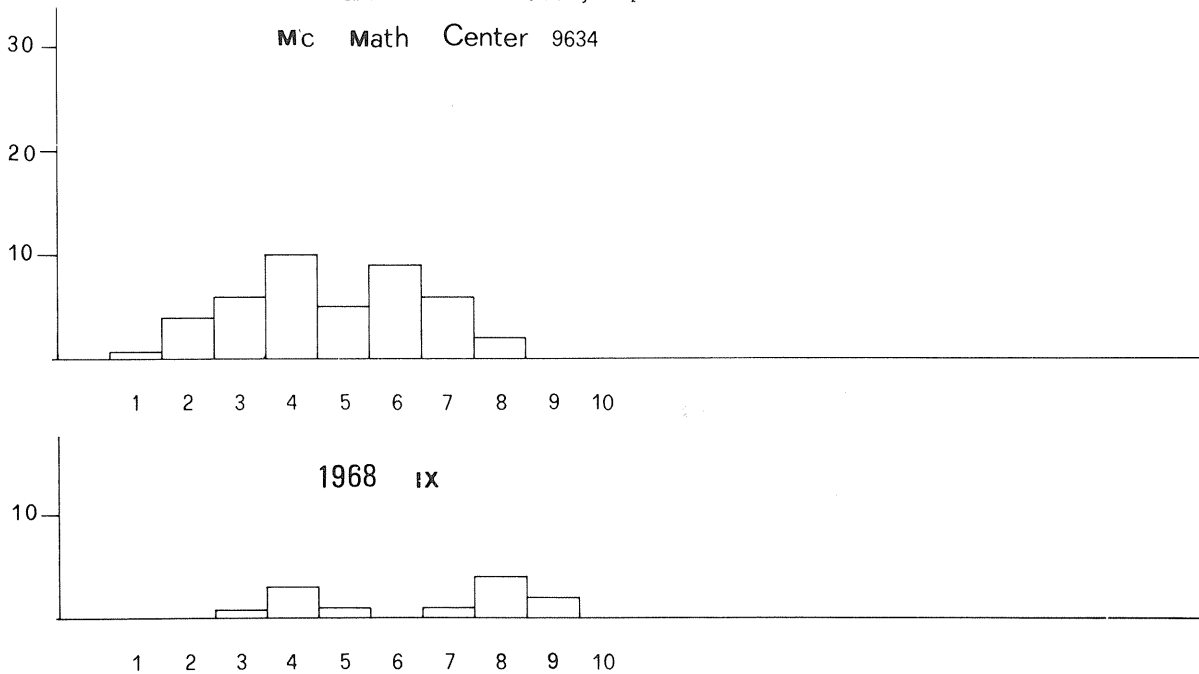


Fig. 1b. Histogram of the flares <1 (above) and =1 (below) associated with the McMath center 9634 (no flare >1 has been observed in the center).

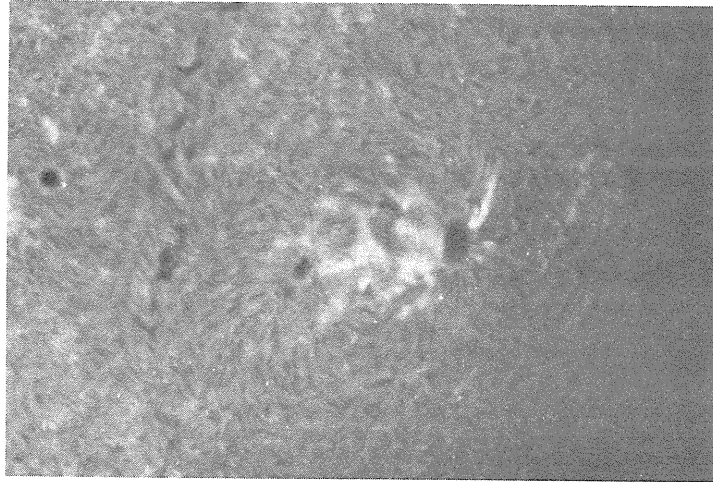


Fig. 2. 1968 September 6, 1045 UT: H $\alpha$  filtergram (courtesy of the Osservatorio Astronomico di Catania).

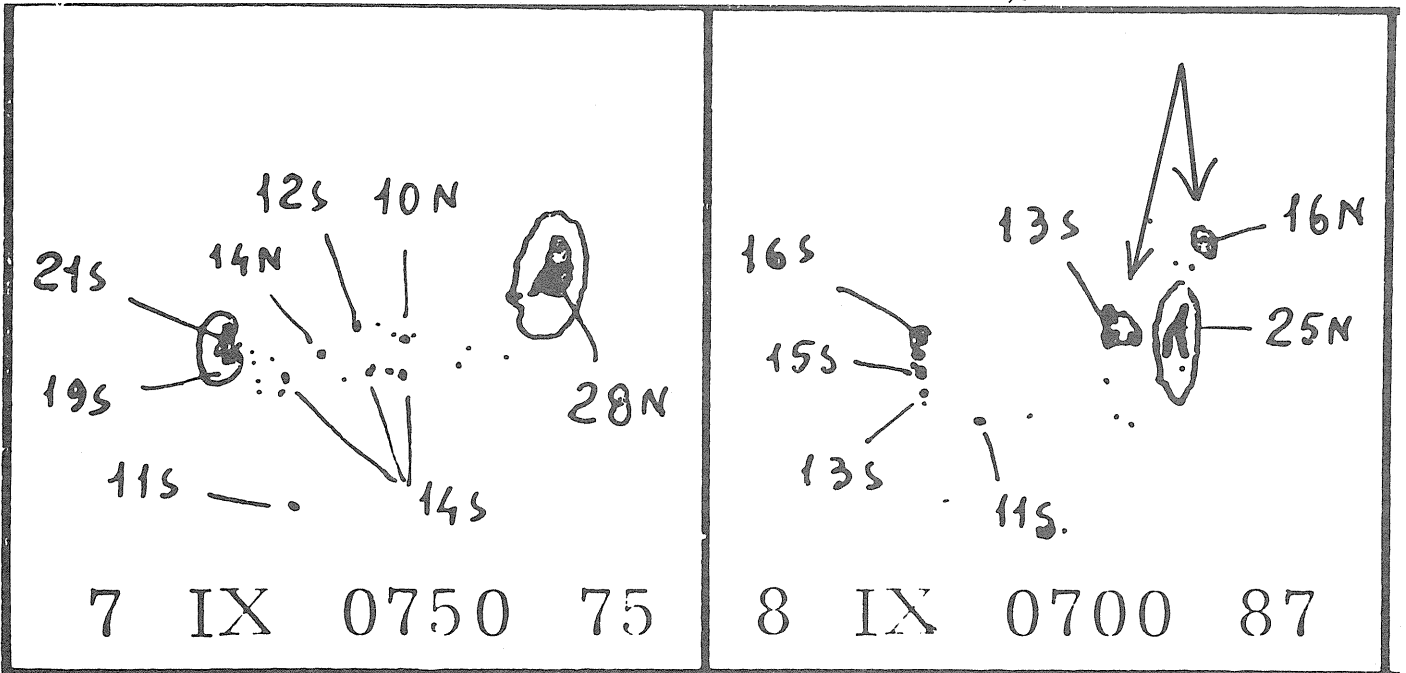


Fig. 3. Region McMath 9634 - Sunspot magnetic configuration - Roma Observatory magnetic observations (the arrows on September 8 indicate the newborn sunspot group).

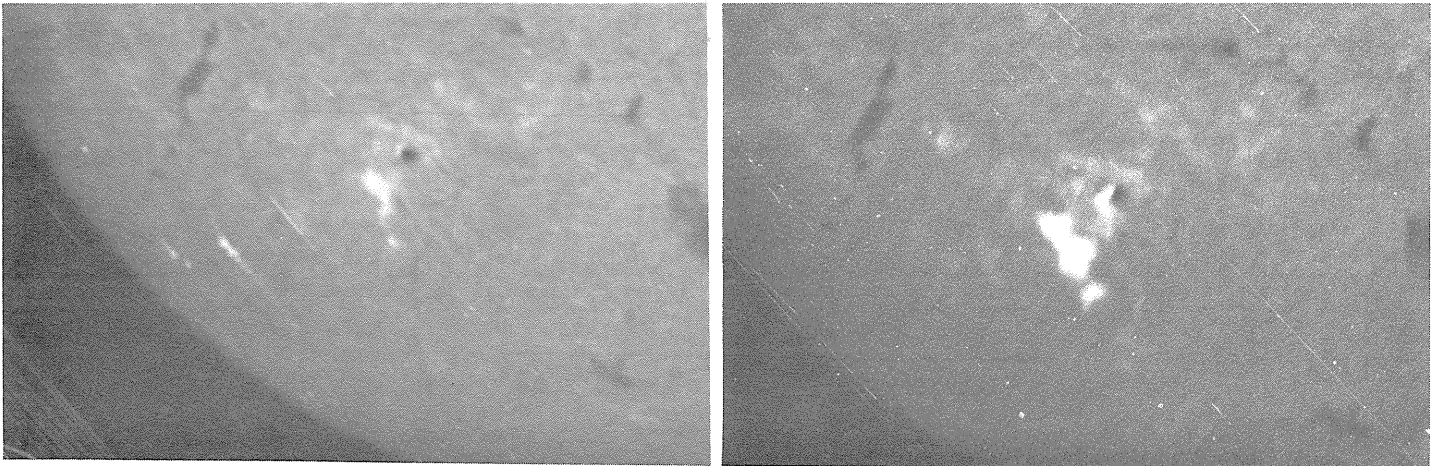


Fig. 4. 1968 September 28: left 0735 UT, right 0850 UT H $\alpha$  filtergrams (Osservatorio Astronomico di Roma).

# "Sunspots Associated with the Proton Flares of Late October 1968"

by

Patrick S. McIntosh  
Space Disturbances Laboratory  
ESSA Research Laboratories, Boulder, Colorado

In the study of previous proton-flare sunspot groups [Gopasyuk and Moreton, 1967; McIntosh, 1968, 1969; Sakurai, 1967] sunspot proper motions, sunspot rotation, and rapid sunspot growth have been related to the occurrence of the flares. The region of late October 1968 is no exception. This sunspot group is also outstanding for the rapid changes in appearance resulting from rapid spot growth and motions in all parts of the region.

The proton flare of 30 October can be related in position and time to the rapid growth of new spots near a convoluted portion of a longitudinal neutral line. The site of the flare was only one of several areas of high magnetic field gradient across a neutral line in the longitudinal field occurring in this region. This site differed from the others in its rapid development during the 24 hours prior to the flare and in the conspicuous motion of a sunspot toward this site during the same period.

This active region was the third disk passage of a region which formed late on 1 September. If we examine the patterns of faint plage and quiescent filaments which remained after previous active regions decayed, we can trace the activity at the location of the October region continuously as far back as late January 1968. Active regions formed within a  $5 \times 15$  degree area bounded by Carrington longitudes 167 to 182 and heliographic latitudes S10 to S15 on the following dates: a few days before east limb passage on 24 January, 21 March, 9 June, and 1 September. The activity in October can be interpreted as the outbreak of a number of small areas of new magnetic fields superposed on the region marked by the returning leader sunspot which formed during September. Thus, the October passage represents the fifth in a series of emerging regions at the same absolute coordinates on the sun, and it represents the 11th solar rotation since the first region formed.

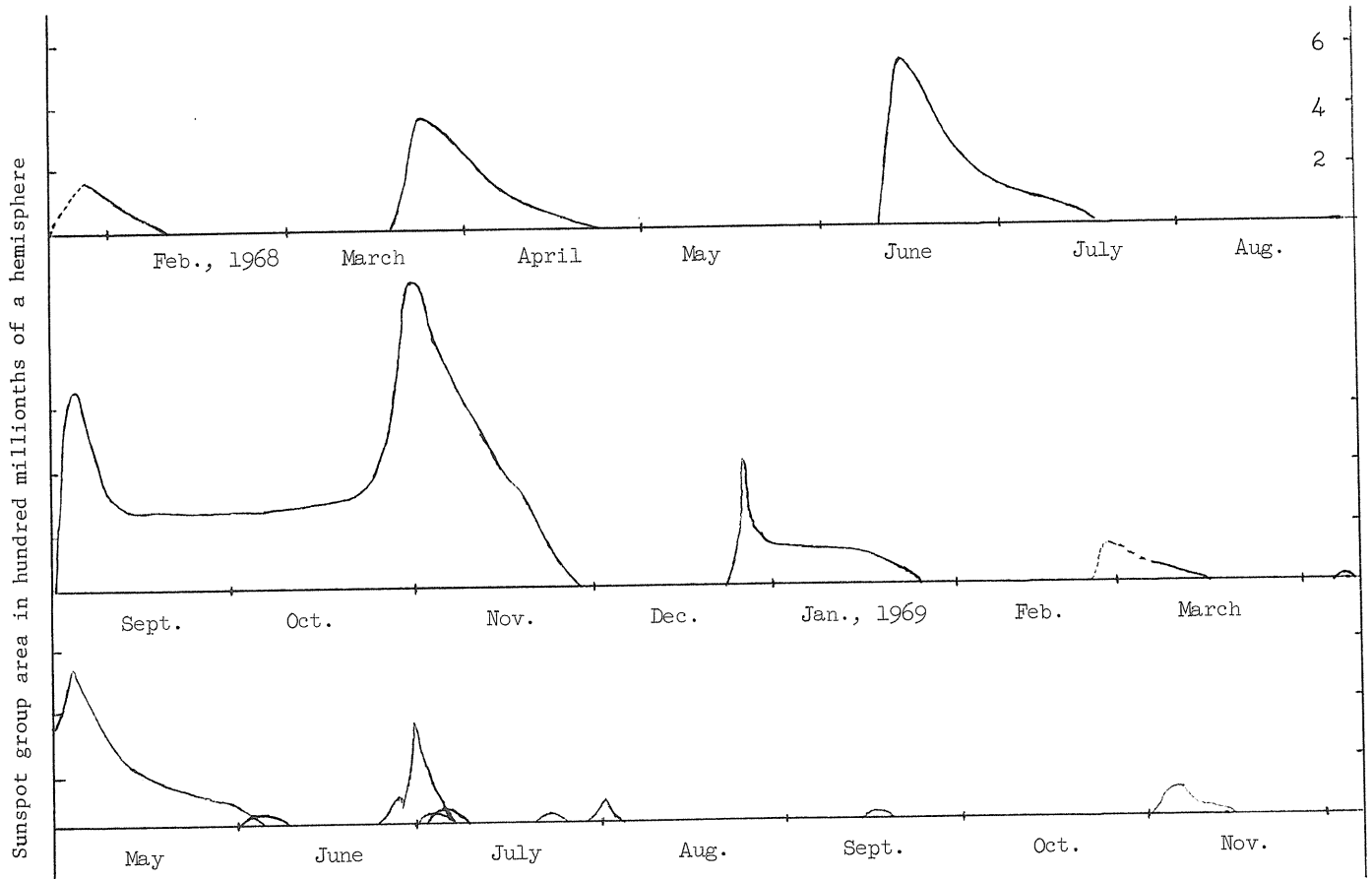


Fig. 1. Approximate sunspot area within a region bounded by S10 to S15 latitude and 167 to 182 degrees Carrington longitude. Extrapolations have been made between west limb passages and returns to east limb.

After the October 1968 disk passage, activity at this location can be traced more-or-less continuously to the present (December 1969). Eight additional new regions have formed since the proton-flare sunspots. Figure 1 depicts all of the observed regions at these solar coordinates by a plot of sunspot group area with time. A quasi-periodic series of sunspot groups is derived, with the first five becoming successively larger in maximum area. A period of 56 days appeared at least five times and a period of 81 days appeared twice. After the large region in October, none of the groups have been as large and the periodicity has not been as marked. Most of the groups have shown more rapid growth than is normally observed in emerging active regions.

The sunspot group which formed in early September was notable for rapid growth to a mature Eac-type\* group of 600 millionths hemispheric area in only 72 hours. The following portion of the region quickly diminished while the leader spot continued to grow in size and field strength, becoming perfectly symmetric during its passage west of central meridian. The form of the group was basically that of a classical bipolar group with little complication.

On the last day before west limb passage new plage formed on the northern side of the leader, establishing a pattern of plage partially encircling a strong spot. This basic pattern was retained for the three subsequent returns of the region.

The second disk passage, beginning on 24 September, consisted of a stable large sunspot (the old leader spot) and a few small attendant spots. More significant was the pattern of plage close to the spot on the north side and an active filament east of and extending south of the spot. This filament disrupted at least three times during the disk passage, followed by major flares each time. The pattern of spots and plage remained virtually the same throughout this disk passage.

The third passage of this region was heralded days before its disk appearance by strong coronal line-emission, loop prominences, and large surges. The region had clearly developed strong magnetic fields and relatively high densities in the corona above the region. The sunspots, when near east limb, consisted once again of the large symmetric leader spot surrounded by smaller spots. Figure 2 depicts the sunspot group from east limb to near central meridian.

The structure of the sunspot group near the time of the proton flares late in the disk passage can be better understood by examining the structure and dynamics of the region throughout the disk passage. The positions of successively emerging new spots and the directions in which these spots move may provide clues for understanding the nature of the optical and radio flares. The magnetic structure of the region can be estimated by combining magnetic polarity measurements from the Crimean Astrophysical Observatory, Sayan Mountain, Kislovodsk, and Rome with the polarities inferred from careful examination of fine structure in  $H\alpha$ . The polarities allow the interpretation of the spot evolution as the successive emergence of possibly six bipolar sets in the near vicinity of the old leader spot remaining from the two previous solar rotations. These sets are numbered in the order of their emergence in Figures 2 and 3. In the southern hemisphere during this solar cycle the leading, or western spots, are normally of north polarity and the follower spots are normally of south polarity. The old returning leader, therefore, was of north polarity.

The sunspots on 22 October presented three significant magnetic areas. The old leader was accompanied by a small decaying bipolar set to the northwest (set #1) and a compact, apparently young, bipolar set to the southwest (set #2). Set #1 had the normal polarity arrangement, but set #2 had reversed polarities, so that the leader of set #2 was the same polarity as the follower of set #1. The leader of set #2 moved westward until the set attained maximum area late on 23 October. This divergence of leader from follower is a normal behavior for simple bipolar sunspot groups.

As the leader of set #2 approached the longitude of the leader of set #1 new spots formed between them to create set #3. The leaders of both set #1 and #2 began to fragment and diminish as the spots of set #3 developed. These spots reached their maximum size late on 24 October and were intermittently seen through the 29th.

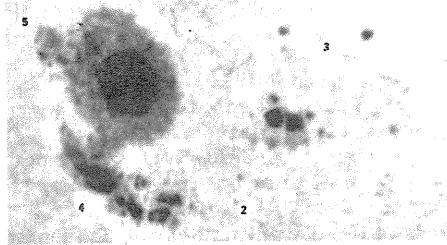
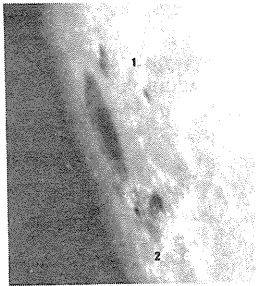
On 24 October new spots formed to the southeast of the old principal spot at the same time that new growth took place in the follower of set #2. The spots near the number 4 at 1636 UT were of south polarity, while the new umbra in the follower of set #2 was north polarity, as the follower had been since its first observation. The south polarity spots quickly grew and coalesced and began a rapid movement to the southwest. By the middle of 25 October penumbra encompassed the umbrae of both polarities, forming a magnetic delta configuration. The rapid growth and movement of the south polarity magnetic field is probably related to significant flares on 23 and 24 October directly over this area.

---

\* This classification is the one now followed by observatories cooperating in the IUWDS interchange of solar data. Devised by the author, it consists of a modified Zurich class, the type of largest penumbra, and the density of sunspots in the interior of the sunspot group.

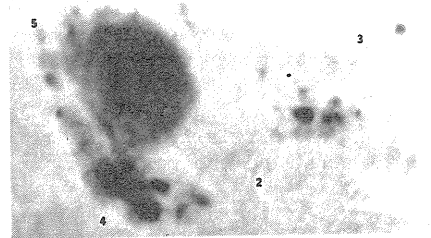
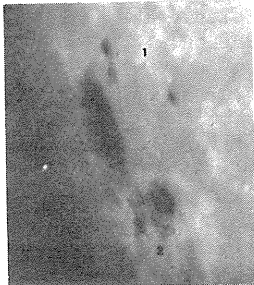
1968

22 OCT  
1456 UT



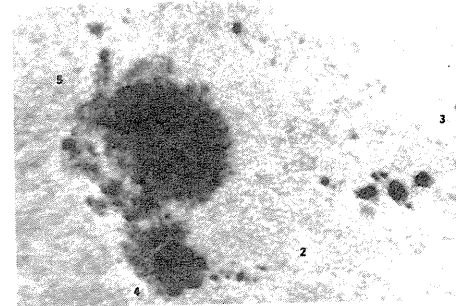
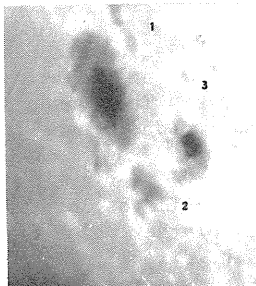
25 OCT  
1502 UT

22 OCT  
2222 UT



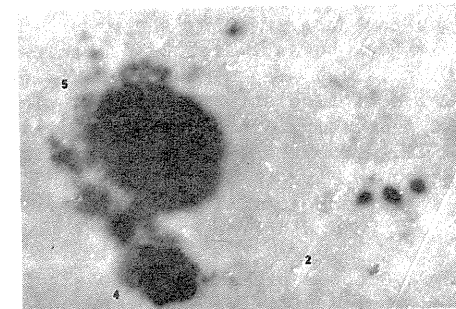
25 OCT  
2330 UT

23 OCT  
1422 UT



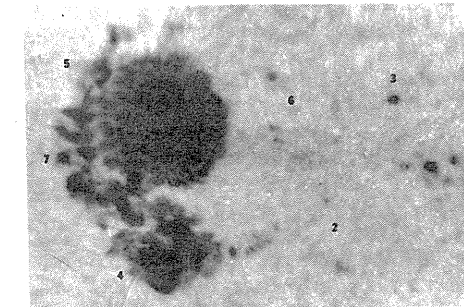
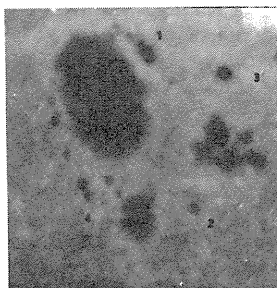
26 OCT  
1510 UT

23 OCT  
2108 UT



26 OCT  
2122 UT

24 OCT  
1636 UT



27 OCT  
1559 UT

10"

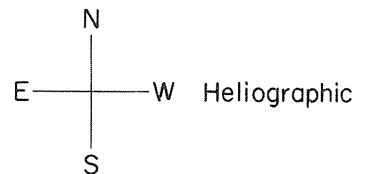


Fig. 2.

The eastern disk passage of sunspots associated with proton flares in October 1968. The numbers indicate bipolar "sets" discussed in the text. Photographs were copies at enlarged scale from small-scale patrol films of the Sacramento Peak Observatory, AFCRL.

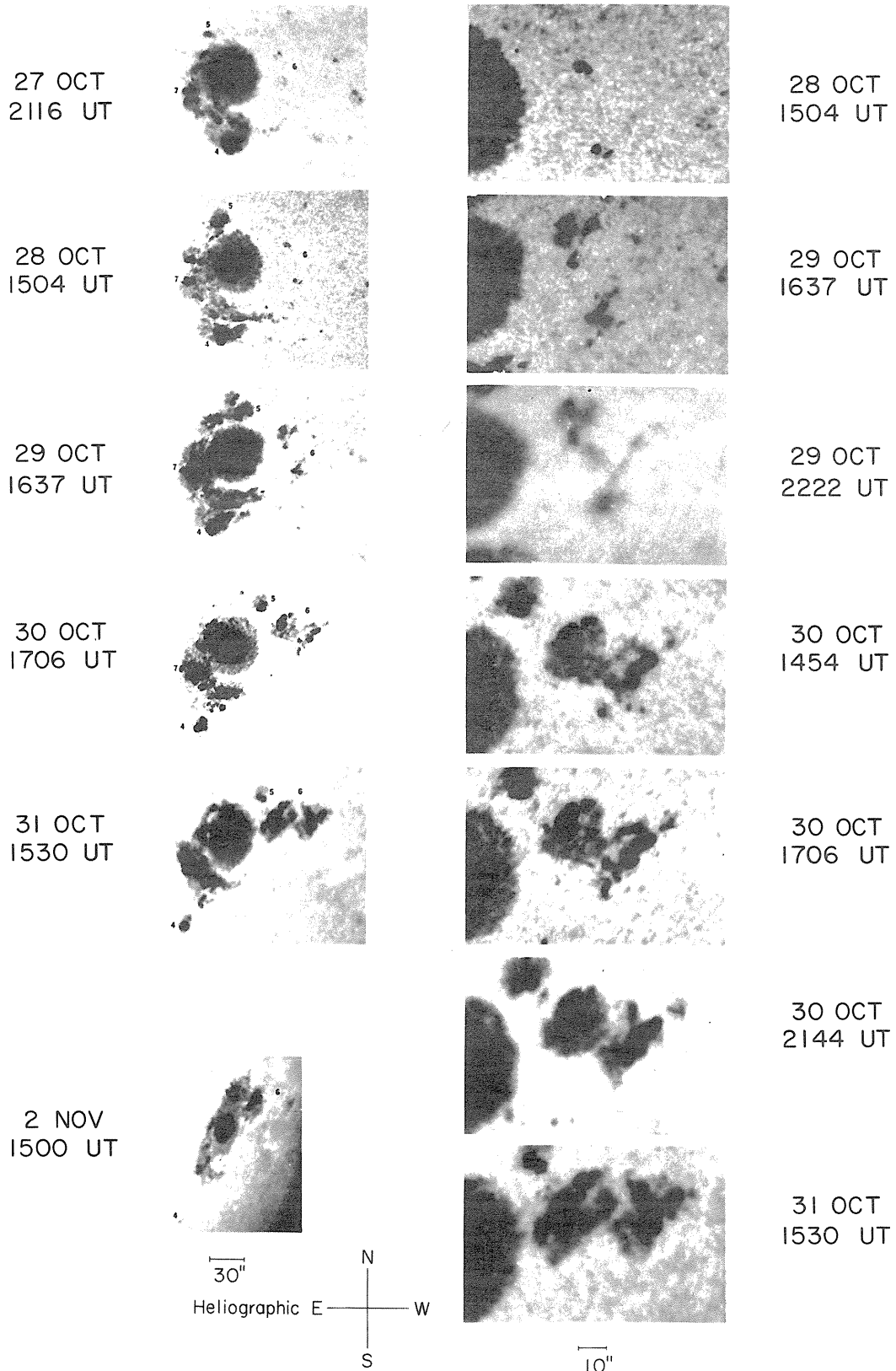


Fig. 3. Left: Daily pictures depict the sunspot group evolution during its very active western disk passage.  
 Right: The rapid development of a bipolar area at the position of the proton flare which began at 2343 UT on 30 October.

The south polarity spot continued to grow and move so that it crowded the north polarity spot at the southern extremity of the region. During the time that the region was west of central meridian the two spots moved slowly together to higher latitude, breaking out of the main mass of penumbra by the middle of 30 October. The pair could be traced until the spots disappeared among bright faculae late on 2 November.

The number 5 refers first to an area of complex growth of penumbra and small spots on the northeast corner of the principal spot, beginning early on 25 October. Spots of both polarity occurred there, but they did not form a clearly defined group. Not until 27 October did strong spots of greater than one-day lifetime form, perhaps in association with the formation of set #6 and spot #7. The principal spot of area 5 developed rapidly and exhibited westward motion relative to the large spot on 28 through 30 October. The approach of #5 spot to the follower spots of set #6 reached a minimum separation close to the time of the proton flare near their position late on 30 October. The path followed by #5 was an arc symmetric about the large spot, with spot #5 moving to higher latitude in its close approach to set #6.

The penumbral filaments surrounding the main spot of the group formed a spiral pattern on the days of best seeing conditions, as if the spot were rotating in the same sense as the motion of spot #5. A rotational velocity of 1 km/sec clockwise was derived for the outer border of the penumbra by assuming an average Evershed gas velocity of 1.5 km/sec and measuring the curvature of the penumbral filaments on 29 October. This spot had a diameter of 38,500 km. so that at the estimated rate of rotation the spot would complete one rotation every 33 hours.

An equally plausible explanation for the curvature of the penumbral filaments would be a curvature in the magnetic field. There often exists conspicuous curvature to the large system of chromospheric fibrils surrounding strong spots when observing in  $H\alpha$ , yet Evershed velocities have not been measured but relatively near to the spots. Since the chromospheric fibrils appear as extensions of penumbral filaments, we might assume that their curvatures have common origins in the shape of the magnetic field. Perhaps the shape of the magnetic field is partially influenced by rotation of active regions, but no clear evidence has yet been assembled.

The velocity of motion for the spot #5 was an order of magnitude slower than the estimated rotational velocity at the penumbral border. Values between 0.12 and 0.20 km/sec were measured on 28 and 29 October.

Spot #7 cannot be paired with other spots to form a bipolar set, but it is significant in that it was of northern polarity in an area dominated by south polarity. Spot #7 did not appear to have any measurable motion, but all of the south polarity spots west of it clearly moved south, then southwest, past this spot. The south-polarity spots continued the pattern of motion first established by the spot labelled #4. This pattern of motion was symmetric about the principal spot, as was the path of spot #5; and, it is important to note that the directions of motion were correlated with polarity. Spot #5 of north polarity moved in a path clockwise around the principal spot. The south-polarity spots near spot #7 moved in paths counterclockwise.

The spots in the southeast portion of the region formed chains that curved around the principal spot and paralleled the longitudinal neutral line in the area. The movement of the south polarity spots was parallel to this line as well. The spots of opposite polarity were closely-spaced, and it may be significant to point out that the character of the penumbra differed between these spots as compared to the typical penumbral structure surrounding symmetric spots. This penumbra was much darker and consisted of elements with larger dimensions. This type of penumbra was noted in proton-flare regions of September 1963, July 1966 and May 1967 [McIntosh; 1968, 1969]. In all cases the peculiar penumbra lay between closely-spaced strong spots of opposite polarity and the orientation of the penumbral filaments paralleled the longitudinal neutral line. It is not yet clear whether such penumbra occurs whenever there are strong gradients in the magnetic field across lines of polarity change or whether this structure is unique to regions which produce proton flares.

Perhaps the most important development in the sunspot group prior to the proton flares late in the disk passage was the formation of set #6. These spots appeared on 27 October, but did not begin their rapid growth until the 29th. On the 28th the negative for 1503:30 UT showed faint photospheric arcs in the granulation extending between the spots of opposite polarity in this set. The arcs were like those observed by Bray and Loughhead [1964] and may represent emerging loops of magnetic field. Late on 29 October new spots formed directly west of the northernmost of the original pair of spots. As these newer spots grew the original spots of northern polarity faded. By early on the 30th penumbra encompassed all the spots in the set. As the time for the proton flare on the 30th approached, the spots of both polarities enlarged and darkened and the penumbra surrounding them also darkened. Spot #5 approaching from the east was closest to set #6 at the time of last picture on the 30th. Note the formation of some very small spots between spot #5 and set #6. At 1706 UT lanes in the photosphere formed extensions of penumbral filaments from the large spot and connected to both the follower of set #6 and these new small spots near spot #5. According to Figure 5 the longitudinal neutral line lay between the small spots and set #6, but consideration of the structuring of the granulation in the vicinity indicates that the new spots were the same

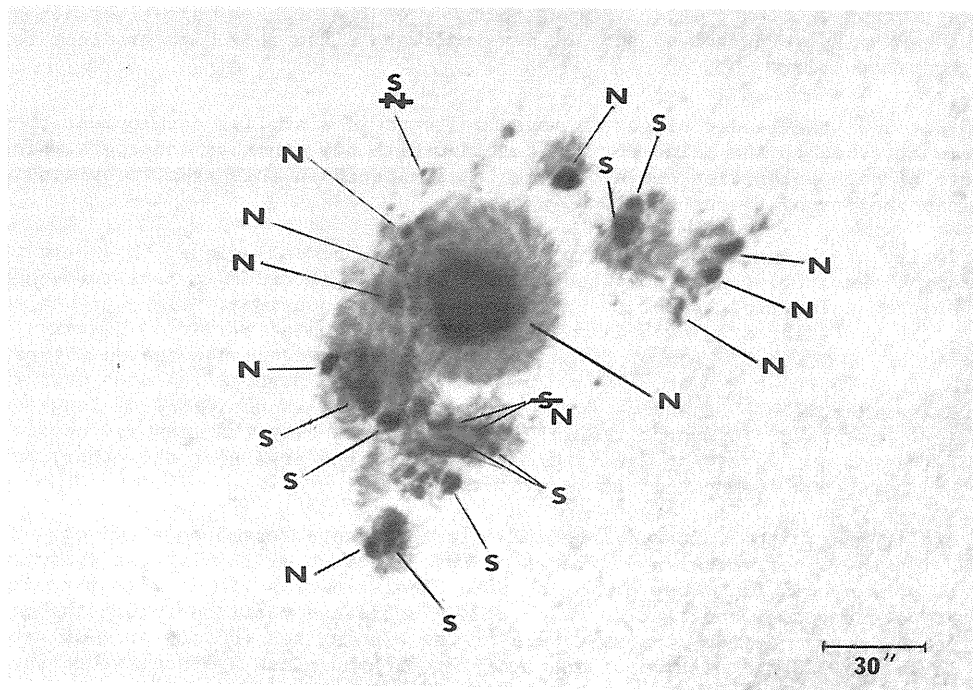


Fig. 4. Magnetic polarities measured at the Crimean Astrophysical Observatory and Sayan Mountain have been combined and placed on a Sacramento Peak photograph for 1706 UT on 30 October. Two polarities are crossed out and replaced with the polarities derived from  $H\alpha$  fine structure. Note the darker penumbra between closely-spaced spots of opposite polarity.

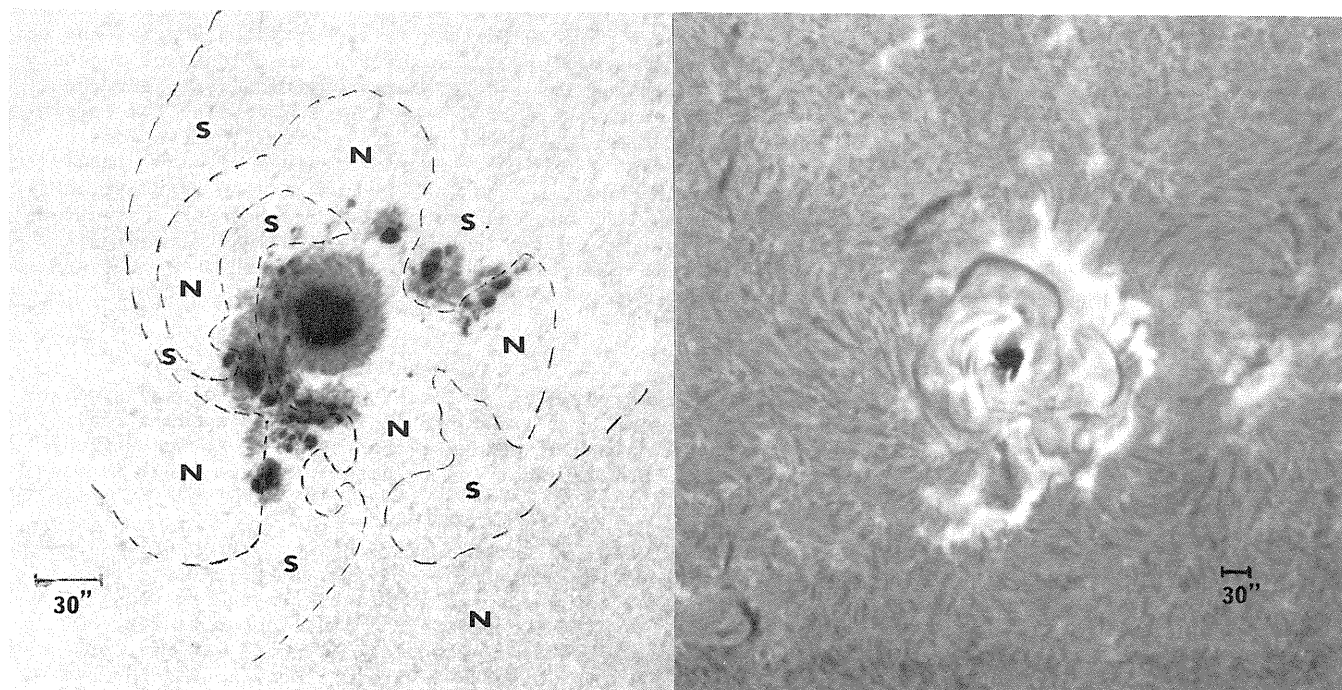


Fig. 5. The wealth of  $H\alpha$  fine structure at right allows the inference of the pattern of magnetic polarities at left.  $H\alpha$  photographs for 29 and 30 October were studied and checked against measured polarities of spots to derive the map. Note the spiral pattern. The spot motions generally paralleled these longitudinal neutral lines.  $H\alpha$  photographed 1542 UT, 29 October by the patrol telescope at ESSA, Boulder, Colorado. White-light photograph was copied from Sacramento Peak Observatory patrol films on 30 October.

polarity as the followers of set #6. If true, then one of the highest magnetic field gradients in the sunspot group lay between spot #5 and the new small spots and this high gradient formed quickly just before the proton flare.

After 30 October, the leader of set #6 moved westward in a similar development to set #2. The follower became attached to the main spot and combined with new penumbra and spots which formed in area #5. Spots of both polarities again became closely-spaced in this area, providing conditions that may explain the strong flares on 2 and 4 November.

The complexity of the magnetic field in this region was almost unique. Magnetic polarities measured at four observatories were combined to make Figure 4 in order to have comprehensive measurements. Even so, the polarities appear to be in error at two locations. Using proven relationships between polarities and filaments, arch-filaments, fibrils and plage corridors [Bruzek, 1967; Martres *et al.*, 1966; Smith, 1968] the region of October 1968 was examined and the map in Figure 5 constructed. It agrees with the polarities in Figure 4 except for two spots. The H $\alpha$  features near these locations were among the least ambiguous in the region for interpretation as positions of longitudinal neutral lines. Therefore, we prefer to accept the inferred polarities over the measured ones. The small size of one of the spots in question, and the complexity of the area near the other, make it highly likely that the measured values should be questionable.

The pattern formed by the inferred lines of polarity change resembles a spiral. This pattern reinforces the impression of rotation derived from the structure of the largest spots and the motions of the smaller spots around it. Most of the pattern consisted of a single highly-convoluted line. The form of the pattern underwent continuous change in shape and position during the complex evolution of the region. For instance, the emergence of the bipolar set #6 consisted of introducing an increasingly large bend in the portion of the line through these new spots. Before the first spots appeared, the line at the location was nearly a straight line in a 90-degree arc around the region.

Finally, the position of the large central spot was examined at the time of its birth in early September, during its second disk passage, and for the three days centered on 30 October. The active region formed in September at Carrington longitude 172 degrees. On the second day of the region's life the leader spot was at 176 degrees and the follower spots appeared at their original longitude. By the fourth day, the sunspot group had reached its maximum area and the leader was at 178 degrees. The leader remained near 178 degrees throughout the next full solar rotation. Late in the second disk passage the spot appeared to begin a slow movement eastward and by 29 October, during its third disk passage, it was located at 172 degrees. On 30 October it was at 171.5 degrees and on 31 October returned to 172 degrees. Without a more careful study of the spot positions, we can only tentatively suggest that the large spot may have reached its most easterly position very near the time of the proton flare of 30 October. This motion may have been important in creating the complex form to the magnetic field. The rate of solar rotation that would be derived from observations of this group on this active disk passage is in agreement with proper motion findings of Ward [1966]. Ward determined from extensive statistical analysis that large sunspot groups have an average longitudinal motion up to 2 per cent less rapid than small groups and groups that are more or less circular in shape move 1.5 to 2.0 per cent less rapidly than groups that have longitudinal dimensions many times larger than their latitudinal extent. The October 1968 region belongs in both categories and might, therefore, be expected to move even more slowly.

### Discussion

It is always dangerous to generalize from a study of a single case, but when a solar active region is carefully observed there emerge some phenomena that are worth at least some speculation. Some of what has been described above could have a major influence on the theory of active region formation and on the formulation of flare models. Some of what can be said from this study is supported by findings from studies of other case histories.

The studies of the July 1966, May 1967 and October 1968 proton-flare sunspot groups all illustrate the value of breaking complex regions into small overlapping bipolar sets [McIntosh, 1968, 1969]. The succession of formation of these sets and their positions relative to the flares give strong suggestions for physical ties between emerging magnetic fields and major solar flares. Since in these three cases the new growth was taking place near much older sunspots, it may be a necessary condition for proton flares that there be interaction between older magnetic fields and the new emerging fields. The older fields should have expanded to greater heights in the corona, but the rate of expansion may differ from one set of fields to another. As the younger set expands it may overtake the older fields and produce complex interaction between the fields. Matter transported upward by the expanding fields might be accelerated and/or dumped back into the chromosphere by the interaction. Furthermore, it could be shown that the orientation of the bipolar flux loops were different between the old and young magnetic field sets. The theorists should examine the implications of crossed field lines as the two loops intermix.

For those interested in forecasting proton flares the results are mixed. It is encouraging that there appear to be conspicuous changes in the magnetic fields prior to the major flares, but

it is important to note the short amount of time between the first appearance of new spots and the flares. Until the spots form and establish a rate of growth and an orientation, it may be impossible to assess their effect on the rest of the active center. On the other hand, the apparent correlation between growth and motions in separated portions of the active center may be a clue that the emergence of new magnetic fields is predictable by the dynamics of the active center. It will be a challenging task to pursue this kind of investigation.

The inference of solar magnetic fields from H $\alpha$  fine structure has become a regular and dependable technique within ESSA's Space Disturbance Forecasting Services. We believe the patterns such as depicted in Figure 5 may reveal important new aspects of active region evolution. They provide a link between the small-scale dynamics observed within active centers and the evolution of solar features with dimensions an order of magnitude larger than the supergranulation.

The spiral pattern in the inferred line of polarity change reinforces the impression of rotation gained from the structure and movements within the spot group. This rotation could be fundamental to the storage of energy emitted in the large flares, as proposed by Stenflo [1969].

Evolution in a large time-scale appears related to the occurrence of specific large flares in that there apparently were quasi-periodic outbreaks of sunspot groups at the same location prior to these flares. This tendency toward regular intervals between outbreaks is a new aspect of the "families" of persistent activity pointed out by Dodson and Hedeman [1968]. One of the "families" mentioned by Dodson and Hedeman was one which persisted at Carrington longitude 160 to 175 degrees in 1965, close to the location of the activity of concern in this paper. Perhaps there might be some longer periods in the occurrence of active regions at a particular heliographic location.

#### Acknowledgements

This study was made possible by the loan of white-light patrol films from the Sacramento Peak Observatory, Air Force Cambridge Research Laboratories. The work of copying these films and preparing the figures was largely by Richard Henke and John Allen. Magnetic polarity data was provided through the services of the World Data Center A, Upper Atmosphere Geophysics, at the ESSA Research Laboratories.

#### REFERENCES

- |   |      |   |
|---|------|---|
| BRAY, R. J. and<br>R. E. LOUGHHEAD                    | 1964 | <u>Sunspots</u> , John Wiley and Sons, plate 3.4.   |
| BRUZEK, A.  | 1967 | "On Arch-Filament Systems in Spotgroups", <u>Solar Phys.</u> , <u>2</u> , 451-461.  |
| DODSON, H. W. and<br>E. RUTH HEDEMAN                  | 1968 | "Some Patterns in the Development of Centers of Solar Activity, 1962-66", <u>I.A.U. Symposium No. 35</u> , ed. by Kiepenheuer, D. Reidel Company, Dordrecht, Holland, 56-63.  |
| GOPASYUK, S. I. and<br>G. E. MORETON                  | 1967 | "Motions of Magnetic Fields and Umbrae Within a Spot Group", <u>Proc. Astron. Soc. of Australia</u> , <u>1</u> , 8.   |
| MARTRES, M. J.,<br>R. MICHARD and<br>I. SORU-ISCOVICI | 1966 | "Morphological Study of the Magnetic Structure of Active Regions in Relation to Chromospheric Phenomena and Solar Flares, II. Location of Bright Plages, Filaments and Flares", <u>Ann. d'Astrophys.</u> , <u>29</u> , 249-253. |
| MC INTOSH, P. S.                                      | 1968 | "Birth and Development of the Sunspot Group Associated with the Proton Flare of July 1966", <u>Annals of the IQSY</u> , <u>3</u> , 10-13.   |
| MC INTOSH, P. S.                                      | 1969 | "Sunspots Associated with the Proton Flare of 23 May 1967", <u>Upper Atmosphere Geophysics Report UAG-5</u> , 14-19.  |
| SAKURAI, K.   | 1967 | "Solar Cosmic-ray Flares and Related Sunspot Magnetic Fields", <u>Report of Ionosphere and Space Research in Japan</u> , <u>21</u> , 113-124.   |
| SMITH, S. F.  | 1968 | "The Formation, Structure and Changes in Filaments in Active Regions", <u>I.A.U. Symposium No. 35</u> , D. Reidel Publishing Co., Dordrecht, Holland, 267-279.  |
| STENFLO, J. O.  | 1969 | "A Mechanism for the Build-up of Flare Energy", <u>Solar Phys.</u> , <u>8</u> , 115-118.  |
| WARD, F.  | 1966 | "Determination of the Solar-Rotation Rate from the Motion of Identifiable Features", <u>Astrophys. J.</u> , <u>145</u> , 416-425.   |

### 3. OUTSTANDING SOLAR FLARES

"Eruptive Flare of October 24, 1968"

by

H. Zirin

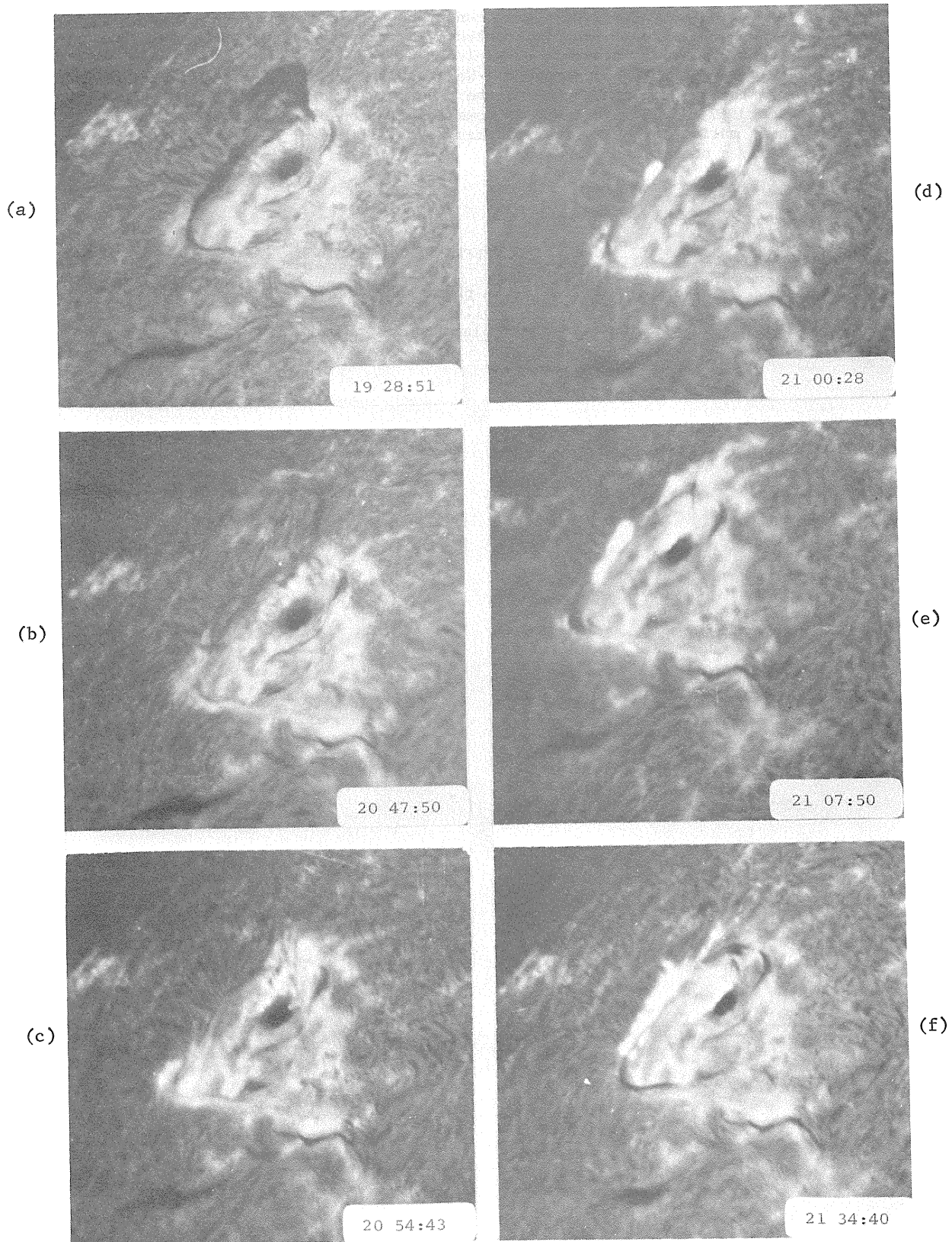
The Hale Observatories  
Carnegie Institution of Washington  
California Institute of Technology  
Pasadena, California

One of the first large events associated with the limb passage of McMath 9740 was a beautiful eruptive flare on 24 October, 1968. We observed this flare simultaneously with the five-inch Caltech Photoheliograph in the center of H $\alpha$  and the large equatorial telescope "Ishak" using a ten-inch objective lens on the blue wing of H $\alpha$ . Mr. Ernest Lorenz assisted in the observations. These simultaneous observations provide a unique picture of an eruptive flare.

Figures 1 and 2 present frames printed to more or less the same scale from the observations with both telescopes. For various reasons, slightly different times are printed. This spot group was a classic example of inverted polarity. The main spot of preceding polarity was almost completely surrounded by bright plage of following polarity. A large prominence overlay the region, and about 1700 UT began to slowly rise. An advanced stage in this development is seen in the first frames of Figures 1 and 2. By 2000 UT, the prominence had broken into very high strands, which were still slowly expanding. At 2035 UT, a more rapid upward motion began, followed by the eruption of the prominence at 2046 UT. The first ionospheric effects appeared at about 2037 UT. The actual eruption of the prominence took place from the southern end, below the spot on our photographs. However, at 2050 UT, there was an extraordinary and rapid outflow from the area at the north end, close to the large spot, and the prominences blew off. The "Ishak" off-band observations have very high resolution (at least 2 seconds of arc) and show extremely violent horizontal motion along the base of the region where the prominence had been, followed by a rapid downward motion near the sunspot at 2058 UT. This rapid downward motion resulted in a very bright region directly above the spot which is easily seen in Figure 1(d) and 2(e). The flow is very turbulent but clearly downward. With the downward flow, this region rapidly reached flare brightness. At the same time, two bright strands of flare emission developed; one along the outer perimeter of the plage, roughly underlying the position previously occupied by the filament; and one along the following edge of the sunspot. As time went on, these two regions became the principal areas of brightness.

Unfortunately, we do not have detailed records of non-optical phenomena associated with this flare. Furthermore, both the hard X-ray detectors on OGO and OSO were not observing in this period. So, our conclusions must be based on data culled from "Solar-Geophysical Data". The flare is of great interest for the study of non-optical phenomena in that we are interested in knowing if the X-ray and other emission is more closely associated with the prominence eruption, which began long before the flare, or with the actual surface brightening which composed the optical flare. VHF stations around 10 MHz, as recorded at Boulder, show a small event at 2040 UT, corresponding to the explosion, and a main event at 2058 UT, corresponding to the H $\alpha$  brightening. One VLF station (Omega, New York), recorded at Boulder, shows a sharp drop at 13.6 kHz at 2038 UT, lasting without interruption to 2110 UT. I am not sufficiently familiar with the X-ray origins of these events to tell which best represents the hard X-ray flux. NRL reports a soft X-ray event beginning 2115 UT and ending 2125 UT, clearly associated with the bright main phase of the flare. The University of Iowa reported a similar event measured with Explorers 33 and 35; however, their event began at 2054 UT with peak at 2124 UT. It is clear that the soft X-rays are more closely associated with the main, bright phase of the flare than with the eruption of the filament. The well-known association between H $\alpha$  brightness and X-ray flux is thus preserved, at least for soft X-rays. However, the evidence from the ionospheric data is that there was a hard X-ray pulse associated with the abrupt eruption of the prominence. All of the observed radio events peaked after 2100 UT, again in association with the development of the bright flare maximum. Only one record, the 2800 MHz emission, began as early as the impulsive eruption with which the flare began.





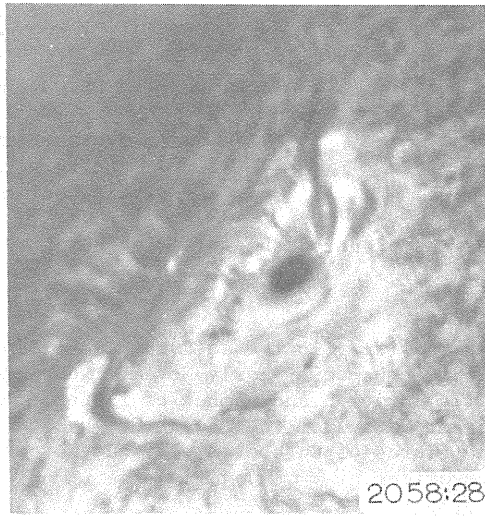
CALTECH PHOTOHELIOGRAPH  
Fig. 1 Observations at California Institute of Technology

24 OCTOBER 1968

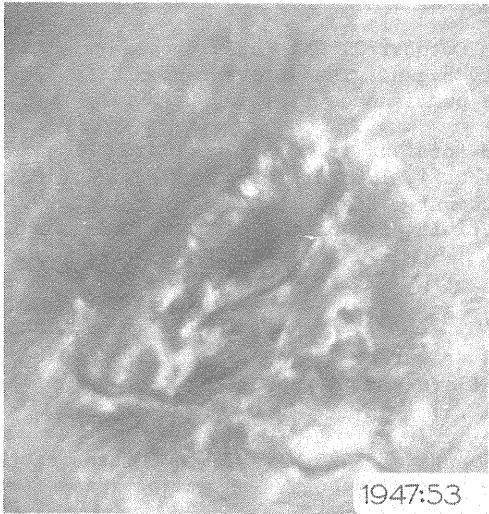
(a)



(d)



(b)



(e)



(c)



(f)



# ISHAK I

Fig. 2 Observations at California Institute of Technology

"Study of the Flares in the Active Region of the Proton Events of  
1968 October 29 - Early November During its Transit October 21 - November 4"

by

G. Godoli, O. Morgante and M. L. Sturiale

Osservatorio Astrofisico di Catania  
Universita di Catania  
Consiglio Nazionale delle Ricerche

[The compiler has prepared the following paragraphs from the outline submitted by G. Godoli.]

Introduction

The flare activity in the active region (S15 and Carrington longitude  $L = 171$ ) of the proton events of 1968 October 29 - early November during the transit October 21 - November 4 has been studied. The daily duration and number of flares of different importance classes have been studied taking into account data from the "Solar-Geophysical Data" IER-FB-296 and 297. The morphology and evolution of the flares of October 27, 29 and November 1 and 2 have been studied taking into account Catania observations.

General remarks on the flare activity during the transit October 21 - November 4

The active region appeared at the east limb on October 21 with only faculae visible. On October 22 the spot appeared and also the flare activity began. The active region disappeared at the west limb on November 4 with only flares and active prominences visible, both with base  $>90^\circ$ .

The total daily duration of flare activity and total daily number of flares of different importance classes during the transit October 21 - November 4, 1968 are given in Fig. 1. Only average values for confirmed flares have been taken into account. Fig. 1 shows that on October 29 the flare activity lasted about 11 hours. Such high flare activity for proton flare regions has been already pointed out by Bruzek [1969].

Flares of October 27

On October 27 two 2b flares have been observed at Catania. The first flare S18 E17 begins at 1238 UT and ends at 1315 UT. Four pictures of the flare are given in the first row of Fig. 2. The flare partially covers the major sunspot umbra.

The second flare S18 E18 begins at 1400 UT and ends at 1425 UT. Four pictures of the flare are given in the second row of Fig. 2. Also this flare partially covers the major sunspot umbra.

Flare of October 29

On October 29 one 2b flare S16 W14 has been observed at Catania. The flare begins at 1115 UT and ends at 1445 UT. This last value is uncertain because the region has been active all day. Pictures showing the most important stages of this flare are given in the last three rows of Fig. 2. This flare has several eruptive centers and partially covers the major sunspot umbra.

Fig. 3 shows the evolution curve of the flare. Projected area is given in  $10^{-4}$  of the solar disk. The flare maximum area is about 30% of the faculae area. The hill on the ascending branch of the evolution curve of Fig. 3 is due to a secondary maximum of the flare.

Flare of November 1

On November 1 one 2b flare S18 W48 has been observed at Catania. The flare begins at 0845 UT and ends at 1045 UT. Pictures showing the most important stages of this flare are given in the first three rows of Fig. 4. The flare partially covers the major sunspot umbra. We notice that this flare is also visible in the Catania  $K_{232}$  spectroheliogram taken at 0910 UT.

Fig. 3 also shows the evolution curve of this flare.

Flare of November 2

On November 2 one 2b flare S13 W67 has been observed at Catania. The flare begins at 1000 UT and ends at 1045 UT. Pictures showing the most important stages of this flare are given in the last two rows of Fig. 4. The flare has several eruptive centers and partially covers the major sunspot umbra.

Fig. 3 also shows the evolution curve of this flare.

REFERENCES

BRUZEK, A.

1969

Flares in the Active Region during the Proton Flare Period of July 1966, *Annals of IQSY*, 3, 82-91.

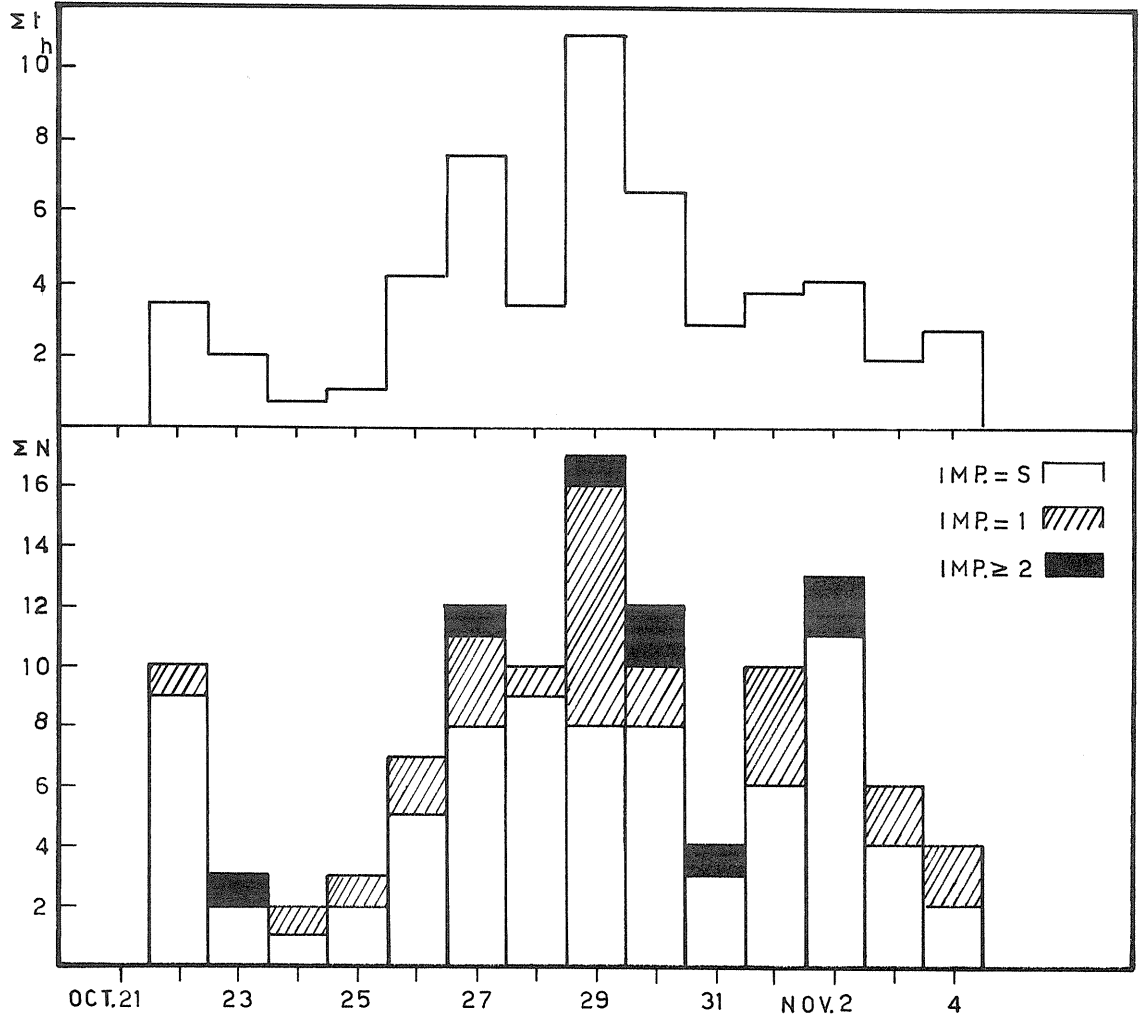


Fig. 1. (above) Total daily duration of flare activity for the transit October 21 - November 4, 1968.  
 (below) Total daily number of flares of different importance classes during the transit October 21 - November 4, 1968.

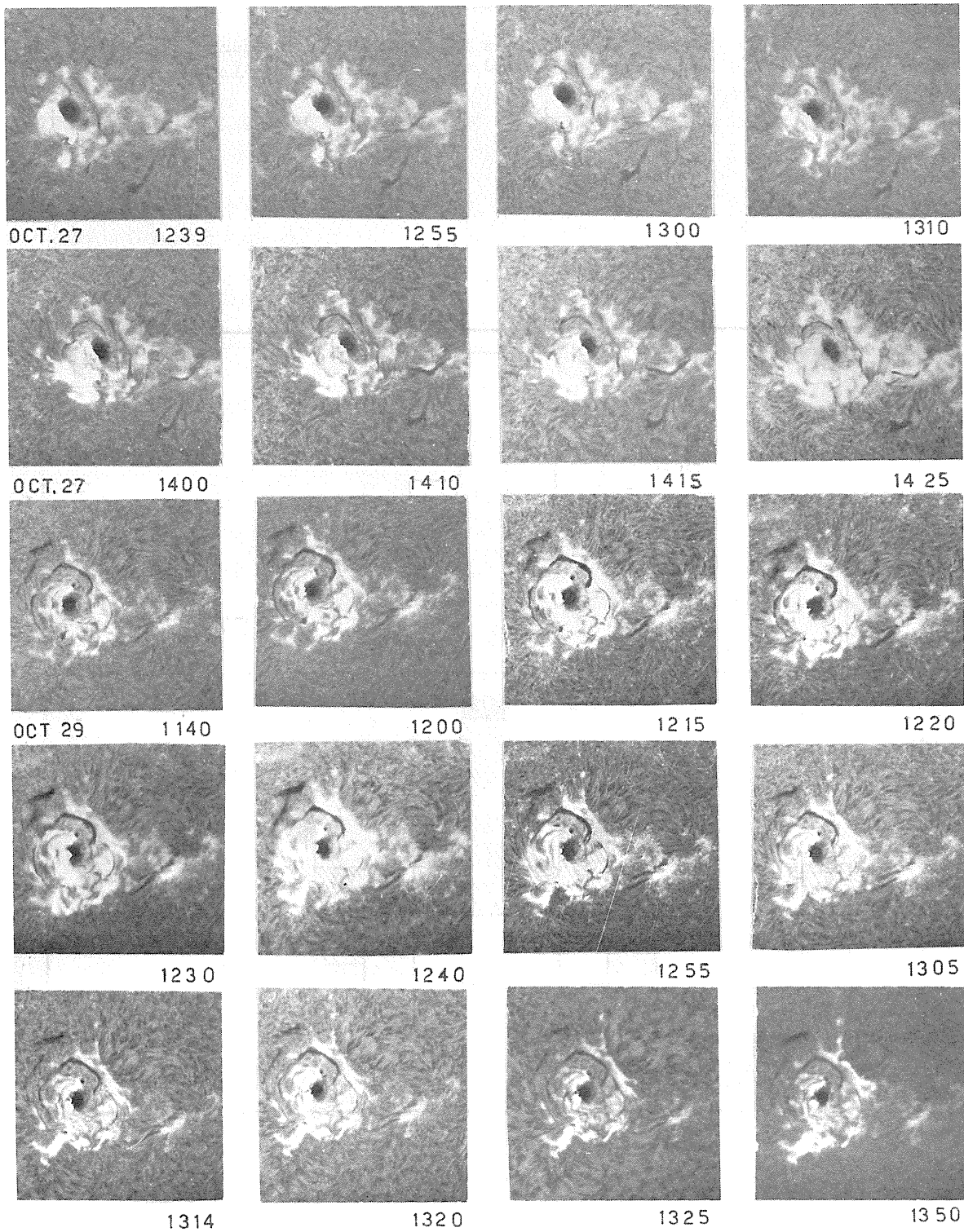


Fig. 2. Flares of October 27 and 29, 1968.

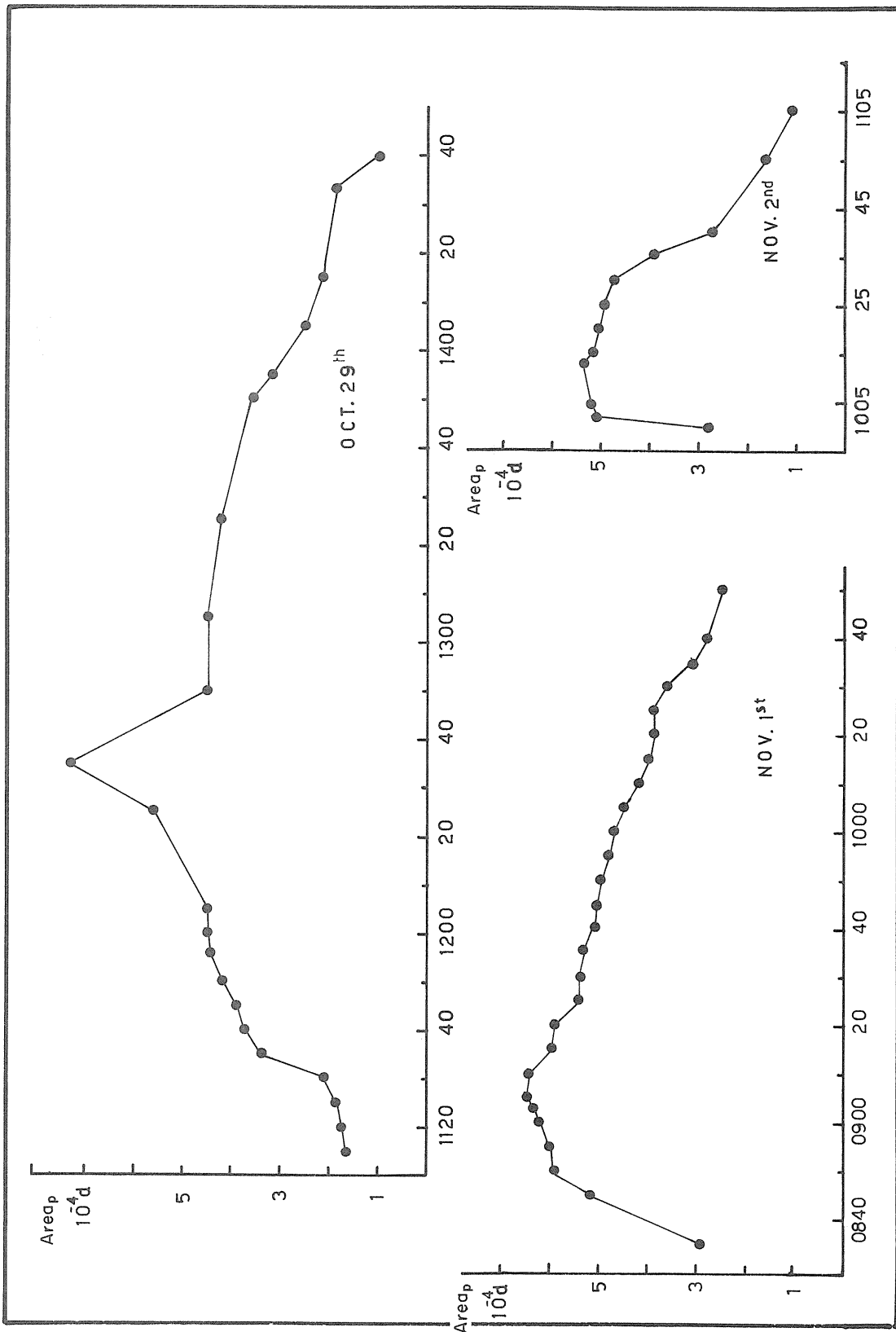


Fig. 3. Projected areas in  $10^{-4}$  of the solar disk (d) for the 2b flares observed at Catania on October 29, November 1, November 2, 1968.

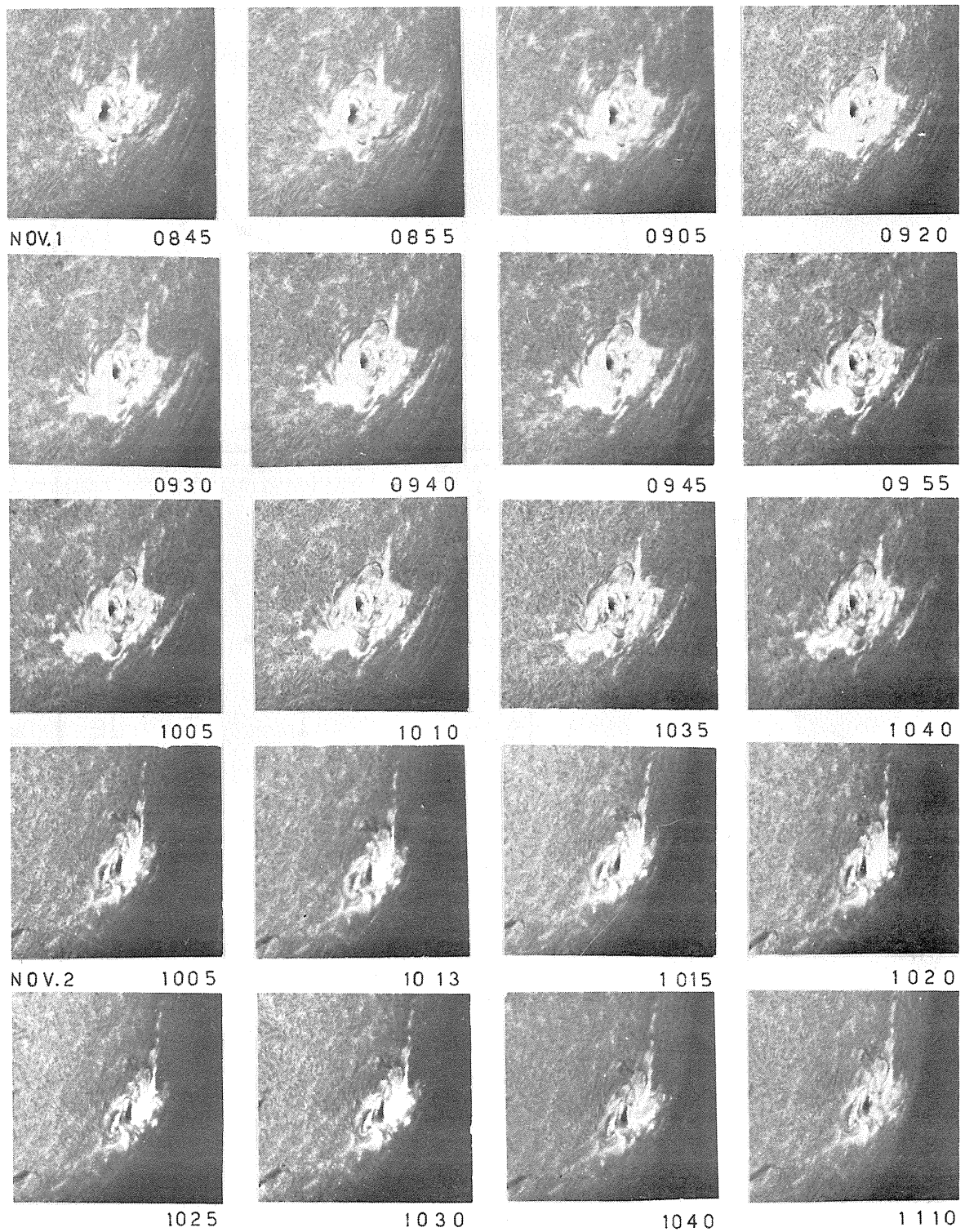
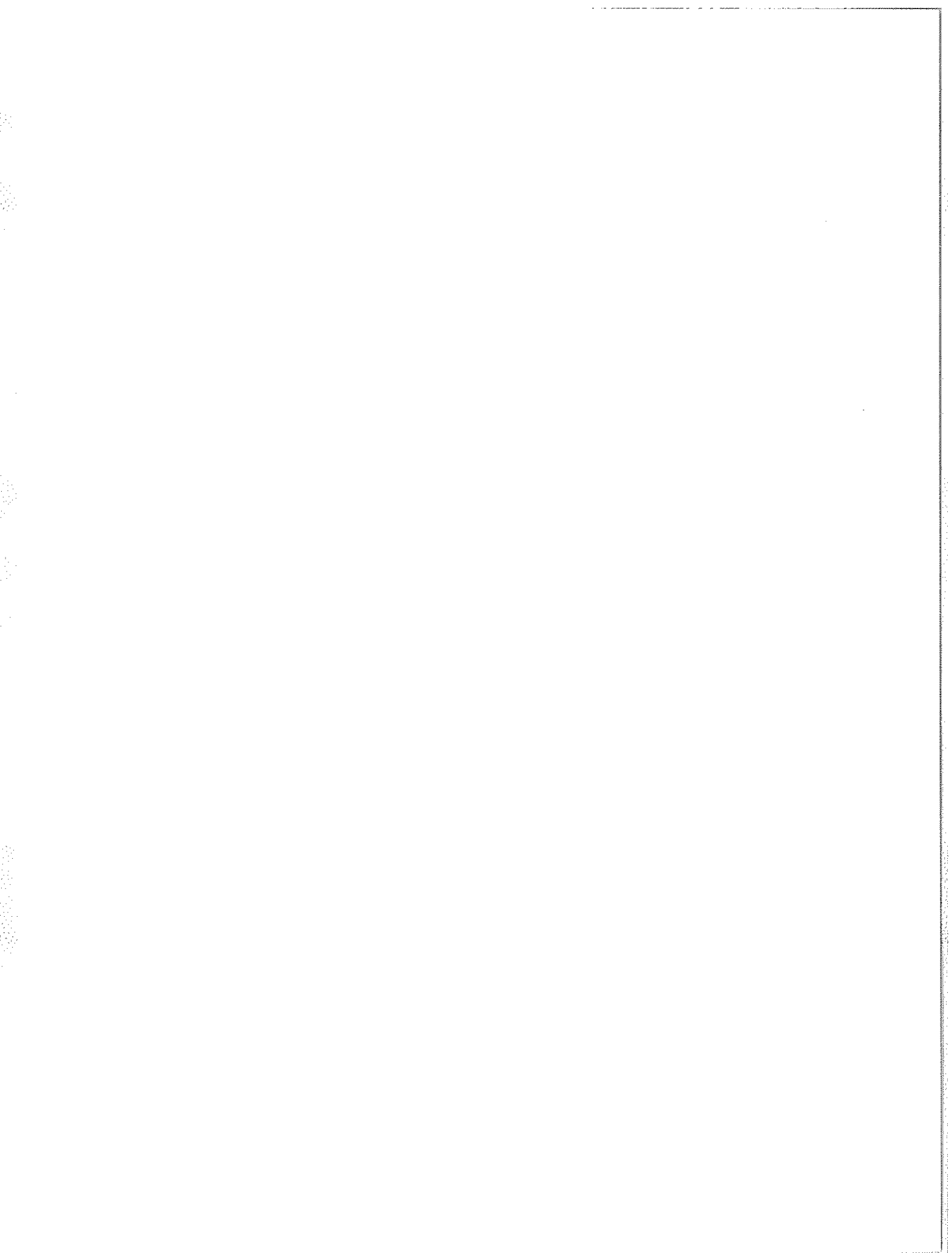


Fig. 4. Flares of November 1 and 2, 1968.



"Six Large Solar Events Recorded by the NASA Solar Particle Alert Network from  
October 27 to November 4, 1968"

by

P. E. Lafferty, J. W. Snyder, and J. H. Reid  
Astronomy Branch, Manned Spacecraft Center  
Houston, Texas

Introduction

The Solar Particle Alert Network (SPAN) is described elsewhere [Robbins and Reid, 1969]. During the period under consideration the three radio and five of the seven optical stations were in operation. The coverage of the sun by the SPAN system is given in Table 1 for the period October 16 to November 4, 1968.

Table 1

Observing periods at the different frequencies of SPAN

Frequency	Total observing time	Percent of possible time
H $\alpha$	434 hours	90.4%
1420 MHz	454 hours	94.6
2695 MHz	478 hours	99.6
4995 MHz	475 hours	99.0

During this period the sun's activity was dominated by two major regions. The first (McMath Region 9735) came around the east limb on October 16 at latitude N13, crossed the central meridian on October 23 and disappeared over the west limb on October 29. The second group (McMath Region 9740) came around the east limb on October 21 at latitude S16, crossed the central meridian on October 28 and passed over the west limb on November 4. The optical telescopes detected 197 flares during the period of which 71 were associated with Region 9735 and 69 associated with Region 9740. The remainder were produced by other groups.

Radio emission was associated with 33 flares in Region 9735 and 40 of the flares in Region 9740. A breakdown of the flare activity and radio bursts is given in Table 2.

Table 2

Distribution of flares (H $\alpha$ ) and radio emissions (R.E.) according to flare importance

Region	Event Type	Flare Importance				Total Events
		S	1	2	3	
Region 9735	H $\alpha$	39	29	3	-	71
	R.E.	16	14	3	-	33
Region 9740	H $\alpha$	31	26	11	1	69
	R.E.	10	19	10	1	40

Region 9740 was responsible for more major flares than Region 9735 and it also produced more radio emission. A detailed study of these two regions is in progress and in this paper are merely shown data on some of the large events recorded by the network between October 27 and November 4.

Treatment of the Radio Burst Data

The gains of the SPAN radio telescope antennas are not precisely known. Consequently, the flux levels for bursts presented here were determined by comparisons between SPAN burst data and that of another observatory (Sagamore Hill). The largest correction necessary was 20 percent.

The computer program used to plot the burst profiles presented was incapable of resolving more than 900 points along the vertical or horizontal axes. Since SPAN radio flux data was sampled once per second, it was necessary to average the flux data to accommodate the plot program. Therefore, very rapid changes of flux are masked somewhat due to averaging.

Descriptive Notes on the Events

Table 3 summarizes data describing seven flares occurring in Region 9740 during the study period. The date, Universal times of beginning, maximum and end, importance classification, heliographic coordinates, measured and corrected areas in square degrees are given.

Table 3

Flare Data Summary									
Event	Date Mo./Da.	Observed UT			Imp.	Mer.		Meas. Area Sq. Deg.	Corr. Area Sq. Deg.
		Start	Max	End		Lat.	Dist.		
1A	10/27	U1249	1251	1306	SN	S17	E15	1.0	1.1
1B	10/27	1318	1321	U1330	2N	S18	E17	4.6	5.5
2	10/30	2350	2404	2440	3B	S15	W36	12.8	16.6
3	10/31	2235	U2251	2320	2B	S13	W50	4.2	7.1
4	11/1	0835	0842	0930	2N	S15	W45	7.2	10.8
5	11/2	0957	1007	1025	2B	S18	W65	4.6	10.1
6	11/4	0524	0529	0606	1B	S14	W90	1.2	4.8

Figures 1a and 1b show the radio burst profiles and selected H $\alpha$  photographs for events 1A and 1B. The early burst is associated with flare 1A and the later one with 1B.

Figures 2a and 2b show the radio profiles and H $\alpha$  photographs for the large event of October 30 (Event 2). Event 3 is shown in Figures 3a and 3b.

The flare of November 1 (Event 4) had a double maximum. After some fluctuations beginning about 0816, the flare got under way at 0835, and reached a peak at 0842. It later increased in brightness to a second maximum at 0903. Radio burst profiles and selected H $\alpha$  photographs for Event 4 appear in Figure 4a and 4b.

The bright flare of November 2 (Event 5) was accompanied by highly complex bursts at the three radio frequencies (see Figures 5a and 5b). The 2695 MHz and 4995 MHz bursts were recorded by both Carnarvon and the Canary Islands. With the exception of some low level variations due to sunset multipath effects at Carnarvon, the burst profiles were identical. The Canary Islands 1420 MHz receiver was not operating at the time of the event. Therefore, in Figure 5a we have presented the Carnarvon burst profile at that frequency. Comparisons of the bursts at the other two frequencies suggested that the large variations in the 1420 MHz Carnarvon bursts were real rather than attributable to multipath effects. Note, in Figure 5a that the 1420 MHz data were not seriously degraded by sunset until about 1026.

The radio burst of Event 6 appeared to be associated with a limb flare (see Figures 6a and 6b). It is interesting that the radio emission was detected before the optical flare became visible. This suggests that the main flare occurred behind the limb and the optical observations were only of a higher part of the flare. Typical post flare loops are shown in Figure 6b.

One of the largest radio events recorded by the SPAN system occurred on October 29, 1968. It is not included here as it has been the subject of a separate paper [Mennella and Reid] which is reproduced with copyright permission on pages 150 to 153 of this Report.

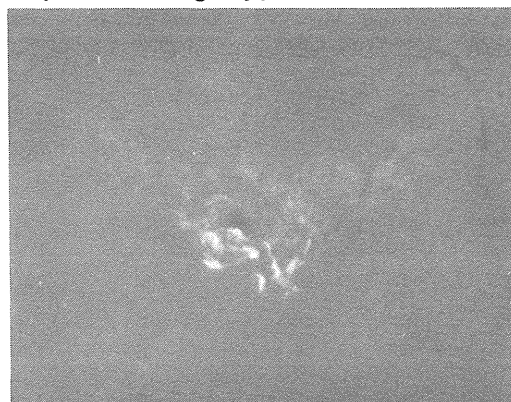
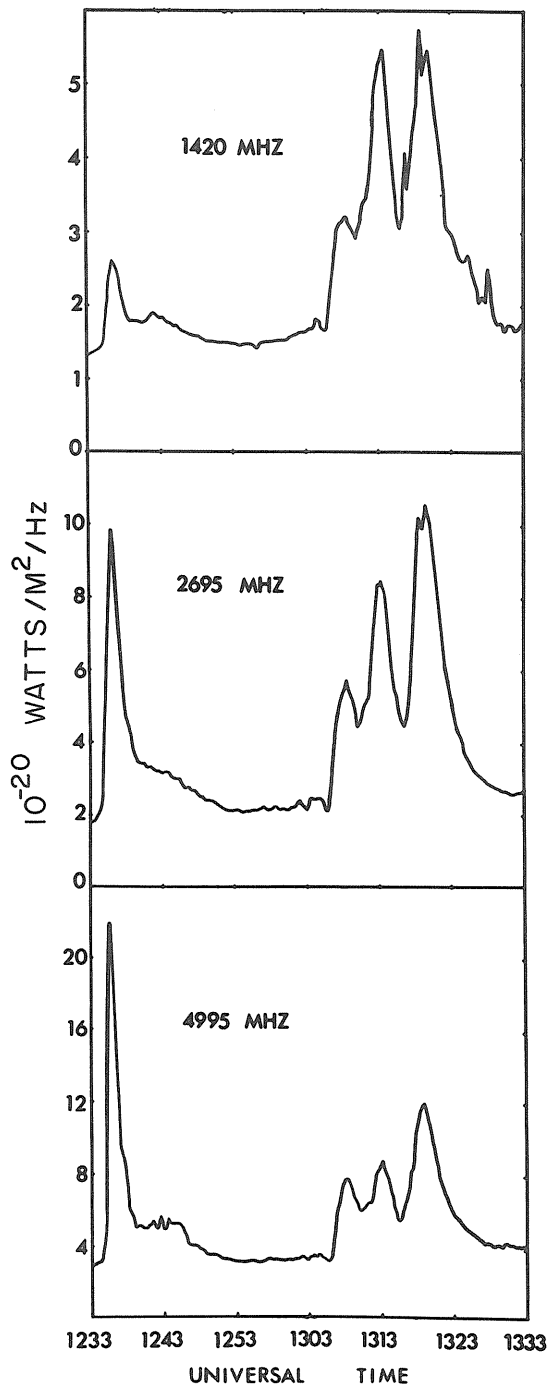
#### REFERENCES

- |                                   |      |  |
|-----------------------------------|------|--|
| MENNELLA, R. A. and<br>J. H. REID | 1969 | Unusual 1 to 5 GHz Solar Radio Emission of 29 October 1968, <u>Astrophysical Letters</u> , <u>3</u> , 129. |
| ROBBINS, D. E. and<br>J. H. REID  | 1969 | Solar Physics at the NASA Manned Spacecraft Center, <u>Solar Physics</u> , <u>10</u> , 502-510.            |

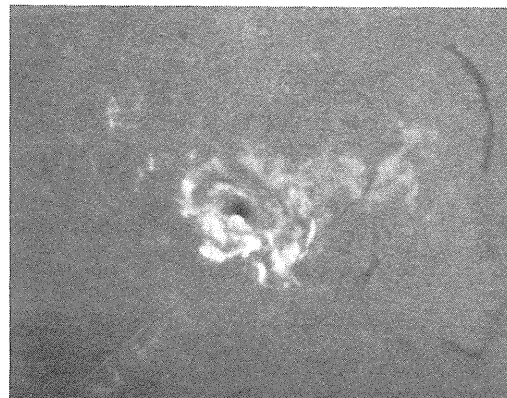
27 OCTOBER 1968

NASA-SPAN-CYI

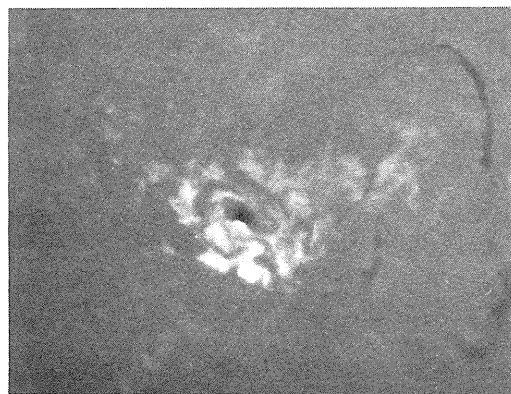
← 5x10<sup>5</sup> km →



1315



1319



1325

Fig. 1a. Solar radio burst recorded on October 27, 1968 by NASA Canary Islands Observatory.

Fig. 1b. Selected H $\alpha$  photographs of class 2N flare at S18 E17 on October 27, 1968, photographed by NASA Canary Islands Observatory.

30 OCTOBER 1968

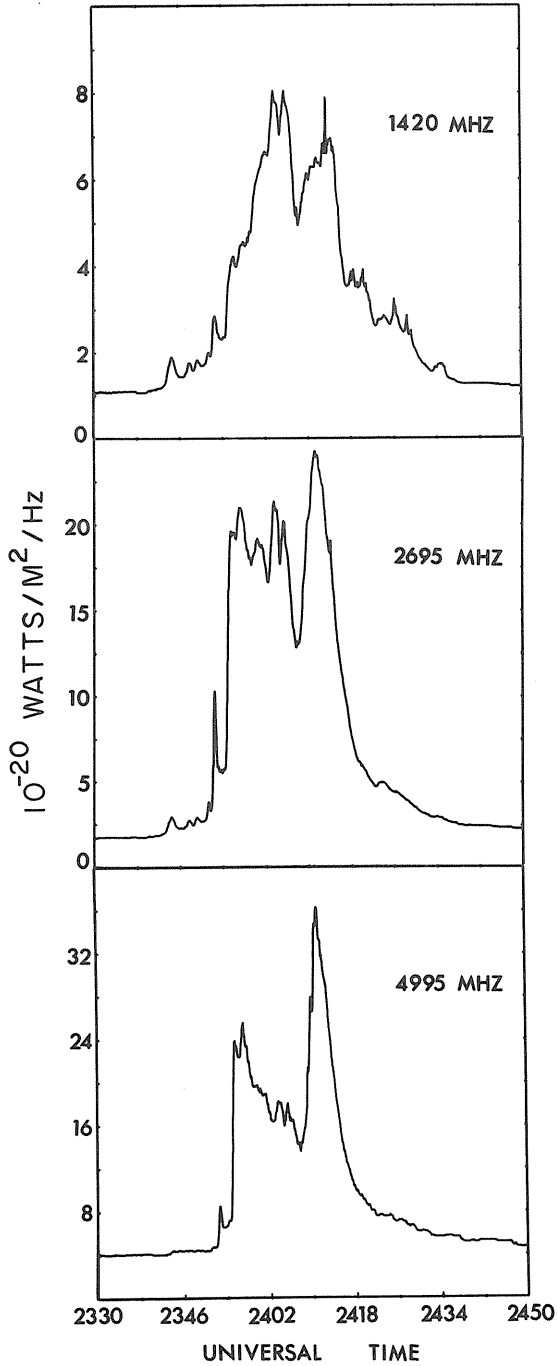


Fig. 2a. Solar radio burst recorded on October 30, 1968 by NASA Observatory at Carnarvon, Australia.

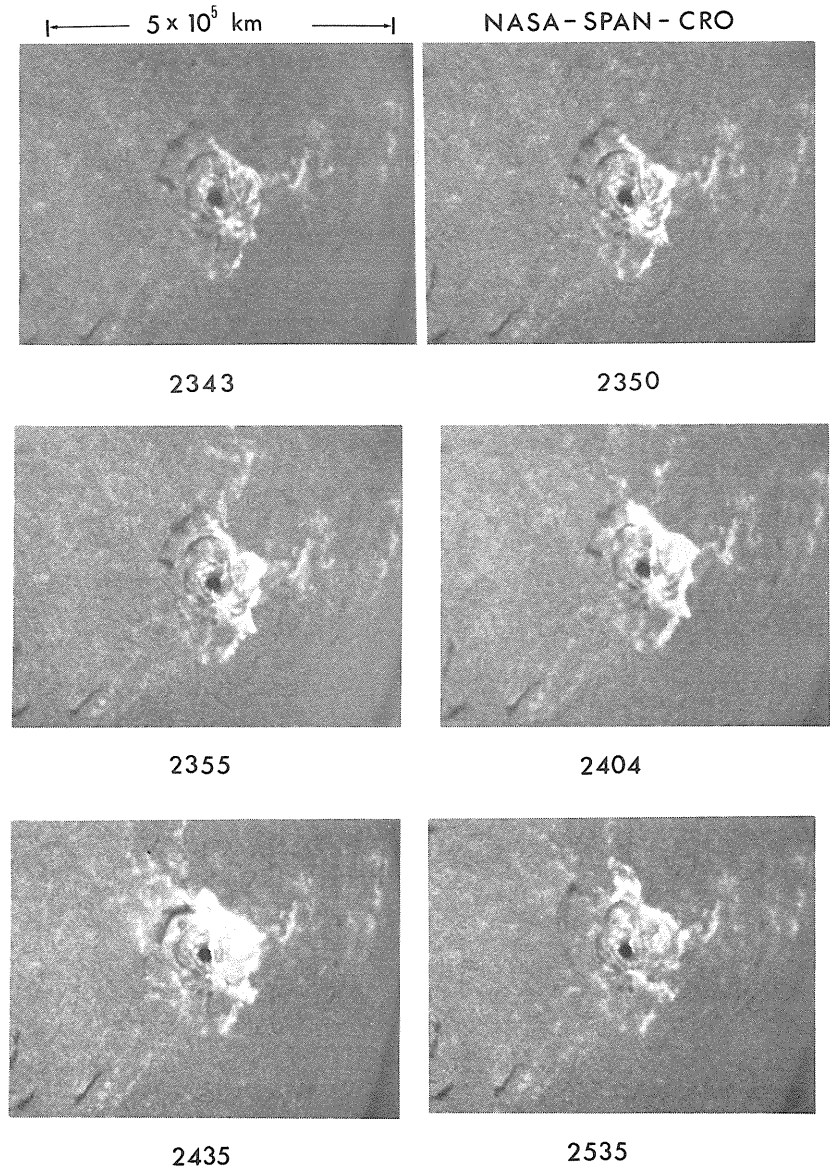
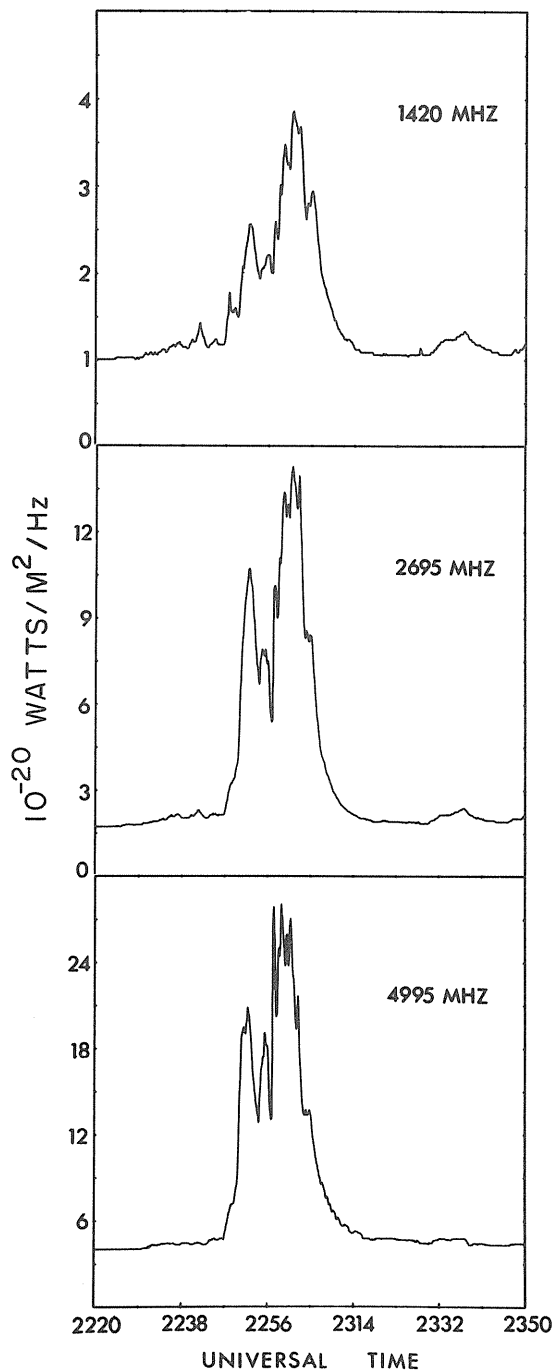


Fig. 2b. Selected H $\alpha$  photographs showing development of class 3B flare at S15 W36 on October 30, 1968, photographed by NASA Observatory at Carnarvon, Australia.

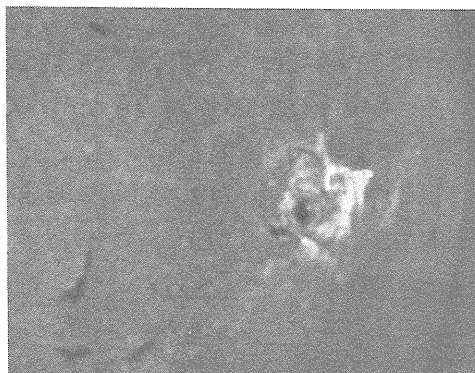
31 OCTOBER 1968

NASA-SPAN - CRO

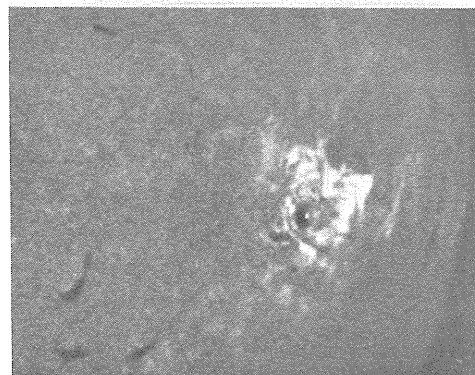
← 5x10<sup>5</sup> km →



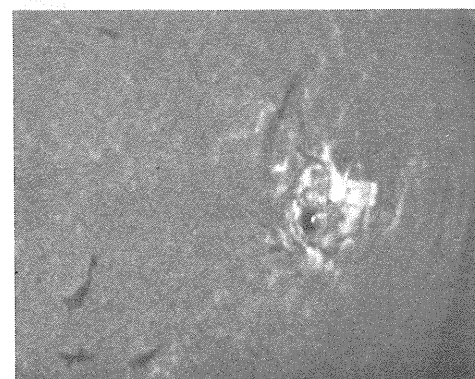
2246



2251



2320



2412

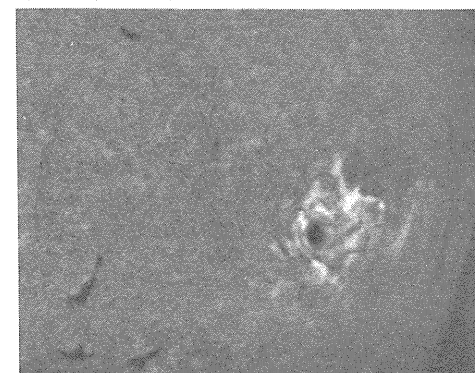


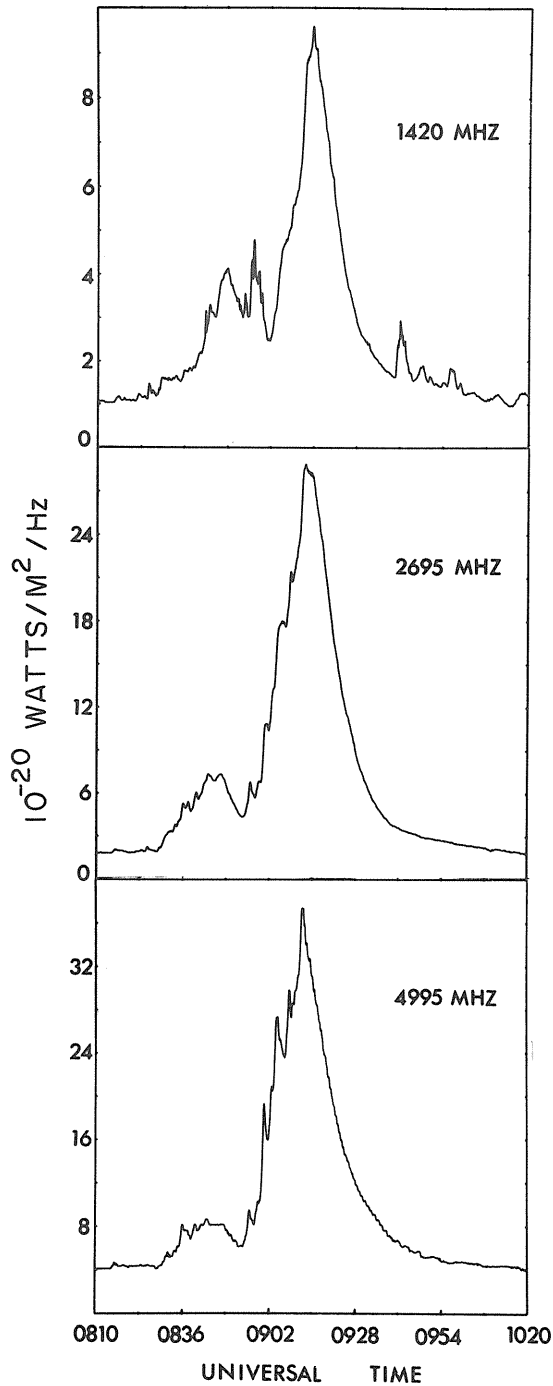
Fig. 3a. Solar radio burst recorded on October 31, 1968 by NASA Observatory at Carnarvon, Australia.

Fig. 3b. Selected H $\alpha$  photographs of class 2B flare at S13 W50 on October 31, 1968, photographed by NASA Observatory at Carnarvon, Australia.

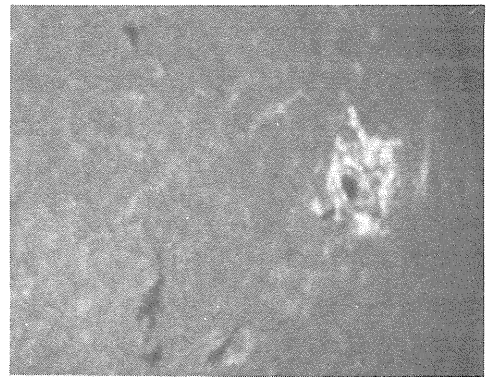
1 NOVEMBER 1968

NASA-SPAN-CYI

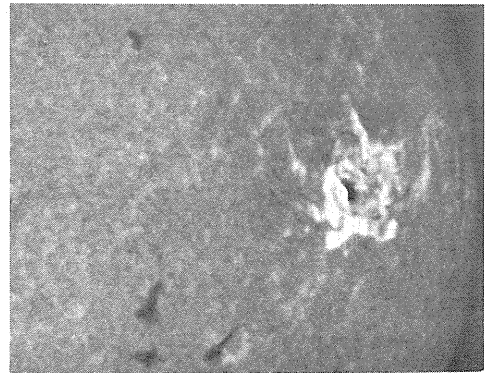
← 5x10<sup>5</sup> km →



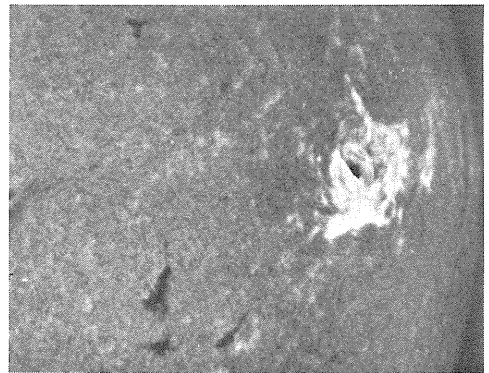
0745



0900



0929



1050

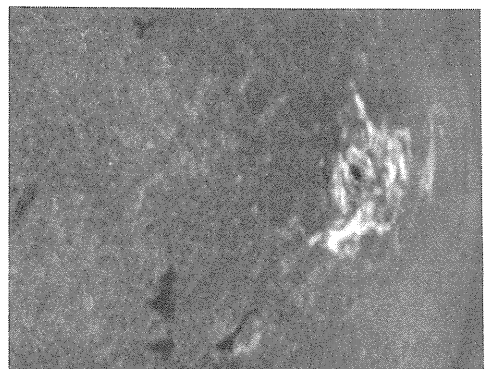


Fig. 4a. Solar radio burst recorded on November 1, 1968 by NASA Observatory at Carnarvon, Australia.

Fig. 4b. Selected photographs during the class 2N flare at S15 W45 on November 1, 1968, photographed by NASA Observatory at Canary Islands.

2 NOVEMBER 1968

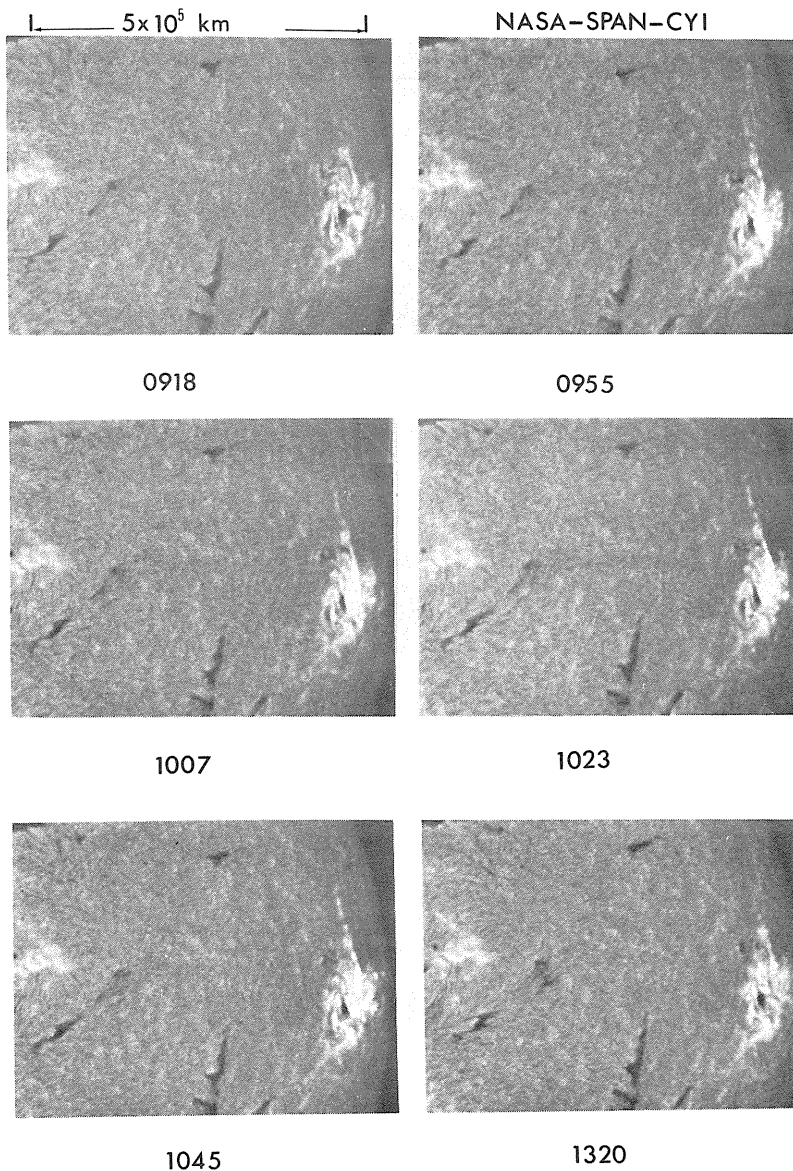
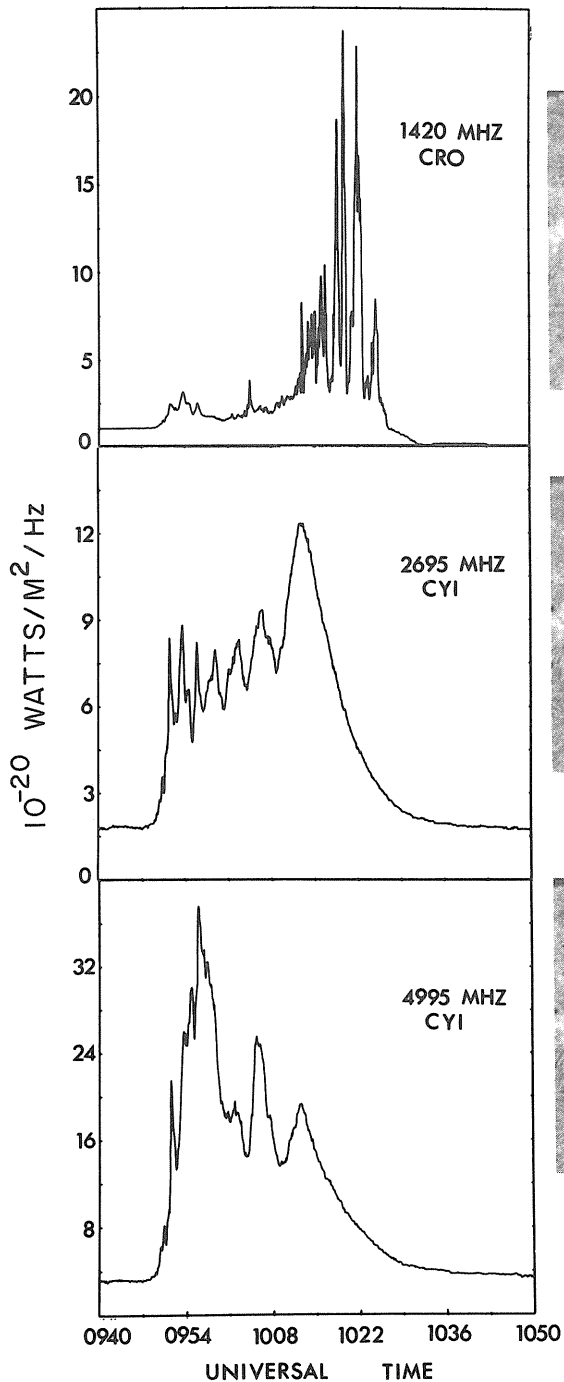


Fig. 5a. Solar radio bursts recorded on November 2, 1968 at the NASA Observatory at Carnarvon (CRO) and the Canary Islands (CYI).

Fig. 5b. Selected H $\alpha$  photographs during the class 2B flare at S14 W65 on November 2, 1968, photographed by NASA Canary Islands Observatory.

4 NOVEMBER 1968

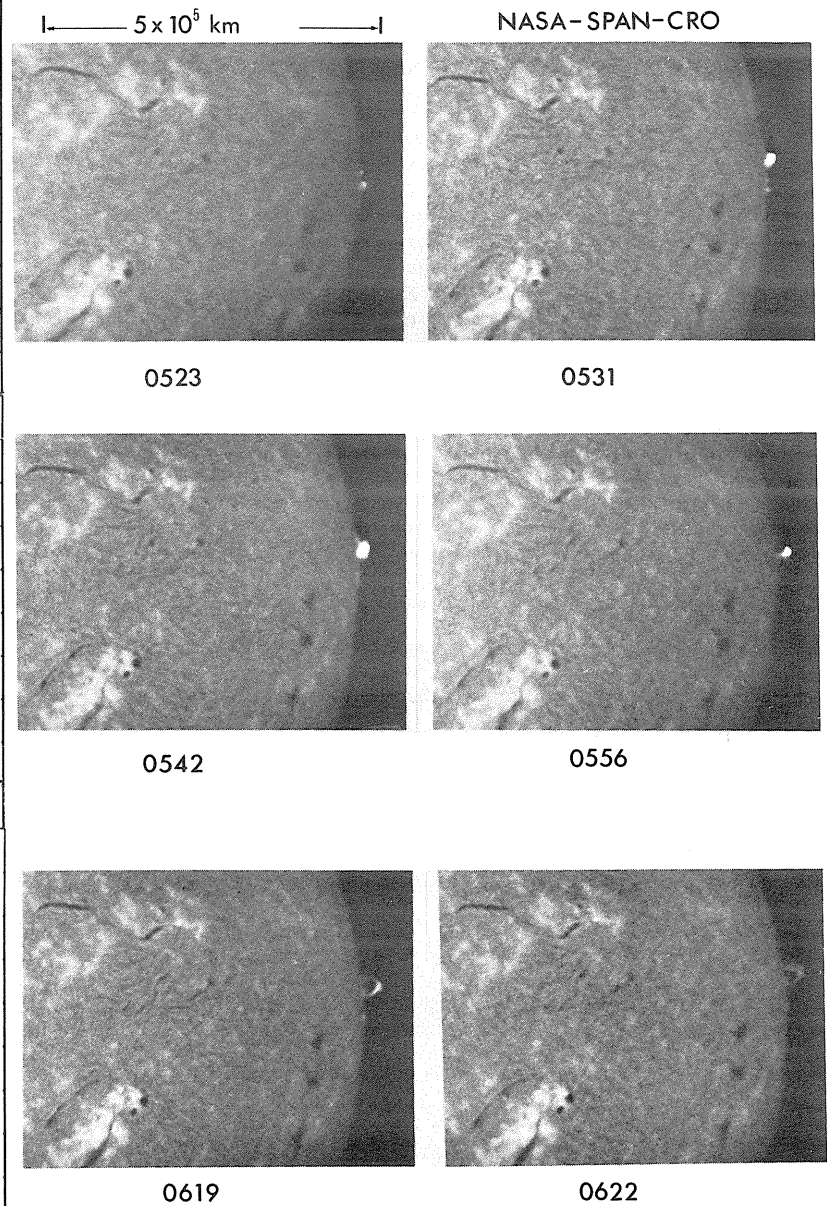
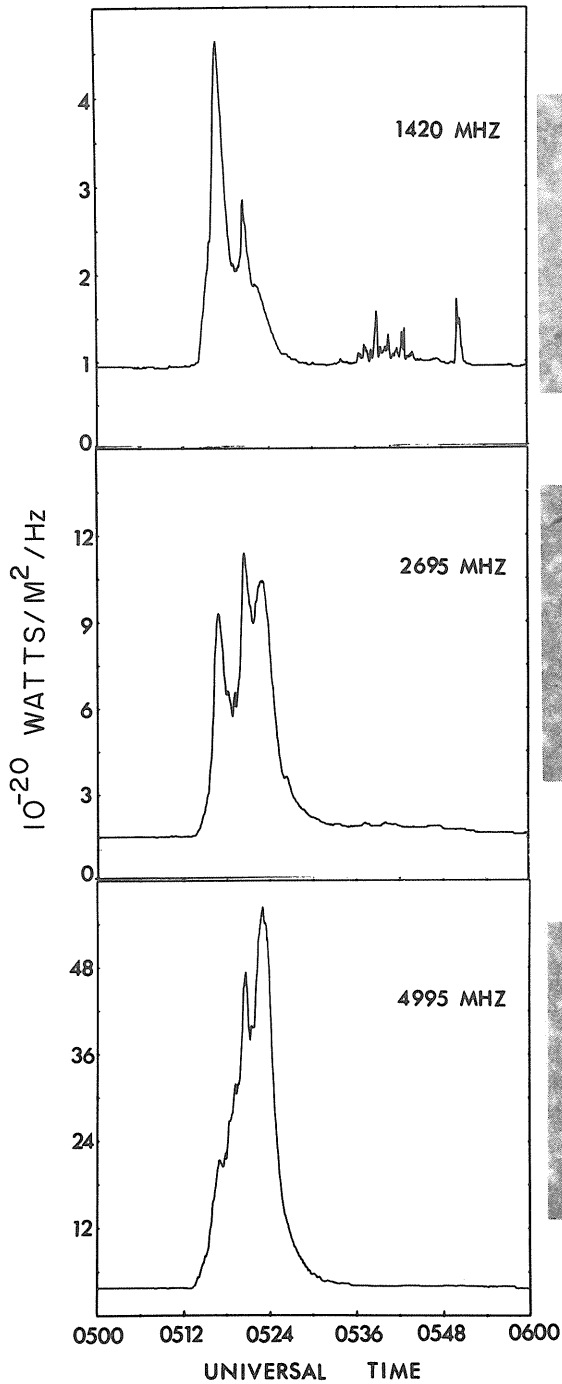


Fig. 6a. Solar radio burst recorded on November 4, 1968 by NASA Observatory at Carnarvon, Australia.

Fig. 6b. Selected H $\alpha$  photographs showing limb flare on November 4, 1968, photographed by NASA Observatory at Carnarvon, Australia.

"A Study of the Film Record of H $\alpha$  Flare of October 30-31, 1968"

by

Richard A. Miller, S. J. and Allan R. Trinidad  
Solar Division  
Manila Observatory, Manila, Philippines

Introduction

McMath plage region 9740 came onto the disk October 21, 1968. It subsequently showed the most interesting development of any center of activity in many months. Gradually the filament and plage structure tightened into a circular form around the main spot. Worthy of note are the parallel bright ribbon structures, surrounding the main spot. Mt. Wilson magnetograms, during the disk passage of this area, showed an increasingly clear island of north magnetic polarity, in a sea of south magnetic polarity. (See pages 8-10 of this Report.) As far as can be judged by a superposition of the plage region from a Manila Observatory H $\alpha$  spectroheliogram of October 30, 1968 at 0040 UT, properly enlarged for a 1:1 comparison with a Mt. Wilson copy of a magnetogram taken 7 hours previously, the brightest of the parallel ribbons, often on either side of curved filaments, straddled the neutral lines. They became the chief flaring regions a day later.

Flare Development

Previous to the flare the curved ribbon structure encircling the east side of the activity center joined with the curved ribbon structure of the west side of the region. This junction was not smooth, but formed an "X", one arm of which was faint. The extension of two of the arms to the west side had a wishbone shape, with a sharp apex, pointed eastward. At this apex at 2342 UT of October 30, 1968 the flare began. The faint arm of the "X" brightened. The flare began to branch out, star-like, from the point of crossing. By 2353 UT this "X" had become a six-pointed star.

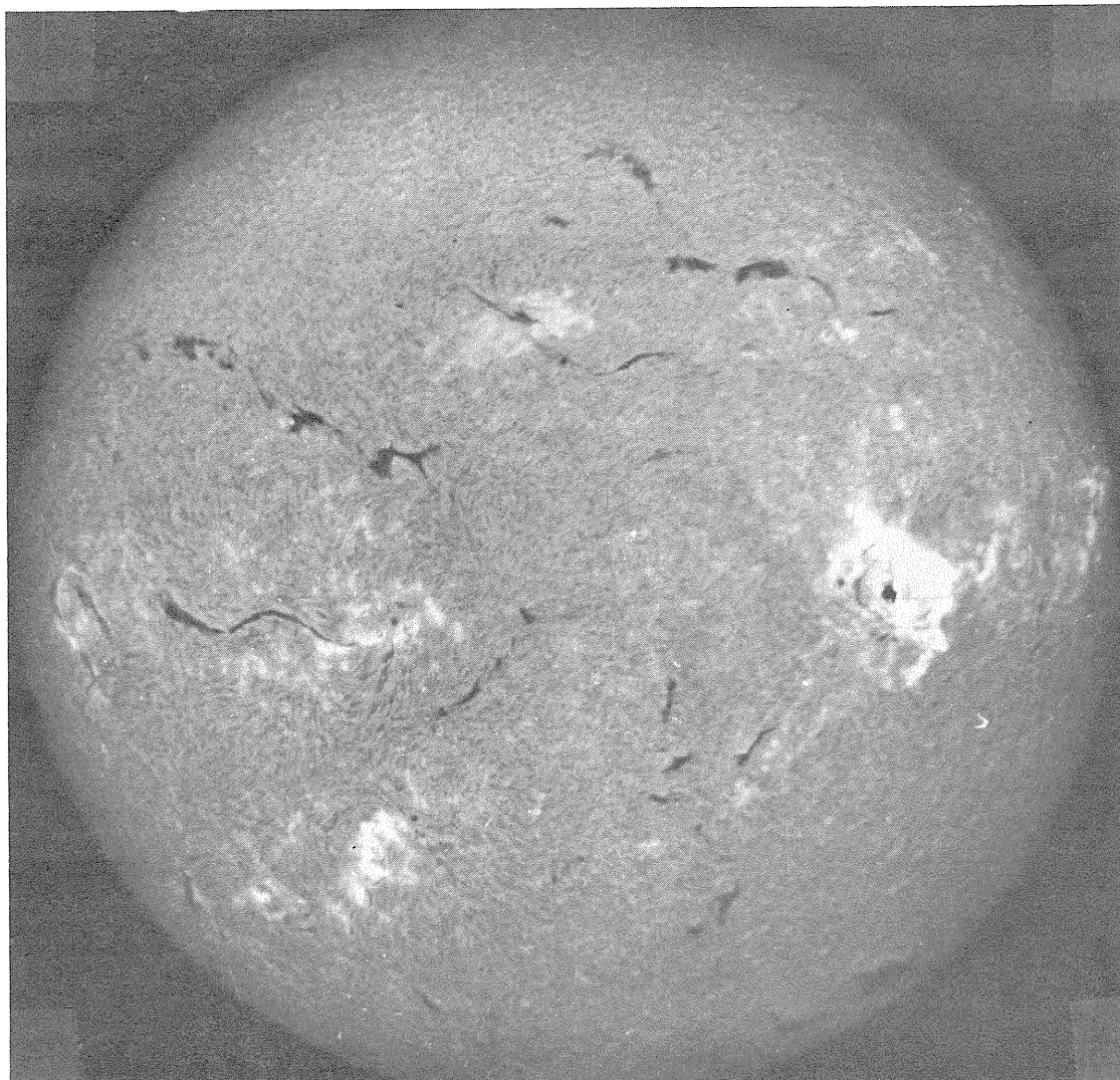


Fig. 1. Filtergram taken with Razdow WS-250 telescope at Manila Observatory of flare maximum at 0013 UT October 31, 1968.

Meanwhile, with a one minute lag in start time, the plage ribbons to the west brightened. By 2353 UT this west section dominated the flare and by 0000 UT of Oct. 31, this section alone measured 15 square degrees uncorrected. This west section put out feelers towards the star formation. The heaviest streamer failed by one degree in projection of ever quite joining a corresponding arm of the star. Another heavy streamer which cut a chord across the west edge of the sunspot umbra, did join up with one of the rays of the star, from 0002.5 UT of Oct. 31, 1968 till 0050 UT when it faded and drew back to the north. The star configuration began to weaken by 0015 UT and was reduced to three rays by 0059 UT. Figure 1 is a photograph of the flare at maximum taken with the Razdow WS-250 telescope at the Manila Observatory.

In an attempt to obtain a 3-dimensional impression of this flare, two strips of film taken one hour apart during the time of the flare were viewed stereoptically. A 3-dimensional effect, as of an object 25 feet away, was obtained because of the 1/2 degree rotation of the sun per hour. The effect of the flare was that of a series of loops, some of which were overlapping. What, with single-eyed vision, appeared to be a crossing of lines of flux clearly shows in three dimensions as one loop superimposed upon the other. The flare in its generic shape fits the loop category according to Smith and Smith's classification [1963].

In 3-dimensions the place of the first brightening of the flare, the site of the star-like formation, was the focal point or the source of a series of loops in the form of a many-streamed fountain viewed from above. Much of the bright flare ribbon formation of 0008 UT and nearby times, by an hour later, was replaced by filamentary structures in absorption. Matter injected during the flare had evidently cooled enough to absorb. The heights of the flare loop structures appeared to be one-half of the distance between their feet or roots. This makes their height to be 50,000 km., the height of the greatest flares observed at the limb. The thickness of these ribbons ranged from 1/2 degree to one degree.

At 0003 UT two filaments 5 and 8 degrees in projection from the large spot on the east side of the flare began to disappear and were completely gone by 0007 UT. The filament nearer the flare had reappeared by 0220 UT but the more distant filament 8 degrees in projection from the large spot had not appeared even by the next day. There were many dark surges at 0017 UT going to the north and others beginning at 0022 UT going to the east, which persistently recurred till after 0220 UT. An impression of an advancing shock front was given by the activations at increasing distances of the surges on the east side of the flare beginning at 0022 UT but no shock moving over great distances was observed on band. The dark surges followed the isogauss pattern of the Mt. Wilson magnetogram and those to the east followed the locus of the former filaments which had disappeared. During the flare there was evidence of deterioration of the fibril structure close by the flaring region, as noted by Ellison and others [1960]. The deterioration was most noted from 0007 UT till 0025 UT and appears to be a solar seeing effect caused by the flare-induced solar turbulence.

#### Analysis

The whole flare area at maximum measured a good bit larger than the reported uncorrected areas, even of this observatory. Thirty-three square degrees was what a careful reading showed. It is realized that the SO-375 film showed turbidity and that 33 square degrees is an upper limit. Because of the dome or hemispherical shape of the flare, it is felt that no correction should be applied to the 33 square degrees, an area quite close to the 28 square degrees corrected of the Tokyo Astronomical Observatory at Mitaka. The flare rates as of importance 4.

If a visual estimate of 1/2 degree is taken as the thickness of the flaring material in a hemispherical shape, the volume of the flare was 33 cubic degrees, or  $4 \times 10^{28}$  cm<sup>3</sup>, the volume of a major flare.

An effort was made to derive the total energy flux per second at the flare maximum from a measurement of the areas weighted according to their emission, as calibrated against the step wedge in units of the background of the neighboring solar region. The density in the flare region was well beyond the straight part of the characteristic curve of the film. Of the flare area 6 degrees averaged an intensity 90% of the continuum, 12 square degrees averaged 60% of the continuum, and 15 square degrees averaged 40% of the continuum. Continuum was taken to be 4 times the background. Assigning 2 Angstroms of line width to the brightest 6 square degrees and 1 Angstrom of line width to the less bright parts of the flare, the total output of the flare at maximum is of the order of  $3.3 \times 10^{26}$  ergs per second. Continuum emission was taken to be  $29 \times 10^{13}$  ergs/sec.-ster-radian- $\text{\AA}$ .



There is an impression given by the sunspot configurations on successive days, that the rotation of the smaller spots takes place around the large spot of the region. For the most part this impression is illusory. The true motion, when correction is made for foreshortening by reduction of the positions of the smaller spots to the positions they would hold relative to the main spot if viewed at the center of the disk, accords with the well known findings of Severny [1964] that the geometrical pattern of sunspots expands after a large flare. Figure 3 shows the changes which did occur from the day previous to the day following the flare.

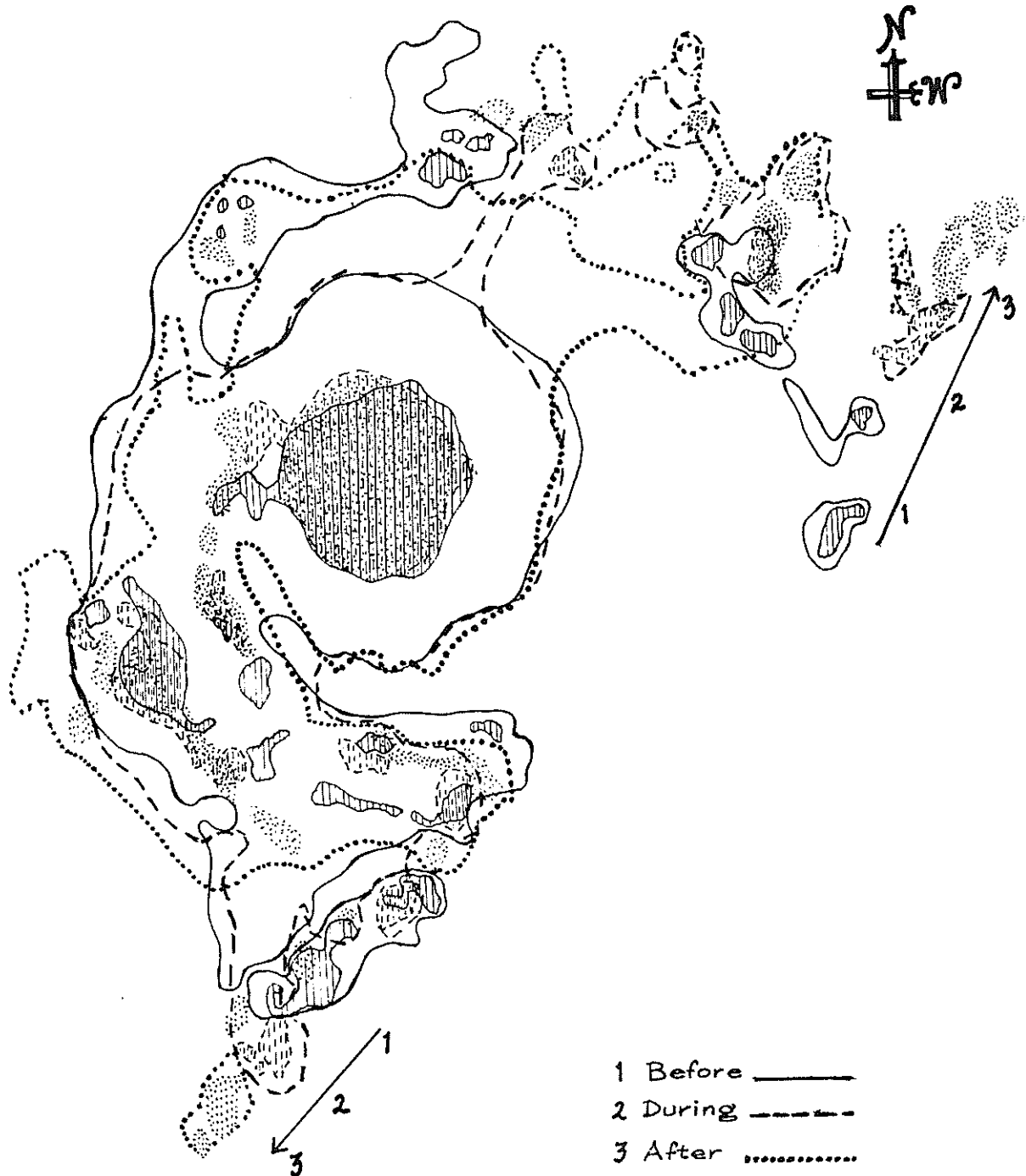


Fig. 3. Drawings of sunspots of the flare region one day before (———), during (- - - - -), and one day after (.....). Expansion of the spot configuration took place.

Vesecky and Meadows [1968] believe that many origins of flares can be explained by the diffusion of a point explosion, during the first two minutes of a flare. Taking the coefficient alpha to represent the slope of  $\log R$ , the radius of a developing feature in km, versus the log of the time in seconds, this flare for its first two minutes at the star formation, had an alpha of 0.4, a result within the limits set by Vesecky and Meadows.

Correlated Effects

The radio events recorded in the ESSA "Solar-Geophysical Data" bulletin coincided for the most part with events observed optically, but there were so many bursts and optical changes that nothing definite can be said about the coincidences. The group of radio bursts of type III began with the beginning of the flare and the next group of type III bursts from 2351 UT to 2428 UT coincided with the general development of the flare. The type II radio emission from 0000 UT to 0005 UT coincided with the filling in of the area between the westernmost ribbon streamer and the spot. Type IV radio emission from 0002.5 UT till 0035 UT accompanied the greatest all-over development, as well as the most intense part of the flare. It may be significant that this type IV began with the completion of the flare ribbon across the western edge of the spot umbra and lasted till this ribbon rather abruptly thinned and faded by 0035 UT on October 31.

The vigor of the event was shown locally by the SID effects at the Manila Observatory. On the SPA (Sudden Phase Anomaly) link to Jim Creek, the advance was  $210^\circ$  at 0016 UT, and  $115^\circ$  on the link to Hawaii. Unusual for the early local time of 8 A.M. was the total fade of the 9.6 MHz radio reception from Tokyo for 2 hours and 5 minutes, beginning at 2355 UT on October 30.

Figure 4 compares the light curve of a consistent section of the western flaring region with the sudden phase anomaly record of the transmission at 18.6 kHz from NLK, Jim Creek, Washington. The two maxima coincide. The flash stage is apparent on the figure going from 0002 UT to 0015 UT.

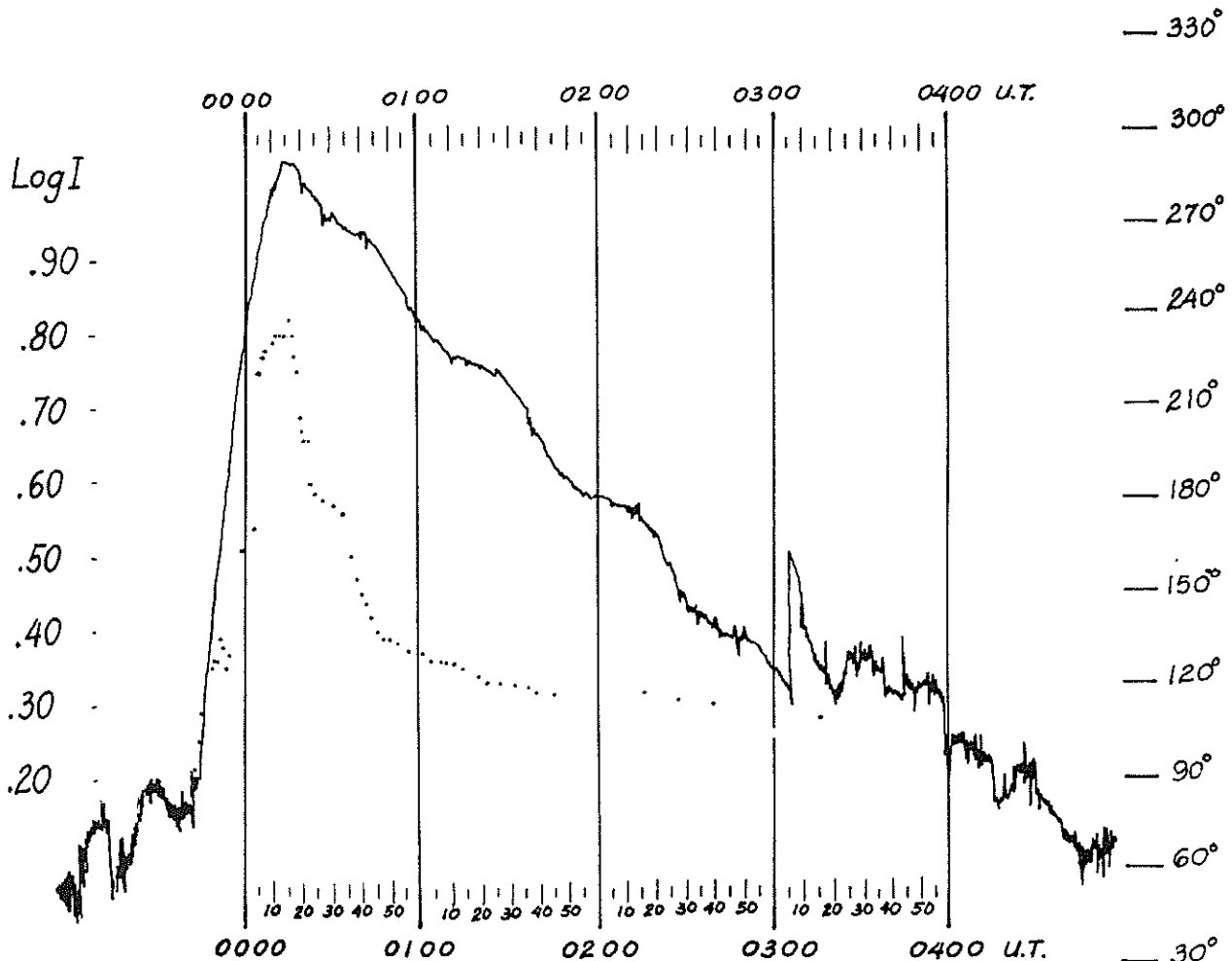


Fig. 4. Comparison of Sudden Phase Anomaly phase recording on NLK (Seattle) to Manila path (————) with light curve of one of the persistent features (.....) in the west side of the flare.

## Conclusion

The flare is a good example of a many filamented structure in loop formations forming a vault into the corona. It was ideally situated on the sun to inject protons into the earth. The dissipation of energy took place along the neutral lines clearly evident in filtergrams after comparison with magnetograms. The flare had almost all the characteristics of a large event, a flash phase, a nimbus, some evidence of a shock front on band, and dark surges, but it did not reach by a factor of two the intensity or energy flux of the greatest flares.

## Acknowledgements

Acknowledgement is made to A. Ambion for the drawings and to the Weather Arm of the U.S. Air Force for the supply of film used in the patrol.

## REFERENCES

- |   |      |   |
|---|------|---|
| ELLISON, M. A.,<br>S.M.P. MCKENNA and<br>J. H. REID | 1960 | The Solar Flare of 1960 April 1, <u>The Observatory</u> , <u>80</u> , 149.  |
| SEVERNY, A. B.                                      | 1964 | On the Behavior of Magnetic Field Associated with Solar Flares, <u>AAS - NASA Symposium on the Physics of Solar Flares</u> , Ed. W. N. Hess NASA SP-50, Washington, D. C. |
| SMITH, H. J. and<br>E.V.P. SMITH                    | 1963 | <u>Solar Flares</u> , Macmillan, New York, 89.  |
| VESECKY, J. F. and<br>A. J. MEADOWS                 | 1969 | The Initial Development of Solar Flares, <u>Solar Physics</u> , <u>6</u> , 80.  |

# "Description of the H $\alpha$ Flares of November 1, 2 and 4, 1968"

by

C. J. Macris and C. E. Alissandrakis  
Astronomical Institute  
National Observatory  
Athens, Greece

## Introduction

The flares of November 1, 2 and 4, 1968 in the active region S15, L = 173° (McMath plage region 9740) were very interesting, being accompanied by important associated events. This region showed intense activity during rotation 1540 (October 22 - November 4, 1968) but, unfortunately, because of unfavorable weather, we observed only the above mentioned flares, which we have characterized as importance 2b. The observations were carried out photographically at the center as well as at the wings of H $\alpha$  (0.0Å,  $\pm$  0.5Å,  $\pm$  1.0Å) using a Halle filter mounted on the 40 cm refractor (f/12.5) of the National Observatory of Athens. The diameter of the image at the prime focus of the 40 cm objective is 50 mm; a negative lens enlarges the focal image 31 times and thus the diameter of the solar disc on the film is 155 mm.

## The Flare of November 1, 1968

The flare appeared successively in three separate parts of the region 9740; Figure 1b shows the sunspot group, drawn from a photograph taken at +1Å, while Figure 1c shows the parts of the region covered by the flare. Some other parts of the plage brightened; however, they did not reach flare brightness. In two cases motion of dark material was observed; radio emission was recorded in the mm and cm bands [Anastassiades and Macris, 1969]. At 8 mm there was an increase of power flux density by  $490 \times 10^{-22} \text{Wm}^{-2} \text{Hz}^{-1}$  units, i.e. almost 25% over the quiet sun level of that day (2000 units). Protons were detected by Explorer 34 satellite 7 hours after flare maximum and X-rays by Explorer 33 and 35 (see "Solar-Geophysical Data").

The main phases of the flare are given below:

	<u>Start</u>	<u>Maximum</u>	<u>End</u>
Part 1	~0806	0850 and 0915	1010
" 2	~0806	0853	0920
" 3	0818	0919	1050

Part 1 of the flare began at ~0806 UT as a brightening of the plage in points 1 (Figs. 1a and 2) of the main spot. The brightening advanced rapidly from 0812 UT (flash phase) towards the main spot (arrow in Fig. 1a) and began to cover its umbra at 0828. On the original negatives one can see two thread-like formations over the umbra (dashed line in Fig. 1a). The coverage begins as an enhancement of one of them.

Part 1 attains a first maximum at 0850 and it is inhomogeneous in intensity, consisting of bright knots and intermediate less bright material; the H $\alpha$  width is ~2Å. For a short period it remains stationary, then the region over the umbra expands eastwards producing a second maximum at 0913, brighter than the first (Figs. 1c and 3); the part of the umbra covered by the flare is about 30%. Part 1 ends at 1010 UT, but the plage remains excited.

Part 2 (Figs. 1a, 1c and 2) begins simultaneously with part 1, as two bright knots (Points marked 2 in Figs. 1a and 2). Nearby points brighten and finally the flare takes the shape of two filamentary structures. The flash phase begins at 0840 and the maximum is at 0853 (Fig. 1c); at maximum it is slightly visible at  $\pm$  1Å. The decline is rather quick and at 0920 it is finished.

Part 3 began after parts 1 and 2 at 0818 UT but it was the brightest and biggest. At first the points marked 3 brighten (Figs. 1c and 2) and at 0845 the flash phase starts with an expansion in the direction of the arrows; in the SE region there was a chain of bright mottles.

The intensity maximum was at 0919 (Figs. 1c and 3) with an H $\alpha$  width  $>2\text{Å}$ . A decrease of intensity follows with a slight increase of area (area maximum 0930). The northern region fades more rapidly than the southern, where brightness falls gradually. At about 1050 UT the brightness of the region does not change, so we may consider the flare finished. The plage remains bright even on the next day (cf. the lower part of Fig. 7a).

An interesting case of displacement of the excitation was observed at ~0900 as a successive brightening of the regions between the facule 3a (Fig. 1a) and the main part of the plage to the north. The whole process lasted 7 minutes. It is evident that it was not a movement of material because the bright knots consisting the region can be traced in successive photographs; this is in agreement with Bruzek [1968].

Two eruptive prominences were observed at the beginning of the flare (excitations of filaments I and II, Fig. 1a). Filament I was active before the flare, visible at  $\pm 1\text{\AA}$  and with significant changes in shape. At 0816 it became invisible at the center of H $\alpha$ , being prominent at  $-0.5\text{\AA}$ , that is it was ascending (Fig. 5). It is very probable that the cause of excitation was part 2 of the flare. Seven minutes later its size was increased and a condensation is formed which moves rapidly to the north and is separated from the main body of the prominence at 0826 (Fig. 6). At 0830 there is also a descending part in the ejected material. Because of its great velocity (of the order of 300 km/sec.) the condensation went out of the observed region of the sun, 25 minutes after its creation. Photographs taken at the center and the wings of H $\alpha$  revealed an excitation of the filament II (Fig. 1a) at about 0816 UT. The filament has a complex structure at  $-0.5\text{\AA}$ , consisting of dark string-like formations (Figs. 5 and 6). At 0857 UT the strings have almost disappeared and finally a quiescent filament is formed.

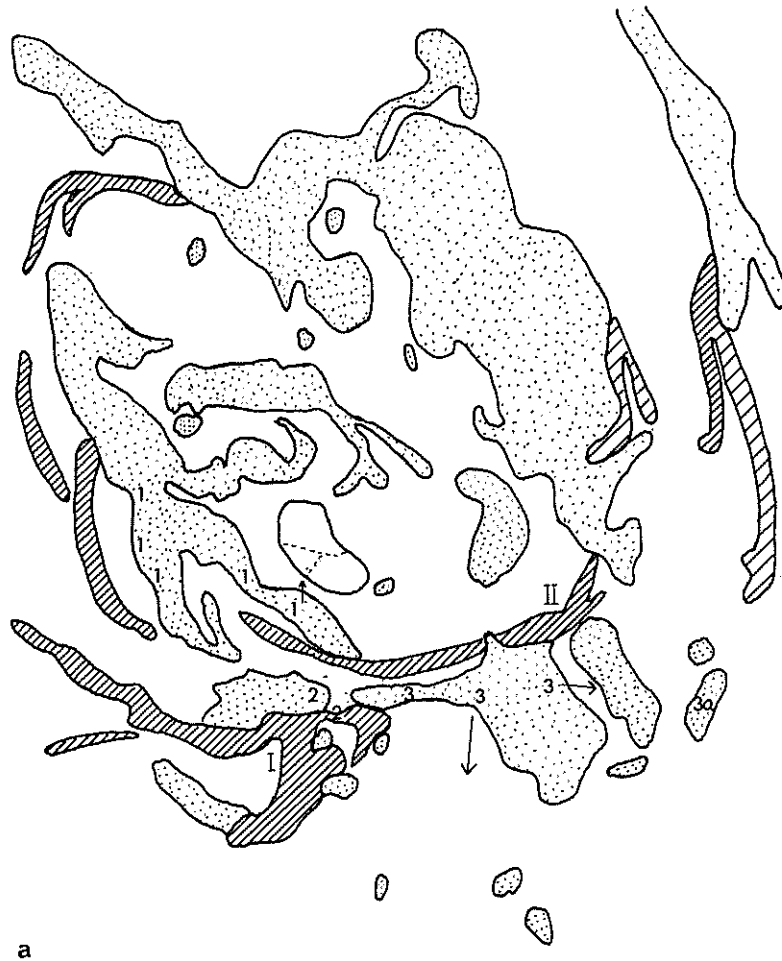


Fig. 1a. The active region S15,  $L = 173^\circ$  on November 1, 1968. Chromospheric drawing at 0755 UT showing plage (dotted), filaments (parallel lines) and the main spot umbra (white). The umbra is partly covered with chromospheric material. The dashed line over the umbra is a faint feature. The numbers indicate the location of the flare.

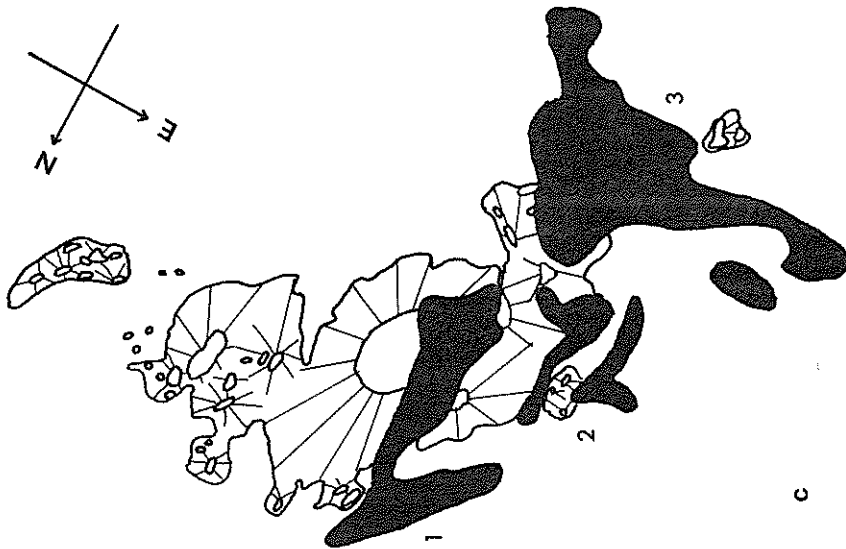


Fig. 1c. The three parts of the flare (black) at their maximum phase. Part 1 and 3 drawn from a photograph at 0919 UT, part 2 at 0853 UT.

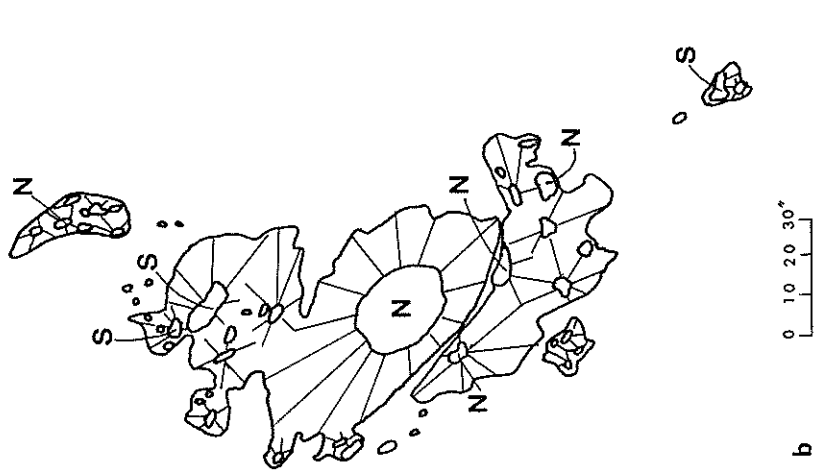


Fig. 1b. The sunspot group drawn from a photograph at  $+1.0\text{\AA}$ . Spot umbrae appear white, penumbrae with radial lines. Polarities according to Rome Observatory data.

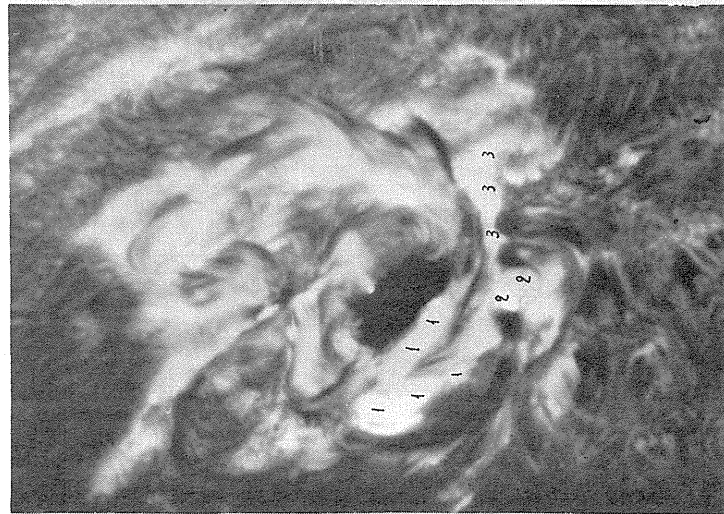


Fig. 2. 08<sup>h</sup> 24<sup>m</sup> 24<sup>s</sup> UT, 0.0Å. The flare 18 minutes after the beginning.

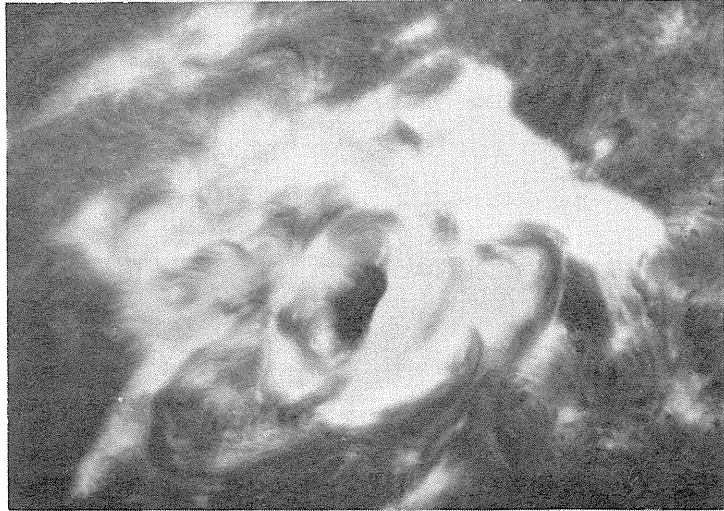


Fig. 3. 09<sup>h</sup> 17<sup>m</sup> 25<sup>s</sup> UT, 0.0Å. The flare near maximum (maximum of Parts 1 and 3 at 0919 UT).

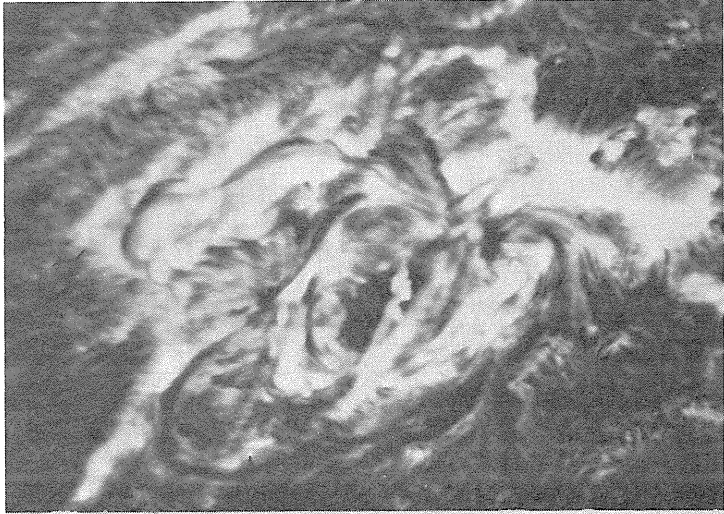


Fig. 4. 10<sup>h</sup> 48<sup>m</sup> 13<sup>s</sup> UT, 0.0Å. The flare near the end.

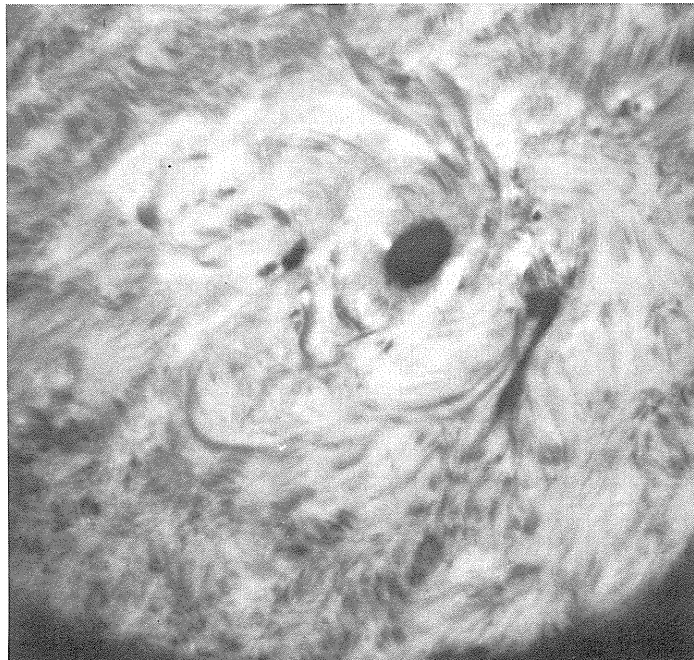


Fig. 5. 08<sup>h</sup> 17<sup>m</sup> 55<sup>s</sup> UT, -0.5Å. Ascending dark material (filaments).

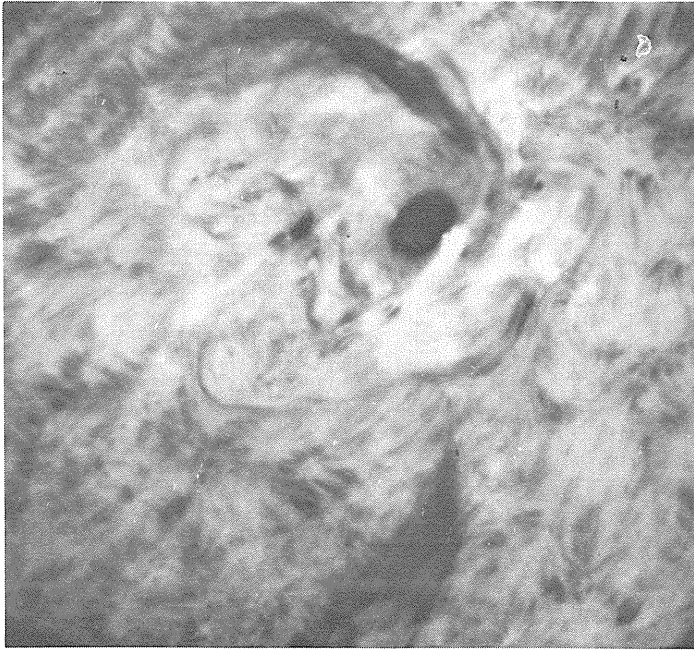


Fig. 6. 08<sup>h</sup> 30<sup>m</sup> 12<sup>s</sup> UT, -0.5Å. Evolution of the filaments. The ejected condensation is visible at the left.

The Flare of November 2, 1968

On November 2, in the same active region we observed a 2b flare on the western part of the spot group. The flare consisted of two separate parts (Fig. 7c) which appeared simultaneously but had a different evolution after maximum.

The main phases of the flare are summarized below:

	<u>Start</u>	<u>Maximum</u>	<u>End</u>
Part 1	0848 UT	~1009	1125 UT
" 2	0848	~1009	1045

Part 1 appeared in facule 1 (Fig. 7a) beside an active filament. Figure 9 shows the beginning of the flare which in its early stage consists of bright knots arranged parallel to the filament, but later it is more homogeneous. The maximum is at ~1009 UT when it is very bright at the center as well as at the wings of the H $\alpha$ , even at  $\pm 1\text{ \AA}$  (Figs. 7c and 9). No movement of material associated with part 1 was observed.

Part 2 began in region 2 (Fig. 7a) at 0848 UT. The maximum was at ~1009 and the end at 1045 UT. A very interesting phenomenon in part 2 is the ejection of a bright surge, begun at 1002 UT, which grew rapidly as shown in Fig. 11. As it is seen on photographs at the center and the wings of H $\alpha$  the material rose from part 2, near the main spot umbra (north polarity), followed the magnetic lines of force and descended in the vicinity of a spot of opposite polarity (Figs. 7b and 10). High resolution photographs show that it consists of thin filaments close to each other.



Fig. 7a. The active region S15 L = 173° on November 2, 1968. The chromosphere at 19<sup>h</sup> 21<sup>m</sup> 23<sup>s</sup>. The plage is dotted, the filaments with parallel lines, the main spot umbra white; the black regions are the remnants of a small flare, the regions enclosed by dashed lines were bright at 0950 UT.

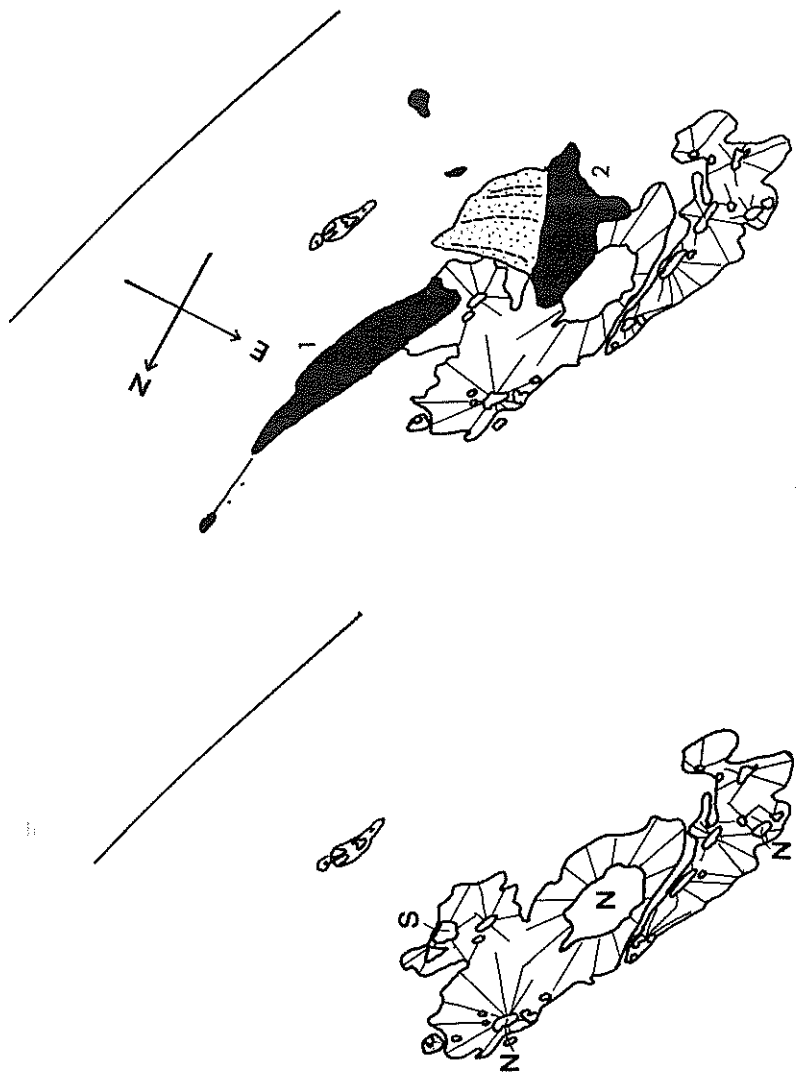


Fig. 7b. The sunspot group from a photo at  $-1.0\text{\AA}$ , (spot umbrae white, penumbrae with radial lines). Polarities according to Rome Observatory data.

Fig. 7c. The flare (black) at 1009 UT superimposed on the group. The dotted part is the surge, which has a filamentary structure (dashed lines).

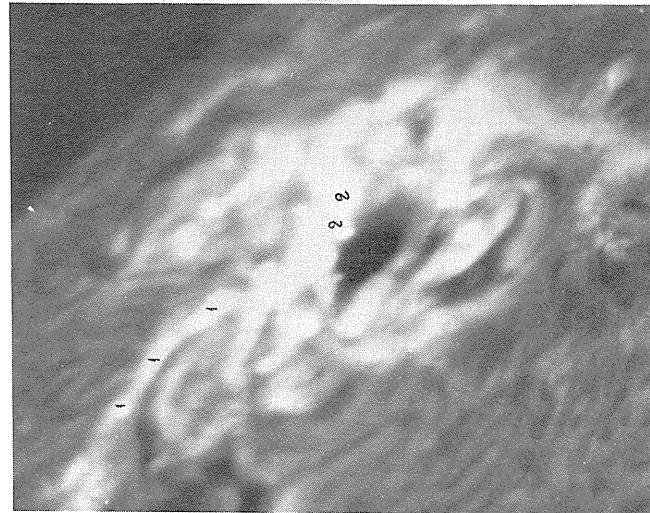


Fig. 8. 09<sup>h</sup> 48<sup>m</sup> 52<sup>s</sup> UT, 0.0Å. The flare at the beginning.



Fig. 9. 10<sup>h</sup> 02<sup>m</sup> 52<sup>s</sup> UT, +1.0Å. The flare before maximum.

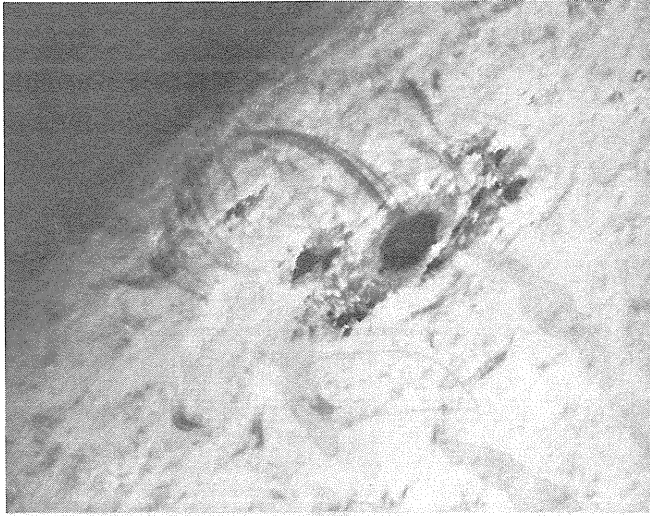


Fig. 10. 11<sup>h</sup> 24<sup>m</sup> 44<sup>s</sup> UT, +1.0Å. The surge fully developed; both ascending and descending branches are seen in this composite photograph.

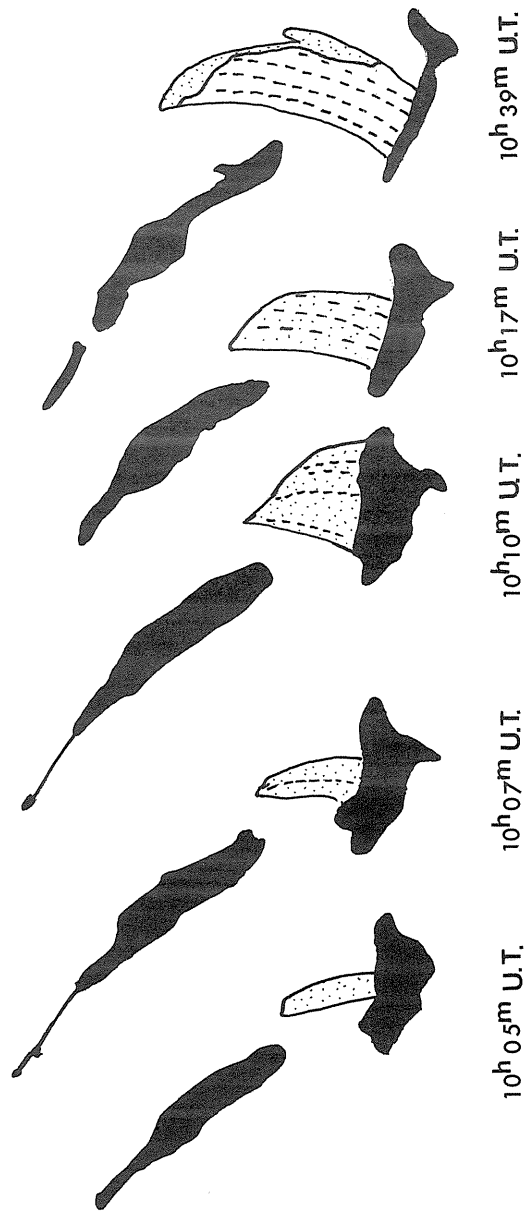


Fig. 11. Development of the surge; flare - black, bright surge - dotted, dark surge - white. The dashed lines show the direction of the filaments consisting the surge.

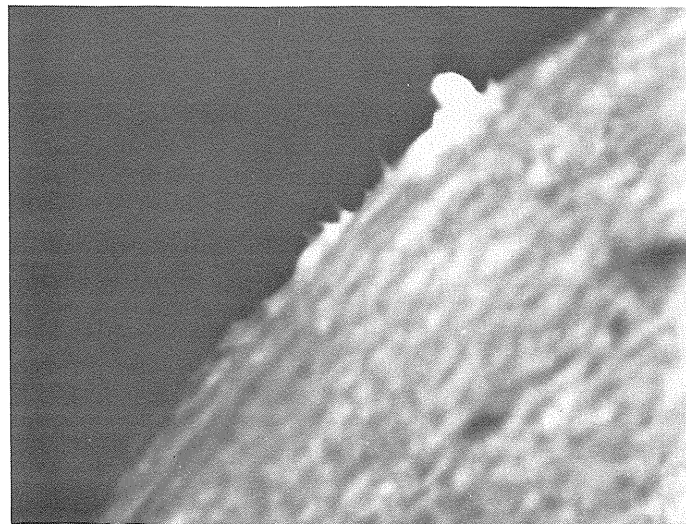


Fig. 12. The flare of November 4, 1968.  
09h 36<sup>m</sup> 33<sup>s</sup> UT, 0.0Å.

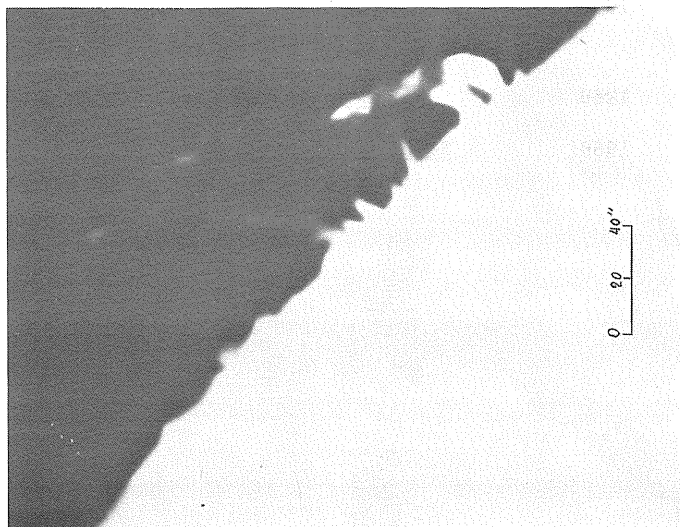


Fig. 13. The flare surge at 09h 37<sup>m</sup> 48<sup>s</sup>  
UT, 0.0Å.



Fig. 14. The surge at 09h 52<sup>m</sup> 02<sup>s</sup> UT,  
0.0Å.

As we have mentioned above, the surge began as an emitting feature, but evolved to an absorbing feature gradually; the change began at first in the lower parts of the surge and propagated to the higher parts. An interesting remark is the following: After maximum and while the surge was developing, the area of part 2 decreased as shown in Fig. 11, and the end of this part is 40 minutes earlier than part 1.

The flare of November 2 gave intense radio emission, X-rays and SID. The excitation went so deeply into the chromospheric layers that the mm outburst was very prominent, the solar flux being much greater than  $4000 \times 10^{-22} \text{Wm}^{-2} \text{Hz}^{-1}$ , that is, there was an increase of more than 100% over quiet sun level [see Anastassiades and Macris, 1969].

#### The Flare Surge of November 4, 1958

At 0932 UT November 4, a flare appeared on the western limb, which originated in McMath Region 9740. Within 10 minutes it evolved rapidly and gave rise to a surge which lasted for a long time after the end of the flare. The photographs reveal a complex movement of the ejected material. Characteristic phases of the event are shown in Figures 12, 13 and 14.

#### REFERENCES

- |                                    |      |   |
|------------------------------------|------|---|
| ANASTASSIADES, M. and<br>C. MACRIS | 1969 | The mm Wave Outbursts of November 1 and 2, 1968, <u>Solar Physics</u> , <u>10</u> , 188-197.  |
| BRUZEK, A.                         | 1968 | On Small Scale Mass Motion Associated with Flares, Mass Motion in <u>Solar Flares and Related Phenomena</u> , Y. Ohman, Ed., 67-70. |
|                                    | 1969 | <u>Solar-Geophysical Data</u> , <u>No. 297</u> , 144.   |
|                                    | 1969 | <u>Solar-Geophysical Data</u> , <u>No. 300</u> , Part II, 86-91.  |

#### 4. SOLAR LIMB PHENOMENA

"Note on the Limb Passage of the Active Region November 2-4, 1968"

by

Charles L. Hyder  
Sacramento Peak Observatory  
Air Force Cambridge Research Laboratories, Sunspot, New Mexico

[The compiler has prepared the following paragraph from correspondence with Dr. Hyder.]

At Sacramento Peak Observatory there are limb data of the large active region crossing the limb during November 2, 1968. Loops were observed in that region November 4 and 5. These data are  $\approx 1\text{\AA}/\text{mm}$  spectra from  $3500\text{\AA}$  to  $9000\text{\AA}$  (the SPO Universal Spectrograph) with associated  $1/2\text{\AA}$  H $\alpha$  and  $1\text{\AA}$   $\lambda 5303$  slit jaw pictures. There may also be HeI D<sub>3</sub> coverage of that limb passage. These studies were done in association with the Harvard OSO experiments at that time. These accumulations are unbelievably rich in data, but it will be a year or more before the quantitative job of data reduction and analysis will be accomplished.

# "Eruptive Prominence Associated with the Solar X-ray Burst of 4 November 1968"

by

Stephen Pinter  
Geophysical Institute of the Slovak Academy of Sciences  
Hurbanovo, Czechoslovakia

During the period 22 October to 4 November 1968 an important active region at S15, L 173° on the solar disk produced two proton flares and terrestrial effects associated with them. Many smaller flares occurred in this region, ending with an importance 1B eruptive prominence on 4 November 1968 which is dealt with in this paper.

The eruptive prominence started in the H $\alpha$  light about 0515 UT on western limb at a position S15 W90. Because the flare was on the limb with part of it projected above the limb, one can follow here the typical space structure of an eruptive prominence which occurred in a proton active region. This limb event was observed in H $\alpha$  also at Mitaka and Norikura, Japan and at the Carnarvon Station, Australia.

Pictures of the corona in H $\alpha$  obtained from the Norikura Coronal Station showed the occurrence of the active prominence in the preflare phase, which was associated with a spray beginning about 0445 UT. The eruptive prominence began in the form of a bright knot at 0515 UT.

Fig. 1 shows the development of the eruptive prominence. Onset of the eruptive prominence is not well seen in the figure. At 0521 UT we can see a bright knot and 9 minutes after we see the development of loop structure of the flare. Maximum of the eruptive prominence was reached at 0529 UT. In the finishing phase of the flare there was a bright ribbon situated above the limb in the corona one hour after the beginning of the event.

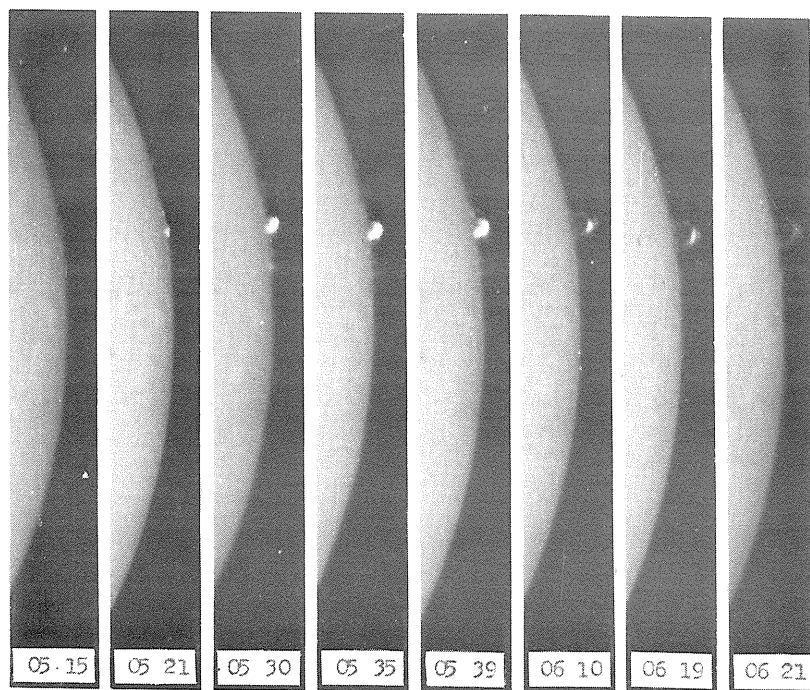


Fig. 1. Development of the eruptive prominence of 4 November 1968. (Courtesy of T. Takakura).

This limb phenomenon was accompanied with X-ray burst and radio burst in different wavelengths.

It follows from the data published by the University of Iowa, Solar X-ray flares (2-12 $\text{\AA}$ ) observed by the satellites Explorer 33 and Explorer 35 that the burst of the soft X-rays (2-12 $\text{\AA}$ ) began at 0458 UT with slow rising of the flux followed by a rapid onset at 0514 UT. The maximum flux,  $F(2-12\text{\AA}) = 0.29 \text{ erg/cm}^2 \text{ sec}^{-1}$  was observed at 0529 UT. This time corresponds to maximum phase of the optical flare.

The flux of soft X-rays was during this phenomenon and it was measured by the satellite Explorer 37. The flux was measured in three wavelengths, namely:

$F(8-20\text{\AA}) > 1.10 \text{ erg/cm}^2 \text{ sec}^{-1}$ ,  
 $F(1-8\text{\AA}) > 0.490 \text{ erg/cm}^2 \text{ sec}^{-1}$  and  
 $F(0.5-3\text{\AA}) > 0.0013 \text{ erg/cm}^2 \text{ sec}^{-1}$ .

Time of onset of hard solar X-rays in the energy range  $E > 20 \text{ keV}$  is at 0524 UT [Masley, 1969].

We can suggest the time of the burst of hard X-rays on the basis of the geomagnetic crochet [Pinter, 1969]. Geomagnetic crochet recorded by Janky Bazar Observatory, USSR [СОЛНЕЧНЫЕ ДАННЫЕ, 1968 No. 11] is shown in Fig. 2. Sudden rising of the intensity of horizontal component begins at 0521 UT. Maximum value of  $30\gamma$  was reached at 0530 UT.

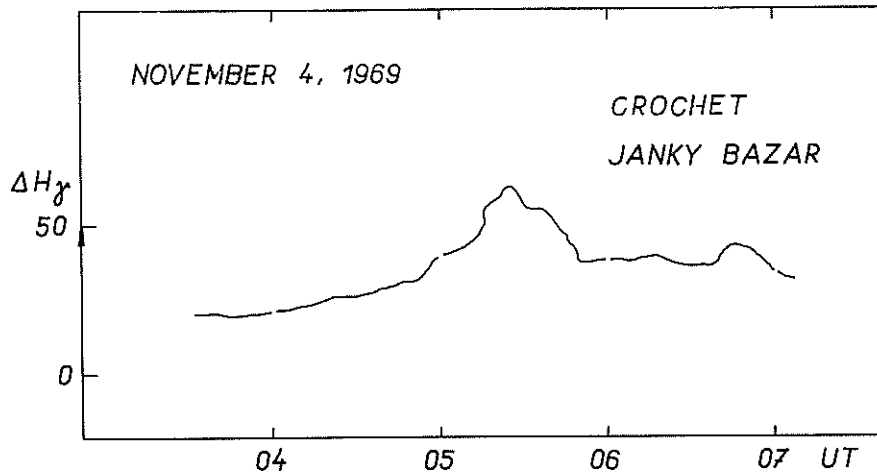


Fig. 2. Geomagnetic crochet of the eruptive prominence of 4 November 1968.

### Conclusion

In the paper it is shown that the soft X-ray radiation associated with eruptive prominence begins at the time when the emission knot begins to expand into space (vertically and tangentially respectively) and evolves into a loop structure. Beginning of hard X-ray radiation in the range 10-50 keV follows the soft X-rays, and it is associated with the explosive phase of the eruptive prominence.

### Acknowledgements

The author is thankful to Prof. Takakura, Astronomical Observatory of the Tokyo University, Japan and Mr. Davies from Carnarvon Tracking Station, Australia for kindly sending HX photocopies for the studied event.

### REFERENCES

- |               |      |  |
|---------------|------|--|
| MASLEY, A. J. | 1969 | Paper presented at 11th International Conference on Cosmic Rays, Budapest, 25 August-4 September 1969. |
| PINTER, S.    | 1969 | <u>Bull. Astr. Inst. Csl.</u> , <u>20</u> , 151.   |

## 5. SOLAR RADIO EVENTS

"Summary of Worldwide Outstanding Solar Radio Emission Events - Fixed Frequency and Spectral"

by

Hope I. Leighton and J. Virginia Lincoln  
Space Disturbances Laboratory  
ESSA Research Laboratories, Boulder, Colorado

The tables list the outstanding events from fixed frequency records as reported from worldwide sources to World Data Center A. The explanation of the type code and the stations included are given at the end of the table. This is the form of presentation currently used in "Solar-Geophysical Data", but at time of publication in "Solar-Geophysical Data" only the Western Hemisphere data were included.

Following the fixed frequency tables, the spectral summaries for October 24 - November 6, 1968 are repeated for the convenience of the reader. These data were first published in "Solar-Geophysical Data" IER-FB-292, pp. 84-86 and IER-FB-293, pp. 72-74.

The station abbreviations are as given in the following list:

### Fixed Frequencies

Code	Station	Geographic		Frequency Range (MHz)
		Lat.	Long.	
ARCE	Arcetri	44N	11E	9285, 1420
BERL	Berlin-Adlershof	52N	13E	9489, 2920, 1470
BORD	Bordeaux	44N	01W	930
BOUL	Boulder	40N	105W	18 (Univ. of Colo.) 184 (ESSA)
CRIM	Simferopol	44N	34E	3100
GORK	Gorky	56N	44E	9100, 3800, 2950, 650, 200, 100
HARS	Harestua	60N	10E	225
HIRA	Hiraiso	36N	140E	500, 200
IZMI	Moscow IZMIRAN	55N	37E	202
KIEL	Kiel	54N	10E	1420, 420, 240
KISV	Kislovodsk	43N	42E	15000, 6100
MANI	Manila	14N	121E	8800, 4995, 2695, 1415
MCMA	McMath-Hulbert	42N	83W	18
NERA	Nederhorst	52N	05E	9500, 3000, 610, 200
NEUS	Neustrelitz	53N	13E	9139, 1490
ONDR	Ondrejov	49N	14E	9400, 808, 536, 260
OTTA	Ottawa ARO	45N	75W	2800
PENN	Penn. State Univ.	41N	78W	10700, 2700, 960, 328
PENT	Penticton	49N	119W	2695
POTS	Potsdam	52N	13E	234, 111, 23
SANM	San Miguel	34S	58W	408
SAOP	Sao Paulo	22S	46W	7000
SLOU	Slough	51N	00E	71000, 19000, 2800
SGMR	Sagamore Hill	42N	71W	35000, 15400, 8800, 4995, 2695, 1415, 606, 245
TOKO	Tokyo	35N	139E	17000, 612
TRST	Trieste	46N	14E	239
TYKW	Toyokawa	34N	137E	9400, 3750, 2000, 1000
UCCL	Uccle	50N	04E	600
VORO	Voroshilov	43N	132E	208
WASH	Wash. State Univ.	47N	117W	486

### Spectral

BOUL	Boulder (U. of Colo.)	40N	105W	7.6-80
CULG	Culgoora (C.S.I.R.O.)	30S	150E	8-222
HARV	Fort Davis	31N	104W	10-580
SGMR	Sagamore Hill (A.F.C.R.L.)	42N	71W	19-41
WEIS	Weissenau	48N	10E	30-1000

# SOLAR RADIO EMISSION OUTSTANDING OCCURRENCES

24 OCTOBER - 6 NOVEMBER 1968

	FREQUENCY STATION	TYPE	STARTING TIME	TIME OF MAXIMUM	DURATION	FLUX DENSITY $10^{22} \text{ Wm}^{-2} \text{ Hz}^{-1}$		INT	REMARKS	
			UT	UT	MINUTES	PEAK	MEAN			
24	1700 TOKO	5	0002.3	0005	7					
	8800 MNL	30	0010.5	0010.5	127.5	82.3	41.2			
	4995 MNL	30	0011.5	0011.5	17	102.3	51.2			
	2695 MNL	30	0011.5	0011.5	16.9	123.4	61.7			
	9400 TYKW	5	0015.7	0016	.7	23.0	7.0			
	8800 MNL	3	0015.8	0016	.5	23.5	11.8			
	4995 MNL	3	0015.6	0016	.8	36.8	18.4			
	3750 TYKW	5	0015.7	0016	.7	15.0	5.0			
	2695 MNL	1	0015.3	0016.1	1.7	5.4	2.7			
	4995 MNL	20	0025.5	0032.8	86.9	65.4	37.7			
	2695 MNL	20	0025.5	0033.6	132.2	53.7	26.9			
	1415 MNL	20	0025.5	0033.8	100.5	37.5	18.8			
	200 GORK	44	0502 E		461 D		5.0			
	100 GORK	44	0502 E		461 D		15.0			
	100 GORK	6	0641.9	0642.5	1	100.0D				
	111 POTS	45	0938.2	0938.5	.5	450.0	60.0			
	100 GORK	6	0938.2	0938.5	.7	110.0D				
	260 ONDR	5	0943	0943	.5	25.0				
	600 UCCL	27	1034	1040	31	5.0	1.0			
	9139 NEUS	1	1036.7	1037.3	3	6.6	2.2			
	9100 GORK	1	1036.9	1037.3	.6	7.8	3.6			
	7000 SAOP	3	1036.4	1036.9	1.4	11.4	5.7			
	7000 SAOP	29	1037.8		3.6					
	3840 GORK	1	1037	1037.2	.7	2.3	1.1			
	111 POTS	5	1105.9	1106	.1	200.0	70.0			
	111 POTS	45	1134.4	1134.4	.1	250.0	60.0			
	100 GORK	6	1134.3	1134.6	.7	110.0D				
	1900 SLOU	1	1304	1304.5	.6	44.0				
	260 ONDR	5	1414	1414	.5	35.0				
	111 POTS	40	1453.9	1507.7	17.2	500.0	2.0			
	2800 OTTA	1	1505	1506	1.5	4.4	2.2			
	2695 SGMR	1	1505.4	1505.8	1.4	5.1	2.0			
	18 MCMA	6	1636	1637	2				1	
	18 MCMA	6	1924	1926	2				1	
	2800 OTTA	4	2045	2134.5	95	180.0	64.0			
	1415 SGMR	22	2051.5	2132.8	56.5D	105.0	35.0			
	184 BOUL	44	2054	2108	163 D	2170.0	1085.0			
	606 SGMR	22	2119	2132.8	29 D	35.9	12.0			
	18 MCMA	6	2139	2140	1				1	
	208 VORO	40	2200	2210	360	150.0				
	2800 OTTA	29	2220		60	15.0	7.5			
	25	208 VORO	24	0008.4	0009	1.6	251.0	56.0		
		208 VORO	24	0011.8	0012	.7	276.0	48.0		
		1415 MNL	41	0204.6	0207.1	17.4	31.6	9.0		
		2695 MNL	41	0206	0207.5	7	14.3	1.4		
		3750 TYKW	5	0224	0225.2	2	9.0	3.0		
		1000 TYKW	5	0322	0322.3	.5	15.0	3.0		
		100 GORK	44	0505 E		337 D		5.0		
2695 MNL		41	0509.3	0518	37.7	12.9	2.6			
1415 MNL		41	0509.7	0510.3	56	31.6	4.5			
111 POTS		5	0715.2	0715	.1	200.0	70.0			
111 POTS		5	0802.6	0802.7	.1	800.0	250.0			
100 GORK		6	0837.5	0837.8	.7	10.0D				
200 GORK		42	0857	0913.3	63	55.0				
100 GORK		6	1011.8	1012.2	1.1	10.0D				
600 UCCL		27	1059	1112	20	6.0	2.0			
7000 SAOP		3	1226.8		1.9	10.8	5.4			
234 POTS		45	1353.8	1353.8	.1	120.0	25.0			
18 BOUL		6	1420	1423	4				1	
2800 OTTA		21	1520	1545	50	6.4	3.2			
2800 OTTA		3	1530.2	1534	4	20.0	9.0			
7000 SAOP		4	1531	1532.7	2.4	21.5	10.7			
8800 SGMR		4	1532.2	1534.1	5.4	11.3	5.6			
4995 SGMR		4	1532.4	1534.2	7.2	47.2	16.5			
2700 PENN		3	1532.3	1534.3	3.5	15.2	7.7			
2695 SGMR		45	1532.8	1533.2	6.9	46.0	18.9			
10700 PENN		20	1533.4	1547.9	27	7.2	4.1			
7000 SAOP		29	1533.4		9					
2700 PENN		29	1535.8	1535.8	18.5	3.8	1.9			
2700 PENN		1	1648.4	1649.2	2	2.7	0.9			
408 SANM		3	1700	1701	1.2	24.0	18.0			
7000 SAOP		22	1853.5		27.8	30.1	15.0			
2800 OTTA		21	1905	1925	45	4.8	2.4			
10700 PENN		20	1907.2	1913.4	32.1	8.2	4.1			
4995 SGMR		45	1907.1	1911.5	11.1	26.2	12.0			
2800 OTTA		21	1907	1911.3	10	6.0	3.0			
2800 OTTA		1	1907	1908	2.2	7.6	3.8			
2700 PENN		20	1907	1909.8	36.8	8.4	2.8			
2695 SGMR		45	1907.7	1909.7	3.8	6.8	3.0			
2800 OTTA		1	1909.2	1910	1.5	7.6	3.8			
7000 SAOP		3	1922	1923.4	3.5	17.2	8.6			
184 BOUL		6	2111	2112	3	2800.0	290.0			
3750 TYKW		5	2316	2317	5	18.0	5.0			
1415 MNL		3	2317.9	2318.2	2.1	10.1	4.6			
2695 MNL		3	2318	2318.2	.7	14.5	6.6			
26		208 VORO	24	0037.5	0038	1.5	306.0	27.0		
		200 HIRA	45	0038	0038	1	250.0	100.0		
		200 HIRA	45	0100	0156	80	190.0	20.0		

# SOLAR RADIO EMISSION OUTSTANDING OCCURRENCES

24 OCTOBER - 6 NOVEMBER 1968

	FREQUENCY STATION	TYPE	STARTING TIME	TIME OF MAXIMUM	DURATION	FLUX DENSITY $10^{-22} \text{ Wm}^{-2} \text{ Hz}^{-1}$		INT	REMARKS
			UT	UT	MINUTES	PEAK	MEAN		
26	3750 TYKW	45	0104	0132	90	52.0	26.0		
	2000 TYKW	45	0104	0132	90	73.0	32.0		
	208 VORO	40	0105	0136	32	255.0			
	500 HIRA	45	0115	0153	60	1290.0	230.0		
	1000 TYKW	45	0122	0151	50	5280.0	630.0		
	612 TOKO	45	0128		39	1450.0D			
	208 VORO	45	0145	0157	25	306.0	127.0		
	260 ONDR	45	0845	0845.5	1.5	35.0			
	9139 NEUS	2	1023	1024	4	6.9	3.7		
	9100 GORK	1	1023.2	1023.8	3.4	9.7	4.4		
	202 IZMI	43	1100		60 D	80.0			
	111 POTS	45	1107 U	1326 U		400.0U			
	260 ONDR	44	1109	1308	100	70.0			
	240 KIEL	45	1110	1250		230.0	80.0		
	234 POTS	45	1112 U	1334 U		70.0U			
	408 SANM	43	1120	1247.7	170	80.0	245.0		
	420 KIEL	45	1140	1243	140	70.0	30.0		
	9139 NEUS	22	1155	1158	8.5	14.0	5.7		
	1500 NEUS	22	1155	1213.7	42	3.7	2.5		
	3100 CRIM	1	1156	1158	9	5.0	2.0		
	2920 BERL	22	1156	1158.2	10				
	3000 NERA	5	1157.6	1158	.8	8.0	4.0		
	9139 NEUS	20	1221 E	1221		2.9			
	9139 NEUS	20	1239.8E	1239.8		5.2			
	2920 BERL	20	1243	1256.5	71				
	3100 CRIM	1	1245	1247	5	4.0	1.0		
	9139 NEUS	20	1249	1257	13	6.9	4.3		
	9139 NEUS	1	1341.5	1342.1	.6	9.5	3.2		
	8800 SGMR	20	1457.5	1511.8	31.1	8.8	4.4		
	2495 SGMR	20	1457	1511.5	32.7	4.2	2.1		
	4995 SGMR	20	1458.7	1511.7	44.1	9.0	4.5		
	15400 SGMR	20	1636.4	1647 U	51.5	18.2U	9.1U		
	8800 SGMR	20		1647 U	36.8D	45.5U	22.8U		
	4995 SGMR	20		1647 U	33.3D	26.2U	13.1U		
	2695 SGMR	20		1647 U	35 D	11.7U	5.8U		
	2800 OTTA	23	1637	1650	60	13.0	5.0		
	2800 OTTA	4	1637.5	1638.5	4	16.8	7.0		
	2700 PENN	20	1852.2	1857.6	32.4	10.8	2.6		
	7000 SAOP	4	1853	1854	2.2	17.4	8.7		
	10700 PENN	3	1856.6	1857.6	16.2	24.0	4.1		
	8800 SGMR	3	1857.3	1857.7	4.2	20.3	8.5		
	4995 SGMR	3	1857.4	1857.8	3	17.9	7.2		
	2800 OTTA	2	1857	1857.5	3	5.6	2.8		
	2695 SGMR	1	1857.5	1857.7	4	5.6	2.3		
	2700 PENN	1	1951.6	1952.7	2.2	5.4	1.3		
	2695 SGMR	1	1951.4	1952.8	5	3.3	1.7		
	8800 SGMR	1	1952.1	1952.6	5	4.5	2.2		
	4995 SGMR	1	1952.2	1952.6	4.2	2.9	1.4		
	2800 OTTA	1	1952	1952.8	1.5	2.8	1.4		
	2800 OTTA	22	2015	2025	30	2.4	1.8		
2695 PENT	1	2126	2126.9	1.5	2.8	1.4			
8800 MNL	23	2355.3	0108.7	95	22.0	4.4			
4995 MNL	23	2357	0108.7	125.3	17.5	3.6			
3750 TYKW	45	2357	2400	100	54.0	14.0			
2695 MNL	23	2357	0108.7	164	33.0	6.6			
9400 TYKW	45	2358	2400	100	50.0	18.0			
8800 MNL	3	2358.6	2359.8	4.1	30.1	15.4			
4995 MNL	3	2358.6	2359.6	4.1	41.9	20.1			
2695 MNL	3	2358.6	2359.8	4.1	22.0	11.0			
2000 TYKW	45	2358	0108	80	17.0	5.0			
1415 MNL	23	2358.5	0108.7	162.5	22.2	4.0			
1000 TYKW	45	2358	0108	80	25.0	4.0			
27	208 VORO	43	0018	0258	282	408.0			
	208 VORO	5	0042	0043.5	2.5	306.0			
	500 HIRA	45	0046	0109.5	183	37.0	12.0		
	208 VORO	27	0047	0304	191	255.0	110.0		
	200 GORK	44	0512 E		348 D		18.0		
	100 GORK	44	0520 E		340 D		30.0		
	9100 GORK	1	0755	0756.1	.5	10.0	3.5		
	9139 NEUS	20	0757.5	0803.5	13.2	7.0	3.6		
	1500 NEUS	46	0759.5	0800.7	2.8	5.1	1.4		
	3840 GORK	1	1000	1002.6	3.7	8.7	4.3		
	260 ONDR	45	1019	1027.5	30	30.0			
	9285 ARCE	21	1101.6	1113	18.5	6.0			
	9139 NEUS	3	1104.5	1109	11	35.0			
	9100 GORK	45	1104.7	1105.1	24	28.0	11.0		
	9100 GORK		1104.7	1108.7		51.0			
	9500 NERA	45	1105	1108.8	7.5				
	3840 GORK	45	1105	1105.7	34.8	21.0	6.0		
	3840 GORK		1105	1109		19.0			
	3100 CRIM	3	1105	1106	35	14.0	5.0		
	3000 NERA	45	1105	1105.6	1	17.0	10.0		
	2920 BERL	3	1105	1109.3	18.3				
	2800 SLOU	28	1105	1106.5	90	12.0			
	9285 ARCE	45	1106	1109.1	7.4	26.0			
	9285 ARCE	45	1106	1105.3	1.8	16.0			
	3000 NERA	29	1106	1109.3	26	11.0	6.0		
9285 ARCE	45	1107.8	1109.1	5.6	26.0				
9139 NEUS	20	1129.5	1132.5	10.5	5.6	3.8			

# SOLAR RADIO EMISSION OUTSTANDING OCCURRENCES

24 OCTOBER - 6 NOVEMBER 1968

	FREQUENCY STATION	TYPE	STARTING TIME	TIME OF MAXIMUM	DURATION	FLUX DENSITY		INT	REMARKS
			UT	UT		MINUTES	PEAK		
27	260 ONDR	45	1130	1206	65		35.0		
	9285 ARCE	20	1132.2	1133	4.4		10.0		
	1500 BERL	1	1132 E	1132			1.9		
	9139 NEUS	4	1141.5	1143.3	32.5		39.0	7.9	
	1500 BERL	20	1141	1157	36.5		3.8	2.5	
	9285 ARCE	4	1142.7	1143.4	2.3		25.5		
	3840 GORK	20	1142.6	1143.4	12.4		9.4	4.6	
	2920 BERL	20	1144 E	1144					
	9285 ARCE	29	1145		37		19.5		
	9100 GORK	20	1147		8.9			11.0	
	3100 CRIM	1	1212	1319	70 D		440.0	140.0	
	2800 SLOU	40	1216.5	1217	7		11.0		
	4995 SGMR	4	1231.8	1235.6	24.9		1860.0	420.0	
	2920 BERL	47	1231	1236	129 D				
	2920 BERL		1231	1319					
	2695 SGMR	3	1231.6	1236	23.4		700.0	150.0	
	9139 NEUS	47	1232.5	1235.5	130 D		1610.0		
	7000 SAOP	47	1232.8	1242.4	64.1		1027.9		
	2800 OTTA	23	1232	1332	290		74.0	23.0	
	2800 OTTA	47	1232	1236	20		570.0	95.0	
	9285 ARCE	47	1233.1		55				OFF SCALE
	9285 ARCE	47	1233.1		7.2				OFF SCALE
	8800 SGMR	4	1233.1	1235.6	27.1		1680.0	400.0	
	3000 NERA	47	1233.4	1236.2	21.6		900.0	200.0	
	2800 SLOU	47	1233	1236.3	23		754.0		
	15400 SGMR	3	1234.3	1235.6	32		1400.0	300.0	
	9500 NERA	47	1234.6	1235.6	19				
	1500 BERL	47	1234.5	1237			132.0		
	1500 NEUS		1234.5	1318.7	125.5D		415.0		OFF SCALE
	1420 ARCE	47	1234.8		55.4				
	1420 ARCE	47	1234.8	1236.8	6		84.0		
	1415 SGMR	45	1234.6	1236.2	20.4		125.0	30.0	
	1415 SGMR	45	1234.6	1236.4	20.4		125.0	30.0	
	10700 PENN	45	1235 E		18 D		1200.0D		
	2700 PENN	45	1235 E		18 D		390.0D		
	960 PENN	45	1235 E		18 D		45.0D		
	808 ONDR	45	1235	1237	5.5				
	1420 KIEL	45	1236	1314	68		360.0	70.0	
	606 SGMR	28	1236	1237	4.5		2.6	1.0	
	9285 ARCE	47	1240.3	1242.6	26.5		141.0		
	1420 ARCE	47	1240.8	1242.6	25.4		36.0		
	606 SGMR	45	1240.5	1242.1	17.8		140.0	25.0	
	536 ONDR	45	1241.5	1243	5		110.0		
	420 KIEL	45	1246	1314			420.0	180.0	
	3000 NERA	28	1255		11.1		60.0	30.0	
	2695 SGMR	28	1255	1303.8	11.2		25.9	12.0	
	1415 SGMR	28	1255	1305.2	11.2		24.6	11.0	
	408 SANM	45	1255	1312.9	60		255.0	71.0	
	4995 SGMR	28	1256.7	1303.9	9.5		23.7	10.0	
	2800 SLOU	47	1256	1319.5	32.5		788.0		
	606 SGMR	28	1258.3	1304.6	7.9		2.9	1.0	
	8800 SGMR	28	1300.2	1304.7	6		12.6	5.0	
	960 PENN	45	1300		31		60.0D		
	240 KIEL	45	1305	1313			600.0	120.0	
	234 POTS	45	1305 U	1313 U			200.0U		
	15400 SGMR	45	1306.2	1318.3	28.8		415.0	105.0	
	10700 PENN	45	1306.2	1318.2	21.5		602.0	272.0	
	9500 NERA	47	1306.3	1318.4	20				
	9285 ARCE	47	1306.3	1308.3	4.1		207.0		
	8800 SGMR	45	1306.2	1318.3	28.4		485.0	95.0	
	4995 SGMR	45	1306.2	1319	28.8		860.0	145.0	
	3000 NERA	47	1306.1	1319.2	29		800.0	300.0	
	2800 OTTA	47	1306	1319.5	25		610.0	230.0	
	2700 PENN	3	1306		21.7		400.0D		
	2695 SGMR	45	1306.2	1318.8	28.8		710.0	135.0	
	1420 ARCE	47	1306.2	1308.3	3.8		133.5		
	1415 SGMR	45	1306.2	1313.5	36.5		390.0	90.0	
	808 ONDR	45	1306	1313	40				
	606 SGMR	45	1306.2	1313	49.8		450.0	95.0	
	536 ONDR	45	1306		44		325.0D		
	328 PENN	45	1306	1313.7	17.7		57.6	23.3	
	225 HARS	45	1307.5	1312	5		800.0		
	9285 ARCE	47	1310.4	1313.2	5.3		213.0		
	1420 ARCE	47	1310		6.1				OFF SCALE
	111 POTS	45	1311 U	1416 U			3500.0U		
	260 ONDR	44	1312		115		75.0D		
	260 ONDR	45	1312 U		40		75.0D		
	9285 ARCE	47	1315.7	1318.4	11.9		268.0D		
	1420 ARCE	47	1316.1		14.1				OFF SCALE
	9139 NEUS		1318.3E	1318.3			730.0		
	328 PENN	40	1323.7		277				
	184 BOUL	43	1323 E		620 D		6480.0D	1085.0	
	10700 PENN	29	1327.7	1327.7	423.3		121.0	60.0	
	9500 NERA	29	1327	1340.5	74				
	9285 ARCE	29	1327.5		79.4		81.0		
	2700 PENN	29	1327.7	1327.7	415.3		33.0	16.5	
	2800 SLOU	29	1328.5	1328.5	75		51.0		
	1420 ARCE	30	1330.2		63		21.5		
	960 PENN	40	1331		320				
	1420 ARCE	22	1332.3	1334	10.8		27.0		

# SOLAR RADIO EMISSION OUTSTANDING OCCURRENCES

24 OCTOBER - 6 NOVEMBER 1968

	FREQUENCY STATION	TYPE	STARTING TIME	TIME OF MAXIMUM	DURATION	FLUX DENSITY $10^{22} \text{ Wm}^{-2} \text{ Hz}^{-1}$		INT	REMARKS
			UT	UT	MINUTES	PEAK	MEAN		
	8800 SGMR	29	1334.6	1334.6	180.4	48.6	20.0		
	15400 SGMR	29	1335	1335	180	85.0	35.0		
	4995 SGMR	29	1335	1335	180	90.2	40.0		
	3000 NERA	29	1335		145 D	75.0			
	2695 SGMR	29	1335	1335	180	64.0	30.0		
	1415 SGMR	29	1342.7	1342.7	197.3	21.0	9.0		
	408 SANM	44	1355	1515	310	149.0	70.0		
	606 SGMR	22	1358	1552	332	160.0	60.0		
	8800 SGMR	20	1810.1	1814.6	21.9	7.4	3.0		
	4995 SGMR	20	1811.2	1819	21.1	2.9	1.5		
	2800 OTTA	20	1815	1820	10	3.2	1.6		
	4995 SGMR	22	1840.8	1844	34.5	8.6	4.0		
	2800 OTTA	22	1842	1845	15	5.4	2.4		
	2700 PENN	20	1843.2	1844	16.6	6.7	2.0		
	2695 SGMR	20	1843.6	1844.1	8.5	7.1	3.5		
	2800 OTTA	1	1957	1959	5	5.4	2.7		
	2700 PENN	20	1957.2	1958.7	14.6	6.0	2.0		
	2695 SGMR	22	1957.3	1959.7	16.9	7.6	3.5		
	208 VORD	27	2200	2301.7	107	95.0	48.0		
28	17000 TOKO	45	0203.4	0203.8	.9	18.0			
	9400 TYKW	5	0203	0204	4	31.0	11.0		
	8800 MNL	3	0203	0203.8	7 D	31.0	15.5		
	3750 TYKW	5	0203	0204	4	43.0	16.0		
	2000 TYKW	5	0203	0204	3	17.0	6.0		
	1415 MNL	3	0203.1	0204.1	6.9D	10.6	5.3		
	1000 TYKW	5	0203	0204	2	3.0	1.0		
	9400 TYKW	45	0348	0350.7	5	11.0	2.0		
	3750 TYKW	5	0406	0409	8	24.0	9.0		
	9400 TYKW	5	0506	0508	7	69.0	15.0		
	9100 GORK	3	0506	0507.4	5	54.0	24.0		
	8800 MNL	3	0506.8	0507.7	16.7	81.9	40.9		
	4995 MNL	3	0506.8	0507.7	16.7	121.9	60.9		
	3840 GORK	3	0506	0507.4	9	63.0	13.0		
	3750 TYKW	5	0506	0508	7	68.0	16.0		
	3100 CRIM	3	0506	0507	6	39.0	10.0		
	2950 GORK	3	0506.2	0507.3	8.6	69.0	17.0		
	2695 MNL	3	0506.8	0507.7	16.7	37.5	18.8		
	2000 TYKW	5	0506	0508	4	12.0	4.0		
	17000 TOKO	5	0507	0507.9	2	14.0			
	9400 TYKW	5	0555	0556	3	26.0	4.0		
	9100 GORK	1	0555.4	0556.1	1.4	17.0	5.6		
	3840 GORK	1	0555.5	0556.5	2.3	7.9	2.2		
	3750 TYKW	5	0555	0556	3	9.0	2.0		
	2000 TYKW	5	0555.5	0556	1	8.0	2.0		
	100 GORK	44	0640 E		320 D		26.0		
	111 POTS	45	0651.1	0651.2	.2	300.0	60.0		
	100 GORK	1	0815	0824.5	66	92.0			
	9285 ARCE	20	0836.4	0837	3	3.5			
	9139 NEUS	22	0836	0836.8	14	11.0			
	2950 GORK	20	0838.4	0846.7	13	8.1			
	2920 BERL	20	0841.7E	0841.7					
	9100 GORK	20	0924.9	0926.8	10.4	11.0	4.2		
	3840 GORK	20	0925.2	0930 U	15.4	2.7	1.2		
	3840 GORK	1	0941.6	0942.1	5.9	7.3	1.5		
	9285 ARCE	21	0949.4	0950.4	27.6	3.5			
	1420 ARCE	2	0953.7	0954.1	1.4	3.0			
	9285 ARCE	1	0954	0954.3	.9	3.5			
	9139 NEUS	20	0954 E	0954		2.9			
	2920 BERL	1	0954 E	0954					
	1500 NEUS	1	0954 E	0954		4.2			
	9100 GORK	20	1046.4	1047.5	15.8	10.0	4.5		
	3840 GORK	20	1046.5	1104.7	18.2	4.9	2.3		
	100 GORK	6	1050	1050.8	3	100.0D			
	9100 GORN	20	1106.4	1112.7	7.3	9.4	2.8		
	7000 SAOP	22	1110.4		5.9	8.7	4.3		
	9139 NEUS	20	1113 E	1113		4.3			
	260 ONDR	5	1131	1131	1	25.0			
	9139 NEUS	20	1149.8E	1149.8		4.3			
	260 ONDR	5	1153	1153	1	45.0			
	111 POTS	5	1232.9	1233	.2	600.0			
	184 BOUL	43	1324 E		615 D		200.0		
	2700 PENN	20	1334.4	1349.2	107.8	14.7	4.7		
	10700 PENN	20	1344.8	1358.7	106.8	22.0	12.1		
	2800 SLOU	20	1345	1349.8	11	15.0			
	1500 NEUS	22	1345	1359	30	3.6	2.6		
	1420 ARCE	22	1345.3	1358.8	29.2	5.0			
	9285 ARCE	22	1346.8	1359	60 U	10.0			
	9139 NEUS	22	1346	1358.8	44	20.0			
	7000 SAOP	21	1346.2		105.1				
	3000 NERA	27	1346.3	1350.8	30	10.0	5.0		
	3000 NERA	5	1348	1348.9	2	8.0	5.0		
	7000 SAOP	3	1356.5	1357.3	1.7	13.0	6.5		
	8800 SGMR	1	1357.7	1358.8	1.6	4.1	1.5		
	4995 SGMR	3	1357.7	1358.7	1.7	7.9	3.0		
	2695 SGMR	1	1357.7	1358.5	1.7	3.5	1.5		
	3000 NERA	5	1358.3	1358.6	1.2	6.0	3.0		
	606 SGMR	46	1358.3	1358.6	1.2	180.0	20.0		
	600 UCCL	45	1359		1	40.0	20.0		
	7000 SAOP	3	1626.4	1630.2	2.3	30.4	15.2		

# SOLAR RADIO EMISSION OUTSTANDING OCCURRENCES

24 OCTOBER - 6 NOVEMBER 1968

	FREQUENCY STATION	TYPE	STARTING TIME	TIME OF MAXIMUM	DURATION	FLUX DENSITY $10^{22} \text{ Wm}^{-2} \text{ Hz}^{-1}$		INT	REMARKS
			UT	UT	MINUTES	PEAK	MEAN		
	10700 PENN	3	1629.3	1630	4.8	16.4	4.1		
	4995 SGMR	3	1629.8	1630.1	1.7	20.4	5.0		
	2800 OTTA	1	1629	1630	2	12.6	6.0		
	2700 PENN	3	1629.1	1630	4.2	12.1	1.6		
	2695 SGMR	3	1629.8	1630.2	1.4	8.8	4.0		
	960 PENN	1	1629.7	1630.3	1.8	1.9	1.0		
	8800 SGMR	3	1630	1630.1	.5	9.0	3.5		
	10700 PENN	3	1942.7	1943.1	4.3	16.4	7.4		
	8800 SGMR	4	1942.6	1943.2	6	20.7	5.0		
	4995 SGMR	4	1942.8	1943.8	8.4	31.3	6.0		
	2700 PENN	1	1942.6	1943.1	4.3	5.7	1.5		
	606 SGMR	1	1942.7	1943.2	1.8	2.1	1.0		
	7000 SAOP	4	1943.2	1943.6	1.7	28.2	14.1		
	2695 SGMR	1	1943	1943.2	4.3	3.3	1.5		
	2695 PENT	1	2127	2127.5	1	2.8	1.4		
	208 VORO	44	2200	0014	360	390.0			
29	612 TOKO	45	0012.3	0012.8	3	22.0			
	500 HIRA	45	0012.7	0012.7	3	100.0	7.0		
	200 HIRA	45	0014	0014	.8	620.0	110.0		
	1000 TYKW	45	0102	0139.5	50	79.0	4.0		
	8800 MNL	20	0241.1	0244.7	15.1	22.5	6.7		
	4995 MNL	20	0241.1	0244.7	15.1	5.0	1.7		
	650 GORK	3	0507.6	0508.1	1	19.5	8.0		
	2695 MNL	23	0508.7	0518	94.6	24.5	12.3		
	1415 MNL	23	0508.7	0516.3	67.6	16.9	8.5		
	3750 TYKW	45	0510	0518	10	27.0	4.0		
	3840 GORK	21	0513	0635 U	313.5	20.0			
	4995 MNL	4	0514	0518	7	22.2	11.1		
	200 GORK	44	0515 E		414 D		60.0		
	100 GORK	44	0515 E		414 D		100.0		
	3840 GORK	3	0516	0518	4	29.0	7.1		
	2000 TYKW	45	0516	0518	3	8.0	2.0		
	1000 TYKW	45	0517.8	0518	1	12.0	5.0		
	2950 GORK	21	0518	0554.1	62.5D	44.0			
	2950 GORK	3	0522.4	0522.9	16	29.0	14.0		
	9400 TYKW	5	0546	0548	20	15.0	3.0		
	8800 MNL	20	0546.1	0548.5	22.6	20.9	10.5		
	4995 MNL	20	0546.1	0548.5	78.4	22.2	11.1		
	3750 TYKW	45	0546	0549	20	15.0	3.0		
	3100 CRIM	3	0546	0549	18	19.0	4.0		
	2695 MNL	20	0546.6	0548.5	10.9	11.0	5.5		
	2000 TYKW	5	0546	0548	20	12.0	2.0		
	1415 MNL	20	0546.6	0548.5	9.4	5.9	2.9		
	3840 GORK	1	0700.2	0701.9	4.3	7.3	2.9		
	202 IZHI	40	0702	0706	4.2	700.0			
	260 ONDR	45	0704.5	0707	3	80.0D			
	111 POTS	45	0710.5	0711.5	1.7	600.0	120.0		
	8800 MNL	3	0727.5	0728.2	18.5	18.6	9.3		
	9139 NEUS	3	0729.5	0730.5	2	11.0	3.1		
	9100 GORK		0735 E		24 D				
	260 ONDR	5	0815	0815	1.5	80.0D			
	9139 NEUS	1	0817.2E	0817.2		6.1			
	111 POTS	45	0817.4	0817.7	.4	500.0	70.0		
	3840 GORK	1	0818.9	0824	6.4	6.6	3.4		
	3100 CRIM	45	0823	0824	4	7.0	2.0		
	3100 CRIM		0823	0825		5.0	15.0		
	600 UCCL	27	0844.5	0930	103.5	16.0	8.0		
	650 GORK	21	0846.8	0954.6	76.3	12.3	4.0		
	650 GORK	20	0846.8	0923.7	76.3	8.4	4.0		
	3100 CRIM	3	0853	0853 D	110 D				
	3100 CRIM	3	0853	0904	11	39.0	12.0		
	9285 ARCE	24	0854		3.6	6.0			
	9100 GORK	21	0854	1146.8	252	48.0			
	3000 NERA	27	0855	0858	98	18.0	10.0		
	1420 ARCE	22	0855	0912	44.7	3.5			
	9139 NEUS	20	0856	0909.5	42	21.0			
	3000 NERA	5	0856.6	0857.2	1	8.0	4.0		
	1500 NEUS	20	0856.5	0909.5	45.5	2.5	1.8		
	9500 NERA	5	0857.1	0857.5	.9				
	9285 ARCE	20	0900	0910.2	39	17.0			
	9285 ARCE	20	0900	0905.5	6	13.0			
	260 ONDR	41	0900		132	80.0D			
	9285 ARCE	20	0906	0910.2	33	17.0			
	200 GORK	41	0935.2	0938.2	11.3	3490.0			
	200 GORK		0935.2	0944		2350.0			
	9139 NEUS	22	0942	0947.4	245	22.0	11.0		
	9285 ARCE	21	0943	0957.7	29.3	10.0			
	9285 ARCE	20	0943.7	0945.5	9.4	17.0			
	9285 ARCE	20	0943.7	0944.4	3.3	13.0			
	239 TRST	45	0943.5	0943.6	.4	860.0	155.0		
	234 POTS	45	0943.5	0943.6	.2	600.0	150.0		
	2920 BERL	21	0945	0958	25.5				
	9285 ARCE	20	0947	0947.5	6.1	17.0			
	3840 GORK	3	0948.3	0954.5	6.9	81.0	40.0		
	1500 BERL	21	0948	1001	20.5	1.9			
	1420 ARCE	21	0948	1000.8	29.4U	2.0			
	9500 NERA	.5	0953.8	0954.3	1.2				
	9285 ARCE	3	0953.9	0954.5	2.4	50.0			
	9139 NEUS	3	0953.5	0954.6	1.5	807.7	32.0		

# SOLAR RADIO EMISSION OUTSTANDING OCCURRENCES

24 OCTOBER - 6 NOVEMBER 1968

	FREQUENCY	STATION	TYPE	STARTING TIME	TIME OF MAXIMUM	DURATION	FLUX DENSITY $10^{-22} \text{ W m}^{-2} \text{ Hz}^{-1}$		INT	REMARKS
				UT	UT	MINUTES	PEAK	MEAN		
				29	9100 GORK	3	0953.8	0954.6		
	3100 CRIM	3	0953	0954	6	52.0	20.0			
	3000 NERA	5	0953.6	0954.4	1.4	50.0	25.0			
	2950 GORK	3	0953.6	0954.3	1.4	30.0	10.0			
	2920 BERL	3	0953.5	0954.4	3.5					
	2800 SLOU	3	0953.5	0954	3.8	37.0				
	1500 BERL	4	0953.5	0954.6	3	22.0	8.0			
	1420 ARCE	3	0953.7	0954.6	1.8	21.0				
	650 GORK	3	0953.7	0954.6	2.6	9.3	3.0			
	239 TRST	40	0953.5	0954.7	1	110.0				
	239 TRST	45	0953.6	0953.6	.6	490.0	69.0			
	234 POTS	45	0953.6	0953.6	1.1	150.0	5.0			
	202 IZMI	5	0953.5	0954	2.5	500.0	300.0			
	200 GORK	48	0953.6	0953.8	3	4140.0				
	111 POTS	45	0953.6	0954.1	3.4	1900.0	250.0			
	100 GORK	48	0953.5	0954.4	7.7	170.00				
	600 UCCL	27	0954.5	0955.5	2.5	14.0	7.0			
	23 POTS	45	0954.2	0954.8	1	6000.0	1500.0			
	1420 ARCE	29	0955.5		3.4	9.5				
	1500 NEUS	1	1010	1010.3		4.3				
	1420 ARCE	1	1010.3	1010.3	.5	3.5				
	9139 NEUS	20	1016.3	1017.3	3.7	6.1	3.2			
	9285 ARCE	23	1111.5	1128.7	243	42.0				
	9139 NEUS	47	1132	1222	190 D	370.0				
	3000 NERA	24	1132	1255	268 D	75.0				
	2920 BERL	47	1132	1226	188 D					
	2920 BERL		1132	1254						
	3840 GORK	28	1134.2	1216.1	44.3	18.0	6.7			
	7000 SAOP	47	1136.6	1248.7	87.4	669.8				
	9285 ARCE	20	1146.7	1147.8	2	26.0				
	10700 PENN	45	1205	1205 E	55 D	650.00				
	2700 PENN	41	1205	1205 E	69 D	185.00				
	960 PENN	41	1205	1205 E	248 D	60.00				
	2695 SGMR	28	1209.3	1218.7	9.4	2.8	1.4			
	9285 ARCE	28	1210.2		8.6	47.0				
	9100 GORK	45	1210	1226.2	45	619.0	92.0			
	9100 GORK		1210	1229.3		330.0				
	4995 SGMR	28	1210	1218.6	8.6	31.9	16.0			
	606 SGMR	28	1210.5	1218.4	7.9	3.7	1.8			
	15400 SGMR	28	1212.9	1218.5	5.6	23.1	11.6			
	9500 NERA	27	1213	1230	60					
	8800 SGMR	28	1213.7	1218.3	4.6	24.7	12.3			
	3100 CRIM	1	1213	1227	120 D	310.0				
	2950 GORK	45	1213.2	1226.5	65 D	225.0				
	2950 GORK		1213.2	1253.4		230.0				
	234 POTS	45	1213	1520 U		5000.0U				
	19000 SLOU	46	1214	1226.5	35	400.0				
	1415 SGMR	28	1214	1218.7	4.7	3.2	1.6			
	650 GORK	45	1215.3	1232.7	58.7D	1090.0				
	650 GORK		1215.3	1219.1		44.0				
	650 GORK		1215.3	1239.4		120.0				
	650 GORK		1215.3	1247.8		280.0				
	650 GORK		1215.3	1256		360.0				
	650 GORK		1215.3	1311.5		240.0				
	408 SANM	47	1215	1236	67	1814.0	252.0			
	260 ONDR	45	1217		165	80.00				
	15400 SGMR	45	1218.5	1226.1	58	485.0	37.8			
	9285 ARCE	47	1218.8	1226.7	18	270.00				
	9285 ARCE	47	1218.8	1222.2	5.7	178.0				
	8800 SGMR	45	1218.3	1226	63.3	630.0	160.0			
	4995 SGMR	45	1218.6	1226.1	60.2	440.0	160.0			
	3840 GORK	45	1218.5	1226.2	48.5	265.0	70.0			
	3840 GORK		1218.5	1229.2		201.0				
	3840 GORK		1218.5	1234.8		152.0				
	2695 SGMR	45	1218.7	1253.4	63.3	215.0	66.7			
	1500 BERL	47	1218	1222	142 D	155.0				
	1500 NEUS		1218	1311		6500.00				
	1420 ARCE	40	1218.6	1233.3	136.4	144.0				
	1415 SGMR	45	1218.7	1310.9	63.5	10900.0	70.0			
	606 SGMR	45	1218.4	1233.1	57.6	2030.0	230.0			
	2800 SLOU	46	1219	1228	27	143.0				
	1420 KIEL	24	1219	1312	56	8500.0	140.0			
	600 UCCL	45	1219.5	1224	168	720.0	97.0			
	9500 NERA	45	1220.5	1222.1	3.4					
	3000 NERA	45	1220.4	1226.4	16.2	160.0	75.0			
	328 PENN	45	1220.6	1249	37.4	330.00	140.00			
	225 HARS	45	1220	1255	190 D	1000.00				
	202 IZMI	47	1220	1256	63	1250.0	500.0			
	420 KIEL	45	1221	1237	176	2500.0	250.0			
	200 GORK	49	1221	1313.6U	53 D	53270.0				
	240 KIEL	45	1222	1405	176	1800.0	350.0			
	9285 ARCE	47	1224.5	1226.7	8.6	270.00				
	9500 NERA	45	1225	1226.2	5					
	808 ONDR	45	1225.5		65	365.00				
	536 ONDR	45	1225.5		95 U	780.0				
	9139 NEUS		1226	1226		14.0				
	2800 OTTA	40	1230	1250	50 D					
	9500 NERA	45	1232.8	1234.6	4					
	9285 ARCE	47	1233.1	1233.7	3.7	131.0				
	9285 ARCE	29	1236.8		45	90.0				

# SOLAR RADIO EMISSION OUTSTANDING OCCURRENCES

24 OCTOBER - 6 NOVEMBER 1968

	FREQUENCY STATION	TYPE	STARTING TIME	TIME OF MAXIMUM	DURATION	FLUX DENSITY $10^{22} \text{ Wm}^{-2} \text{ Hz}^{-1}$		INT	REMARKS
			UT	UT	MINUTES	PEAK	MEAN		
29	100 GORK	49	1237.2	1305.5	36.8	142000.0			
	111 POTS	45	1238 U	1423 U		5000.0U			
	2800 SLOU	46	1246	1253.5	19	143.0			
	3000 NERA	45	1248.8	1253.5	6.2	200.0	50.0		
	7000 SAOP	29	1254.2		120				
	328 PENN	40	1258		177.6				
	10700 PENN	29	1300	1300		130.0D			
	1420 ARCE	40	1302 E	1302		149.5			OFF SCALE
	2800 SLOU	46	1305	1312	19	73.0			
	3000 NERA	45	1306.5	1311	7.5	80.0	40.0		
	408 SANM	45	1308	1311.5	5	231.0	75.5		
	2700 PENN	29	1314.4	1314.4		50.0D			
	606 SGMR	23	1316	1403.8	107	70.0	18.6		
	4995 SGMR	30	1318.8	1318.8	343.6	25.2	12.6		
	2695 SGMR	30	1322	1322	311.3	25.3	12.6		
	1415 SGMR	30	1322.2	1322.2	405.1	43.7	21.8		
	408 SANM	29	1325	1405	110	299.0	125.0		
	184 BOUL	43	1325 E		615 D		1304.0		
	606 SGMR	3	1335.7	1337.3	62	85.0	40.0		
	2695 SGMR	21	1336.6	1355.3	57.6	11.7	5.9		
	9285 ARCE	20	1337	1355.1	42.2	47.0			
	2800 OTTA	23	1337	1350	65	7.2	3.6		
	2695 SGMR	3	1338.8	1339.5	2.1	11.5	5.7		
	1415 SGMR	46	1338	1340.5	35.9	50.0	6.8		
	1415 SGMR	46	1338	1407.6	35.9	50.0	6.8		
	2800 OTTA	1	1339	1339.5	2	9.0	4.5		
	4995 SGMR	22	1342.2	1349.6	32.1	7.5	3.8		
	328 PENN	5	1347.3	1402.2	37.7	100.0	40.8		
	2695 SGMR	1	1348.4	1348.8	2.9	6.9	3.5		
	2695 SGMR	1	1354.6	1355.1	1.9	4.8	2.4		
	23 POTS	45	1403 U	1517 U		6000.0U			
	4995 SGMR	3	1421.9	1424.4	6.7	16.3	8.1		
	2695 SGMR	45	1422.5	1425.5	5.4	13.8	5.8		
	1415 SGMR	22	1422	1424.6	8.4	12.4	6.2		
	2800 OTTA	1	1424	1424.5	2	7.2	3.6		
	18 MCMA	41	1437	1447	11				
	2800 SLOU	46	1507 U	1524 U	60 D	500.0D			
	3000 NERA	47	1515.8	1522.5	44 D	3800.0			
	2800 OTTA	47	1515.7	1523	80	3900.0	1240.0		
	2700 PENN	45	1515.8		60.8	819.0D	460.0D		
	2695 SGMR	47	1515.9	1519.2	37.4	6040.0	1790.0		
	1420 ARCE	47	1515.2						SUNSET
	1415 SGMR	47	1515.6	1524.3	52.4	81000.0D			
	606 SGMR	47	1515.8	1521.8	22.5	260000.0D	5000.0		
	328 PENN	45	1515.6		24.8	270.0D	230.0D		
	19000 SLOU	46	1516.5	1522	21	220.0			
	15400 SGMR	47	1516.7	1522	21.8	340.0	200.0		
	10700 PENN	3	1516.6	1522.1	63.4	470.0	135.0		
	7000 SAOP	47	1516.1	1522.2	20.9	790.3			
	4995 SGMR	47	1516.8	1531.5	35.2	1040.0	240.0		
1420 KIEL	24	1516	1525		35000.0	1000.0			
408 SANM	47	1516	1517.5	54	8500.0	2005.0			
9500 NERA	47	1517.5	1522.1	43 D					
9285 ARCE		1517.5						SUNSET	
8800 SGMR	47	1517	1522.1	35.5	670.0	170.0			
600 UCCL	24	1517	1625 U	55 D	1350.0D				
420 KIEL	45	1517			20000.0U	5000.0			
240 KIEL	45	1518	1525		6000.0	2000.0			
184 BOUL	48	1520	1520 U	18	6480.0D	5060.0			
7000 SAOP	29	1537		57					
15400 SGMR	29	1538.5	1538.5	67.4	120.0	60.0			
606 SGMR	29	1538.3	1538.3	157.3	120.0	60.0			
328 PENN	29	1540.4	1540.4	71.2	18.3	9.2			
8800 SGMR	29	1552.5	1552.5	43.2	120.0	60.0			
4995 SGMR	29	1552	1552	46	485.0	240.0			
2695 SGMR	30	1553.3	1553.3	59.4	300.0	150.0			
1415 SGMR	29	1608	1608	10.9	35.1	17.5			
960 PENN	29	1613.6	1613.6		30.0D				
2700 PENN	29	1616.6	1616.6	20.6	45.0	22.5			
10700 PENN	29	1620	1620	54.6	36.7	18.4			
2800 OTTA	45	1647.5	1649	6	34.0	20.0			
2800 OTTA	45	1647.5	1649	6	34.0				
2800 OTTA	45	1651.5	1652	2	34.0				
408 SANM	3	1650	1650.8	1.5	51.0	27.0			
2800 OTTA	29	1653.5	1653.5	25	8.0	4.0			
4995 SGMR	20	1708.5	1709.2	8.3	5.4	2.7			
2800 OTTA	1	1708.5	1709.3	2	5.6	2.8			
4995 SGMR	3	1754.3	1754.9	2.4	22.4	11.2			
2800 OTTA	1	1754.5	1755	2	5.6	2.8			
2695 SGMR	1	1754.4	1754.9	2.1	6.4	2.5			
2800 OTTA	22	1820	1824	18	5.6	2.8			
2700 PENN	3	1829	1829	.2	13.5	2.3			
10700 PENN	3	1831.9	1832	1.7	11.7	2.7			
960 PENN	3	1831.9	1832	.4	9.3	4.7			
2700 PENN	1	1832	1832.1	2	3.1	1.1			
328 PENN	5	1833.6	1833.9	.4	17.8	5.9			
7000 SAOP	45	1846.4	1851.8	13.6	84.8				
10700 PENN	3	1847	1851.9	12.7	64.1	11.6			
8800 SGMR	45	1847.3	1851.9	19.3	86.0	20.3			
4995 SGMR	45	1847.1	1849.1	6.6	130.0	52.0			

# SOLAR RADIO EMISSION OUTSTANDING OCCURRENCES

24 OCTOBER - 6 NOVEMBER 1968

	FREQUENCY STATION	TYPE	STARTING TIME	TIME OF MAXIMUM	DURATION	FLUX DENSITY $10^{22} \text{ W m}^{-2} \text{ Hz}^{-1}$		INT	REMARKS
			UT	UT	MINUTES	PEAK	MEAN		
30	2700 PENN	3	1847.2	1849	5.7	32.2	12.7		
	2695 SGMR	45	1847.5	1849.3	5.5	35.7	21.3		
	960 PENN	45	1848.3	1849.1	11.5	24.7	1.3		
	2700 PENN	29	1852.9	1852.9	22.3	8.0	4.0		
	4995 SGMR	29	1853.7	1853.7	13.7	15.0	7.5		
	2695 SGMR	29	1853	1853	13.2	8.1	4.0		
	2695 SGMR	1	2043.1	2043.7	1	4.4	1.3		
	4995 SGMR	3	2100.3	2101.3	3.4	12.2	6.1		
	2695 SGMR	3	2100.4	2101.5	2.2	9.7	3.9		
	8800 SGMR	1	2101.1	2101.3	1.9	6.8	3.4		
	2800 OTTA	1	2101	2101.5	1	2.5	1.2		
	2800 OTTA	1	2116.5	2117	2	5.4	2.7		
	2800 OTTA	1	2136.8	2137	1	3.0	1.5		
	2800 OTTA	1	2157	2158	3	3.0	1.5		
	208 VORO	44	2200	0108	360	545.0			
	500 HIRA	45	0020.5	0113.8	156.5	270.0	10.0		
	9400 TYKW	29	0040		210	80.0	30.0		
	3750 TYKW	29	0040		240	60.0	20.0		
	2000 TYKW	29	0040		170	50.0	17.0		
	8800 MNL	4	0132.5	0134	29.2	58.0	4.5		
	4995 MNL	4	0132.3	0134	22.7	54.0	4.8		
	2695 MNL	4	0132.3	0134.1	37.7	28.4	2.8		
	1415 MNL	4	0132.3	0133.9	17.7	42.6	4.2		
	9400 TYKW	5	0133	0134	10	52.0	13.0		
	3750 TYKW	45	0133	0134	10	42.0	9.0		
	2000 TYKW	45	0133	0134	10	17.0	4.0		
	1000 TYKW	45	0134	0134.4	20	32.0	4.0		
	3750 TYKW	5	0216	0217	2	8.0	3.0		
	8800 MNL	4	0247.5	0248.5	4.5	17.9	6.7		
	4995 MNL	4	0247.5	0248.4	4.5	12.7	4.8		
	9400 TYKW	5	0248	0248.5	2	21.0	7.0		
	3750 TYKW	5	0248	0248.5	2	3.0	1.0		
	1415 MNL	2	0248	0248.8	4	5.9	2.5		
	600 UCCL	45	0631 E		70 D				
	3840 GORK	1	0633.7	0634.9	5.1	11.0	4.4		
	260 ONDR	44	0640		500	85.0D			
	202 IZMI	44	0700		300	400.0			
	111 POTS	40	0737 U	0753 U	49 U	4400.0	100.0		
	9100 GORK	21	0750.5	0836.9	74.5	16.0	6.0		
	6100 KISV	5	0750.5	0752	5	50.0	9.5		
	3840 GORK	45	0750	0752.5	36.3	83.0	8.0		
	3840 GORK		0750	0801.3		28.0			
	3000 NERA	45	0750.9	0752.5	2.3	70.0	30.0		
	2920 BERL	3	0750.5	0752.5	251.9				
	9139 NEUS	3	0751	0752.3	24	24.0	5.0		
	9100 GORK	1	0751.7	0752.5	3.3	27.0	7.2		
	8800 MNL	3	0751.7	0752.3	1.1	27.2	13.6		
	4995 MNL	3	0751.2	0752.3	1.6	84.3	42.2		
	3100 CRIM	45	0751	0752.5	35				
	3100 CRIM	3	0751	0752.5	5	95.0	30.0		
2695 MNL	3	0751.2	0752.5	1.6	46.7	23.4			
1500 NEUS	3	0751.5	0752.5	15	10.8	3.6			
1420 ARCE	3	0751.8	0752.7	1.7	11.5				
1415 MNL	3	0751.7	0752.5	1.1	11.3	5.6			
234 POTS	45	0751.9	0752.2	.4	120.0	20.0			
2800 SLOU	3	0752.6	0753.8	3	55.0				
1420 ARCE	30	0753.5		57 U	5.0				
6100 KISV	45	0759.5	0801	3.5	20.0	5.0			
9139 NEUS	4	0800.5	0801.4	2.5	173.3	4.1			
9100 GORK	1	0800.6	0801.4	2	20.0	7.9			
9285 ARCE	20	0801.4	0801.7	1.6	7.0				
8800 MNL	3	0801.2	0801.5	2.8	27.7	11.3			
4995 MNL	3	0801.2	0801.5	2.8	29.3	14.8			
3100 CRIM	3	0801	0802	3	27.0	9.0			
3000 NERA	45	0801	0801.2	1.3	15.0	9.0			
2920 BERL	4	0801	0801.5	1.7					
2695 MNL	3	0801.2	0801.5	2.8	8.8	4.4			
1500 NEUS	22	0801	0801.5	2	2.4	1.8			
1420 ARCE	20	0801.4	0801.5	1	3.5				
1415 MNL	1	0801.2	0801.5	2.8	1.7	.9			
234 POTS	45	0824.1	0824.1	.1	350.0	70.0			
3840 GORK		0830		15 D					
3100 CRIM	20	0830	0830 D	90					
3100 CRIM	20	0830	0841	90	13.0	4.0			
600 UCCL	45	0912	0915	8	8.0				
9500 NERA	40	0915	0915.8	6					
3100 CRIM	3	0916	0924	8	37.0	12.0			
3000 NERA	27	0916.6	0923.5	39	17.0	8.0			
9139 NEUS	20	0917	0923.5	70	15.0	7.8			
2920 BERL	20	0917	0923.5	38					
9100 GORK	20	0918.3	0920	28.3	18.0	10.0			
9285 ARCE	20	0919.7	0923.4	32	10.0				
1500 NEUS	20	0919	0923.5	24	3.5	2.3			
1420 ARCE	21	0919	0927	23.2	2.5				
1420 ARCE	20	0922.6	0923.7	3.4	2.5				
2800 SLOU	20	0929	0935.5	39	16.0				
3840 GORK		0930 E		20 D					
9139 NEUS	22	1102	1117.3	25	9.8				
3000 NERA	27	1105	1120.9	30	13.0	6.0			

# SOLAR RADIO EMISSION OUTSTANDING OCCURRENCES

24 OCTOBER - 6 NOVEMBER 1968

	FREQUENCY	STATION	TYPE	STARTING TIME	TIME OF MAXIMUM	DURATION	FLUX DENSITY		INT	REMARKS
				UT	UT	MINUTES	$10^{22} \text{ Wm}^{-2} \text{ Hz}^{-1}$ PEAK	MEAN		
30	2920	BERL	22	1105	1117	32				
	1500	NEUS	22	1105	1117	37	5.0	2.8		
	3100	CRIM	28	1106	1117	25	25.0	8.0		
	9285	ARCE	22	1111	1117.3	26.8	6.0			
	7000	SAOP	45	1113.6	1116.4	4.4	17.9	8.9		
	9100	GORK	1	1115.4	1117.2	5.7	12.0	5.0		
	3000	NERA	45	1115.5	1116.1	2.5	16.0	10.0		
	2800	SLOU	46	1115	1117	9	144.0			
	7000	SAOP	29	1118		7.4				
	600	UCCL	5	1120.5		.5	18.0	4.0		
	536	ONDR	5	1120	1120	1.5	190.0			
	10700	PENN	20	1201 E	1336.7	570 D	100.0D	40.0D		
	2700	PENN	20	1202 E	1436	570 D	45.0D	20.0D		
	960	PENN	40	1208		82				
	15400	SGMR	21	1215.9	1252	484.2U	52.0	26.0		
	8800	SGMR	21	1216.2	1246	491.3U	81.0	40.5		
	606	SGMR	23	1216.3	1340.2	557.7D	37.3	18.6		
	1415	SGMR	21	1217.6	1417.5	556.4D	18.7	9.4		
	2695	SGMR	21	1218.9	1251.5	401.2	41.9	20.9		
	3840	GORK	3	1225.5	1227.8	4.6	31.0	15.0		
	4995	SGMR	21	1228.6	1255.6	485.4U	80.0	40.0		
	9139	NEUS	22	1230	1252.3	140 D	64.0			
	4995	SGMR	3	1230.7	1232.7	5.5	28.2	11.3		
	2920	BERL	22	1230	1251.5	140				
	2920	BERL		1230	1342.2					
	15400	SGMR	3	1231.3	1232.9	3.8	12.3	5.0		
	9100	GORK	3	1231.4	1232.6	2.6	65.0	25.0		
	8800	SGMR	3	1231.3	1232.7	4.7	34.0	14.0		
	7000	SAOP	45	1231.6		53.2	49.1	26.8		
	3100	CRIM	40	1231	1252	60 D	53.0			
	3000	NERA	24	1232	1341	60	35.0			
	1415	SGMR	1	1232	1232.3	2.2	1.8	.9		
	2800	OTTA	23	1235	1340	275	50.0	20.0		
	2800	OTTA	23	1235	1250	50	32.0			
	15400	SGMR	3	1237.4	1238.5	2.9	14.7	6.0		
	8800	SGMR	3	1237.5	1238.5	3.1	27.6	12.0		
	4995	SGMR	3	1237.4	1238.5	2.9	36.7	14.7		
	2700	PENN	20	1237.3	1336.8	115.7	37.6	15.1		
	2695	SGMR	3	1237.9	1238.5	1.7	9.7	3.8		
	1500	BERL	22	1237	1252	133	10.0			
	1415	SGMR	1	1237.9	1238.5	1	3.1	1.2		
	3000	NERA	5	1238	1238.5	2	15.0	8.0		
	2800	OTTA	1	1238	1238.5	1	9.0	4.5		
	4995	SGMR	45	1242.2	1251.8	12.6	21.1	8.4		
	15400	SGMR	3	1245.6	1247.4	2.9	10.3	5.2		
	8800	SGMR	45	1246.7	1247.4	8	28.5	13.2		
	1415	SGMR	1	1251.2	1252	1.9	4.9	2.4		
	240	KIEL	45	1253 E	1253 U		800.0	250.0		
	18	BOUL	41	1256 U	1305	20				
	18	MCMA	48	1258 U	1302	6 U				
	111	POTS	45	1305 U	1427 U		3000.0U			
	23	POTS	45	1306 U	1443 U		400.0U			
	606	SGMR	4	1311	1311.7	.9	185.0	37.0		
	600	UCCL	5	1311.5		1	117.0	50.0		
	536	ONDR	5	1311.5	1311.5	1.5	80.0			
	420	KIEL	45	1316	1318 U		400.0D	50.0		
	7000	SAOP	22	1321.5	1355.3	57	58.0	29.0		
	8800	SGMR	23	1324.6	1338	63.6	29.0	14.5		
	4995	SGMR	23	1325	1339.7	83.8	46.6	23.3		
	2800	OTTA	23	1325	1340	225	50.0			
	2695	SGMR	23	1326.5	1341.5	96.3	24.2	12.1		
	184	BOUL	43	1326 E		615 D		2170.0		
	15400	SGMR	22	1331.3	1357.6	107.8	22.5	11.2		
	1420	ARCE	40	1331.6	1338.5	69				
	1415	SGMR	46	1331.6	1431.3	74.3	2430.0	245.0		
	960	PENN	41	1331.2		70.8	70.0D			
	8800	SGMR	46	1332.7	1334.8	5.1	71.0	14.8		
	3000	NERA	27	1332	1343	148 D	35.0			
	1500	BERL	47	1332	1407.2	68	305.0			
	1500	NEUS		1332	1431.2		1472.0			
	1420	KIEL	24	1332	1433		1000.0D	120.0		
	606	SGMR	46	1332.7	1338.7	116.8	320.0	75.0		
	808	ONDR	45	1333	1339	15				
	328	PENN	41	1333.8	1336.8	68.8	110.0			
	2695	SGMR	3	1334.4	1336	2.7	13.6	5.4		
	4995	SGMR	3	1335.4	1336.8	2.2	17.0	6.8		
	3000	NERA	40	1335	1342.3	25	16.0			
	2800	OTTA	40	1335	1340	10	12.0			
	536	ONDR	45	1336	1337.5	25	365.0			
	234	POTS	45	1336 U	1350 U		450.0U			
	2695	SGMR	4	1337.3	1338.1	4	11.5	4.6		
	8800	SGMR	3	1338.1	1338.7	2.9	12.4	5.0		
	4995	SGMR	3	1338.4	1338.8	1.1	9.9	4.0		
	420	KIEL	45	1338 E	1338		400.0D	30.0		
	600	UCCL	45	1339		110				
	260	ONDR	45	1340.5U		20	85.0U			
	8800	SGMR	3	1341.6	1342.3	1	13.8	5.6		
	4995	SGMR	3	1341.8	1342.2	1	13.3	5.3		
	2695	SGMR	45	1341.6	1342.3	5	12.7	5.1		
	9139	NEUS		1342 E	1342		58.0			

# SOLAR RADIO EMISSION OUTSTANDING OCCURRENCES

24 OCTOBER - 6 NOVEMBER 1968

	FREQUENCY STATION	TYPE	STARTING TIME	TIME OF MAXIMUM	DURATION	FLUX DENSITY $10^{-22} \text{ W m}^{-2} \text{ Hz}^{-1}$		INT	REMARKS
			UT	UT	MINUTES	PEAK	NEAR		
30	408 SANM	45	1350	1431	160	61.0	27.5		
	240 KIEL	45	1353 E	1353		900.0	80.0		
	960 PENN	29	1442	1442	51	4.7	2.3		
	328 PENN	29	1442	1442	87.5	18.3	9.2		
	960 PENN	45	1448.7	1448.9	1.3	16.4	4.2		
	328 PENN	45	1448.7	1448.9	.6	124.0	47.2		
	960 PENN	45	1458.1	1458.6	1.9	7.0	2.0		
	328 PENN	45	1458.3	1458.7	.7	45.8	14.0		
	4995 SGMR	45	1621.8	1622.4	1.5	12.9	6.4		
	2800 OTTA	40	1621.7	1623.7	2	30.0			
	2700 PENN	45	1621.5	1622.3	2	25.3	5.3		
	2695 SGMR	45	1621.8	1622.4	1.2	23.0	9.2		
	408 SANM	29	1630	1728.3	110	33.0	15.0		
	18 BOUL	41	1827	1830	5			1	
	18 MCMA	41	1827	1830	9			1	
	2800 OTTA	26	1905		50	6.4			
	2800 OTTA	20	2027	2029	20	4.0	2.0		
	208 VORO	44	2200	0009	360	455.0			
	500 HIRA	45	2242	0006.5	118	5050.0	200.0		
	8800 MNL	46	2338.3	0011.2	40.7	1950.0	438.0		
	4995 MNL	46	2338.3	0011.2	40.7	2855.0	642.0		
	2695 MNL	46	2339.5	0011.3	39.5	1680.0	378.0		
	1415 MNL	46	2339.5	0005.7	39.5	610.0	137.0		
	200 HIRA	45	2339	0009	60	790.0	130.0		
	9400 TYKW	45	2340	2411	60	2000.0	500.0		
	3750 TYKW	45	2340	2411	60	2150.0	600.0		
	2000 TYKW	45	2340	2403.8	60	1200.0	450.0		
	1000 TYKW	45	2340	2408.6	60	475.0	170.0		
	2695 PENT	45	2343	2350		75.0			DUR. SUNSET
	208 VORO	47	2344	2355	56	311.0	232.0		
17000 TOKO	45	2353	0011.4	40	940.0				
17000 TOKO	29	2353			90.0				
31	612 TOKO	45			37 D	1070.0D			
	8800 MNL	29	0019	0019	184	40.8	20.4		
	4995 MNL	29	0019	0019	153	75.0	36.6		
	2695 MNL	29	0019	0019	264	61.2	28.5		
	1415 MNL	29	0019	0019	191	34.6	16.9		
	208 VORO	27	0100	0154.5	55	161.0	112.0		
	100 GORK	44	0503 E		357 D		240.0		
	200 GORK	44	0520 E		344 D		20.0		
	500 HIRA	45	0525	0712	135	330.0	40.0		
	650 GORK	46	0615.3	0803.1	232	300.0			
	650 GORK		0615.3	0641.7		185.0			
	650 GORK		0615.3	0705.2		180.0			
	650 GORK		0615.3	0742.7		150.0			
	650 GORK		0615.3	0818.3		116.0			
	3100 CRIM	20	0620	0620 D	140				
	3100 CRIM	20	0620	0659	140	14.0	5.0		
	1415 MNL	46	0635.8	0712.2	56.2	112.9	56.5		
	612 TOKO	45	0635.3	0643.5	42	373.0			
	2695 MNL	21	0636.8	0701	143.2U	12.6	6.3		
	1000 TYKW	45	0636	0712.2	60 D	120.0	25.0U		
	3840 GORK	21	0638.9	0708.7	92.9	12.0	6.2		
	1500 NEUS	46	0640 E	0712	80	126.0			
	600 UCCL	45	0640 U		260 D				
	260 ONDR	44	0640		485	70.0			
	8800 MNL	21	0641.6	0701	92.2	9.0	4.5		
	4995 MNL	21	0641.6	0701	138.4U	21.0	10.5		
	2950 GORK	21	0641.5	0712	48.5	114.0	7.0		
	2950 GORK	20	0641.5		48.5		3.5		
	202 IZMI	44	0700	0740	300	300.0			
	100 GORK	24	0700	0717.1	88.2	974000.0D			
	9139 NEUS	3	0710.5	0712.1	8	29.0	6.4		
	2920 BERL	4	0710	0712.7	160				
	2920 BERL	20	0710	0835					
	8800 MNL	3	0711.7	0712.2	1.1	31.5	15.8		
	4995 MNL	3	0711.5	0712.2	5.3	163.5	81.8		
	3840 GORK	45	0711.1	0712.1	5.8	103.0	20.0		
	3750 TYKW	5	0711.3	0712	2 U	90.0U	38.0U		
	3100 CRIM	3	0711	0712	5	35.0	12.0		
	3000 NERA	45	0711.3	0712	1.2	80.0	40.0		
	2950 GORK	45	0711.3	0712	5.6	105.0	23.0		
	2695 MNL	3	0711.4	0712.2	6.9	90.5	45.5		
	2000 TYKW	45	0711.3	0712.2	5	110.0	30.0		
	234 POTS	45	0711.6	0711.8	.5	2000.0	130.0		
	200 GORK	24	0714.2	0742.1	56.4	850.0			
	9100 GORK		0717 E		30 D				
	9139 NEUS	20	0730	0830	145	8.0			
	240 KIEL	45	0753 E	0753		500.0	30.0		
	1420 ARCE	4	0816.8	0819.6	6.7	123.0			
	1415 MNL	46	0816.6	0819.6	43.4U	172.7	86.3		
	1500 BERL	4	0817	0819.5	97	160.0	17.0		
1420 KIEL	24	0818	0821	27	210.0	80.0			
1420 ARCE	29	0823.5		83.3	55.0				
9139 NEUS		0855 E	0855						
3100 CRIM	20	0915	0930	80	11.0	4.0			
1500 BERL	1	1201.6	1201.6		2.3				
536 ONDR	5	1312.5	1312.5	1.5	125.0				
184 BOUL	43	1328 E		610 D					

# SOLAR RADIO EMISSION OUTSTANDING OCCURRENCES

24 OCTOBER - 6 NOVEMBER 1968

	FREQUENCY STATION	TYPE	STARTING TIME	TIME OF MAXIMUM	DURATION	FLUX DENSITY $10^{22} \text{ Wm}^{-2} \text{ Hz}^{-1}$		INT	REMARKS	
			UT	UT	MINUTES	PEAK	MEAN			
31	420 KIEL	45	1418 E	1418			200.0	5.0		
	10700 PENN	3	1713.6	1715	5		17.8	8.9		
	18 MCMA	41	1715	1727	17				2	
	18 MCMA	6	1927	1929	3				1	
	2800 OTTA	23	2223	2238	85 D		30.0			
	500 HIRA	45	2228	2252	48		190.0	25.0		
	9400 TYKW	45	2231 U	2257.4	100		2270.0	300.0		
	3750 TYKW	45	2231 U	2301	100		800.0	190.0		
	2000 TYKW	45	2233 U	2301.1	100		720.0	145.0		
	1000 TYKW	45	2233 U	2259.6	100		195.0	38.0		
	208 VORO	47	2238	2255	39		333.0	173.0		
	200 HIRA	45	2238	2355.5	40		470.0	160.0		
	8800 MNL	46	2239.3	2257.4	91.2		1905.0	601.6		
	4995 MNL	46	2239.3	2257.4	91.2		2060.0	722.0		
	2695 MNL	46	2239.3	2301.2	91.2		1112.0	445.4		
	1415 MNL	46	2239.3	2300.8	91.2		254.5	85.4		
	2695 PENT	47	2247	2301	28		890.0	400.0		
	2695 PENT	47	2247	2252	10		570.0			
	184 BOUL	48	2248	2256 U	22		6480.0D			
	2695 PENT	47	2257	2301	18		890.0			
	17000 TOKO	45	2300 D		50 D		400.0D			
	612 TOKO	45	2300 D	2302.9U	35 D		143.0U			
	500 HIRA	45	2327 D	2328.4	17 D		50.0	10.0		
	1	208 VORO	5	0119	0119.8	1.5		272.0	92.0	
		200 HIRA	45	0120	0121.2	1.5		490.0	120.0	
		9400 TYKW	5	0151.5	0152.2	4		11.0	2.0	
		8800 MNL	3	0151.7	0152.1	3.3		11.5	4.6	
		4995 MNL	3	0151.7	0152.1	3.3		9.0	4.5	
		3750 TYKW	5	0151.5	0152.2	4		5.0	1.0	
		2695 MNL	1	0151.7	0152.2	4.8		6.4	2.5	
		2000 TYKW	5	0151.5	0152.2	4		8.0	1.0	
1415 MNL		3	0151.4	0152.2	5.1		7.7	3.4		
1000 TYKW		5	0151.5	0152.2	4		12.0	2.0		
2000 TYKW		45	0440.4	0441.7	2.5		8.0	3.0		
1000 TYKW		45	0440.4	0441.7	2.5		10.0	2.0		
3100 CRIM		3	0525	0530	6		15.0	5.0		
1000 TYKW		45	0539.9	0550.7	13		38.0	5.0		
3100 CRIM		20	0540		95					
3100 CRIM		20	0540	0623	95		7.0	2.0		
500 HIRA		45	0544	0546.6	9.5		270.0	60.0		
612 TOKO		45	0545.4	0546	5.6		666.0			
9100 GORK		20	0618	0626.2	13		14.0	4.0		
8800 MNL		3	0621.8	0626.6	9.7		13.7	4.5		
1000 TYKW		5	0621.9	0626.2	6		50.0	15.0		
4995 MNL		4	0622.5	0626.3	8.7		22.2	6.7		
3750 TYKW		45	0622	0626.2	6		22.0	8.0		
3100 CRIM		3	0622	0623	5		25.0	8.0		
2695 MNL		4	0622.4	0626.3	7.3		15.4	7.1		
2000 TYKW		45	0622	0626.2	6		19.0	6.0		
1415 MNL		4	0622.4	0626.3	7.4		33.3	12.3		
500 HIRA		45	0622.5	0626.3	6		420.0	160.0		
612 TOKO		45	0623.6	0626	3.9		4090.0D			
9400 TYKW		45	0625	0626.2	3		12.0	2.0		
1500 NEUS		3	0706.7E	0706.7			7.3			
260 ONDR		41	0728		472		85.0D			
1500 NEUS		1	0746.1E	0746.1			2.2			
200 GORK		44	0755		275			45.0		
100 GORK		44	0755		275			65.0		
3100 CRIM		47	0756	0912	210		1232.0	410.0		
9500 NERA		28	0800	0843	56					
3000 NERA		28	0800	0825.4	29		35.0	15.0		
1500 BERL		47	0802.5	0849	212.5		355.0			
1500 NEUS		29	0802.5	0914.5			977.0			
1420 KIEL		45	0804	0918	109		550.0	80.0		
2920 BERL		47	0805 U	0905	203 U					
2920 BERL		29	0805 U	0912.3						
3800 GORK		47	0806	0912.5	124		2170.0	420.0		
2950 GORK		45	0806.6	0845.5	147.1		500.0			
2950 GORK		45	0806.6	0912.4			1640.0			
9100 GORK		47	0807.1	0912.4	112.9		1930.0	386.0		
650 GORK		46	0810.3	0833.5	134.1		190.0			
650 GORK		46	0810.3	0844.5			250.0			
650 GORK		46	0810.3	0859.4			270.0			
650 GORK	46	0810.3	0912.6			280.0				
650 GORK	46	0810.3	0943.3U			2560.0				
930 BORD	45	0811	0932	116		5100.0	1000.0			
536 ONDR	45	0812.5		107		330.0D				
260 ONDR	45	0812	0952.5	108		80.0				
9285 ARCE	28	0815.4		38.9		109.0		OFF SCALE		
9139 NEUS	47	0815	0904.7	200		1330.0				
9139 NEUS	29	0815	0912.3			1850.0				
8800 MNL	46	0815	0844.8	37.3		300.0	45.0			
4995 MNL	46	0815	0843.4	38.5		385.0	64.0			
2695 MNL	46	0815	0843.4	39.5		430.0	58.0			
1420 ARCE	47	0815 E		73.2D				OFF SCALE		
1420 ARCE	47	0815 E	0857.2	47 D		219.0		OFF SCALE		
1415 MNL	46	0815	0842.5	44.8		315.0	42.0			
808 ONDR	45	0821		100						
420 KIEL	45	0824	0900	106		400.0	80.0			

# SOLAR RADIO EMISSION OUTSTANDING OCCURRENCES

24 OCTOBER - 6 NOVEMBER 1968

	FREQUENCY STATION	TYPE	STARTING TIME	TIME OF MAXIMUM	DURATION	FLUX DENSITY $10^{22} \text{ W m}^{-2} \text{ Hz}^{-1}$		INT	REMARKS
			UT	UT	MINUTES	PEAK	MEAN		
1	2800 SLOU	47	0825.5	0912.5	91.5	2030.0			
	3000 NERA	45	0829.6	0912.4	38	2325.0	1000.0		
	19000 SLOU	47	0830	0912.3	75	1000.0			
	234 POTS	45	0830 U	0841 U	97	175.0	40.0		
	111 POTS	45	0833 U	0906 U	61	200.0	40.0		
	9285 ARCE	47	0854.3		33.2				
	9500 NERA	45	0855.6	0912.3	55				
	1420 ARCE	47	0902		26.2				
	9285 ARCE	29	0927.5		114	240.0			
	1420 ARCE	30	0928.2		138	136.0			
	1420 ARCE	46	0939.8	0941.3	20.6	207.0			
	1420 ARCE	46	0939.8	0941.3	5.4	207.0			
	19000 SLOU	29	0945	0945	48	64.0			
	1420 ARCE	46	0945.2	0948.2	7.9	120.5			
	9500 NERA	29	0950		110				
	1420 ARCE	46	0953.1	0956.4	7.3	104.0			
	2800 SLOU	30	0957	0957	138	74.0			
	100 GORK	6	0957.2	0957.5	1.9	1600.0D			
	9100 GORK	30	1000	1000	159	86.0	32.0		
	3000 NERA	29	1008		105	70.0	35.0		
	3800 GORK	29	1010	1012.1	97.2	45.0	19.0		
	1420 ARCE	40	1019.7	1023.7	7	86.5			
	9100 GORK	45	1139.1	1139.9	5.3	223.0	44.0		
	9100 GORK	45	1139.1	1141.2		142.0			
	408 SANM	45	1206.6	1210	5.9	840.0	528.0		
	4995 SGMR	45	1207.2	1209.8	7.9	300.0	75.0		
	808 ONDR	45	1207	1210.5	6				
	650 GORK	4	1207.4	1210.3	5.5	700.0			
	536 ONDR	45	1207		10	310.0D			
	10700 PENN	45		1209.8		176.0D			
	9139 NEUS	4	1208.5	1210	10.5	195.0	52.0		
	7000 SAOP	47	1208.8	1210.1	7.4	9256.0			
	2920 BERL	4	1208.5	1209.7	95				
	2800 SLOU	3	1208.5	1210	8	72.0			
	2700 PENN	45		1209.9		53.0D			
	2695 SGMR	45	1208.3	1209.9	7.5	82.0	20.0		
	2695 SGMR	45	1208.3	1210.3	7.5	82.0	20.0		
	1500 BERL	4	1208.5	1210	7.5	34.0			
	1420 ARCE	4	1208.5	1210	2.6	35.0			
	1415 SGMR	45	1208.7	1209.9	4.4	32.0	8.0		
	960 PENN	45		1210.3		35.0D			
	606 SGMR	45	1208	1210.2	7	1840.0	215.0		
	420 KIEL	45	1208	1212	6	2000.0	80.0		
	328 PENN	45		1211.2		270.0D			
	260 ONDR	45	1208.5		5.5	85.0D			
	15400 SGMR	45	1209.1	1209.7	7.8	111.0	25.0		
	9500 NERA	45	1209.2	1210 U	5	126.0			
	9285 ARCE	45	1209.2	1209.9	3	126.0			
	9285 ARCE	45	1209.2	1209.9	1.6	126.0			
	8800 SGMR	45	1209.1	1209.8	7.2	250.0	60.0		
	3800 GORK	4	1209	1210	9	115.0	21.0		
	3100 CRIM	3	1209	1210	9	110.0	35.0		
	3000 NERA	45	1209	1210 U	6	95.0	40.0		
	2950 GORK	3	1209	1209.9	7.7	93.0	20.0		
	930 BORD	45	1209	1211	4	139.0	23.0		
	239 TRST	47	1209.6		3.2	200.0			
	234 POTS	40	1209.7	1210.9	2.9	4000.0	250.0		
	225 HARS	45	1209	1210.5	3.5	550.0	50.0		
	111 POTS	40	1209.3	1212.2	3.6	1200.0	30.0		
	19000 SLOU	3	1210.5	1211.3	1.5	39.0			
	9285 ARCE	45	1210.8	1211.2	1.4	70.0			
	1420 KIEL	5	1210	1212	5	80.0	30.0		
	239 TRST	45	1210.8	1211	.6	2680.0D	139.0D		
	1420 ARCE	29	1211.1		3.1	13.5			
	239 TRST	45	1211.5	1211.5	.1	2030.0			
	9285 ARCE	29	1212.2		6	46.0			
	606 SGMR	1	1247.8	1247.9	.8	7.0	3.0		
	7000 SAOP	21	1255.8		17.7				
	1500 BERL	4	1257.5	1258.5	1.5	7.6	1.6		
	1420 ARCE	4	1258	1258.5	1.2	14.0			
	1415 SGMR	40	1258	1258.4	4.7	10.4	2.0		
	930 BORD	45	1258	1258.5	1	54.0	6.0		
	606 SGMR	41	1258.1	1301.3	6.9	240.0	60.0		
	536 ONDR	45	1258.5	1302	3.5	310.0D			
	111 POTS	40	1258.3	1314	16	300.0	1.0		
	23 POTS	40	1301.3	1302.6	13.1	25000.0	200.0		
	7000 SAOP	3	1303.9	1305.1	1.6	23.4	11.7		
	4995 SGMR	3	1303.9	1304.8	2.4	10.2	4.0		
	15400 SGMR	1	1304.3	1305.3	2.7	4.9	2.0		
	9285 ARCE	20	1304	1305	2.8	10.0			
	9139 NEUS	4	1304	1304.8	3	16.0	7.0		
	8800 SGMR	3	1304.6	1304.8	2.2	20.4	8.0		
	234 POTS	40	1304.5	1326.3	21.8	350.0	1.0E		
	606 SGMR	41	1312.6	1314.2	2.6	37.8	7.0		
	7000 SAOP	40	1320		13.5	9.3	4.6		
	8800 SGMR	1	1325.9	1326.6	4.1	5.1	2.0		
	4995 SGMR	1	1326.2	1326.4	.8	3.4	1.5		
	2695 SGMR	1	1326.3	1326.4	1.9	2.3	1.0		
	184 BOUL	44	1330 E		608 D		2170.0		
	15400 SGMR	1	1331.2	1331.9	2.8	4.9	2.0		

# SOLAR RADIO EMISSION OUTSTANDING OCCURRENCES

24 OCTOBER - 6 NOVEMBER 1968

	FREQUENCY	STATION	TYPE	STARTING TIME	TIME OF MAXIMUM	DURATION	FLUX DENSITY		INT	REMARKS
				UT	UT	MINUTES	$10^{-22} \text{ Wm}^{-2} \text{ Hz}^{-1}$			
							PEAK	MEAN		
1	9139	NEUS	20	1331.5E	1331.5		5.7			
	8800	SGMR	1	1331.3	1331.7	2.2	4.1	2.0		
	4995	SGMR	1	1331.1	1331.5	2.7	6.1	2.5		
	2920	BERL	2	1331.6E	1331.6					
	2695	SGMR	1	1331.1	1331.5	3.4	2.3	1.0		
	2800	SLOU	20	1413	1426	24	21.0			
	111	POTS	45	1417.8	1418.1	.8	1400.0	250.0		
	2800	OTTA	20	1422	1426	12	3.4	1.7		
	1415	SGMR	1	1434.5	1435.7	2.6	1.0	.5		
	606	SGMR	41	1434.5	1435.6	2.5	22.7	5.0		
	7000	SAOP	23	1439.3		31.8				
	2700	PENN	20	1450.9	1455.9	22.7	7.5	3.7		
	960	PENN	20	1450.9	1456.7	18.8	4.3	1.5		
	10700	PENN	20	1451.8	1455.8	17.6	7.7	4.1		
	8800	SGMR	22	1451.2	1455.6	22.2	11.2	4.5		
	7000	SAOP	3	1451.6	1453	1.4	158.9	79.4		
	4995	SGMR	22	1451.1	1455.5	23.9	11.9	5.0		
	2800	OTTA	2	1451.5	1455.5	6.5	7.2	3.6		
	2695	SGMR	2	1451.2	1455.6	6.6	7.4	3.0		
	1415	SGMR	3	1451.2	1451.3	2.9	9.6	4.0		
	606	SGMR	45	1451.1	1451.7	5.9	260.0	70.0		
	1415	SGMR	22	1459.8	1504	16.2	3.4	1.5		
	2695	SGMR	21	1502.9	1508.6	8.2	6.0	3.0		
	2800	OTTA	2	1503	1519	8	7.2	3.6		
	960	PENN	24	1510	1806		3.4			
	606	SGMR	4	1514.2	1514.5	.8	17.8	4.0		
	408	SANM	40	1530	1730	135	10.0	7.8		
	240	KIEL	45	1617 E	1617		450.0	30.0		
	10700	PENN	3	1624.9	1630.5	8.1	112.0	27.7		
	960	PENN	1	1624	1624.7	1.2	4.5	0.7		
	328	PENN	45	1624	1624.8	2	275.0D	35.0D		
	2700	PENN	3	1625.8	1630.5	7.2	27.6	10.4		
	2800	OTTA	21	1626	1628.3	20	7.4	3.2		
	960	PENN	45	1626	1630.2	12.6	8.3	1.6		
	7000	SAOP	45	1627.8	1629.4	10.1	18.7	9.3U		
	328	PENN	45	1628	1629.8	4.7	37.5	4.0		
	15400	SGMR	4	1629.6	1630.6	5.8	59.0	12.0		
	8800	SGMR	4	1629.5	1630.6	19.5	290.0	55.0		
	4995	SGMR	4	1629.4	1630.6	20.3	240.0	45.0		
	2800	OTTA	4	1629.2	1630.5	5	26.0	11.0		
	2695	SGMR	4	1629.4	1630.6	18.6	47.6	10.0		
	1415	SGMR	45	1629.6	1630.3	15.7	9.4	2.5		
	606	SGMR	4	1629.7	1630.3	1.3	11.8	3.0		
	10700	PENN	29	1633	1633	13.4	36.0	10.5		
	2700	PENN	29	1633	1633	14.2	5.7	2.9		
	18	MCMA	6	1659	1701	4			1	
	18	BOUL	6	1700	1703	3	1.0			
	15400	SGMR	3	1713.9	1714	2.1	27.4	6.0		
	10700	PENN	3	1713.7	1714	2.3	33.2	5.3		
	10700	PENN	40	1730		40				
	8800	SGMR	21	1747.3	1751.6	72.9	6.1	3.0		
	4995	SGMR	21	1747.9	1802.7	47.8	7.8	3.9		
	2695	SGMR	21	1749.7	1802.2	68.4	2.9	1.5		
	8800	SGMR	3	1758.4	1758.6	1.6	14.1	7.0		
	7000	SAOP	3	1758.6	1759	.8	46.7	23.3		
	4995	SGMR	3	1758.4	1758.6	1.4	10.9	5.4		
	2800	OTTA	1	1758.2	1758.6	1.8	4.2	2.1		
	2700	PENN	1	1758.3	1758.6	2.2	5.0	1.3		
	2695	SGMR	1	1758.6	1758.7	2.7	4.0	2.0		
	606	SGMR	45	1802.2	1802.3	.6	160.0	10.8		
	8800	SGMR	1	1805.9	1806	3.1	4.7	2.3		
	960	PENN	45	1815.6	1819.8	7	6.8	1.6		
	15400	SGMR	45	1818.6	1820.8	13.6	14.8	4.9		
	10700	PENN	45	1818.3	1819.5	7.9	34.2	10.7		
	8800	SGMR	45	1818.5	1819.6	9.6	38.1	12.7		
	7000	SAOP	45	1818.1		3.7	37.4	18.7U		
	4995	SGMR	45	1818.8	1819.7	8.7	30.9	10.3		
	2800	OTTA	2	1818.5	1819	4.5	4.0	2.0		
	2700	PENN	20	1818	1820.5	9	6.9	3.6		
	2695	SGMR	45	1818.5	1819.3	8.5	6.4	3.2		
	1415	SGMR	45	1818.3	1819.6	5.9	3.1	1.0		
	1415	SGMR	45	1818.3	1820.8	5.9	3.1	1.0		
	328	PENN	41	1818	1847.3	98	105.0			
	606	SGMR	1	1820.4	1820.5	.6	1.1	.4		
	7000	SAOP	29	1822.7		3				
	4995	SGMR	1	1830.4	1830.6	1.4	1.7	.6		
	2800	OTTA	2	1830.2	1830.5	1	4.2	2.1		
	2700	PENN	2	1830.2	1830.4	2	7.6	0.7		
	2695	SGMR	3	1830.3	1830.4	2.7	7.5	2.5		
	8800	SGMR	3	1928.2	1929.9	6.9	31.5	10.5		
	960	PENN	20	1928.1	1937.3	15.2	2.9	1.2		
	10700	PENN	3	1929.6	1930.2	8.7	23.6	6.3		
	7000	SAOP	4	1929.6	1930.3	1.9	32.7	16.3		
	2700	PENN	20	1929.7	1930.2	11.3	6.6	1.7		
	606	SGMR	1	1929.9	1930.3	1.2	1.6	.5		
	15400	SGMR	1	1930.2	1930.3	1.3	5.1	1.7		
	4995	SGMR	3	1930	1930.4	10	25.5	8.5		
	2800	OTTA	1	1930	1930.2	2	4.2	2.1		
	2695	SGMR	1	1930.2	1930.3	1.7	3.5	1.2		
	1415	SGMR	1	1932.5	1932.6	.5	2.1	.7		

# SOLAR RADIO EMISSION OUTSTANDING OCCURRENCES

24 OCTOBER - 6 NOVEMBER 1968

	FREQUENCY	STATION	TYPE	STARTING TIME	TIME OF MAXIMUM	DURATION	FLUX DENSITY		INT	REMARKS
				UT	UT	MINUTES	$10^{22} \text{ Wm}^{-2} \text{ Hz}^{-1}$ PEAK	MEAN		
1	8800	SGMR	21	1941	1950.4	46.1	6.6	3.3		
	8800	SGMR	1	1944.6	1945.5	1.5	6.6	2.2		
	4995	SGMR	21	1945.2	1956.8	41.9	5.2	1.6		
	4995	SGMR	28	1945.2	2003	17.8	21.4	10.7		
	8800	SGMR	45	1947.9	1949.6	2.2	8.8	2.0		
	1415	SGMR	28	1952.6	2003	10.4	3.1	1.5		
	960	PENN	45	1952.3	2004.1	33	65.0D	7.0D		
	2800	OTTA	21	1955	2008	35	11.4	5.4		
	2695	SGMR	28	1955.9	2003.1	7.2	6.9	3.4		
	606	SGMR	45	1955.6	1957.2	2.9	240.0	20.0		
	15400	SGMR	28	1956.1	2003.1	7	7.4	3.7		
	10700	PENN	45	1956.6	2004.5	18.4	2330.0	229.0		
	8800	SGMR	3	1956.8	1956.9	.7	19.9	6.6		
	7000	SAOP	4	1956.7	1957.5	2.2	308.5	154.5		
	4995	SGMR	3	1956.7	1956.9	2.7	24.8	8.3		
	2700	PENN	45	1956.4	2004.5	16.2	276.0	26.5		
	2695	SGMR	1	1956.3	1956.5	2.1	7.1	2.7		
	8800	SGMR	28	1959.4	2002.8	3.4	20.4	10.2		
	606	SGMR	45	2000.5	2004.5	22.4	2030.0	105.0		
	8800	SGMR	4	2002.8	2004.6	15.6	3390.0	500.0		
	7000	SAOP	45	2002.3	2009.7	19.5	18.7	9.3U		
	184	BOUL	48	2002	2002	8	6480.0D			
	15400	SGMR	4	2003.1	2004.6	19.4	4180.0	550.0		
	4995	SGMR	4	2003	2004.6	20.3	1250.0	215.0		
	2800	OTTA	4	2003	2004.8	6	390.0	44.0		
	2695	SGMR	4	2003.1	2004.6	16.1	380.0	66.0		
	1415	SGMR	4	2003	2004.7	19.8	600.0	100.0		
	328	PENN	45	2003.4	2004.7	8.8	460.0D	30.0D		
	408	SANM	45	2004 E	2005	16 D	552.0	144.0		
	2800	OTTA	46	2009	2011.6	4	42.0	25.0		
	2700	PENN	29	2012.6	2012.6	16.6	5.2	2.6		
	2700	PENN	3	2013.7	2015.1	4.2	10.5	4.3		
	2800	OTTA	2	2014	2015	3	9.8	4.9		
	10700	PENN	29	2015	2015	13.8	43.0	21.5		
	2800	OTTA	4	2020.8	2021	.8	18.0	6.0		
	408	SANM	40	2020	2031	40	19.0	9.0		
	328	PENN	41	2022	2038.6	68	35.2			
	2695	PENT	1	2112	2112.2	1	2.8	1.4		
	2695	PENT	1	2124.5	2124.8	1.5	2.8	1.4		
	9400	TYKW	45	2232.7	2242.9	20	195.0	22.0		SUNRISE
	3750	TYKW	45	2232.7	2242.9	20	68.0	12.0		
	2000	TYKW	45	2232.7	2242.9	20	26.0	4.0		
	2695	PENT	1	2233	2233.5	2	6.4	3.2		
	500	HIRA	45	2240.5	2243	7	120.0	15.0		
	8800	MNL	46	2242.2	2242.8	7.3	137.0	68.0		
	4995	MNL	46	2242.1	2242.8	7.4	107.0	54.0		
	2695	PENT	4	2242	2242.7	6	21.0	6.0		
	2695	MNL	46	2242	2242.8	7.5	23.9	11.9		
	1415	MNL	46	2242	2242.8	7.5	13.7	6.8		
	1000	TYKW	45	2242.7	2242.9	3	27.0	9.0		
	208	VORO	44	2300	0035	240	400.0			
	208	VORO	27	2300	2301	58	238.0	125.0		
	612	TOKO	45	2306.9	2307.1	.4	313.0			
	208	VORO	27	2358	0035	102	156.0	125.0		
2	9400	TYKW	45	0036	0037.5	10	101.0	19.0		
	8800	MNL	46	0036.2	0037.5	12.2	121.0	61.0		
	4995	MNL	46	0036.2	0037.5	12.2	87.0	43.3		
	3750	TYKW	45	0036	0037.5	10	47.0	9.0		
	2695	MNL	4	0036.2	0037.5	10.1	25.2	12.6		
	1415	MNL	46	0036.2	0037.5	10.1	7.7	3.9		
	17000	TOKO	45	0037	0037.4	7.5	47.0			
	2000	TYKW	45	0037	0038	3	6.0	2.0		
	1000	TYKW	5	0037	0038	3	2.0	1.0		
	9400	TYKW	45	0055	0055.5	2	56.0	13.0		
	8800	MNL	4	0055	0055.6	2.4	56.0	28.0		
	4995	MNL	4	0055	0055.6	2.4	22.7	11.4		
	3750	TYKW	45	0055	0055.5	2	5.0	1.0		
	2695	MNL	4	0106.9	0111.9	12.1	8.0	4.0		
	1415	MNL	2	0106.8	0111.9	12.2	6.0	3.0		
	9400	TYKW	45	0107	0111.8	7	105.0	11.0		
	8800	MNL	46	0107.7	0111.9	11.3	90.0	44.8		
	4995	MNL	46	0107.8	0111.9	11.2	16.5	8.3		
	3750	TYKW	45	0108	0111.8	4	8.0	2.0		
	17000	TOKO	45	0111.2	0111.8	.8	92.0			
	2000	TYKW	5	0111	0111.8	1	4.0	2.0		
	1000	TYKW	5	0111	0111.8	1	6.0	2.0		
	9400	TYKW	5	0131	0131.5	1	13.0	4.0		
	8800	MNL	3	0131.6	0131.8	.3	15.6	6.7		
	4995	MNL	3	0131.6	0131.8	.3	10.3	6.2		
	3750	TYKW	5	0131	0131.5	1	5.0	2.0		
	9400	TYKW	5	0209	0211.7	5	8.0	2.0		
	8800	MNL	1	0209.7	0210.5	3.3	4.5	2.3		
	4995	MNL	3	0209.7	0210.5	3.3	16.5	8.3		
	3750	TYKW	5	0209	0211.7	5	11.0	4.0		
	2695	MNL	1	0209.7	0210.5	3.3	5.3	2.7		
	1415	MNL	1	0209.7	0210.5	3.3	3.4	1.7		
	2000	TYKW	5	0210	0211.7	2	3.0	1.0		
	3750	TYKW	5	0238.5	0238.7	1	8.0	3.0		
	2000	TYKW	5	0238.5	0238.7	1	2.0	1.0		

# SOLAR RADIO EMISSION OUTSTANDING OCCURRENCES

24 OCTOBER - 6 NOVEMBER 1968

	FREQUENCY STATION	TYPE	STARTING TIME	TIME OF MAXIMUM	DURATION	FLUX DENSITY $10^{-22} \text{ W m}^{-2} \text{ Hz}^{-1}$		INT	REMARKS
			UT	UT	MINUTES	PEAK	MEAN		
2	1000 TYKW	5	0238.5	0238.7	1		4.0		1.0
	612 TOKO	45	0238.5	0238.7	.6		182.0		
	2695 MNL	20	0251.5	0251.5	18.5		5.3		2.6
	1415 MNL	22	0251.3	0300.3	18.7		2.7		1.4
	8800 MNL	20	0253.3	0302.5	16.7		6.7		3.4
	4995 MNL	20	0253.3	0302.5	16.7		8.3		4.2
	17000 TOKO	45	0332.3	0332.8	4.5		370.0		
	9400 TYKW	45	0332	0332.8	5		455.0		43.0
	3750 TYKW	45	0332	0332.8	7		49.0		8.0
	2000 TYKW	45	0332	0332.8	7		12.0		1.0
	1000 TYKW	45	0332	0332.8	5		17.0		2.0
	612 TOKO	45	0332.1	0332.6	3		148.0		
	9400 TYKW	5	0513	0514.3	2		37.0		4.0
	9100 GORK	1	0513.3	0514.3	1.8		30.0		14.0
	8800 MNL	21	0513.3	0528.4	24.1		15.7		6.7
	4995 MNL	21	0513.3	0520.7	19.1		11.1		4.4
	3800 GORK	1	0513.3	0513.9	1.3		3.4		1.7
	3750 TYKW	5	0513	0514.3	2		5.0		2.0
	8800 MNL	3	0514.1	0514.2	.8		44.8		22.2
	4995 MNL	3	0514.1	0514.2	.8		31.1		15.5
	650 GORK	40	0518.1	0525	8.9		15.0		6.0
	9400 TYKW	45	0605	0606.8	2		22.0		6.8
	8800 MNL	3	0605.9	0606.2	2.4		15.7		8.9
	4995 MNL	3	0605.9	0606.2	2.4		22.2		8.0
	3750 TYKW	45	0605	0606.8	3		16.0		3.0
	3100 CRIM	45	0605	0605.5	4		10.0		3.0
	3100 CRIM		0605	0606			10.0		4.0
	3100 CRIM		0605	0607			12.0		6.0
	2695 MNL	3	0605.9	0606.2	2.4		14.4		7.1
	1415 MNL	3	0605.9	0607.8	2.4		16.8		6.0
	1000 TYKW	45	0605	0606.8	3		16.0		18.0
	9100 GORK	45	0626.7	0630	6.6		49.0		13.2
	2695 MNL	4	0627.7	0629.8	4.8		26.4		2.2
	1415 MNL	1	0627.7	0629.8	4.8		4.4		59.0
	4995 MNL	4	0628	0629.8	6		118.0		10.0
	3100 CRIM	3	0628	0630.5	8		30.0		7.0
	2000 TYKW	5	0628	0630	5		14.0		42.6
	8800 MNL	4	0629.1	0629.8	4.9		85.0		5.5
	9100 GORK	29	0633.3	0642.3	18.7		13.0		6.4
	9139 NEUS	1	0704.2E	0704.2			6.4		11.0
	1500 NEUS	1	0710.8E	0710.8			11.0		6.0
	1500 NEUS	4	0711 U	0711.4	1		16.0		2.8
	3800 GORK	20	0721.5	0726.2	6.9		5.6		5.0
	9139 NEUS	1	0726.2E	0726.2			5.0		360.0
	202 IZMI	5	0731	0731.3	.6		360.0		2.2
	1500 NEUS	1	0749 E	0749			2.2		120.0
	536 ONDR	45	0752.5	0814.5	30		120.0		300.0
	202 IZMI	5	0807.8	0808	.8		300.0		350.0
	23 POTS	40	0808.9	0810.3	9.1		2000.0		7.0
	9285 ARCE	22	0809.7	0812.7	6 U		7.0		13.0
	9139 NEUS	22	0809.5	0812	5.1		13.0		5.8
	9139 NEUS	1	0809.5	0859.5			3.0		4.0
	3800 GORK	21	0809.5	0817.8	12.3		4.0		2.2
	9100 GORK		0810 E		60 E				7.0
	3100 CRIM	1	0810	0813	6		7.0		2.0
	1500 NEUS	46	0810.5	0812	2.5		6.0		2.0
	1420 ARCE	46	0810.7	0812	3		6.5		8.5
	380 GORK	1	0810.2	0812	3.6		8.5		2.8
	260 ONDR	41	0825	0825	340		80.0D		4.0
	1500 NEUS	1	0826 E	0826			4.0		5.0
	1420 ARCE	1	0826.2E	0826.2			5.0		350.0
	234 POTS	45	0830	0830	.1		1750.0		35.0
	1500 NEUS	46	0832.3	0832.5	1.7		35.0		2.2
	1420 ARCE	8	0832.5E	0832.5	.6		53.0		6.7
	1500 NEUS	4	0841.3	0841.7	.7		6.7		8.0
	1420 ARCE	4	0841.4	0841.8	.7		8.0		400.0
	202 IZMI	40	0841.6	0842.4	1.4		400.0		15000.0
	23 POTS	5	0847.3	0847.4	.3		15000.0		5000.0
	1500 NEUS	1	0859.8E	0859.8			2.0		1.5
	1420 ARCE	2	0859.8	0859.9	.4		1.5		105
	808 ONDR	45	0915		70		80.0D		117.7U
	260 ONDR	45	0922						0927
	2920 BERL	45	0923.7	0927	117.7U				0956
	2920 BERL	47	0923.7	0923.7					1012.7
	2920 BERL	29	0923.7	1012.7					0937.4
	9500 NERA	28	0924	0937.4	25				10
	9400 SLOW	46	0924	0927.5	10		81.0		143.5
	9285 ARCE	21	0924.5	1111.2	143.5		13.0		52.0
	9139 NEUS	45	0924.5	0927.5	125.5U		52.0		6600.0
	9139 NEUS	47	0924.5	0955.7			6600.0		3450.0
	9139 NEUS	29	0924.5	1005			3450.0		30000.0
	23 POTS	40	0924.7	0926.3	2.7		30000.0		40.0
	9285 ARCE	45	0925.6	0927.6	8.8		40.0		40.0
	9285 ARCE	45	0925.6	0927.6	4		40.0		53.0
	9100 GORK	45	0925	0927	20		53.0		600.0
	3100 CRIM	47	0925	1011	126		600.0		16.0
	3000 NERA	28	0925	0943.3	24		16.0		14.0
	2800 SLOW	46	0925	0927.5	7		14.0		27.0
	1500 NEUS	46	0925	0926.5	8.5		27.0		45.0
	19000 SLOW	3	0926.5	0927	1.5		45.0		

# SOLAR RADIO EMISSION OUTSTANDING OCCURRENCES

24 OCTOBER - 6 NOVEMBER 1968

	FREQUENCY STATION	TYPE	STARTING TIME	TIME OF MAXIMUM	DURATION	FLUX DENSITY $10^{22} \text{ Wm}^{-2} \text{ Hz}^{-1}$		INT	REMARKS
			UT	UT	MINUTES	PEAK	MEAN		
2	1420 ARCE	41	0926.2		3.5				
	1420 ARCE	4	0926.2	0926.6	1.2	32.0			
	536 ONDR	45	0926	0931.5	7	155.0			
	420 KIEL	45	0926	0954	69	400.0D	80.0		
	19000 SLOU	28	0928	0949	21	45.0			
	1420 ARCE	8	0928.4E	0928.4		20.5			
	9285 ARCE	45	0929.6	0931.4	4.8	23.0			
	1420 ARCE	4	0929.7	0930.8	2.3	28.5			
	1420 KIEL	45	0930	0932	3	60.0	20.0		
	2800 SLOU	28	0932	0944	15	14.0			
	9400 SLOU	28	0934		14	18.0			
	2920 BERL	1	0934 E	0934					
	1500 BERL	47	0938	1019.8	88 U	1950.0			
	1500 NEUS	29	0938	1022		1857.0			
	9100 GORK	47	0945	0956 U	50	43700.0			
	536 ONDR	45	0946.5		72	345.0D			
	9285 ARCE	47	0947.8		35.2				OFF SCALE
	7000 SAOP	47	0947.5	0956.4	20.5	4731.9			
	9400 SLOU	47	0948	0956 U	75 U	2580.0D			
	2800 SLOU	47	0948	0956 U	180	310.0D			
	1420 ARCE	47	0948 U		54 U				
	19000 SLOU	47	0949	0955.7	55 U	6300.0			OFF SCALE
	9500 NERA	45	0949.4	0956	39				
	3000 NERA	45	0949.2	1012.6	51	925.0	500.0		
	1420 KIEL	45	0949	1019	46	2700.0	600.0		
	23 POTS	45	0949	1025 U	48	4000.0	45.0		
	930 BORD	45	0949	1023	59	10000.0	1200.0		
	202 IZMI	47	0949	1009	40	800.0	200.0		
	111 POTS	45	0949 U	0954 U	48	1600.0	120.0		
	3800 GORK	47	0950 E	0956	81 E	970.0			
	239 TRST	47	0950.4	0953	5 D	750.0			
	234 POTS	45	0950 U	1005 U	40	300.0	100.0		
	225 HARS	45	0950	0953	35	550.0	150.0		
	240 KIEL	45	1006 E	1006		800.0	10.0		
	408 SANM	45	1010 E		25 D				
	7000 SAOP	29	1013.1		68.5				
	9285 ARCE	29	1023		42.6	136.0			
	9500 NERA	29	1028.6		45				
	3000 NERA	29	1040		43	15.0	8.0		
	202 IZMI	40	1052	1055	3.5	300.0			
	408 SANM	45	1053.8	1054.5	3.7	19.0	12.0		
	234 POTS	5	1054.2	1054.2	.1	175.0	60.0		
	239 TRST	45	1055	1055.1	.3	240.0	30.0		
	23 POTS	45	1056.1	1058.1	4.2	6000.0	170.0		
	1500 NEUS	3	1141.5	1142	1	92.0			
	1500 NEUS	2	1141.5E	1141.5		4.4			
	1420 ARCE	8	1142	1142.2	.6	67.0			
	23 POTS	40	1142	1145.4	3.7	4000.0	100.0		
	1500 NEUS	3	1145	1145.2	.5	21.0			
	1420 ARCE	2	1145	1145.3	.4	4.5			
1500 NEUS	1	1146 E	1146		2.5				
23 POTS	5	1152.9	1153	.2	2000.0	700.0			
2920 BERL	22	1153	1201.3	13 U					
9285 ARCE	22	1155	1201.5	14.4	10.0				
9139 NEUS	22	1155	1201.3	13	14.0	3.5			
7000 SAOP	3	1201.2	1201.5	1.3	11.6	5.8			
1500 NEUS	1	1201.4E	1201.4		3.5				
1420 ARCE	1	1201.4E	1201.4	.5	3.0				
7000 SAOP	3	1204.7	1205.7	1.9	9.7	4.8			
234 POTS	45	1223.4	1223.5	.2	200.0	30.0			
9139 NEUS	20	1229.5E	1229.5		4.7				
2920 BERL	22	1229.5E	1229.5						
1500 NEUS	3	1229.5E	1229.5		12.0				
1420 ARCE	8	1229.6E	1229.6		36.0				
9285 ARCE	1	1236.5	1236.7	1	3.0				
9139 NEUS	1	1236.5E	1236.5		4.7				
9285 ARCE	1	1245.7	1246	.6	7.0				
9139 NEUS	3	1245.7E	1245.7		12.0				
8800 SGMR	3	1245.5	1245.7	.9	12.9	6.4			
7000 SAOP	3	1245.9	1247	1.4	15.5	7.7			
4995 SGMR	1	1245.4	1245.6	1	3.4	1.7			
2920 BERL	1	1307.7E	1307.7						
1500 NEUS	3	1307.7E	1307.7		6.7				
1420 ARCE	8	1307.8E	1307.8		8.0				
1420 ARCE	1	1314.3E	1314.3		4.0				
23 POTS	45	1314.3	1315.6	6.4	4000.0	400.0			
1500 NEUS	4	1315.7	1316	1.3	20.0	4.2			
1420 ARCE	4	1315.8	1316.2	.8	52.0				
184 BOUL	44	1330 E		608 D					
15400 SGMR	20	1402.7	1403.1	16.1	8.7	4.4			
8800 SGMR	20	1402.6	1405	14	7.4	3.7			
4995 SGMR	20	1404.5	1406	9.5	3.7	1.8			
1420 ARCE	8	1428.7	1429.7		10.0				
1415 SGMR	3	1429.5	1429.6	.3	7.8	4.0			
606 SGMR	3	1429.3	1429.5	.7	24.8	12.3			
606 SGMR	1	1436.7	1436.8	3.5	3.8	1.9			
4995 SGMR	21	1451.7	1522	77.5	13.9	6.9			
8800 SGMR	21	1452	1523.5	66	17.0	8.5			
960 PENN	45	1452.7	1457	18.5	14.1	1.9			
2695 SGMR	21	1454	1525	65	3.2	1.6			

# SOLAR RADIO EMISSION OUTSTANDING OCCURRENCES

24 OCTOBER - 6 NOVEMBER 1968

	FREQUENCY STATION	TYPE	STARTING TIME	TIME OF MAXIMUM	DURATION	FLUX DENSITY $10^{22} \text{ Wm}^{-2} \text{ Hz}^{-1}$		INT	REMARKS
			UT	UT	MINUTES	PEAK	MEAN		
2	15400 SGMR	21	1455.8	1522.3	90.2	18.9	9.4		
	1420 ARCE	45	1455.4	1455.6	2.5	9.0			
	1415 SGMR	2	1455	1455.5	2.4	6.2	2.1		
	930 BORD	40	1455	1456	3	24.0	4.0		
	606 SGMR	1	1455.3	1455.4	.9	6.5	2.3		
	7000 SAOP	41	1511.5		30.2				
	7000 SAOP	28	1511.5		7.4				
	10700 PENN	45	1512.5	1519.7	33.3	155.0	22.2		
	2700 PENN	3	1512.5	1531.4	29.5	31.8	7.4		
	960 PENN	45	1512.1	1520.1	26.3	23.5	1.5		
	2800 SLOU	45	1513	1520	10 U	34.0			
	1415 SGMR	41	1513.8	1520	8.1	5.2	1.3		
	606 SGMR	41	1514.2	1519	7.1	17.8	3.6		
	328 PENN	45	1515	1521.1	8.9	47.5	7.5		
	1420 ARCE	41	1517.3		8				SUNSET
	1420 ARCE	4	1517.3	1517.5	.5	13.5			
	15400 SGMR	45	1518.5	1520	20	115.0	46.0		
	8800 SGMR	3	1518.8	1519.9	3	140.0	67.0		
	7000 SAOP	3	1518.9	1520.2	4.4	132.0	66.0		
	3000 NERA	45	1518.9	1520	2	14.0	7.0		
	19000 SLOU	45	1519.1	1519.7	16 U	49.0			
	9500 NERA	45	1519	1519.9	2.5				
	9400 SLOU	45	1519	1521.1	16 U	258.0			
	9285 ARCE	41	1519		14.3D				SUNSET
	9285 ARCE	4	1519	1520	2	92.0			
	4995 SGMR	3	1519	1520	7.7	105.0	34.0		
	2800 OTTA	41	1519		30				
	2800 OTTA	3	1519	1519.8	2.5	11.0	5.5		
	2695 SGMR	3	1519.5	1520	1.9	8.5	4.2		
	1420 ARCE	45	1519	1519.2	2	9.0			
	930 BORD	45	1519	1520.5	2	73.0	5.0		
	9285 ARCE	29	1521		3.3	18.5			
	7000 SAOP	45	1523.3	1531.5	11.9	58.2	19.1U		
	9285 ARCE	3	1524.8	1525.2	1.6	18.5			
	2800 OTTA	1	1524.5	1525	1.5	2.2	1.1		
	606 SGMR	45	1524.3	1531.9	22.5	47.5	9.4		
	328 PENN	45	1524.2	1543.5	27.2	266.0D	31.0D		
	1420 ARCE	8	1525.2	1525.2		23.0			
	4995 SGMR	45	1526.8	1531.5	12.1	87.0	28.0		
	2695 SGMR	45	1526.9	1531.4	14.1	38.0	16.0		
	408 SANM	41	1526.6	1542.9	20.9	696.0	144.0		
	9285 ARCE	3	1527.8	1528.5	1.8	16.0			
	8800 SGMR	45	1527.2	1531.5	9.1	48.8	19.6		
	3000 NERA	45	1527.1	1531.7	8	60.0	35.0		
	2800 OTTA	46	1527	1531.5	13	40.0	20.0		
	2800 OTTA	46	1527	1528	2.5	20.0			
	2800 OTTA	46	1529.5	1531.5	10.5	40.0			
	1415 SGMR	21	1527.1	1533.9	21.9	4.4	2.2		
	9285 ARCE	45	1530.6	1531.5	5.6D	29.5			
	9500 NERA	45	1531	1532.3	4				
7000 SAOP	29	1535.2		6.4					
1415 SGMR	20	1537.2	1538.1	8.8	1.8	.9			
960 PENN	20	1541.9	1543.4	32.8	3.0	1.6			
2800 OTTA	1	1542.5	1544	7.5	9.2	4.2			
2700 PENN	3	1542.6	1544	4.8	9.4	3.9			
18 BOUL	6	1557	1559	3	1.0				
18 HCHA	6	1600	1600	1					
2800 OTTA	20	1630	1730	205	12.0	6.0		1	
10700 PENN	20	1633.2	1659.3	107.8	19.3	5.0			
8800 SGMR	1	1659.4	1659.5	1.5	5.5	2.8			
4995 SGMR	20	1659	1728.7	127.4	8.5	4.3			
2695 SGMR	20	1700.2	1728.7	38.5	4.1	2.1			
606 SGMR	1	1743.2	1743.3	1.5	2.7	1.4			
408 SANM	43	1815	1844	120	40.0	11.0			
10700 PENN	3	1910.9	1913.5	9.1	26.1	7.9			
15400 SGMR	3	1912	1913.5	4.5	18.9	9.4			
8800 SGMR	3	1912.7	1913.6	2.1	9.2	4.6			
10700 PENN	3	1958.7	1959.4	2	13.2	4.8			
2800 OTTA	20	2018	2021	50	4.0	2.0			
2695 PENT	1	2146.2	2146.5	.5	4.2	2.1			
9400 TYKW	45	2327	2333.2	25	11.0	3.0			
3	17000 TOKO	45	0002.2	0002.4	.4	48.0			
	9400 TYKW	5	0002.3	0002.6	2.5	85.0	17.0		
	8800 MNL	3	0002.2	0002.5	2.9	80.0	40.1		
	4995 MNL	3	0002.2	0002.5	3.1	42.5	21.8		
	3750 TYKW	5	0002.3	0002.6	1.5	15.0	5.0		
	2695 MNL	3	0002.3	0002.5	3.2	12.7	6.4		
	1415 MNL	3	0002.3	0002.5	4.2	74.0	24.2		
	208 VORO	5	0002	0002.5	1	398.0	211.0		
	200 HIRA	45	0002.2	0002.5	.5	1160.0	340.0		
	9400 TYKW	5	0009	0009.4	1	2.0	1.0		
	3750 TYKW	5	0009	0009.4	1	2.0	1.0		
	9400 TYKW	5	0138.8	0139	.7	10.0	2.0		
	200 HIRA	45	0208	0208.8	2	990.0	50.0		
	9400 TYKW	5	0209.7	0210.1	.8	21.0	5.0		
	3750 TYKW	5	0209.8	0210.1	.7	3.0	1.0		
	2695 MNL	1	0209.9	0210.1	.9	3.8	1.9		
	2000 TYKW	5	0209.8	0210.1	.8	4.0	1.0		
	1415 MNL	3	0209.9	0210.1	.9	13.0	6.5		

# SOLAR RADIO EMISSION OUTSTANDING OCCURRENCES

24 OCTOBER - 6 NOVEMBER 1968

	FREQUENCY	STATION	TYPE	STARTING TIME	TIME OF MAXIMUM	DURATION	FLUX DENSITY		INT	REMARKS
				UT	UT	MINUTES	$10^{22} \text{ Wm}^{-2} \text{ Hz}^{-1}$ PEAK	MEAN		
3	1000	TYKW	45	0209.2	0210.1	1.5	128.0	10.0		
	208	VORO	5	0209	0209.7	1.5	361.0	160.0		
	8800	MNL	3	0210	0210.1	.8	20.0	10.0		
	4995	MNL	3	0210	0210.1	.8	17.0	8.5		
	9400	TYKW	45	0427.5	0427.7	.5	26.0	5.0		
	9400	TYKW	5	0529	0530.7	6	12.0	4.0		
	9400	TYKW	5	0646.3	0646.9	1.5	25.0	4.0		
	3750	TYKW	5	0646.5	0647	1	2.0	1.0		
	8800	MNL	3	0710	0710.4	1.8	34.2	16.0		
	4995	MNL	3	0710	0710.4	1.8	22.2	11.1		
	2695	MNL	3	0710	0710.4	1.8	13.8	6.9		
	1415	MNL	3	0710	0710.4	2.7	20.8	10.4		
	9500	NERA	45	0711	0711.1	1.1				
	9139	NEUS	3	0711	0711.1	1	18.5			
	3750	TYKW	5	0711	0711.5	1	9.0U	3.0		SUNSET
	3100	CRIM	1	0711	0711.5	2	7.0	2.0		
	3000	NERA	5	0711.1	0712	1.2	12.0	6.0		
	2000	TYKW	5	0711	0711.5	1	14.0	5.0		
	1000	TYKW	45	0711	0711.5	1	15.0	5.0		
	3800	GORK	1	0720.3	0722.5	3.7	7.9	3.9		
	3800	GORK	1	0843.6	0846.5	6.9	7.1	4.0		
	9139	NEUS	20	0911.5E	0911.5		2.8			
	239	TRST	45	0918.9	0918.9	.2	125.0	49.0		
	260	ONDR	45	0919	0927.5	20	85.0D			
	9285	ARCE	21	0921.8	0923.3	16.4	6.5			
	9139	NEUS	22	0922	0927.5	15	9.7			
	9139	NEUS		0922	0934		6.5	3.5		
	202	IZMI	40	0924		13	300.0			
	9285	ARCE	20	0927.4	0927.9	2.6	6.5			
	930	BORD	45	0927	0927.6	1	18.0	2.0		
	239	TRST	45	0927.1	0927.5	.6	540.0	76.0		
	234	POTS	45	0927.3	0927.4	.2	250.0	30.0		
	239	TRST	45	0931.6	0932.2	.8	660.0	69.0		
	234	POTS	40	0933.8	0934.1	2.8	140.0	2.0		
	111	POTS	45	0933.8	0933.9	.3	400.0	80.0		
	9285	ARCE	1	0934	0934.5	1	4.0			
	239	TRST	45	0935.3	0935.5	.3	290.0	73.0		
	9400	SLOU	3	1009.5	1009.6	.5	54.0			
	9285	ARCE	1	1015.8	1016.3	2.2	6.5			
	9139	NEUS	1	1015.5	1016.2	2	8.2	3.3		
	260	ONDR	45	1204.5		37	85.0D			
	4995	SGMR	1	1216	1217.8	2.3	4.4	2.2		
	3000	NERA	45	1216.5	1217.8	1.9	6.0	3.0		
	2695	SGMR	3	1216	1217.3	3.6	7.6	3.0		
	1500	NEUS	4	1216.5	1218	2.2	22.0	3.9		
	1415	SGMR	4	1216.1	1217	2.1	14.0	3.7		
	606	SGMR	1	1216.3	1217.8	2.9	3.9	1.9		
	2920	BERL	22	1217	1218	1.5				
	1420	KIEL	45	1217	1218	21	30.0	12.0		
	1420	ARCE	4	1217.2	1218.2	1.8	16.0			
1420	ARCE	31	1219	1224	13	-22.5				
3100	CRIM	3	1220	1237		25.0				
1500	NEUS	1	1220.8E	1220.8		4.2				
1500	NEUS	1	1222 E	1222		3.0				
239	TRST	45	1223.8	1223.9	.3	280.0	73.0			
2920	BERL	1	1230.8E	1230.8						
1500	NEUS	1	1230.8E	1230.8		4.2				
1420	ARCE	1	1230.7	1230.9	.7	3.5				
606	SGMR	45	1230.4	1239.4	20.5	490.0	31.9			
19000	SLOU	41	1232.6	1233	12.4	25.0U				
15400	SGMR	45	1232.6	1233.4	10.2	22.2	10.7			
10700	PENN	45		1233.1		80.0D				
9285	ARCE	45	1232.5	1233.4	8.7	56.0				
9285	ARCE	45	1232.5	1233.4	4	56.0				
9139	NEUS	46	1232	1233.3	150 D	58.3				
9139	NEUS		1232	1239.6		41.5				
9139	NEUS	31	1232	1249.5		-13.5				
8800	SGMR	45	1232.9	1233.2		83.0	18.8			
7000	SAOP	41	1232.7		10.3					
7000	SAOP	3	1232.7	1233.4	1.6	79.0	39.5			
4995	SGMR	45	1232.6	1233.3	8.2	120.0	29.9			
3000	NERA	40	1232.8	1233.4	8	85.0				
2920	BERL	46	1232.7	1233.4						
2920	BERL	46	1232.7	1239.6						
2920	BERL	31	1232.7	1250 U						
2700	PENN	45		1233.2		58.0D				
2695	SGMR	45	1232.8	1233.2	8.6	77.0	27.6			
1500	NEUS	46	1232.5	1234	87.5	84.0				
1500	NEUS		1232.5	1240		68.0				
1500	NEUS	31	1232.5	1255		3.0				
1420	ARCE	46	1232.5	1233.5	13.8	79.0				
1420	ARCE	46	1232.5	1233.5	2.8	79.0				
1415	SGMR	45	1232.6	1239.6	10.5	100.0	35.0			
960	PENN	45		1236.6		300.0D				
536	ONDR	45	1232.5	1240.5	12	280.0				
328	PENN	45	1232.7	1233	1.2	101.0	15.6			
240	KIEL	45	1232 E	1232		2000.0D	7.0			
9500	NERA	40	1233	1233.2	7					
9400	SLOU	41	1233.3	1234	10	174.0				
2800	OTTA		1233 E	1233.5	12 D	72.0			DUR SUNRISE	

# SOLAR RADIO EMISSION OUTSTANDING OCCURRENCES

24 OCTOBER - 6 NOVEMBER 1968

	FREQUENCY	STATION	TYPE	STARTING TIME	TIME OF MAXIMUM	DURATION	FLUX DENSITY $10^{-22} \text{ Wm}^{-2} \text{ Hz}^{-1}$		INT	REMARKS
				UT	UT	MINUTES	PEAK	MEAN		
3	1420	KIEL	45	1233	1241	11	250.0	100.0		
	23	POTS	40	1233.2	1239.3	6.3	10000.0	250.0		
	930	BORD	45	1233	1237	11	450.0	39.0		
	808	ONDR	45	1233	1239.5	8.5				
	420	KIEL	45	1233	1240	11	400.0D	100.0		
	239	TRST	45	1233	1233.1	.8	5600.0D	566.0D		
	234	POTS	40	1233	1233.1	8.6	3500.0	40.0		
	111	POTS	40	1233	1239.1	6.2	1000.0	10.0		
	1420	ARCE	46	1235.3	1236.8	3.8	49.5			
	9285	ARCE	45	1236.5	1236.9	2.7	27.0			
	7000	SAOP	3	1236.1	1236.8	2.1	27.1	13.5		
	328	PENN	45	1238.9	1238.9	1.6	130.0	20.0		
	239	TRST	40	1238.9	1239.6	1.6	3960.0	170.0		
	9285	ARCE	45	1239.2	1239.8	2	34.0			
	7000	SAOP	45	1239.1	1239.6	1.2	38.3	19.1U		
	1420	ARCE	46	1239.1	1239.7	7.2	77.0			
	9500	NERA	31	1240	1245	20 U				
	7000	SAOP	29	1240.3		2				
	3000	NERA	31	1240.7	1250	80	12.0	6.0		
	9285	ARCE	31	1241.2	1247.4	10	38.0			
	1420	ARCE	31	1246.3	1247.3	7.6	15.0			INTERFERENCES
	1500	NEUS	1	1309 E	1309		3.5			
	2800	OTTA	20	1310	1325	30	3.0	1.5		
	1500	NEUS	45	1310	1311	1.3	7.0	2.1		
	1500	NEUS	1	1329 E	1329		3.8			
	10700	PENN	20	1346.1	1511.6	199.7	32.8	17.1		
	2700	PENN	20	1346.1	1535.6	307.4	9.1	4.2		
	2800	OTTA	24	1350		20	6.0			
	2800	OTTA	22	1425	1450	115	6.0	3.6		
	10700	PENN	3	1639.3	1641.1	9.1	61.4	10.1		
	8800	SGMR	3	1640	1641.1	4.7	34.0	16.2		
	4995	SGMR	20	1640.9	1642.4	8.1	5.8	2.8		
	2695	SGMR	1	1640.9	1641.2	.9	1.8	.9		
	184	BOUL	6	1640	1640	1	1810.0	900.0		
	2700	PENN	1	1641	1641.1	1.6	3.5	1.0		
	960	PENN	3	1642.2	1642.3	.6	8.1	1.9		
	8800	SGMR	29	1644.7	1644.7	13.1	8.3	4.2		
	10700	PENN	20	1708.4	1709.7	17.4	16.4	3.5		
	15400	SGMR	3	1709.4	1709.7	1	15.0	7.5		
	8800	SGMR	3	1709.2	1709.7	1.4	10.6	5.3		
	4995	SGMR	3	1709.3	1709.8	1.6	17.0	8.5		
	2800	OTTA	41	1709.2		11				
	2800	OTTA	3	1709.2	1710	2	10.6	5.3		
	2700	PENN	3	1709.1	1709.8	4.7	13.4	5.1		
	2695	SGMR	3	1709.2	1709.8	3	12.7	6.3		
	960	PENN	45	1709.2	1709.9	6.8	48.3	6.6		
	328	PENN	5	1709.3	1709.5	.3	17.4	11.6		
	2700	PENN	3	1714.8	1719.3	5.4	12.2	4.4		
	184	BOUL	6	1714	1714	1	2700.0	1300.0		
	2800	OTTA	1	1715	1715.5	2	2.0	1.0		
	328	PENN	5	1715.1	1715.2	.5	52.0	11.6		
	1415	SGMR	4	1718.7	1719.3	2.5	97.0	33.0		
	606	SGMR	4	1718.3	1719.1	2.2	145.0	36.0		
	15400	SGMR	1	1719.2	1719.6	.8	4.0	2.0		
	8800	SGMR	1	1719.2	1719.5	1	3.7	1.7		
	4995	SGMR	1	1719.3	1719.6	1	5.1	2.5		
	2800	OTTA	1	1719	1719.2	1	9.2	4.6		
	2695	SGMR	3	1719	1719.3	1	9.7	4.3		
	960	PENN	45	1719	1719.4	1.6	52.1	17.4		
	328	PENN	5	1719.2	1719.3	1	8.7	2.3		
	606	SGMR	45	1741.3	1741.6	1.2	170.0	19.6		
	328	PENN	45	1741.2	1741.4	.8	75.2	9.4		
	10700	PENN	3	1803.7	1810.2	21.2	22.4	5.7		
	8800	SGMR	3	1808.9	1810.8	3.5	13.8	6.8		
	15400	SGMR	1	1809.9	1810.5	1.4	5.5	2.8		
	1415	SGMR	1	1810.2	1810.3	.4	2.0	1.0		
	328	PENN	45	1828.7	1829.1	1.1	60.5	20.3		
	960	PENN	45	1829	1829.1	1	96.0	64.0		
	960	PENN	45	1839.5	1840.3	1.1	28.6	13.8		
	328	PENN	45	1839.7	1840.3	1	39.9	15.2		
	960	PENN	29	1840.6	1841.5	26.4	12.5	4.5		
	184	BOUL	43	1927	2100	115	434.0	220.0		
	2700	PENN	1	1932.3	1934.2	7.3	7.5	2.5		
	15400	SGMR	3	1933.9	1934.3	1.3	11.0	3.7		
	10700	PENN	3	1933.4	1934.2	2	12.3	6.1		
	8800	SGMR	3	1933.9	1934.3	1.1	13.8	4.6		
	4995	SGMR	3	1933.8	1934.3	3.7	10.2	3.4		
	2695	SGMR	1	1933.7	1934.2	4.7	6.2	3.2		
	1415	SGMR	3	1933.8	1934.4	2.9	8.5	4.3		
	960	PENN	3	1933.5	1934.2	3.4	9.2	2.6		
	606	SGMR	4	1933.7	1934.3	1.8	15.7	4.9		
	7000	SAOP	3	1934	1934.4	1.7	13.5	6.7		
	2800	OTTA	1	1934	1934.5	2	5.2	2.6		
	328	PENN	5	1934.2	1934.3	.2	5.5	2.8		
	606	SGMR	4	1952.3	1952.4	1.3	39.2	15.6		
	606	SGMR	45	2032.5	2032.5	1.5	82.0	15.0		
	328	PENN	45	2036.3	2039.3		79.9			
	10700	PENN	3	2037.4	2038.9		25.2			
	8800	SGMR	45	2037.5	2039.5	5.6	30.4	15.0		
	4995	SGMR	45	2037.8	2038.8	5.4	34.0	17.0		

# SOLAR RADIO EMISSION OUTSTANDING OCCURRENCES

24 OCTOBER - 6 NOVEMBER 1968

	FREQUENCY STATION	TYPE	STARTING TIME	TIME OF MAXIMUM	DURATION	FLUX DENSITY $10^{-22} \text{ Wm}^{-2} \text{ Hz}^{-1}$		INT	REMARKS
			UT	UT	MINUTES	PEAK	MEAN		
	2800 OTTA	4	2037.5	2038.8	5.5	49.0	11.0		
	2700 PENN	3	2037.4	2038.7		41.4	17.4		
	2695 SGMR	4	2037.8	2038.8	5.3	35.2	30.4		
	1415 SGMR	45	2037.6	2038.9	5.6	74.0	7.2		
	960 PENN	45	2037.5	2038.7	5.8	70.2	15.0		
	606 SGMR	45	2037.2	2037.7	5.8	200.0	-3.8		
	2800 OTTA	32	2043	2100	53	-7.6	160.0		
	500 HIRA	45	2322.5	2323	1	460.0			
4	3750 TYKW	5	0030	0031.3	15	6.0	2.0		
	9400 TYKW	5	0217.5	0217.9	5	7.0	4.0		
	9400 TYKW	45	0346	0347.5	5	8.0	3.0		
	3750 TYKW	45	0346	0347.5	5	6.0	5.0		
	9400 TYKW	5	0432.8	0433.2	3	36.0			
	3800 GORK	47	0459.3	0522.9	119 D	1720.0			
	9400 TYKW	45	0513	0520.7	26	8000.0	2300.0		
	9100 GORK	47	0513	0523.9	37	2130.0			
	8800 MNL	46	0513	0520.6	20	6400.0	3200.0		
	4995 MNL	46	0513	0523	20	4300.0	2100.0		
	3750 TYKW	45	0513	0523.2	26	1800.0	400.0		
	2695 MNL	46	0513.2	0520.6	18.9	730.0	375.0		
	2000 TYKW	45	0513	0517	20	470.0	125.0		
	1415 MNL	45	0513.2	0517	13.8	360.0	178.0		
	17000 TOKO	45	0514		21	2600.0D			
	3100 CRIM	47	0514	0523	86	240.0	80.0		
	1000 TYKW	45	0514	0517	19	385.0	85.0		
	612 TOKO	45	0515.3	0517.1	9	185.0			
	1415 MNL	30	0527	0533	68	12.8	6.0		
	2695 MNL	30	0532.1	0533	62.9	33.8	17.5		
	1415 MNL	40	0532.8	0539.2	38.2	71.0	35.0		
	8800 MNL	30	0533	0533	62	115.0	57.5		
	4995 MNL	30	0533	0533	62	88.0	43.4		
	2000 TYKW	29	0533		60	8.0	4.0		
	2000 TYKW	45	0533	0540.3	20	90.0	10.0		
	17000 TOKO	29	0535			104.0			
	2695 MNL	40	0536.6	0539.7	34.4	12.5	6.2		
	1000 TYKW	40	0538	0550.5	14	95.0	9.0		
	9400 TYKW	29	0539		80 D	95.0	35.0U		
	9400 TYKW	45	0539	0548	11	20.0	7.0		
	3750 TYKW	29	0539		90 D	30.0	15.0U		
	3750 TYKW	45	0539	0547.5	15	13.0	5.0		
	9100 GORK	30	0550	0550	109	61.0	18.0		
	1000 TYKW	45	0558.5	0605.2	11	140.0	30.0		
	9400 TYKW	5	0606	0607	4	8.0	4.0		
	3750 TYKW	5	0606	0607	4	4.0	2.0		
	9400 TYKW	5	0618	0619.5	6	55.0	13.0		
	9100 GORK	3	0618.3	0619.5	2	45.0	22.0		
	8800 MNL	3	0618.1	0619.7	4.9	50.6	25.3		
	4995 MNL	3	0618	0619.7	5	43.4	24.8		
	3800 GORK	30	0618 E		54				
	3800 GORK	3	0618.5	0619.4	1.9	15.0	8.0		
	3750 TYKW	5	0618	0619.5	13	24.0	8.0		
	2695 MNL	3	0618.3	0619.7	4.7	12.5	6.2		
	2000 TYKW	45	0618.5	0619.6	6	69.0	9.0		
	111 POTS	5	0651	0651	.1	200.0	70.0		
	260 ONDR	44	0750	1110.5	250	75.0			
	1500 NEUS	20	0814.5E	0814.5		1.5			
	3800 GORK	21	0815 E	0835	96 E	7.7	5.7		
	3100 CRIM	1	0822	0825	5	7.8	2.0		
	3000 NERA	5	0823.6	0824.9	2.2	7.0	3.0		
	2920 BERL	1	0823	0825	3				
	3800 GORK	1	0824.5	0825	1	3.6	1.7		
	2800 SLOU	23	0905	0934.2	44	10.0			
	3100 CRIM	41	0906	0908	9	4.0	1.0		
	3100 CRIM		0906	0915		8.0	3.0		
	9285 ARCE	20	0908.8	0909.4	1.8	3.5			
	9139 NEUS	20	0908	0909.4	3.7	6.7	3.5		
	3800 GORK	1	0908.5	0909	1	3.5	1.7		
	2920 BERL	22	0908	0909	8				
	2920 BERL		0908	0914.5					
	930 BORD	5	0909	0909	1	24.0	2.0		
	9285 ARCE	20	0912.6	0915.3	11	6.0			
	9139 NEUS	20	0913	0916.5	5.5	3.2	2.7		
	3000 NERA	5	0913.8	0914.6	1.2	9.0	5.0		
	1500 NEUS	1	0913.7	0914.6	1.3	2.8	0.8		
	1420 ARCE	1	0913.8	0914.7	1.4	1.5			
	3800 GORK	1	0914.2	0914.6	1	5.9	2.8		
	240 KIEL	45	0920 E	0920		2000.0D	35.0		
	3100 CRIM	1	0925	0926	3	4.0	1.0		
	9285 ARCE	20	0926.6	0927.2	1.7	9.5			
	9139 NEUS	1	0926.3	0927	3	8.3	4.0		
	3800 GORK	1	0926.3	0927	1.8	5.9	3.0		
	2920 BERL	20	0926.5	0927.2	2.5				
	3100 CRIM	3	0933	0934	3	10.0	3.0		
	3000 NERA	5	0933.3	0934.4	1.7	10.0	5.0		
	2920 BERL	4	0933.6	0934.6	3.4				
	1500 NEUS	45	0933.5	0934.6	3.5	12.0	3.5		
	3800 GORK	1	0934.1	0934.5	1.3	8.3	4.1		
	1420 ARCE	46	0934	0934.9	3	10.0			
	1500 NEUS	1	0940.7E	0940.7		4.0			

# SOLAR RADIO EMISSION OUTSTANDING OCCURRENCES

24 OCTOBER - 6 NOVEMBER 1968

	FREQUENCY STATION	TYPE	STARTING TIME	TIME OF MAXIMUM	DURATION	FLUX DENSITY $10^{-22} \text{ Wm}^{-2} \text{ Hz}^{-1}$		INT	REMARKS
			UT	UT	MINUTES	PEAK	MEAN		
4	1420 ARCE	1	0940.7	0940.9	.8	1.0			
	2920 BERL	1	0941 E	0941					
	9285 ARCE	20	0951.2	0953.8	7	6.5			
	9139 NEUS	20	0952.7E	0952.7		5.4			
	9139 NEUS	20	0956.5E	0956.5		5.4			
	408 SANM	41	1010 E	1041.6	60 D	30.5	14.0		
	606 SGMR	22	1257.3	1304.7	16.9	6.2	3.0		
	8800 SGMR	22	1304.1	1306.2	8.2	7.7	3.0		
	7000 SAOP	22	1304.1		3	8.3	4.1		
	4995 SGMR	22	1304.1	1306.4	7.9	11.2	5.0		
	15400 SGMR	2	1305.9	1306.1	6.4	4.5	2.0		
	2800 OTTA	1	1305.5	1306.3	2	2.8	1.4		
	9139 NEUS	1	1306.5E	1306.5		5.4			
	2920 BERL	2	1306 E	1306					
	2695 SGMR	22	1306	1306	8.2	3.7	1.5		
	1500 BERL	1	1306 E	1306		1.2			
	9139 NEUS	1	1311.5E	1311.5		2.7			
	2920 BERL	1	1311.5E	1311.5					
	1500 NEUS	1	1311 E	1311.5		2.0			
	2800 OTTA	26	1700		5	2.4			
2800 OTTA	1	2104.7	2105	4	3.0	1.5			
2695 PENT	24	2140		5	2.4				
5	9400 TYKW	5	0248.5	0248.8	1.5	15.0	3.0		
	3750 TYKW	45	0248.5	0248.7	1.5	28.0	8.0		
	2000 TYKW	45	0248.5	0248.8	1.5	67.0	20.0		
	1000 TYKW	45	0248.5	0248.8	1.5	20.0	8.0		
	2000 TYKW	5	0429	0429.2	.5	6.0	2.0		
	1000 TYKW	5	0429	0429.2	.5	41.0	10.0		
	3750 TYKW	45	0434.5	0435.4	1.5	8.0	4.0		
	2000 TYKW	45	0434.5	0435.4	1.5	22.0	3.0		
	1000 TYKW	45	0434.5	0435.1	1	125.0	15.0		
	9400 TYKW	5	0435	0435.4	1	5.0	1.0		
	1000 TYKW	40	0532	0532.4	1.5	45.0	8.0		
	260 ONDR	5	1122.5	1122.5	1	20.0			
	1500 NEUS	2	1233.5	1234.3	1.8	4.6	1.7		
	1420 ARCE	4	1234.3	1234.4	1	6.0			
	3100 CRIM	1	1235	1238	5	6.0	2.0		
	960 PENN	45	1236.1	1238.3	2.7	20.4	2.3		
	10700 PENN	3	1237.4	1238.3	1.8	8.2	2.0		
	3000 NERA	45	1237	1238.2	1.6	10.0	4.0		
	2920 BERL	2	1237	1238.4	3				
	2700 PENN	3	1237	1238.3	2.8	9.0	2.8		
	1500 NEUS	41	1237	1238.4	2.3	65.0			
	1420 ARCE	41	1237.3		2				
	1420 ARCE	8	1237.3	1237.3		24.0			
	1420 ARCE	8	1237.7	1237.7		17.0			
	930 BORD	40	1237	1238	2	45.0	5.0		
	15400 SGMR	1	1238.2	1238.3	.3	5.0	2.5		
	9285 ARCE	1	1238.2	1238.4	.6	3.5			
	9139 NEUS	1	1238.4E	1238.4		3.4			
	8800 SGMR	1	1238.2	1238.3	.5	1.0	.5		
	4995 SGMR	1	1238.2	1238.3	1.4	7.0	3.5		
	2695 SGMR	3	1238.1	1238.2	.6	8.1	4.0		
	1420 KIEL	45	1238	1239	2	300.0	80.0		
	1420 ARCE	4	1238.2	1238.3	1	88.0			
	1415 SGMR	3	1238.1	1238.2	.6	110.0	45.0		
	606 SGMR	1	1238.2	1238.3	.5	1.7	1.0		
	15400 SGMR	3	1342.3	1343.3	3.2	33.2	8.0		
	10700 PENN	3	1342.1	1343.3	3.5	46.0	12.6		
	9400 SLOU	3	1342.5	1343	2	90.0			
	9139 NEUS	4	1342.6	1343.3	4.4	45.6	14.4		
	8800 SGMR	3	1342.5	1343.3	8.2	59.0	14.0		
	7000 SAOP	3	1342.6	1343.3	2.8	115.2	57.6		
	4995 SGMR	3	1342.6	1343.3	8	80.0	20.0		
	3000 NERA	5	1342.5	1343.6	2.5	80.0	35.0		
	2920 BERL	3	1342.7	1343.5	3.6				
	2800 SLOU	3	1342	1342.3	9.5	76.0			
	2800 OTTA	3	1342.5	1343.5	2.5	86.0	22.0		
	2700 PENN	3	1342.5	1343.3	6.8	79.9	10.3		
	2695 SGMR	3	1342.5	1343.3	11	92.0	22.0		
	1500 NEUS	4	1342.6	1343.3	4.4	380.0			
	1420 ARCE	3	1342.6	1343.3	3.6	368.0			
1415 SGMR	3	1342.6	1343.3	6.4	780.0	190.0			
960 PENN	3	1342.3	1343	7.2	86.0D	12.0D			
930 BORD	40	1342	1344	7	380.0	120.0			
808 ONDR	45	1342.5	1344	5					
606 SGMR	45	1342.6	1344	6.4	185.0	15.0			
9500 NERA	45	1343.1	1343.4	1.5					
9285 ARCE	3	1343	1343.5	1	40.0				
1420 KIEL	5	1343	1344	3	600.0	250.0			
260 ONDR	5	1343.5	1343.5	1	25.0				
9285 ARCE	29	1344		3	20.0				
536 ONDR	5	1344.5	1344.5	1	135.0				
2800 OTTA	30	1345		7	3.0	1.5			
328 PENN	5	1346.4	1346.9	.8	11.0	5.5			
1500 NEUS	4	1347.7	1348.3	1.3	31.0	11.0			
960 PENN	3	1347.9	1348.2	.9	29.1	7.0			
2920 BERL	1	1348.3E	1348.3						
2800 OTTA	1	1348	1348.3	1	6.2	2.0			

# SOLAR RADIO EMISSION OUTSTANDING OCCURRENCES

24 OCTOBER - 6 NOVEMBER 1968

	FREQUENCY STATION	TYPE	STARTING TIME	TIME OF MAXIMUM	DURATION	FLUX DENSITY $10^{-22} \text{ Wm}^{-2} \text{ Hz}^{-1}$		INT	REMARKS
			UT	UT	MINUTES	PEAK	MEAN		
	2700 PENN	1	1348	1348.1	.9	5.2	2.4		
	1420 KIEL	5	1348	1349	2	75.0	25.0		
	1420 ARCE	3	1348.1	1348.3	2	20.0			
	2800 OTTA	32	1755	1820	80	-3.8	-1.9		
	2700 PENN	24	1858	2028.3		7.2			
	2800 OTTA	21	2000	2125	150 D	9.4			
	606 SGMR	22	2010.8	2012.1	31.7	8.0	3.0		
	2800 OTTA	1	2011	2012.5	4	2.8	1.4		
	2695 SGMR	22	2011.8	2019.7	26.3	6.9	3.0		
	1415 SGMR	22	2011.4	2018.5	33.7	9.0	4.0		
	4995 SGMR	22	2016.4	2018.6	16.6	5.6	2.5		
	8800 SGMR	22	2018.2	2022.5	14.8	6.3	3.0		
	2800 OTTA	21	2116	2128	25	5.0	2.5		
	2800 OTTA	1	2116	2118.5	5	6.2	3.1		
6	8800 MNL	3	0248.4	0248.8	1.6	11.1	4.4		
	4995 MNL	20	0248.4	0248.8	11.6	22.0	7.3		
	2695 MNL	3	0248.3	0248.8	2.2	21.3	10.7		
	1415 MNL	46	0248.3	0248.8	2.2	93.0	46.5		
	8800 MNL	1	0434.7	0435.3	3	4.6	2.3		
	4995 MNL	3	0434.7	0435.3	3.3	12.3	5.5		
	2695 MNL	3	0434.3	0435.4	3.7	8.6	4.3		
	1415 MNL	4	0434.3	0435	4	12.3	4.7		
	8800 MNL	3	0704.7	0705.1	1	22.9	11.5		
	4995 MNL	3	0704.7	0705.1	1	13.6	6.8		
	2695 MNL	3	0704.7	0705.2	1	10.7	5.4		
	1415 MNL	1	0704.7	0705.2	1.2	3.8	1.9		
	9400 SLOU	21	0856	0918.2	32	90.0			
	1420 ARCE	21	0917.9	0919.3	10.2	3.0			
	1420 ARCE	1	0917.9	0918.2	.6	3.0			
	1500 NEUS	1	0918.1E	0918.1		4.7			
	1500 NEUS	1	0919.3E	0919.3		2.9			
	1500 NEUS	1	0922.2E	0922.2		2.5			
	1420 ARCE	1	0922	0922.2	.6	1.5			
	2920 BERL	1	1111.8	1112	1.5				
	1500 NEUS	3	1111.9	1112	1.1	19.0	1.2		
	9285 ARCE	1	1112	1112.3	1	6.5			
	9139 NEUS	1	1112	1112.2	1	6.5	2.5		
	2800 SLOU	3	1112	1112	.2	16.0			
	1420 ARCE	1	1112.1	1112.1	1	3.0			
	7000 SAOP	3	1225.5	1226.2	5.3	439.7	219.8		
	19000 SLOU	3	1226.3	1226.5	.8	47.0			
	15400 SGMR	3	1226.6	1226.8	1	43.4	22.0		
	9500 NERA	5	1226.8	1227	1.2				
	9400 SLOU	3	1226.5	1227	8.5	138.0			
	9285 ARCE	3	1226.6	1227	1	30.5			
	9139 NEUS	3	1226.5	1227	5.5	40.0	8.8		
	8800 SGMR	3	1226.7	1226.9	1.6	59.0	22.5		
	4995 SGMR	45	1226.6	1226.7	3.3	275.0	64.0		
	3000 NERA	5	1226.6	1227.1	6	175.0	35.0		
	2920 BERL	3	1226.5	1227	11				
	2800 SLOU	3	1226.7	1226.8	12	188.0			
	2695 SGMR	45	1226.6	1226.8	10.7	155.0	21.9		
	1500 NEUS	3	1226.5	1227.2	19	38.0	15.0		
	1420 ARCE	3	1226.5	1227.1	2.3	38.5			
	1415 SGMR	3	1226.4	1227	8	39.4	13.5		
	9285 ARCE	29	1227.7	1227.7	7.4	12.0			
	1420 KIEL	5	1227	1228	6	50.0	20.0		
	536 ONDR	5	1227	1227	1	125.0			
	1420 ARCE	29	1228.8	1228.8	4.2	14.5			
	15400 SGMR	1	1302.5	1302.8	1.3	6.1	3.3		
	8800 SGMR	1	1302.5	1302.7	.7	4.5	2.4		
	4995 SGMR	1	1302.4	1302.6	2.5	3.4	1.2		
	2695 SGMR	1	1302.5	1302.7	.9	1.8	1.0		
	536 ONDR	45	1330.5	1330.5	6	75.0			
	260 ONDR	45	1330.5	1330.5	4	70.0			
	234 POTS	40	1330.2	1331.2	1	500.0	15.0		
	225 HARS	45	1330	1331	2	170.0	50.0		
	111 POTS	40	1330.2	1330.2	1.2	800.0	20.0		
	2700 PENN	1	1650.6	1650.9	.5	2.3	1.7		
	1415 SGMR	3	1650.9	1651	.3	8.3	2.3		
	960 PENN	1	1650.8	1650.9	.3	2.2	1.5		
	606 SGMR	3	1650.7	1650.9	.5	15.4	6.2		
	960 PENN	1	1816.7	1818.3	1.9	3.4	0.7		
	2700 PENN	1	1817.9	1818.2	2.2	3.5	1.2		
	40E SANM	45	1835	1835.5	1	36.0	12.0		
	40B SANM	3	1843.5	1844.5	1.5	40.0	19.0		

# SOLAR RADIO EMISSION SPECTRAL OBSERVATIONS

24 OCTOBER - 6 NOVEMBER 1968

DATE	TIMES OF OBSERVATION		STATION	EVENTS									SPECTRAL TYPE								
	START UT	END UT		DECIMETRIC BAND			METRIC BAND			DEKAMETRIC BAND											
				START UT	END UT	INT.	START UT	END UT	INT.	START UT	END UT	INT.									
10 24	0000	0655	CULG				0001	0002.5	2								IIIG.v				
			CULG				0003	0055	1	0003	0055	1						IV			
			CULG				0244.5	0247	2	0244.5	0247	2							CONT		
			SGMR																		
			WEIS				1134.4	1134.7	1											IIIB	
			HARV				1330	2040	1											IN	
			BOUL				1337	1338.8												IIIG	
			HARV				1629	1630	2	1630										IIIG	
			BOUL				1629.7	1630												III	
			BOUL				1650.9	1651.4												IIIG	
			HARV				1651		2	1651										IIIG	
			BOUL				1719.6	1719.8												III	
	BOUL				1827.1	1827.3												III			
	HARV				1859	1900	1	1859	1900	1	1859	1900	1					IIIG			
	BOUL				1859	1859.6												IIIG			
	BOUL							1908.5	1908.8	1								III			
	HARV				2055	2100	3	2059	2106	3								IV			
	HARV							2057	2120	2								II			
	CULG							2058	2120	2	2104	2120	2					IIH			
	BOUL							2058.3	2119.4									II			
	CULG							2108		1	2108							IIIB			
	HARV							2111	2200	2								IC			
	CULG							2113		1	2113							IIIB			
	BOUL							2119.4	2200									IV			
	CULG							2122	2135	1								IIIG			
	HARV							2127		1	2127							IIIG			
	BOUL							2127	2127.6									IIIG			
	CULG							2129	2227	1								IV			
	HARV							2137	2139	2	2138							IIIG			
	CULG							2137.5	2138.5	2	2137.5	2138.5	2					IIIG			
	BOUL							2137.6	2138.2									IIIG			
	HARV							2200	2340	1								IN			
	BOUL							2200	2255									CONT			
	CULG							2222	2400	1	2222	2400	1					IIIN			
	BOUL							2245	2246.3									IIIG			
	BOUL							2250.2	2251.4									IIIG			
	HARV							2302	2303	1	2302	2303	1					IIIG			
	CULG							2302	2303	2	2302	2303	2					IIIG			
	BOUL							2302.3	2303.1									III			
	CULG							2306.5	2307	1	2306.5	2307	1					IIIG			
	BOUL										2306.6	2307.3	1					IIIG			
	CULG							2345.5		1								IIIB			
	10 25	0000	0626	CULG				0000	0440	1	0000	0440	1					IIIN			
				CULG				0008.5	0013	2	0018.5	0013	2						IIIG.v		
				CULG				0040.5	0041	1	0040.5	0041	1						IIIG		
				CULG				0103.5	0105	1	0103.5	0105	1							IIIG	
				CULG				0209			0209										IIIB
				CULG				0322	0342	2	0322	0342	2								IIIGG
CULG							0340													IIIB.U	
CULG							0559	0605	2	0559	0605	2								IIIG	
CULG																					
SGMR																					
WEIS										1012.1	1012.7	1								IIIG	
WEIS										1022.4	1022.6	1								IIIG	
WEIS								1043.6	1043.8	1								IIIG			
WEIS								1345	1514	2								IS			
HARV								1345	1620	1								IN			
WEIS								1434.4	1434.6	1								IIIB			
BOUL								1434.4	1436.7									IIIG			
HARV								1437	1438	1								IIIG			
BOUL								1441.6	1445.2									IIIG			
HARV								1504	1505	2								IIIG			
WEIS								1504.4	1504.6	2								IIIG			
BOUL								1504.4	1505									III			
BOUL											1511.7	1512	1					III			
HARV								1711	1727	1	1711	1727	1					IIIN			
BOUL								1711.4	1717.3									IIIG			
BOUL								1726.5	1726.9									III			
HARV								1924	1926	1	1924	1926	2					IIIG			
BOUL								1924.3	1926.2									IIIG			
BOUL								1941	1941.5									III			
BOUL								2018.7	2019.1									III			
BOUL								2044.6	2045									III			
BOUL								2111.4	2114.8									IIIG			
CULG								2111.5	2115	2	2111.5	2115	2					IIIG.v			
HARV								2112	2114	2	2114							IIIGG			
CULG								2157	2202	1	2157	2202	1					IIIG			
BOUL								2157.5	2201.8									IIIG			
HARV								2231		2								IIIG			
CULG								2231	2231.5	3	2231	2231.5	1					IIIG.U			
BOUL								2231.2	2231.9									III			
CULG								2306		1	2306							IIIB			
CULG								2334	2337	1	2334	2337	1					IIIG			
CULG								2346.5	2350.5	2	2346.5	2350.5	2					IIIG			

# SOLAR RADIO EMISSION SPECTRAL OBSERVATIONS

24 OCTOBER - 6 NOVEMBER 1968

DATE	TIMES OF OBSERVATION		STATION	EVENTS									SPECTRAL TYPE	
	START UT	END UT		DECIMETRIC BAND			METRIC BAND			DEKAMETRIC BAND				
				START UT	END UT	INT.	START UT	END UT	INT.	START UT	END UT	INT.		
10 26	0000	0700	CULG				0004	0009	2	0004	0009	2	IIIG	
			CULG				0038	0038.5	1				IIIG,U	
	CULG				0045	0048	1					IIIG		
	CULG				0059	0118	1	0059	0118	1	IIIGG			
	CULG				0115	0130	1	0115	0130	1	UNCLF			
	CULG				0120	0215	1	0120	0215	1	I			
	CULG				0511	0512	1	0511	0512	1	IIIG			
	CULG				1115	1500	2					I		
	0655	1625	WEIS										CONT	
	1000	2400	SGMR				1330	1540	2		1200	1300	IC	
1330	2344	HARV				1540	2002	1				IN		
		HARV	1702	1705	1	1702	1705	1				IIIG		
	2044	2400	HARV											
			CULG											
10 27	0000	0647	CULG				0120	0145	1				I,CONT	
			CULG				0145	0400	2				I,CONT	
	CULG				0204	0400	2	0204	0400	2		I		
	CULG				0400	0600	1					IS,CONT		
	0735	1635	WEIS				1040	1600	3				IIIB	
			WEIS				1121.9	1122.1	1				CONT	
	1000	2200	SGMR							1230	1630		IIIB	
			SGMR							1241	1241.6		IIIB	
			SGMR							1303	1303.4		IIIB	
			WEIS	1307	1534	2							IV	
	1312	1506	BOUL				1312	E 1651					IV	
			SGMR							1315	1320		IIIG	
			SGMR							1329	1332		IIIG	
	1330	2343	HARV	1330	E 1830	3	1330	E 1800	3				IV	
			HARV				1330	E 1830	3					
		BOUL				1651	1859.6							
		HARV				1740	1804	2	1740	1804	2	CONT		
		HARV				1800	1840	2				IIIN		
		HARV				1840	1920	1				IC		
		HARV	1843	1846	2	1843	1846	2				I		
		BOUL				1859.6	1940					IIIG		
		HARV				1920	2103	1				CONT		
		BOUL				1953	1953.7					IN		
		BOUL										IIIG		
	2210	2400	CULG											
10 28	0000	0645	CULG				0103	0107	1				IIIG	
			WEIS											
	1100	2200	SGMR										I	
	1330	2342	HARV				1330	1553	1				III	
	1321	1614	BOUL				1415.9	1416.7					IIIG	
			BOUL							1530.1	1531.1	2	IIIG	
			BOUL	1543	1544	2							IC	
			HARV				1553	2340	2				III	
			BOUL							1600.7	1600.9	1	III	
			BOUL							1623.7	1624	1	III	
	1621	1628	BOUL							1629.3	1631.9	3	IIIG	
	1629	2345	HARV	1630	1631	1	1630	1631	2	1630	1631	2	IIIG,V	
			BOUL							1631.9	1700	2	CONT	
			HARV				1636	1642	2	1638	1642	2		
			BOUL							1638.1	1643.5	3	II	
		BOUL												
		BOUL				1700	2000						CONT	
		HARV	1943		1	1943	1944	2	1943	1944	2	IIIG		
		BOUL				1943	1947.6						IIIG	
		BOUL							2138.7	2139	2	III		
	2206	2209	CULG				2208	2209	1				IIIG	
	2211	2400	HARV				2221	2400	1				I	
			CULG							2250.6	2254	1	IIIG	
			BOUL											
10 29	0000	0633	CULG				0000	0530	1				I	
			CULG				0012	0013	1	0012	0013	1	IIIG	
	CULG				0014	0015	2	0014	0015	2	IIIG			
	CULG				0042	0103	2	0042	0103	2	IIIGG			
	CULG				0117.5	0119	1	0117.5	0119	1	IIIG			
	CULG				0132	0148	1					UNCLF		
	CULG				0226.5		1	0226.5		0226.5		1	IIIB	
	CULG				0433.5	0445.5	1	0433.5	0445.5	1	0433.5	0445.5	1	IIIG
	CULG									0517		1	IIIB	
	CULG						0654	0655	2	0654	0655	2	IIIG,V,U	
	0655	1610	WEIS	0700	1517	2							IN	
			WEIS	0705.5	0706.1	3							IIIG	
			WEIS				0707.7	0707.9	1				IIIG	
			WEIS				0952.6	0957	3				IIIG,V	
	1100	2200	SGMR							1218	1252		CONT	
		WEIS	1225	1540	3							IV		
		SGMR							1245.2	1248		IIIG		
		SGMR							1248.5	1252		V B		
		SGMR							1252	2200		IV		
1113	2345	BOUL				1311	E 1524					IV		
1328	2341	HARV	1328	E 1440	2	1328	E 1440	3				IV		
		HARV	1328	1500	2									
		HARV				1328	E 2120	3				IIIN		
		HARV				1440	1516	2				IC		
		HARV	1440	1516	1	1440	1516	2				IV		
		HARV	1454	1456	2	1454	1456	2				IIIG		
		WEIS	1515.7	1539	3							IV		

# SOLAR RADIO EMISSION SPECTRAL OBSERVATIONS

24 OCTOBER - 6 NOVEMBER 1968

DATE	TIMES OF OBSERVATION		STATION	EVENTS									SPECTRAL TYPE	
	START UT	END UT		DECIMETRIC BAND			METRIC BAND			DEKAMETRIC BAND				
				START UT	END UT	INT.	START UT	END UT	INT.	START UT	END UT	INT.		
10 29	2037	2400	HARV	1516	1547	3	1516	1538	3				IV	
			BOUL				1524	2125				3	CONT	
			CULG				2037	2400	1				I	
			HARV				2120	2340	2				IC	
10 30	0427 0658 1100	0425 1640 2200	CULG				0000	0105	1				I	
			CULG				0000	0636	1	0000	0636	1	IIIN	
			CULG				0105	0600	2				I	
			WEIS				0600	0636	1				I	
			SGMR				0658	1327	2			1230	1350	IS
			WEIS				1255	1545	2					CONT
			WEIS	1313.2	1409	1								IV
			HARV				1328	E 1600	3					IIIGG
			HARV	1328	E 1917	2								IC
			WEIS	1335.5	1337.2	2								IV
			HARV	1336	1340	3	1337		2			1350	1630	IIIGG
			10 31	0655 1100 1330 1317	1605 2200 2340 2349	CULG				0000	0639	1		
CULG							0002.5	0035	1				IV	
CULG							0004	0005	1				IIIG	
CULG							0009	0010	3	0009	0010	3	IIIG,V	
CULG							0010	0020	2				UNCLF	
CULG							0010	0025	1	0010	0025	1	IIIGG	
CULG							0013.5	0014	3	0013.5	0014	3	IIIG	
CULG							0017.5	0021	2	0017.5	0021	1	II	
WEIS	0655	1505				2								IC
WEIS	0711.7	0712.2				2								IIIG
SGMR							1312.3	1312.6	1					IIIG
11 01	0750 1100 1330 1317	1620 2200 2340 2350				WEIS				0750	1508	2		
			WEIS				0851.7	0900.5	2				II	
			WEIS	0853	0915	1							IV	
			WEIS	0925	0952	2							IV	
			WEIS	1208.9	1213	2								III,UNCLF
			SGMR							1210.5	2015	1211.5		CONT
			SGMR											IIIB
			WEIS				1247.8	1248	2					IIIB
			SGMR							1248	1248.5			IIIB
			SGMR							1258	1304			IIIG
			WEIS	1258.3	1304.6	2								IIIGG
			WEIS				1312	1314.5	2					IIIGG
SGMR				1326.1	1326.5	1	1312	1315.3			IIIG			
WEIS							1327	1328			IIIB			
SGMR											IC			
HARV	1330	2340		1330	E 2340	2	1350	E 1956	2	1350	E 1956	CONT		
BOUL	1317	2350								1402.8	1406.5	IIIG		
SGMR										1433	1436.5	IIIG		





# SOLAR RADIO EMISSION SPECTRAL OBSERVATIONS

24 OCTOBER - 6 NOVEMBER 1968

DATE	TIMES OF OBSERVATION		STATION	EVENTS									SPECTRAL TYPE
				DECIMETRIC BAND			METRIC BAND			DEKAMETRIC BAND			
	START UT	END UT		START UT	END UT	INT.	START UT	END UT	INT.	START UT	END UT	INT.	
11 05	1317	2345	BOUL				1724.3	1724.7	1	1724.3	1724.7	1	IIIG
			BOUL							2011.5	2012	1	III
			BOUL				2030.9	2031.2	1	2030.9	2031.2	1	III
	2129	2329	CULG				2146.5		1	2146.5		1	IIIB
			BOUL				2147.1	2147.4	2	2147.1	2147.4	2	III
2346	2400	CULG											
11 06	0000	0056	CULG										
	0106	0551	CULG										
	0552	0603	CULG										
	0605	0637	CULG										
	1100	2200	SGMR				0631.5		1	0631.5		1	IIIB
	.0751	1550	WEIS				1330	1331.7	2				IIIGG
	1348	2347	BOUL				1447	1447.7	2	1447	1447.7	2	IIIG
			BOUL							1512.4	1513.6	2	III
			BOUL				1524.2	1524.4	2				III
			BOUL				1938.7	1939.7	2	1938.7	1939.7	2	IIIG
	1346	2336	HARY				1939		1	1939		2	IIIG
	2032	2348	CULG				2117	2118	1				IIIG
			CULG				2251	2258	1	2251	2258	1	IIIGG
			BOUL				2253.7	2358.7	2	2253.7	2358.7	2	IIIG
		2357	2400	CULG									

"Millimeter Radio Emission of McMath Plage No. 9740"

by

G. Feix

Astronomical Institute of the University of Bochum\*

Instrumentation

The observational data used in this report were carried out by an equatorially mounted paraboloid antenna 10 m in diameter. The antenna is provided with a movable feedhorn in order to make solar scans of high position accuracy by means of lateral defocussing. The stepped shift of the feed in declination produces a line raster type scan at fixed separations of 1.6' in declination while in hour angle direction every 0.7' or 2.3 sec an intensity data point is obtained. The parameter of the beam and the efficiency of the instrument are summarized in Table 1.

Table 1

Stockert Radio Observatory

Efficiency of a 10 m  $\phi$  parabola antenna operated at 36 GHz

BEAMWIDTHS	MIN.of ARC	EFFICIENCY $\eta$ :		
		relative pattern	antenna ohmic** loss	total
3 db beam (uniformly illuminated)	3.02 '	0.82	0.43	x 0.61 = 0.26
3 db beam (measured)	3.1' x 3.6 '			
pattern angle (integrated power pattern normalized to unity)	4.6 ' = $\Omega_A^{1/2}$	0.53		

Apparent Temperature:  $T_A = \eta S D^2 / 3.5 \cdot 10^{-23}$ ;  $T_A = 1^\circ$  K at the receiver terminal, if  $\eta=0.26, D=10$  m and  $S=134 \cdot 10^{-26} \text{ Wm}^{-2}\text{Hz}^{-1}$

Flux per beamwidth of the quiet sun:  $S_\theta = 1900 \cdot 10^{-22} \left( \frac{\Omega_A}{\Omega_\theta} \right) = 39.2 \cdot 10^{-22} \pm 5\% \text{ Wm}^{-2}\text{Hz}^{-1}$

\*\*including losses and mismatch on the line: receiver - antenna

Due to the South-declination of the sun during its observation period and due to inclement weather conditions of the season mm-observations were secured only  $\pm 2$  to 3 hours around the meridian transit per day. The time deviation between Ephemeris transit and culmination of the sun at the site of the radio telescope is 26.9min. The latitude of this instrument which is operated by Stockert Radio Observatory is  $N50^\circ 34' 14''$ .

Observations

There is evidence that the most intensive activity during the period October 1968 on into early November 1968 occurred in the region of McMath plage No. 9740. This plage became optically visible on Oct. 21 and disappeared on Nov. 3 beyond the solar west limb. At 36 GHz ( $\lambda = 8.3$  mm) this plage was not detected before Oct. 23 and was not observed any more after Oct. 31. No activity was found within the mentioned daily 4-to 6-hour observation period until Oct. 27. Up to that time the mm-radio emission of 9740 is just the same as what is observed for a moderately active region of an intensity excess of approximately 10% of the quiet sun (Fig. 1). On Oct. 27, one day before the central meridian passage of the plage, the first mm-burst was received (Fig. 2). This burst-flare event of the optical importance 2 B was as summarized in the "Solar-Geophysical Data" IER-FB 296 the second large burst in the history of 9740.

An examination of the mm-flux of two further events of remarkable importance Oct. 29 and Nov. 2 (Fig. 3) revealed in accordance with the event of Oct. 27 a close correlation between radio burst emission and bright flare emission. Table 2 gives a summary of those  $\geq 2$  B flares which were observed within our daily patrol interval. Both intensity curves of Fig. 2 show a typical intense peak followed by a significantly increased postburst.

\* Work was performed at Stockert Radio Observatory, Bonn, G.F.R.

Table 2

Solar Flares of the Importance 2 B assigned to Plage 9740 covered by 36 GHz Radio-Observations

Flare and Group Number*	Date 1968	Time		36 GHz	Remarks
		Start	End		
18750	Oct. 27	1241	1309	observed	H , Z
18819	Oct. 29	1114	1445	observed	Z
18851	Oct. 30	1234	1510	not observed	H , Z
18910	Nov. 02	0949	1108	observed	Z , M

H = flare with high velocity dark surge

M = white light flare

Z = major sunspot umbra covered by flare

\*Source of Data: "Solar-Geophysical Data" IER-FB 291 and IER-FB 292, issued Nov. 1968 and Dec. 1968, respectively.

The large time displacement between the maxima of the flash phase and the postburst increase of more than 30 minutes and even more than 1 hour on Oct. 27 is striking; usually this time interval remains in the range of only a few minutes for the majority of bursts observed. Primarily, it is a matter of choice, whether one describes this type of burst as a single event or as two separate bursts; however, at no time between the initial impulsive phase and the postburst phase did the intensity drop to preburst level.

Final activity of this plage has been observed on Nov. 2 around 1054 UT. The flare had already developed to the decay phase, when the antenna beam acquired this event. The sequence of the corresponding flare was attained by optical observatories as follows:

Start : 0949 UT  
 Maxima: 0957; 1012; 1026 UT  
 End : 1108 UT

The burst emission was detectable even longer at mm-wavelengths. As Fig. 4 demonstrates, the burst was still visible at 1330 UT; however, within the following hour this emission disappeared from our records completely. As mentioned above, no steady emission of the plage layer remained on the records after the burst on Nov. 2.

Summary

The observation of McMath plage No. 9740 at 36 GHz during its passage from the east limb to the west limb has been discussed. Three distinct burst events were observed on Oct. 27, Oct. 29 and Nov. 2, 1968. No outstanding activity of this plage was found before Oct. 27, 1968.

Oct. 26, 1968

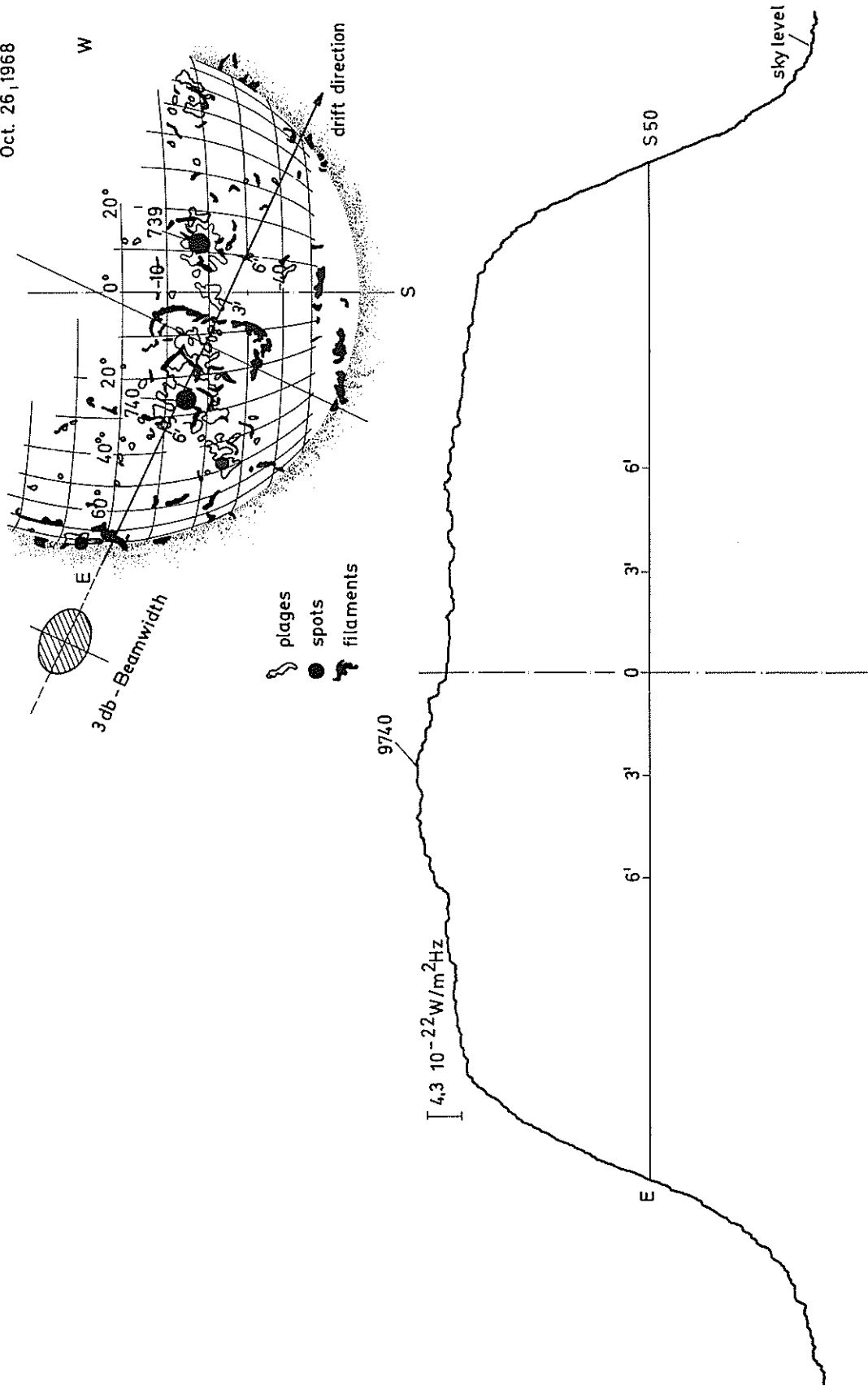


Fig. 1. Solar drift curve of October 26, 1968 noon. Frequency: 36 GHz.

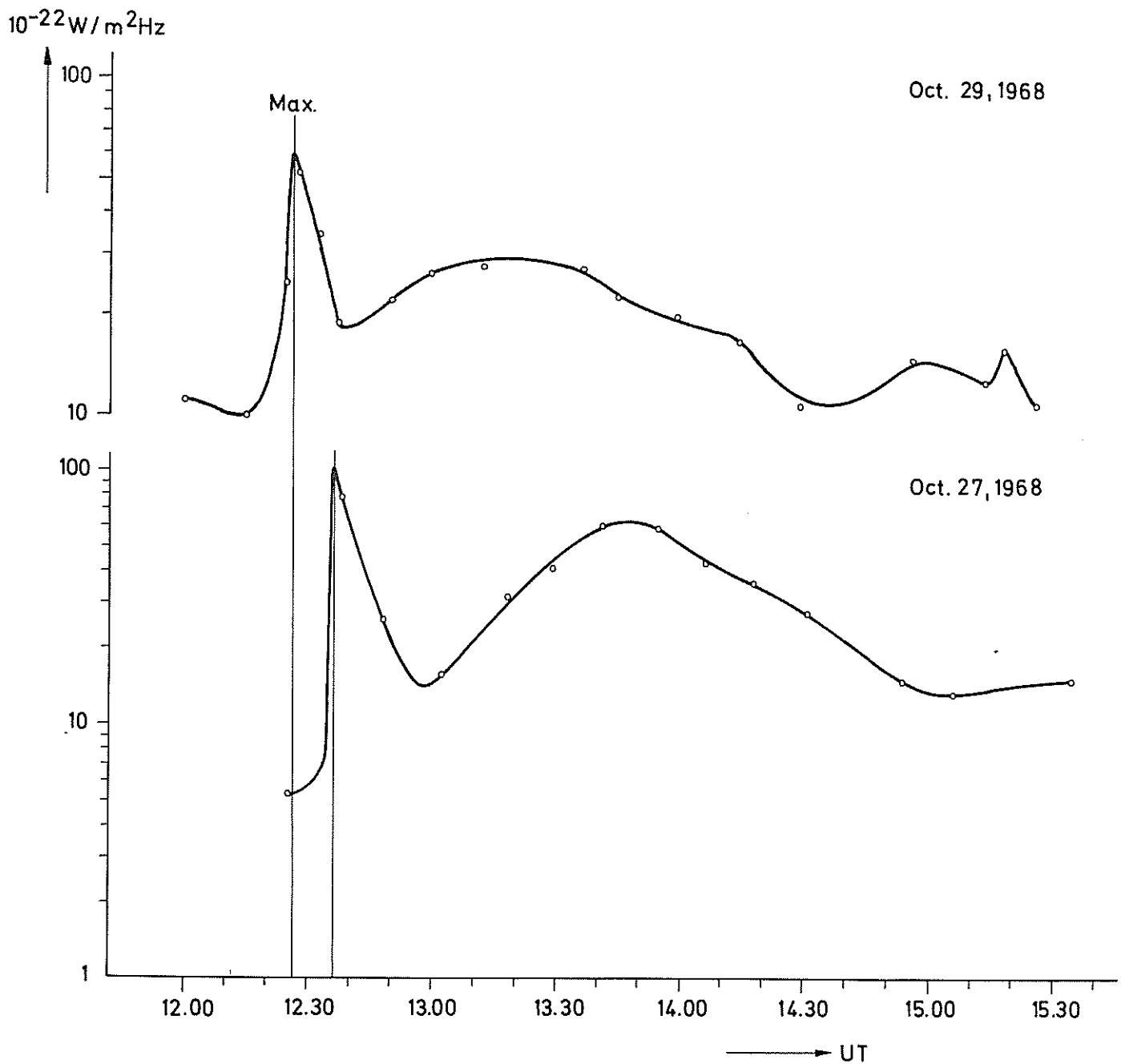


Fig. 2. Solar burst sequences at 36 GHz October 27 and 29, 1968.

Nov. 2, 1968

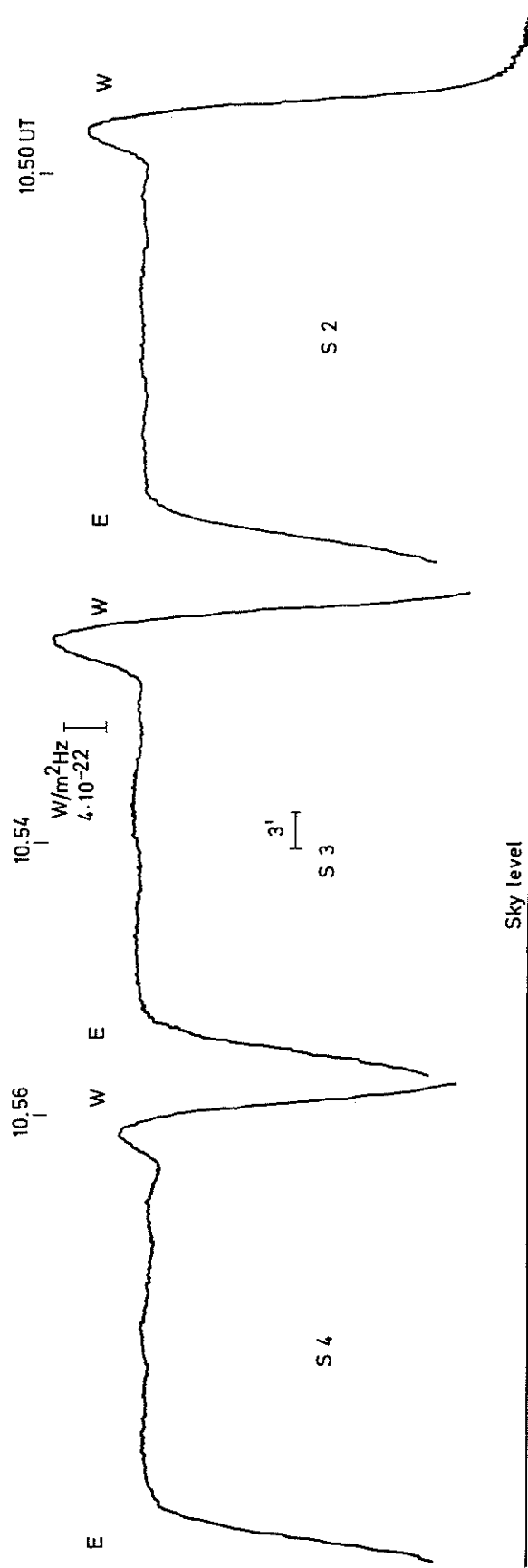
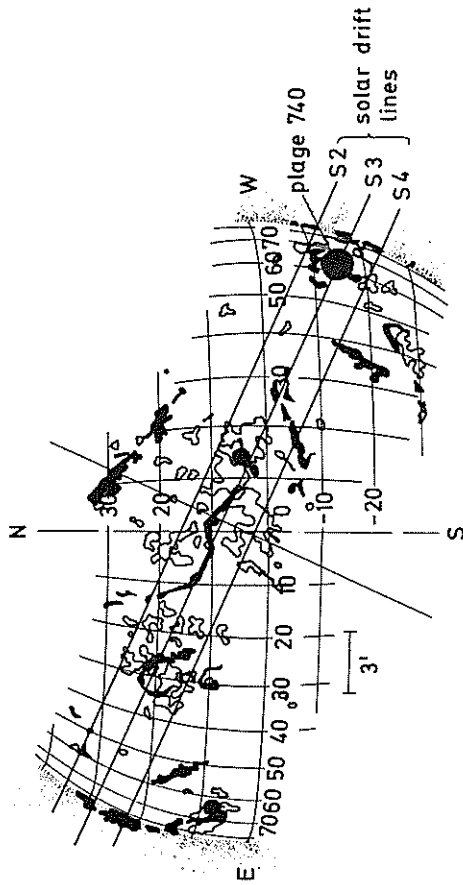


Fig. 3. Solar drift curves showing limb burst at the decay phase November 2, 1968. Curve separation 1.6'.

Nov. 2, 1968

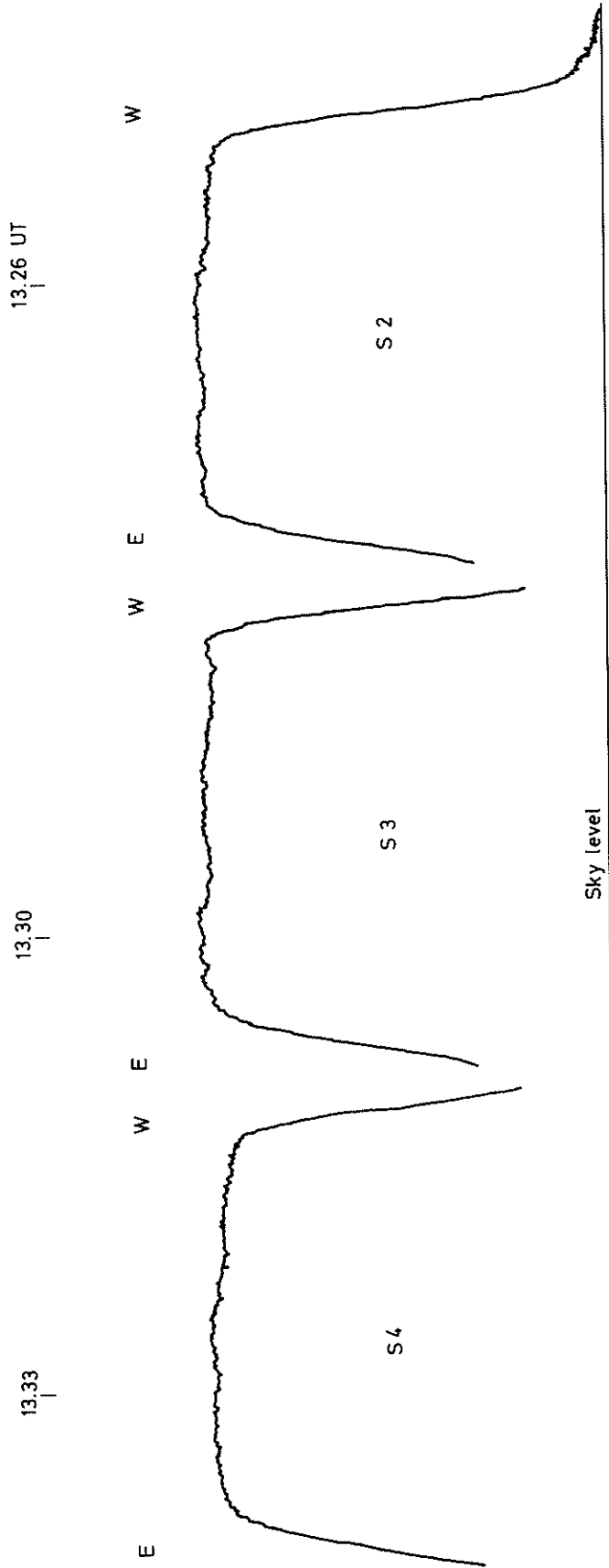


Fig. 4. Solar drift curves of the burst of Fig. 3 immediately before the end of the burst. Curve separation 1.6'.

# "Radio Burst Spectra Associated with Proton Flux Increases"

by

D. S. Lund  
 Space Disturbances Laboratory  
 ESSA Research Laboratories  
 Boulder, Colorado

## Introduction

During late October and early November 1968, McMath-Hulbert Region Number 9740 produced a series of flares that resulted in enhanced proton fluxes in the interplanetary medium. These flares, with their associated radio bursts, seemed promising grounds for testing two ideas; Is there a one-to-one correspondence between "U Bursts" (as defined later) and proton-accelerating flares? Does the information carried in the radio spectra readily determine the relativistic electron spectra and the total number of such electrons associated with the basic flare mechanism? Such questions were the departure point for the study here described. We have taken our proton data from IMP F measurements of directional proton flux (with energy greater than 10 Mev) as reported in "Solar-Geophysical Data". Six definite increases in flux have been identified, and two possible (small, gradual) further increases are suggested. These latter two events occurred early in the development of the region, before it crossed the Central Meridian. The dates and times of these increases are listed in Table 1.

Table 1

<u>PROTON FLUX INCREASE</u>	<u>OPTICAL FLARE MAXIMUM</u>	<u>RADIO SPECTRUM</u>
Date/Time UT	Time UT (Importance)	Time UT (Figure Number)
26/1100-1600* Oct 68	0119 (1N)*, 0854 (SN)*	None
27/1700-2000*	1237 (1B)*, 1324 (2N)*	1236 (Fig. 1)*
29/1700	1234 (2B)*	1226 (Fig. 2), 1522 (Fig. 3)*
30/1400	1253 (2B)	1336 (Fig. 4)
31/0200	0013 (3B)	0011 (Fig. 5)*
01/1700 Nov 68	0844 (1N)	0913 (Fig. 6)
01/2400	2010 (1B)	2005 (Fig. 7)*
04/0600	0542 (1B)	0520 (Fig. 8)
* Weak, gradual	* Questionable association	* Detailed comments in text

For the listed increases, we suggest that the flares listed in the second column were the proton sources. Of the last five listed, four identifications are clear (flux increase within four hours of a flare of large area). The increase noted on 01/1700 UT November is thought to have originated in the 1N flare of 01/0844 UT by reason of a large burst at millimetric wavelengths, and the absence of intervening major flares. The time delay between flare and flux increase seems long, but not inordinately. The first three events in the list are regarded as questionable in association. The first event is too tentative to bear scrutiny, but the second event is probably associated with the 1237 UT flare on the 27th, by reason of association with a major radio event. The third event listed in Table 1 is interesting. The flare listed has minor radio association at centimetric wavelengths, but is in time coincidence with the onset of deka-metric Type IV. On the other hand, a major centimetric burst was observed at 1522 UT, but no optical flare was associated with this event. All flares are listed by their times of maximum intensity, and all listings were taken from the Confirmed Flares listings of the "Solar-Geophysical Data".

The third column of Table 1 lists the times of the flare-associated radio spectra. Seven of the eight bursts show flux in excess of 1000 flux units (one flux unit =  $10^{-22} \text{Wm}^{-2} \text{Hz}^{-1}$ ) at some frequency above 1000 MHz. The spectra are crude, since reported peak fluxes have been used, and these are not always given at the same time for different frequencies. Time differences greater than several minutes are, however, excluded. The data have been taken from "Solar-Geophysical Data", from the Air Force Cambridge Research Laboratories' Geophysics and Space Data Bulletin, and from the monthly reports of the Toyokawa Observatory of Nagoya University and the Slough Solar Radio Observatory of the Radio and Space Research Station.

## Idealized Synchrotron Spectra

The spectrum of gyroemission from a non-relativistic electron moving in a constant magnetic field consists of a delta function at the gyrofrequency. As the electron energy is increased, harmonics of the gyrofrequency appear, and as the energy approaches relativistic values, the intensity of the harmonics becomes greater than the intensity of the fundamental. The radiation is polarized, such that if viewed perpendicular to the magnetic intensity vector it appears linearly polarized, while if viewed along the field it is circularly polarized. Gyroemission at relativistic energies is called synchrotron emission.

The spectral characteristics of the radiation from a large number of particles will be the same as above if the particle energy distribution is monoenergetic. If not monoenergetic, the spectral form of the radiation represents an integration over some electron energy range, of the product of the radiation from an individual electron multiplied by the electron energy distribution. In this case, the electron energy spectrum is assumed to be [Lin et al., 1968]

$$N(E)dE = KE^{-\gamma}dE \quad (1)$$

where  $N(E)$  is the relativistic electron density in the energy interval from  $E$  to  $E + dE$  and  $K$  and  $\gamma$  are constants. The radio spectra often show a broad maximum, and at higher frequencies (higher than the frequency corresponding to maximum flux):

$$S \sim \nu^{-\alpha}$$

where  $S$  is the spectral flux density,  $\nu$  is the frequency and  $\alpha$  is a constant.

The indicated integration, when combined with the assumption (1) yields a simple connection between spectral indices for particles and radio flux

$$\alpha = \frac{\gamma-1}{2} \quad (2)$$

Most observed spectra show a flux decrease at lower frequencies (lower than the frequency corresponding to maximum spectral flux density)

$$S \sim \nu^{\beta}$$

which is thought to be the result of absorption. This absorption may be due to free-free opacity (either within the emitting region or above it) or to synchrotron self-absorption, or to the Razin Effect. This effect [Razin, 1960] is more precisely, a suppression of emissivity when the refractive index is substantially less than unity, but is often discussed as if it were an "absorption". If due to synchrotron self-absorption, theory indicates  $\beta = 2.5$ . If due to Razin Effect,  $\beta > 2.5$ . If due to free-free self-absorption

$$\beta = 2 - \left(\frac{\gamma-1}{2}\right) \leq 2.5 \quad (3)$$

By observing  $\beta$ , we may infer the dominant absorption mechanism. Once the absorption mechanism has been identified, a characteristic length,  $\ell$ , may be defined as the reciprocal of the absorption coefficient and an estimate of emitting volume made, assuming spherical symmetry. For synchrotron self-absorption, for example

$$V = \frac{\pi \ell^3}{6} = 2\pi \times 10^{12} S^{3/2} H_{\perp}^{3/4} \nu^{-15/4} R^3 \quad (4)$$

where  $V$  is the source volume in  $\text{cm}^3$ ,  $S$  is in units of  $10^{-22} \text{Wm}^{-2} \text{Hz}^{-1}$ ,  $H$  in Gauss,  $\nu$  in megaHertz, and  $R$  is the distance from source to observer in cm. Similar arguments are often used in the study of sizes of Quasi-Stellar Objects [Kellerman, 1966].

We may now complete our discussion by specifying how  $K$  in Equation (1) is calculated. Ginzburg and Syrovatskii [1965] discuss this point. Their result is

$$K = \frac{7.4 \times 10^{21} R^2 S}{a(\gamma) H V} \left( \frac{\nu}{6.26 \times 10^{18} \text{H}} \right)^{\frac{\gamma-1}{2}} \quad (5)$$

where

$$a(\gamma) = \frac{\frac{\gamma-1}{2} \sqrt{3} \Gamma\left(\frac{3\gamma-1}{12}\right) \Gamma\left(\frac{3\gamma+19}{12}\right) \Gamma\left(\frac{\gamma+5}{4}\right)}{8 \sqrt{\pi} (\gamma+1) \Gamma\left(\frac{\gamma+7}{4}\right)}$$

and  $H$  is averaged over all field orientations. This result is in CGS units, with symbols as defined previously. Integration of Equation (1) then yields the total number of electrons with energy greater than  $E_0$  within the emitting

$$N_{\tau}(E > E_0) = \frac{KV}{\gamma - 1} E_0^{1-\gamma} \quad (6)$$

In the calculations that follow, we have assumed a field of 200 Gauss.

### Observed Burst Spectra

In general, the observed spectra fall into four distinct types: The first is a simple synchrotron emission spectrum showing synchrotron self-absorption at the lower frequencies (Figure 1); the second is a simple synchrotron emission spectrum showing free-free absorption at the lower frequencies (Figure 5); the third is a complex spectrum such as Figure 7 that has been called a "U burst" in the literature [Castelli *et al.*, 1967]; finally a complex spectrum with a large peak at lower frequencies and a high-frequency synchrotron "tail" (Figure 3). We will now discuss these four bursts in greater detail.

A. Burst on October 27, 1968 at 1236 UT. The high frequency roll-off of the spectrum of this burst leads to  $\gamma = 1.8$ . The low-frequency slope of the spectrum is 2.5, indicating that the absorption mechanism is indeed synchrotron self-absorption. The size of the emitting region is calculated to be 17 arc seconds, although if we apply the correction discussed by Braude [1966], it would be about 5 seconds. The volume is then found to be  $9.7 \times 10^{26} \text{ cm}^3$  and  $K = 3,200$  using Equations (4) and (5). The total number of relativistic electrons is about  $2.9 \times 10^{31}$ . The absence of the Razin Effect at a frequency of 606 MHz indicates an upper limit to the electron density (for electrons of all energies) within the emitting region as  $1.7 \times 10^{10}$ . Low density such as this indicates that the duration of the burst should reflect the energy loss time scale from synchrotron radiation [Takakura, 1960]. The observed e-folding time for the burst was about 40 seconds. For an electron of 0.5 Mev to radiate away its kinetic energy to an e-th in the observed time, a field of 1900 Gauss is required. This is believed to be an untenable value, and we conclude that the dominant loss mechanism for electron energy is not synchrotron radiation.

B. Burst on October 31, 1968 at 0011 UT. This burst was associated with the largest optical flare, and with one of the two largest proton flux increases. It is difficult to analyze, both by reason of lack of sufficient high frequency data, and because of the flux observed at 1415 MHz. The lack of high frequency data means that we cannot calculate  $\gamma$  from the high frequency roll-off as was done for the previous case. The slope of the low-frequency roll-off is less than 2.5, and we would ascribe the observed value to free-free absorption, were it not for the flux value at 1415 MHz. All other flux values between 1000 and 5000 MHz fit a straight line well, indicating a  $\gamma$  of 2.70 as calculated from Equation (3). If we were to assume the 1415 MHz value as correct, it would appear that this was a "U burst". Since we have not observed "U burst" spectra as narrow in frequency as would be required by the 1000 MHz flux value we believe that the 1415 MHz flux value is in error. The burst may still be a "U burst", but if so the low-frequency minimum is below 1000 MHz.

If now we enforce the condition that the free-free absorption coefficient (in the emitting region) must be greater than the synchrotron self-absorption coefficient (in the emitting region)

$$\frac{0.1 \times N_e^2}{T_e \nu} > 0.014 (3.5 \times 10^9)^{\gamma} K H_{\perp}^{\frac{\gamma+2}{2}} \nu^{-\left(\frac{\gamma+4}{2}\right)}$$

and assuming the smallest plausible values for  $K$  (say  $10^3$ ),  $H_{\perp}$  (take 50 gauss) and  $T_e$  (we try a chromospheric value of  $10^4$ ) we find that  $N_e$  must be greater than  $10^{12} \text{ cm}^{-3}$ . We conclude that this implausible consequence suggests free-free absorption which is external to the emitting region. Such a dominant absorption can only result from a) high electron density, and/or b) low temperature. This opacity is above the emitting region, and cannot have gotten there simultaneously with the microwave burst (characteristic length of order  $10^{10} \text{ cm}$ , say, requires such material to be in position before the burst, if relativistic speeds are to be avoided). Thus the radio evidence suggests a superposed region of chromospheric density and/or temperature above the synchrotron emission region. As may be seen in the discussion of the optical aspects of this flare elsewhere in this volume, this particular flare had several brightenings, and an associated high-speed ejection. Such earlier events may be the source of the opacity which the radio chronology requires.

C. Burst on November 1, 1968 (2005 UT). It has long been known that spectra of the larger radio bursts when averaged over many such bursts, had a distinct minimum near 1000 MHz [Takakura, 1959]. More recently Castelli and Aarons [1969] have argued that such a spectrum is an excellent diagnostic for short-term prediction of PCA events. Unfortunately, the "U burst" shown in Figure 7 does not permit much analysis of the high frequency portion of the burst. The slope of the low-

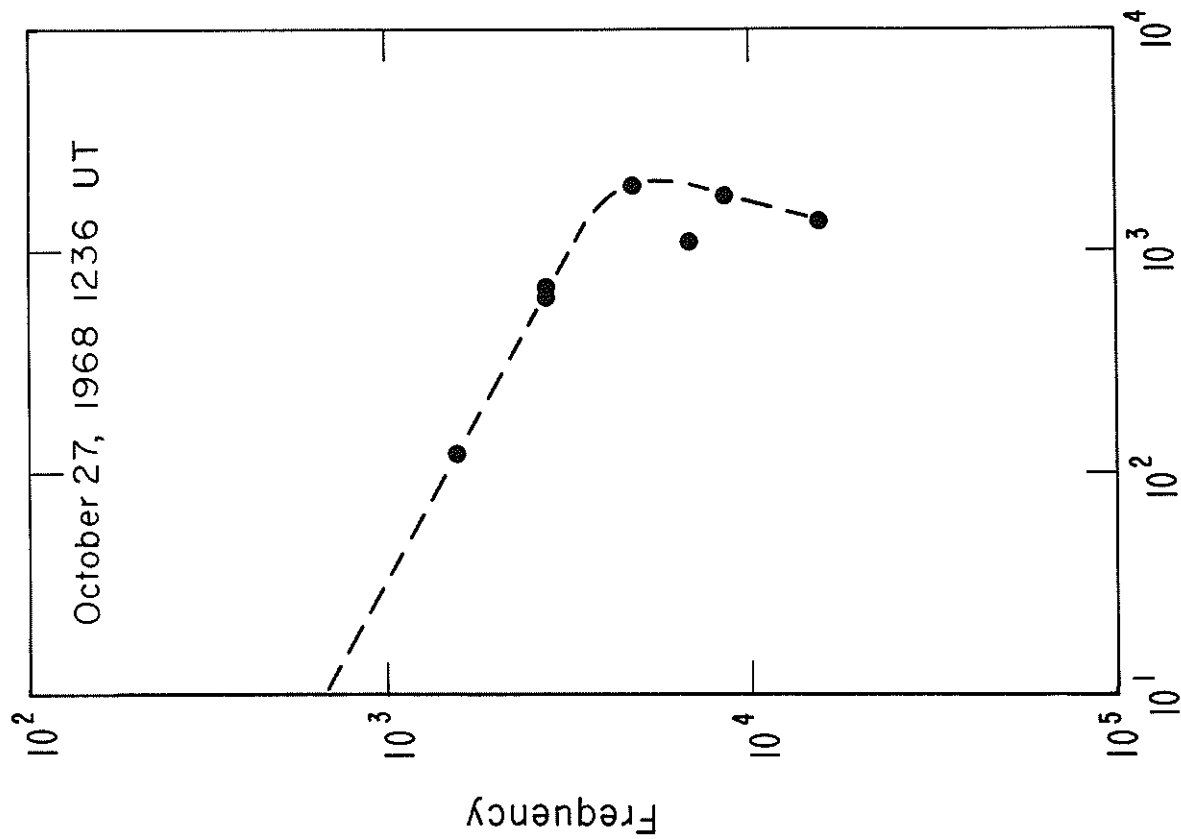


Fig. 1. Spectral flux density as a function of frequency for the burst of October 27, 1968 at 1236 UT. Units of flux are  $10^{-22} \text{Wm}^{-2} \text{Hz}^{-1}$  and frequency is in MHz.

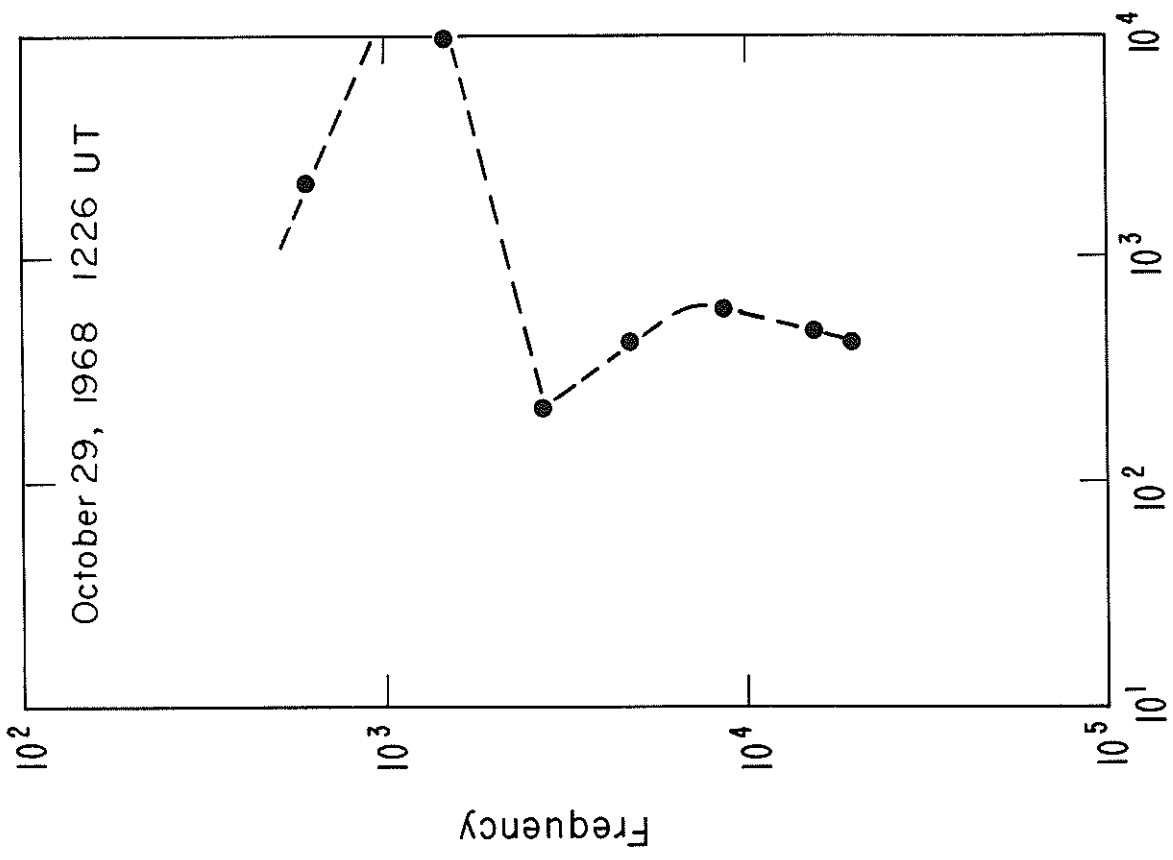


Fig. 2. Spectral flux density as a function of frequency for the burst of October 29, 1968 at 1226 UT.

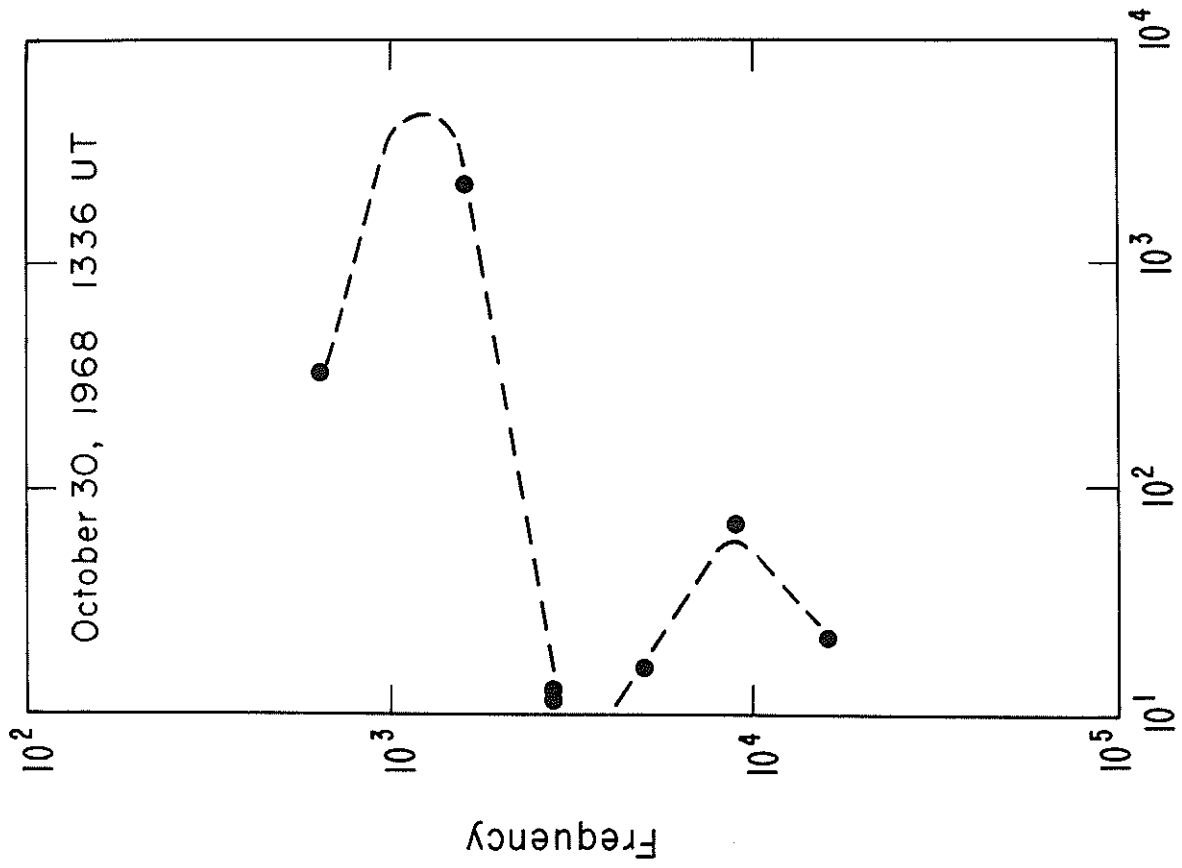


Fig. 4. Spectral flux density as a function of frequency for the burst of October 30, 1968 at 1336 UT.

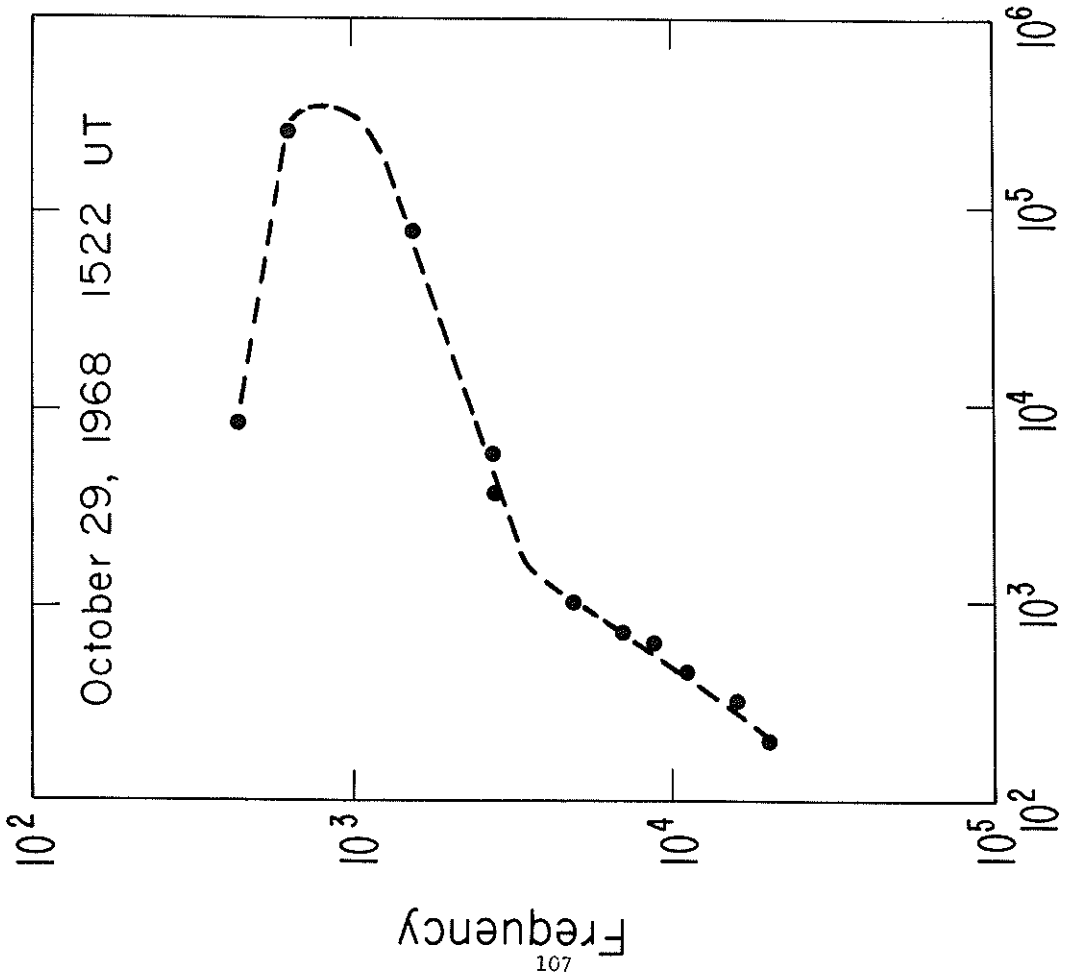


Fig. 3. Spectral flux density as a function of frequency for the burst of October 29, 1968 at 1522 UT.

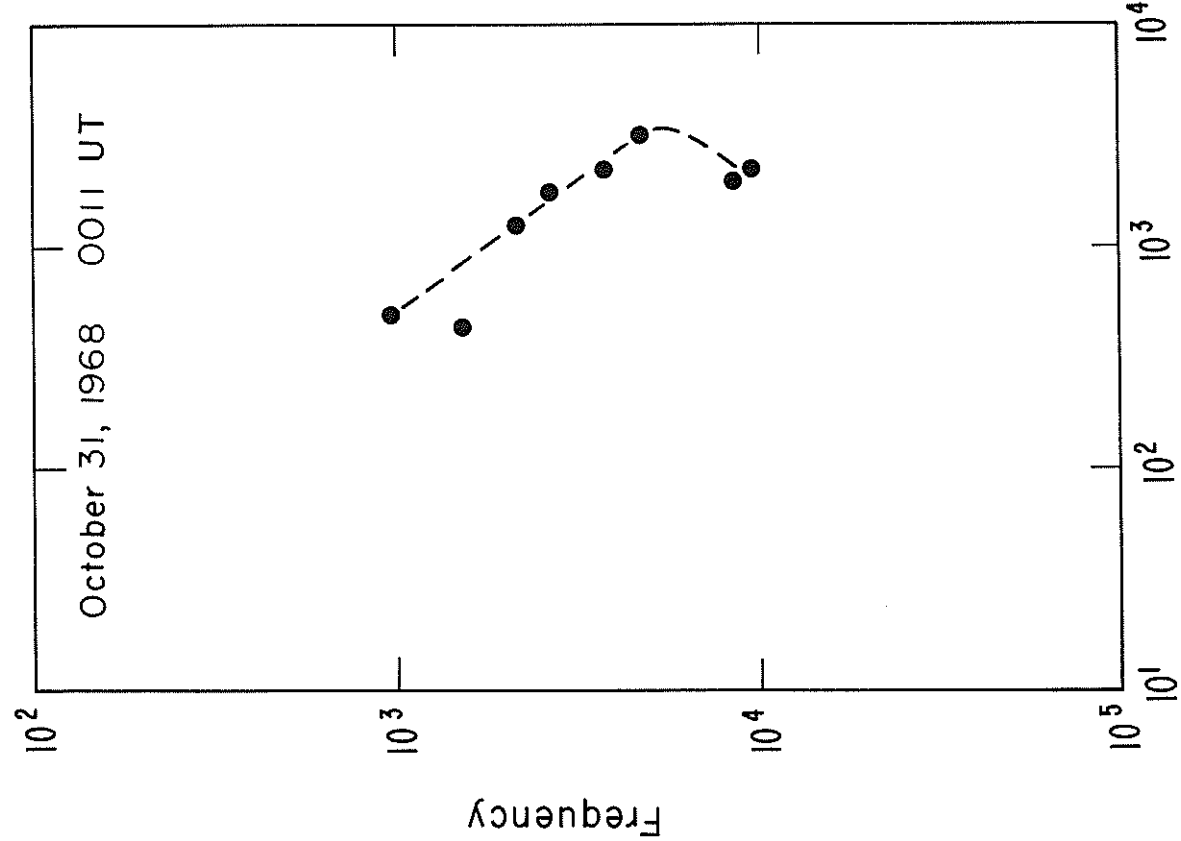


Figure 5. Spectral flux density as a function of frequency for the burst of October 31, 1968 at 0011 UT.

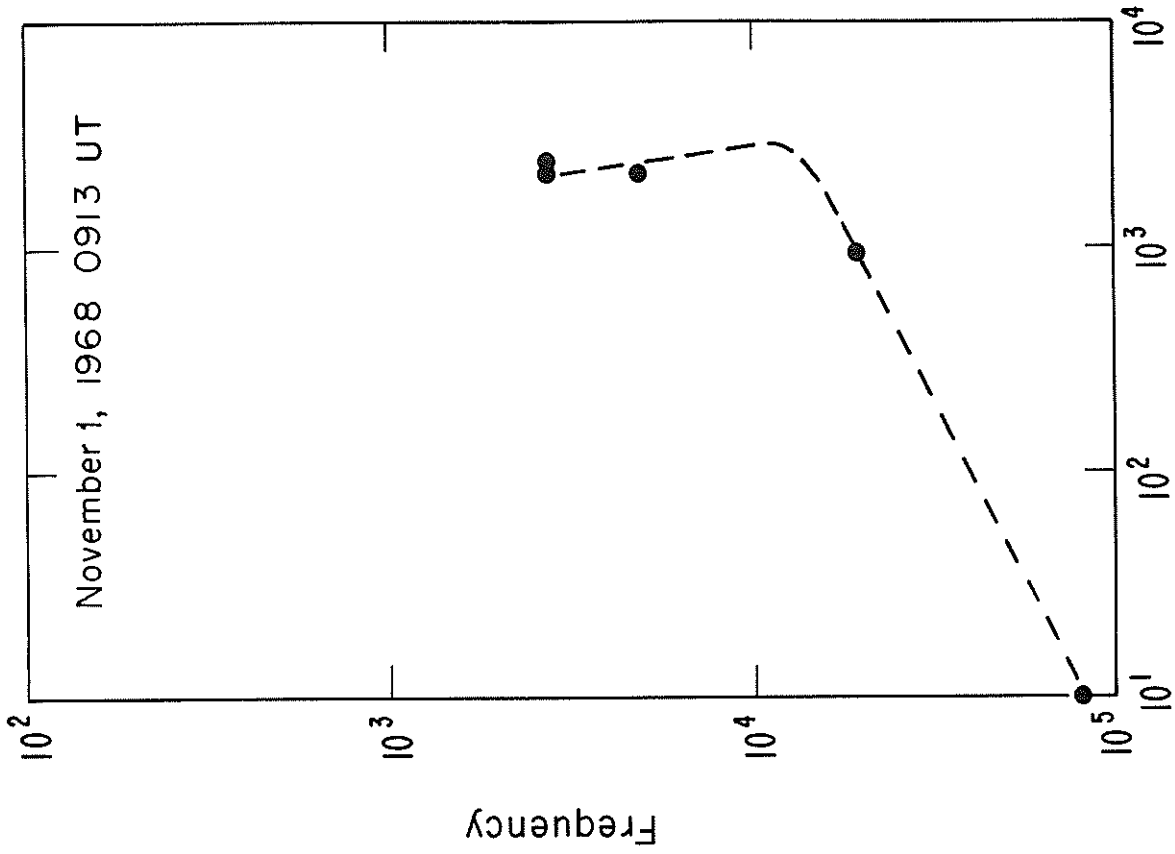
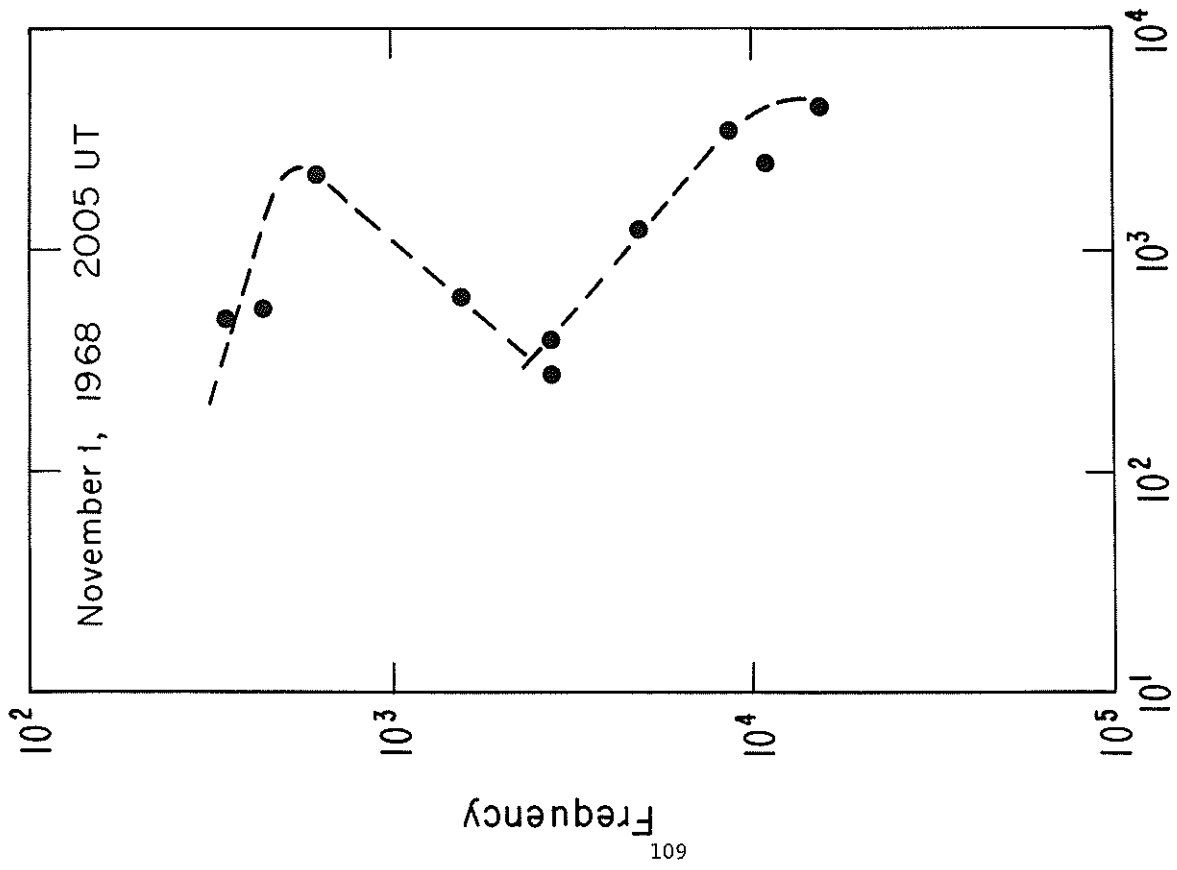
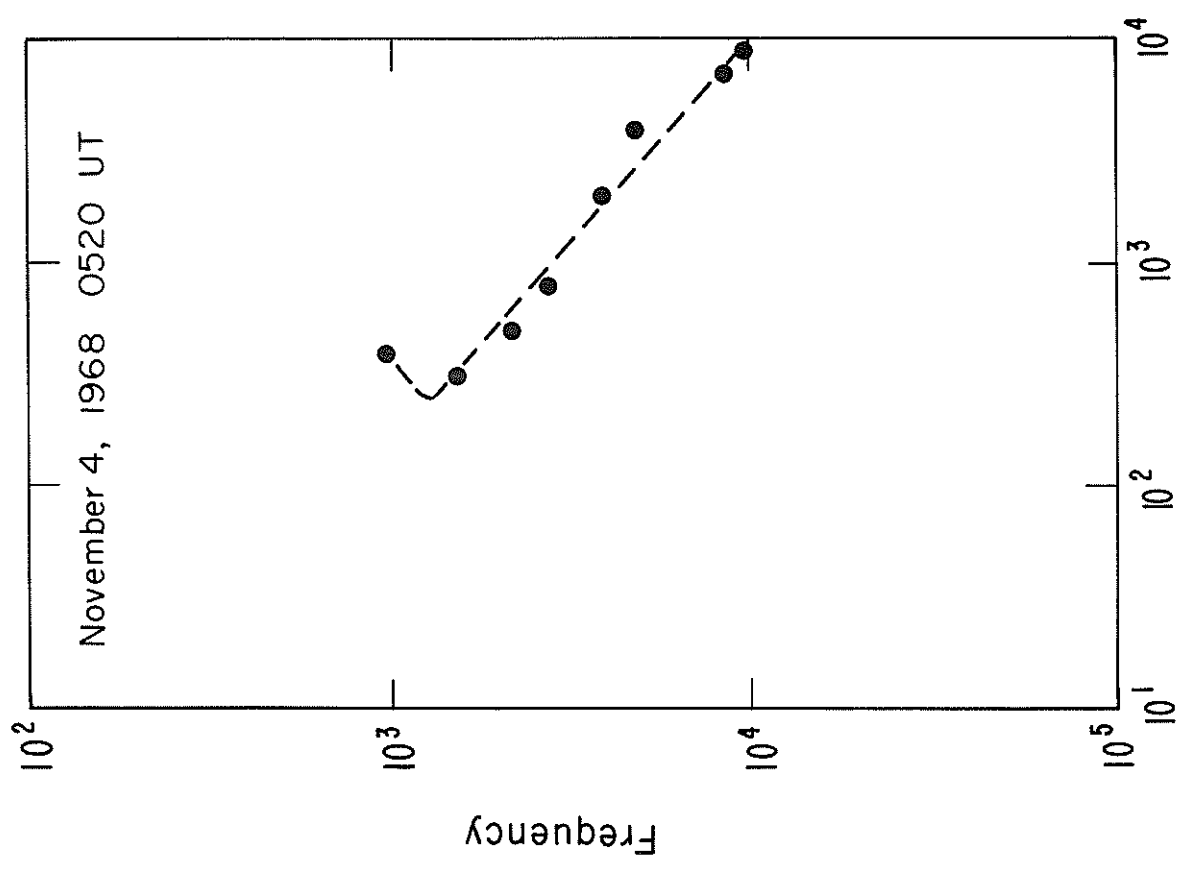


Figure 6. Spectral flux density as a function of frequency for the burst of November 1, 1968 at 0913 UT.



Spectral Flux Density

Fig. 7. Spectral flux density as a function of frequency for the burst of November 1, 1968 at 2005 UT.



Spectral Flux Density

Fig. 8. Spectral flux density as a function of frequency for the burst of November 4, 1968 at 0520 UT.

frequency roll-off of the centimetric burst (between 2700 and 5000 MHz) appears to be 2.5, indicating synchrotron self-absorption. The high frequency roll-off of the decimetric burst (between 600 and 2700 MHz) would indicate a  $\gamma$  of 3.8, but past experience with "U bursts" for which wider-range spectra are available indicates differing  $\alpha$ 's for centimetric and decimetric bursts, thus suggesting that the decimetric burst may not be of synchrotron origin. This impression seems strengthened by polarization measurements. Below 600 MHz, this spectrum seems to indicate Razin Effect absorption, although with the discrepancy between fluxes at 328 and 408 MHz, such a conclusion is not a very strong one. All that can be said about the centimetric burst is that if we do indeed see the spectral maximum at perhaps 16,000 MHz, then the source volume was of order  $4 \times 10^{25} \text{cm}^3$ , or perhaps less if the Braude correction is included. We note that this burst seems to have been associated with a modest increase in the proton flux observed by IMP F, but a smaller increase than was produced by the events on the 31st, the 4th, and earlier on the 1st.

D. The burst of November 29, 1968 (1522 UT). The classical "U burst", often has centimetric and decimetric peaks of comparable magnitudes. In addition,  $\alpha$ 's for the decimetric portion are often between 1 and 3. By contrast, the spectrum of Figure 3 shows a decimetric peak which almost obscures the centimetric burst (it appears as a tail on the decimetric burst, with its maximum buried). Further, the sharply peaked nature of the spectrum of the decimetric burst ( $\alpha \sim 4$ ) suggests further inquiry. For the centimetric burst  $\gamma = 3.0$ , and since the maximum flux and its corresponding frequency are obscured, further analysis is not possible. In the case of the decimetric burst, the very steep slope of the low-frequency roll-off again suggests Razin Effect absorption. If this is a correct assumption, then the electron density is about  $10^{10} \text{cm}^{-3}$ . The plasma frequency would then be about 900 MHz, which is sufficiently close to the observed decimetric flux maximum to suggest that emission at either the plasma frequency or the upper hybrid frequency (approximately 1000 MHz, under stated assumptions) need investigation as potential explanations. It appears that the burst of the 29th (1226 UT) and the 30th (1336 UT) may be further examples of this type, but with unobscured synchrotron maxima.

### Conclusions

One may easily judge the importance of millimetric observations to this study. Since few observatories have extended their facilities into this spectral region, the foregoing analyses are obviously hampered. Despite the small size of the sample (which results from the limitations just mentioned) several conclusions may be drawn:

A. If one generalizes the definition of the "U Burst" to include all spectra showing multiple flux maxima then 5 of the 8 spectra displayed show such form. The score may be higher, since low frequency measurements are lacking in the three remaining cases. Conversely, a "U Burst" that occurred on October 31st at 2257 UT, [Castelli and Aarons, 1969] does not seem to be associated with any proton flux increase observed by IMP F.

B. The small size of the inferred sources - of order one to ten arc-seconds - is beyond the resolving power of known instruments. Thus the source sizes derived from interferometric measurements, as in Kundu [1959] need careful reexamination.

C. Consistent absence of observed Razin Effect in the centimeter-wavelength region indicates upper bounds on electron densities of the order of chromospheric densities. This observation argues (somewhat weakly) against emission models that depend upon compression.

D. The presence of free-free absorption in the (optically) largest flare, and the fact that such a spectrum has been observed in a number of other cases, indicates the presence of density/temperature values, of magnitude comparable to lower chromospheric values, at surprisingly great heights.

### REFERENCES

- |   |      |  |
|---|------|--|
| BRAUDE, S. Ya                                       | 1966 | "Reabsorption of Synchrotron Radiation in Discrete Sources", <u>Soviet Astronomy - AJ</u> , 9, 893-895   |
| CASTELLI, J. P.,<br>J. AARONS, and<br>G. A. MICHAEL | 1967 | "Flux Density Measurements of Radio Bursts of Proton - Producing Flares and Nonproton Flares", <u>Journal of Geophysical Research</u> , 72, 5491-5498.                                   |
| CASTELLI, J. P., and<br>J. AARONS                   | 1969 | "Radio Burst Spectra and the Short Term Prediction of Solar Proton Events", Paper presented at <u>XV Electromagnetic Wave Propagation Meeting of AGARD</u> , St. Jovite, Quebec, Canada. |
| GINZBURG, V. L., and<br>S. I. SYROVATSKII           | 1965 | <u>Annual Review of Astronomy and Astrophysics Volume 3</u> , edited by L. Goldberg, A. J. Deutsch and D. Layzer, pp. 297-350, Annual Reviews, Inc., Palo Alto, Calif.                   |

- KELLERMANN, K. I. 1966 "On the Interpretation of Radio-Source Spectra and the Evolution of Radio Galaxies and Quasi-Stellar Sources", Astrophysical Journal, 146, 621-633
- KUNDU, M. R. 1959 "Structures et Propriétés des Sources d' Activité Solaire sur Ondes Centimétriques", Annales d'Astrophysique, 22, 1-100.
- LIN, R. P., S. W. KAHLER, and E. C. ROELOF 1968 "Solar Flare Injection and Propagation of Low-Energy Protons and Electrons in the Event of 7-9 July, 1966", Solar Physics, 4, 338-360.
- RAZIN, V. A. 1960 "Contribution to the Theory of Spectra of Radio Emission from Discrete Sources Below 30 Mc/s", News of Higher Education Institutions, Ministry of Higher Education, Radio Physics Series, 3, 73-87.
- TAKAKURA, T. 1959 "Paris Symposium on Radio Astronomy", edited by R. N. Bracewell, pp. 562-570, Stanford University Press, Stanford, California.
- TAKAKURA, T. 1960 "Synchrotron Radiation from Intermediate Energy Electrons and Solar Radio Outbursts at Microwave Frequencies", Publications of the Astronomical Society of Japan, 12, 325-351.

"Solar Radio Activity in Plage #9740 22 October - 4 November 1968"

by

John P. Castelli, Air Force Cambridge Research Laboratories  
Walter Clark, Air Weather Service  
William O'Brien, Air Force Institute of Technology  
Santimay Basu, University Calcutta

Introduction

Although the current sunspot cycle had earlier witnessed important southern hemisphere activity; e.g. the 9 June 1969 proton event at longitude  $240.0^\circ$  [Badillo *et al.*, 1969], the first really extended period during which important radio bursts emanated from that hemisphere occurred in late October and early November 1968. Almost complete time surveillance of the centimeter wavelength radio sun was assured to the U.S. Air Force by its broad coverage at discrete frequencies between 606 and 15,400 MHz at the Sagamore Hill Radio Observatory (Hamilton, Mass.) and a complementary patrol at the Manila Observatory, Philippines. The present discussion draws mainly from the observations of these stations. However, two important bursts occurred on 1 and 2 November which were obscured to Air Force patrols but were recorded by European observations.

McMath Plage 9740

McMath Plage #9740, the source of myriad and important radio bursts was first observed on 22 October 1968. Before it had passed around the west limb on 4 November, it had produced at least 131 flares and subflares. Forty-nine were associated with radio bursts. Nine of the flares were importance 2 or greater.

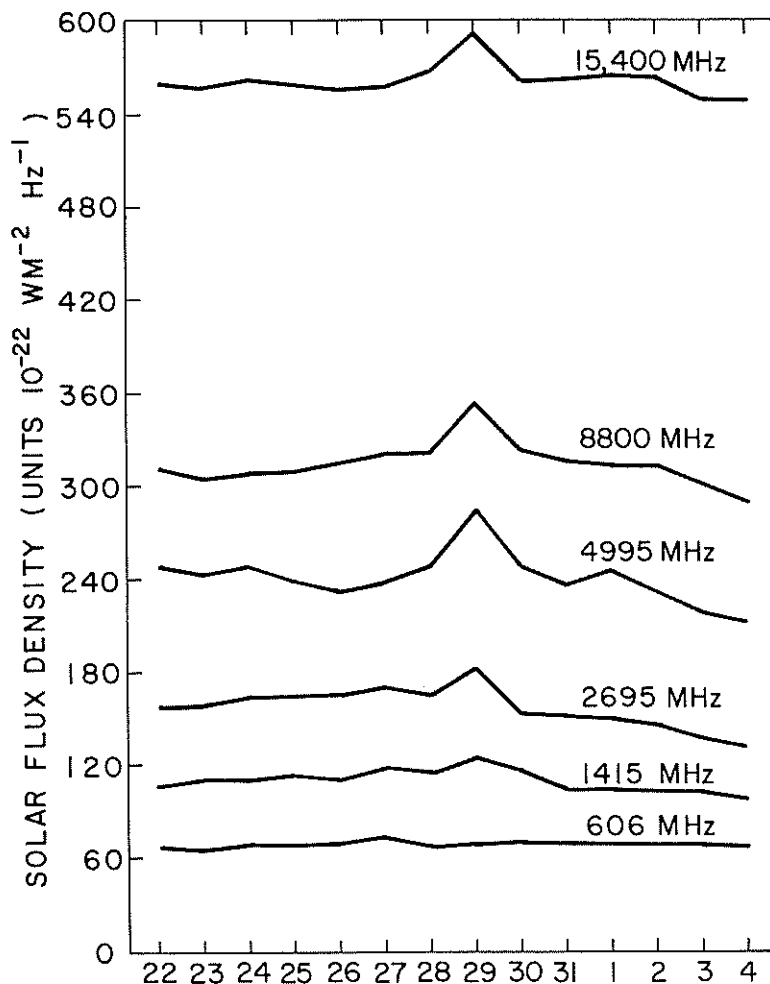


Fig. 1. Variation of undisturbed solar flux between 22 October and 4 November 1968. Bursts were observed every day.

During the same period the undisturbed sun was only moderately hot and day-to-day intensity variations of the slowly varying component were unimpressive, see Fig. 1. Bursts were observed on each day of the period.

### Region Productivity

The flare-burst production history of region #9740 is shown in Fig. 2. All classes of confirmed flares are included. Only flare correlated bursts are indicated. The total of 131 flares and 49 bursts give a fairly high burst-flare productivity rate of 37%. In addition, about 16 bursts occurred which may have originated in the same region but which had no reported optical correlation. Some of these had intensities as high as 290 flux units and 40-50 flux units were common. Since they occurred generally in the most active period of plage #9740 passage across the visible disk, we believe they originated in #9740. This apparent absence of flare association may not be surprising since one of the largest bursts at approximately 1515 UT on 29 October had only a sub-flare normal (-N) association and was detected by only one optical observatory at a time when others were on patrol. It is not unusual to have bursts at 606 MHz and lower without flare association; however, it is unusual to have the situation so pronounced at 8800 MHz. The largest number of "no-flare" bursts occurred on 1 November.

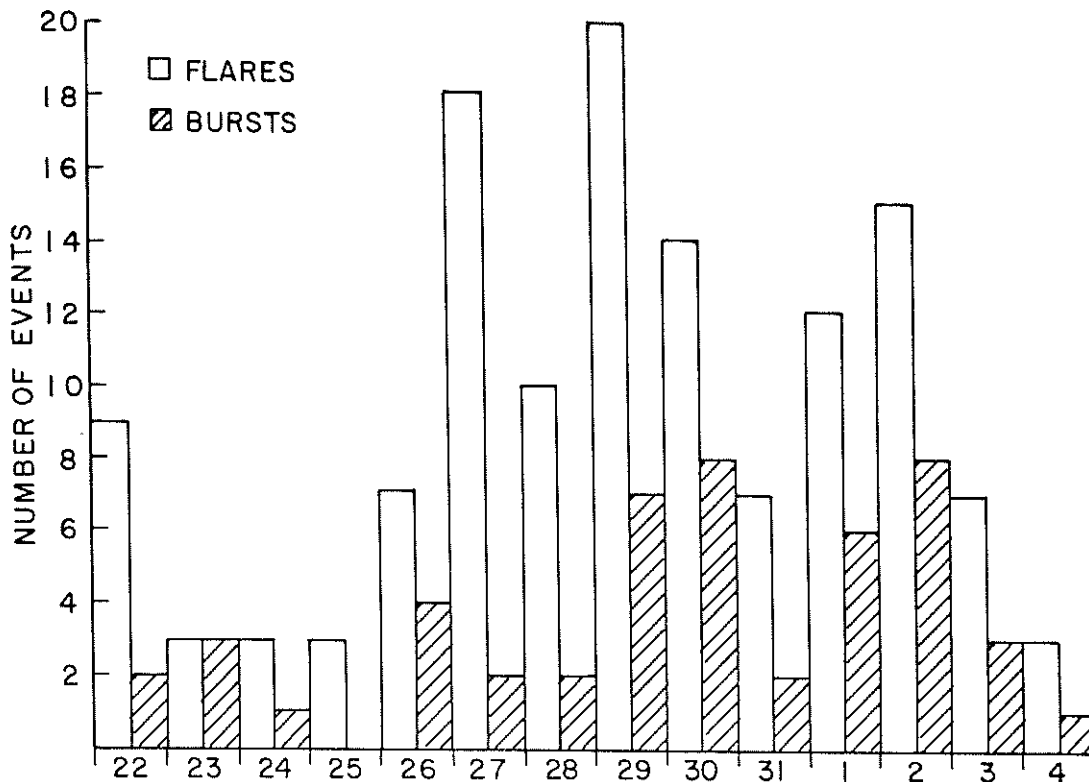


Fig. 2. Distribution of confirmed flares (all classes) and correlated bursts in passage of McMath plage #9740 across visible disk, 22 October - 4 November 1968.

The relatively quiet radio days shown in Fig. 2 cannot be taken as an indicator of absence of important activity. Proton activity was certainly associated with events on 31 October and 4 November and possibly 27 October which were otherwise quiet days.

During the same period there were at least 9 flares rated importance 2 or greater by both ESSA and the Air Weather Service (AWS) Solar Forecast Center. Possibly a few of the weaker events should be upgraded in view of the intense radio bursts correlation. Table 1a lists all of these events and also whether they were associated with a burst  $\geq 500$  flux units. All except a 2N flare at 0601 UT on 2 November had such association. Table 1a is a compilation of AWS collected flare data.

There was a somewhat larger number of bursts (13) during the same period whose peak fluxes exceeded an arbitrary level of 500 f.u. in any part of the patrolled spectrum. This is only five more than the number of flares  $\geq$  importance 2 with 500 f.u. burst association. They are listed in Table 1b. Events marked with an asterisk (\*) all had considerably less than the 1000 f.u. at  $\lambda \approx 3$  cm. One of the criteria defined by some of the present authors [Castelli *et al.*, 1967] as necessary for a principal PCA is that intensities of at least 1000 f.u. must be achieved near 3 centimeters.

The remaining events (marked +) satisfied this criterion and each seems to have contributed toward proton activity - some dramatically and others less brilliantly. These conclusions are based on information listed in ESSA "Solar-Geophysical Data" IER-FB 291, privately communicated riometer absorption data from A. D. Masley, and especially ATS-1 satellite proton data privately communicated from G. A. Paulikas.

Table 1a  
Flares  $\geq$  Importance 2 in Plage 9740  
22 October - 4 November 1968

Date	Begin Time UT	Position	Flare Impt.	Flare Long. ( $10^{-22} \text{Wm}^{-2} \text{Hz}^{-1}$ )	>500 f.u.	Burst Spectrum U-Shape	Zurich Sun-Spot Type (a)	Mt. Wilson Magnetic Class (b)
23 Oct *	2356	S12, E59	2B	175.17°	Yes		D	BY(-)
27 Oct *	1318	S17, E18	2N	169.26	Yes		D	$\delta(6)$
30 Oct *	1334	S18, W28	2N	175.55	Yes		D	No obs.
30 Oct +	2339	S14, W37		179.01	Yes	Yes	D	No obs.
31 Oct +	2232	S15, W49	2N	178.44	Yes	Yes	D	$\delta(-)$
1 Nov +	0820	S17, W47	2B	171.05	Yes	Yes	E	$\delta(5)$
2 Nov +	0601	S20, W58	2N	170.03	No		E	
2 Nov +	0949	S14, W66	2B	176.01	Yes	Yes	D	$\delta(5)$
4 Nov +	0520	S15, W90	2B	176.14	Yes	Yes	D(3 Nov)	No obs.

Table 1b  
Bursts  $\geq$  500 Flux Units in any Part of Patrolled dm-cm  $\lambda$  Spectrum  
with Associated Flare  $<$  Importance 2

27 Oct +	1235	S16, E18	1B		Yes	Yes	D	$\delta(6)$
29 Oct *	1216	S16, W12	1B		Yes		D	$\delta(-)$
29 Oct *	1515	S14, W19	-N		Yes		D	$\delta(-)$
1 Nov *	1210	S12, W51	-N		Yes		C	$\delta(5)$
1 Nov +	2002	S13, W56	1B		Yes	Yes	E	$\delta(5)$

(a) Data based on AWS Measurements.

(b) See ESSA Solar-Geophysical Data Bulletin IER-FB 291 and 292 for times and details.

#### Important Non-Proton Burst Spectra

The most impressive of the former group (\*) with flare association no greater than sub-flare normal importance (-N) began about 1515.6 on 29 October. The burst was both complex and of long duration. The spectra of the principal peaks are shown in Fig. 3. Burst mean flux is also shown. In spite of the great intensity and long duration, the spectra are not those we associate with proton events. The absence of the U-shape with over 1000 f.u. at 3 cm was decisive in our not predicting a proton event. One also finds that the integrated flux at 3 cm is considerably less than  $10^{-15} - 10^{-17}$  joules  $\text{m}^{-2} \text{Hz}^{-1}$ , a requirement which appears to be valid for proton events [Straka and Barron, 1969]. The remarkable thing about this event besides its intensity is that emission at the higher frequencies generally began later and peaked later than at the lower frequencies.

The addition of data points at 184 and 408 MHz shows that the peak of the burst spectrum was probably in the 500-600 MHz range. The steepness of the slope between 184 and 606 MHz was probably greater than -5. The steepness of the slope in the high frequency direction is greater than 6 or 7.

The optical correlation of this event with a subflare in plage #9740 at approximately the same starting and maximum times as the burst, which was reported by one observatory seems not to have been universally accepted. By way of confirmation we offer that in view of the less nebulous association of a weaker radio event at 1218 within this region but one with the same general spectrum as the burst presently under consideration, we conclude that the event at 1515 UT was indeed located at S14 W19.

Another event in this region with a spectrum similar to that cited above, peaking near 1415 MHz at 1432.3 on 30 October with 2430 f.u. and with very high spectral indices on both the high and low frequency sides was recorded. It is significant that the only three major bursts over this period of 24 hours each had the same general spectrum as that shown in Fig. 3. Flare importance ranged from -N to 2N but none were related to particle emission. During this period the "Zurich" sunspot configuration of the principal group within the plage was essentially H according to the Sacramento Peak patrol classification. The magnetic configuration of the region was delta according to the Mt. Wilson classification. This subject will be discussed later in greater length.

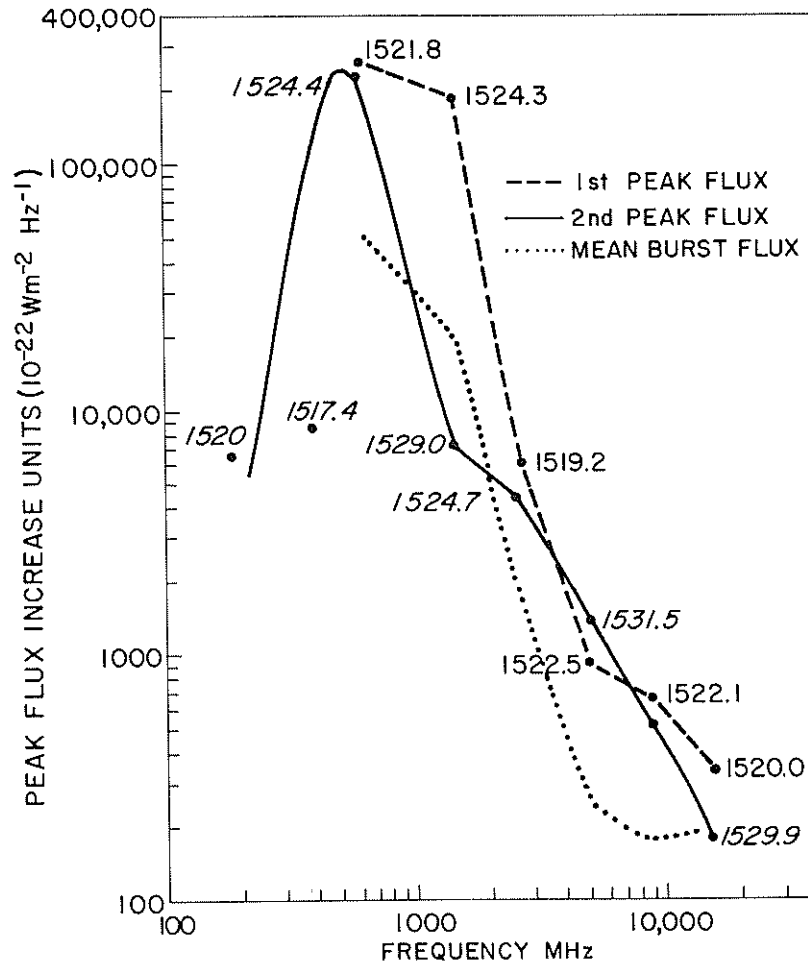


Fig. 3. Peak flux spectrum of great burst of 29 October 1968. The associated sub-flare normal (-N) in excellent time agreement was located S14, W19 in plage #9740.

#### Proton Burst Spectra and Events

Following this brief trio of bursts, there followed during the next five days a chain of six major bursts each of which had a "U" shape spectrum which had been statistically related to Polar Cap Absorption (PCA) events [Castelli & Aarons, 1969]. The few false alarms encountered have been reduced by the invocation of satellite measurements of particles according to a study at AFCRL [O'Brien, 1969]. The one interruption in the chain occurred on 1 November at 1210 UT when a small flare (-N) again triggered a burst whose spectrum was reminiscent of the three discussed above.

The relation between the six similar bursts occurring between 2338 UT on 30 October and 0513 on 4 November to different class flares and proton activity is diagrammed in Fig. 4. Even before 30 October, specifically on 27 October at 1318 UT, a complex "U" shaped peak flux spectral event seems to have been responsible for an increase in the 5-21 Mev particle flux recorded by the ATS-1 satellite. There is some evidence too that a slight increase in riometer absorption on the 29th may have been caused by this event. Profiles of this burst are shown in Fig. 5. The configuration may not be a facsimile of the more typical proton flare-burst which we shall see later.

Spectra of the 6 above referenced bursts are shown in Fig. 6. Note that each spectrum is similar in that the flux exceeds 1000 units at approximately 3 cm wavelength, the spectral slope is rising in the high frequency direction, there is a drop to low values in the decimeter range and that flux values rise again in the long wavelength direction. Where no meter wavelength data were available, the dekameter Type IV burst confirmed the necessary and important low frequency emission.

In idealized form, the spectra were rising in the high frequency direction. However, two of the events on 30 and 31 October showed a rounding off and actual reversal of slope direction between 4995 and 8800 MHz. A third event of 4 November may have shown a reversal between 8800 MHz and 17 GHz but there is some question about the true maximum of the 17 GHz value published. Three of the events on 1 and 2 November show flux still rising at the highest monitored frequency for the reporting station; in one instance 15,400 MHz, in two other instances this was at 9400 MHz. The 9400 MHz

## LEGEND

- (F) = FLARE  $\geq$  IMPORTANCE 2  
 F = FLARE  $\leq$  IMPORTANCE 2  
 B = RADIO BURST PEAK  $\geq$  500 FLUX UNITS ( $10^{-22}$   $\text{wm}^{-2}$   $\text{Hz}^{-1}$ )  
 SOMEWHERE BETWEEN 606 & 15,400 MHz.  
 U = BURST PEAK  $>$  1000 FLUX UNITS NEAR  $\lambda \cong 3$  cm.,  
 DIP IN DM. RANGE AND LARGE M- $\lambda$  BURST OR  
 DEKAMETER TYPE IV  
 (P) = POLAR CAP ABSORPTION EVENT CORRELATION  
 P = APPARENT PARTICLE INCREASE ASSOCIATION BY  
 SATELLITE SENSORS; PCA UNCONFIRMED.

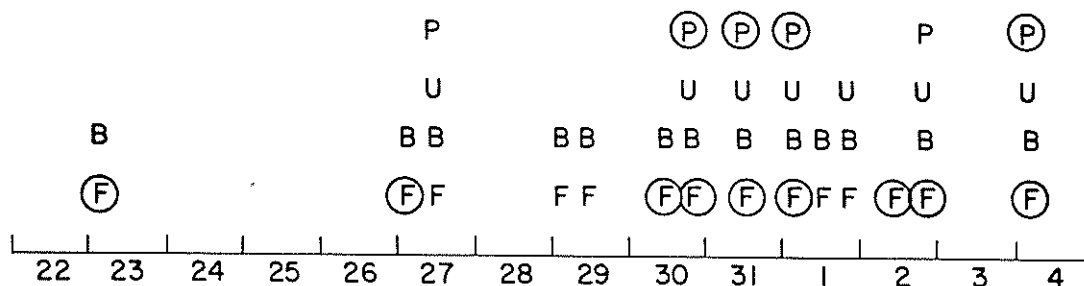


Fig. 4. Distribution of bursts  $\geq$  500 flux units in plage #9740 between 22 October and 4 November 1968 according to date, flare, spectra and proton association.

data were reported by Heinrich-Hertz Institute. One can only speculate on the probable reversal point. The minima brought about by the crossover point of high and low frequency burst sources is also quite variable. It is not clear that where the dip or crossover point is high the short wavelength synchrotron peak is also high on the frequency scale or that there is any relation between the two.

Profiles of the available bursts for this period are shown in Figs. 7-10. Only the event of 1 November at about 2005 shown in Fig. 9 has an uncertain correlation with proton activity. Fig. 7, 8 or 10 might be called classical examples of proton flare-bursts. The events had long duration and also slow rise times.

### The PCA Correlation

In a period with so many large bursts with particle association, it is difficult to correlate the precise influences of each with PCA events. It is well established that the event late on 30 October and early 31 October was the source of the first principal PCA which reached 3.9 dB at Thule before 1600 on 31 October. It appears also that the complex event at 2239 on 31 October provided a second PCA to increase the previously declining riometer absorption. We believe too that the extremely large burst peaking near 0912 UT on 1 November was responsible for holding the riometer absorption at Thule constant and even increasing it somewhat on 2 November.

Because of the complicated absorption pattern between 1 and 4 November it is difficult to precisely associate the 2002 UT event on 1 November with geophysical activity. The same situation prevails for the 0954-1020 UT burst on 2 November. It is felt that the event on 4 November at 0513 UT was responsible for the 1.6 dB absorption event later that day. The correlation of all these bursts with a variety of other geophysical phenomena will receive more extensive attention in another paper.

### Correlation of Burst Locations with Specific Sunspot and Magnetic Configurations

Table 1a - 1b also lists sunspot and magnetic field data. There are several obvious trends which emerge from relating the flare-burst locations of events with sunspot and magnetic configurations. The first is that the principal spot group in plage #9740 had, according to Mt. Wilson data, a delta magnetic configuration from the time of the first important event on 27 October until the region passed beyond the west limb. This fact is significant in view of the present high burst

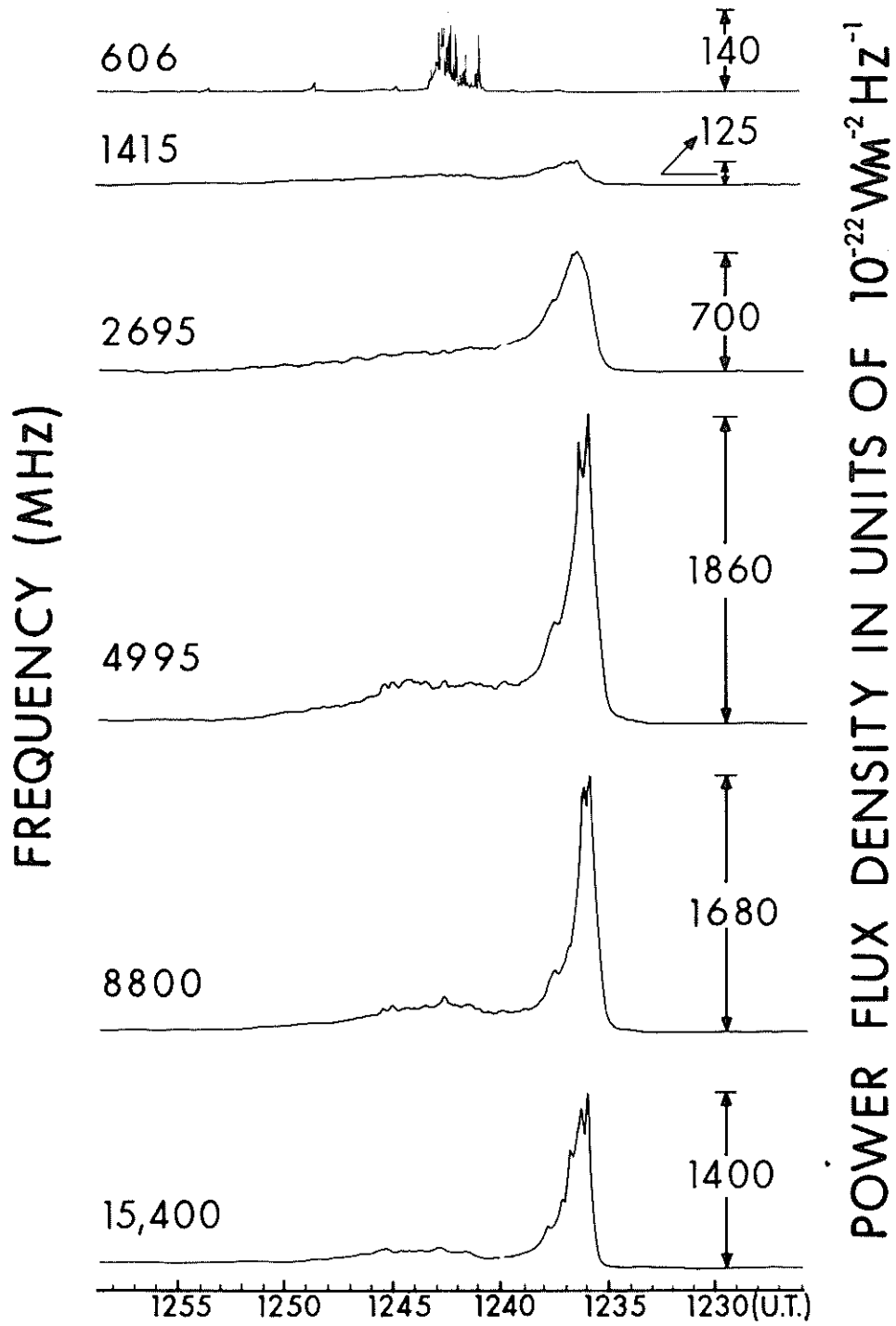


Fig. 5. Complex and simple 2 radio burst observed on 27 October 1968 Sagamore Hill Radio Observatory, Hamilton, Mass.

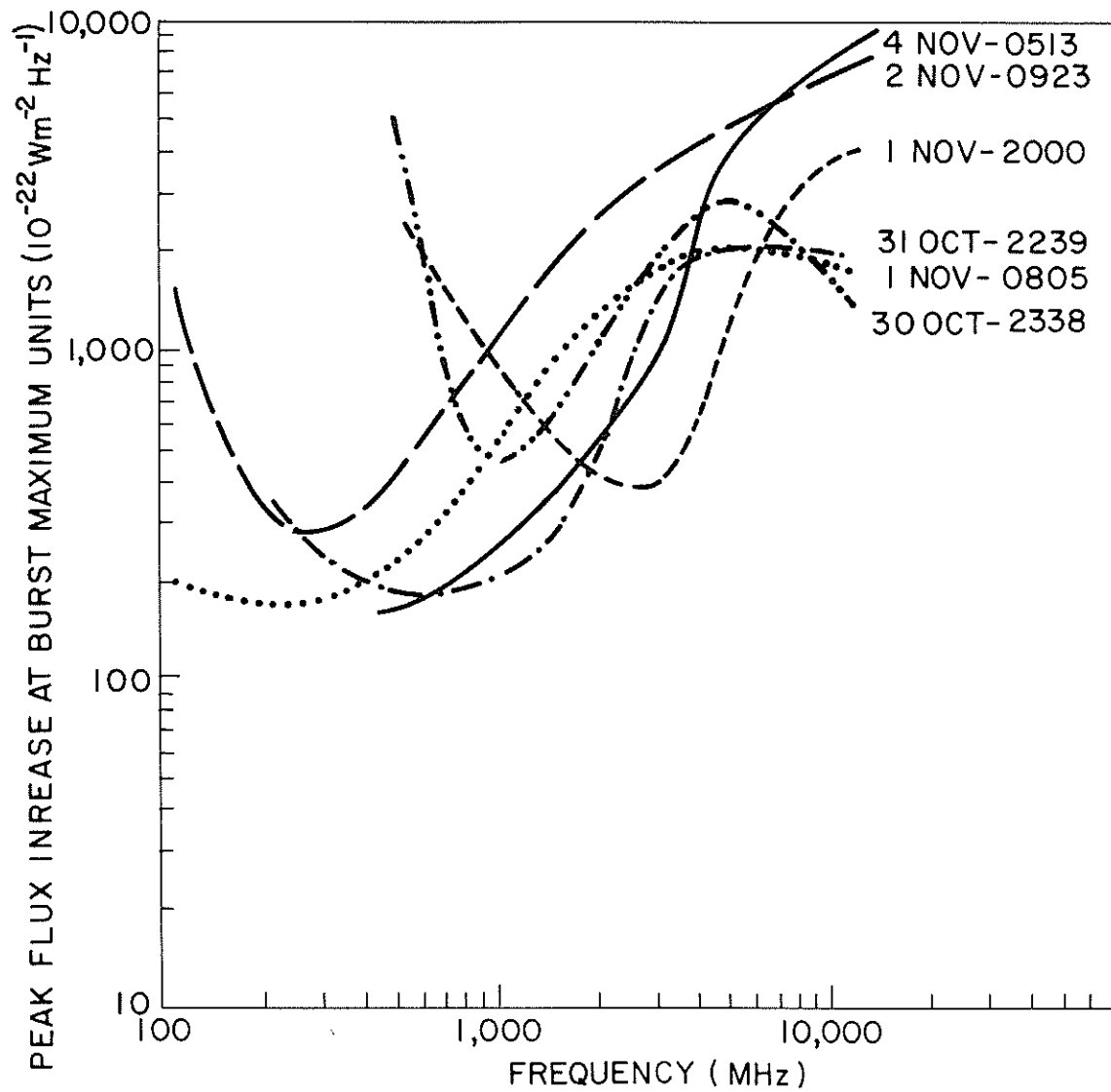


Fig. 6. Peak flux spectra of proton flare radio bursts 30 October - 4 November 1968. Start times are for radio bursts.

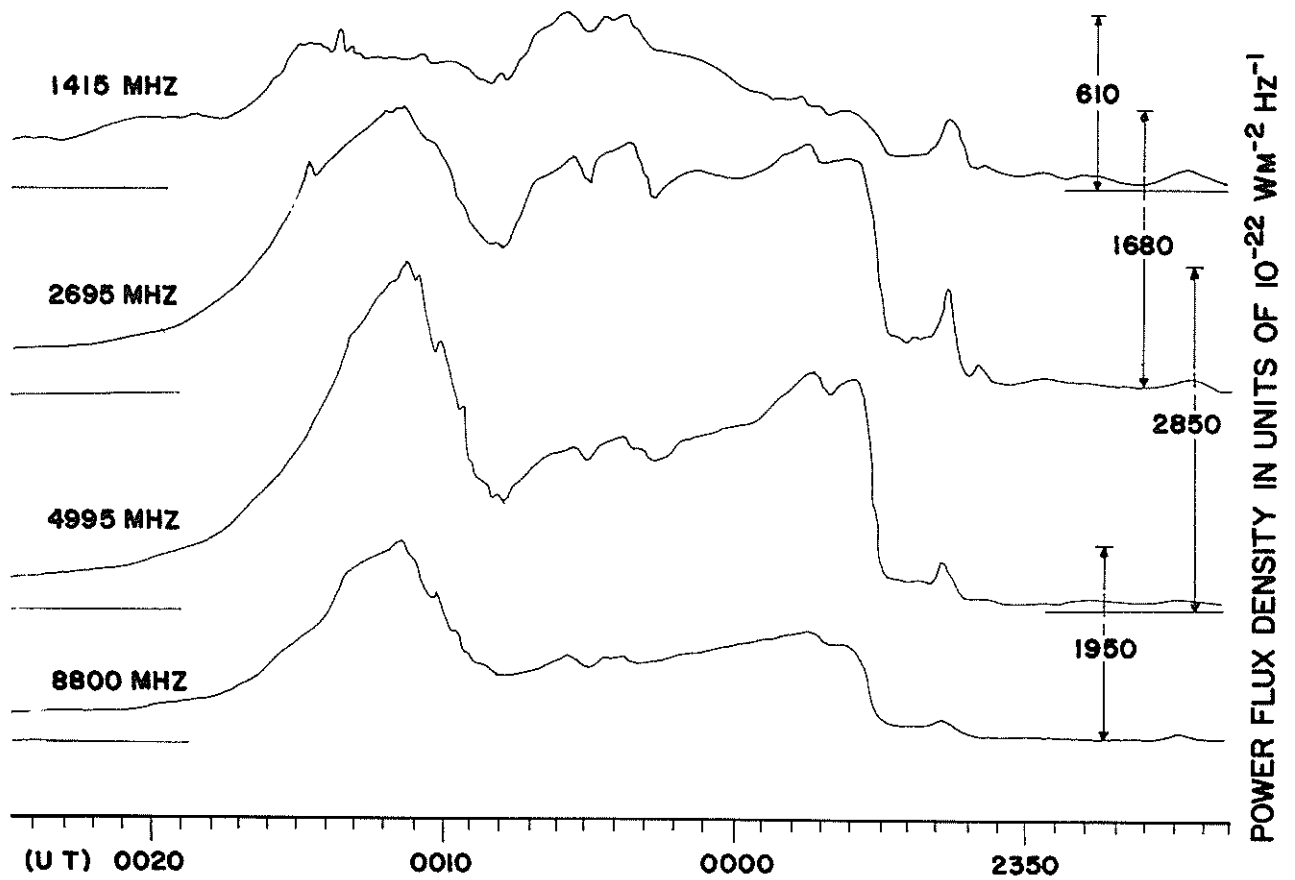


Fig. 7. Complex radio burst observed 30-31 October 1968 at Manila Radio Observatory.

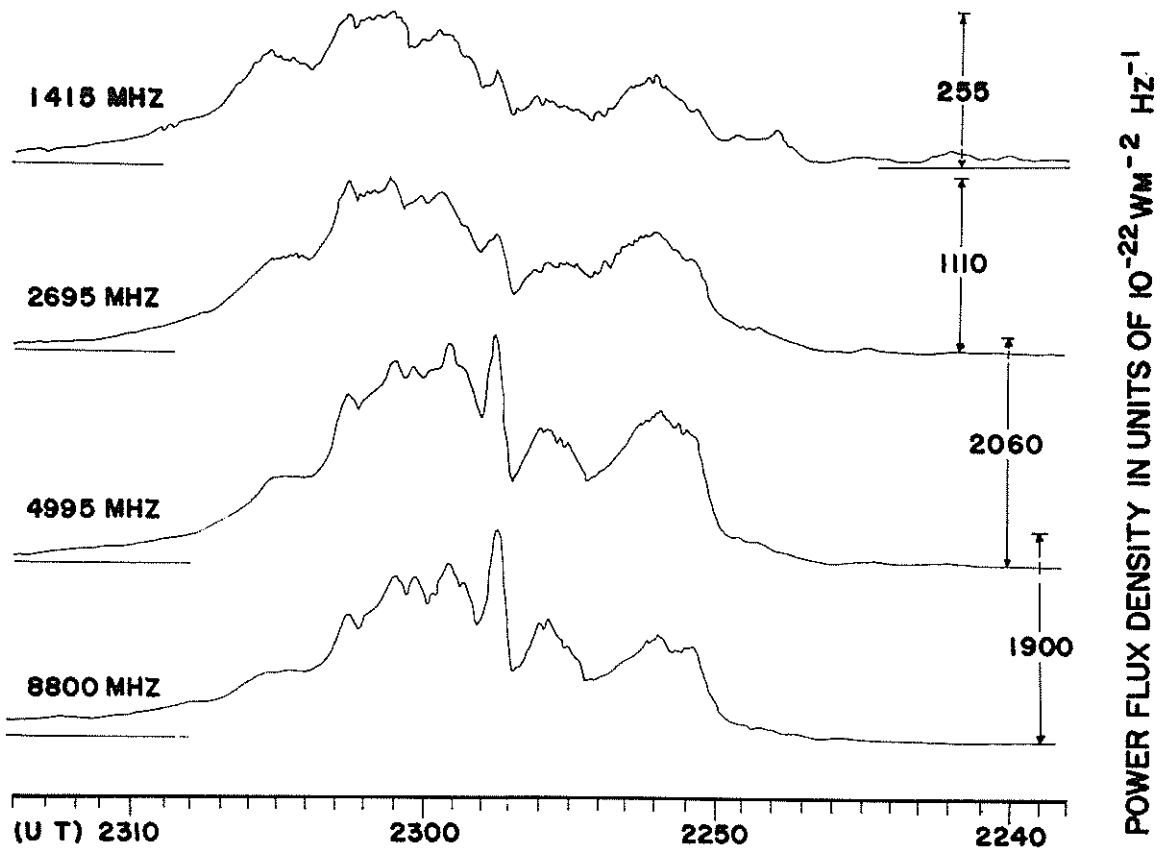


Fig. 8. Complex radio burst observed 31 October 1968 at Manila Radio Observatory.

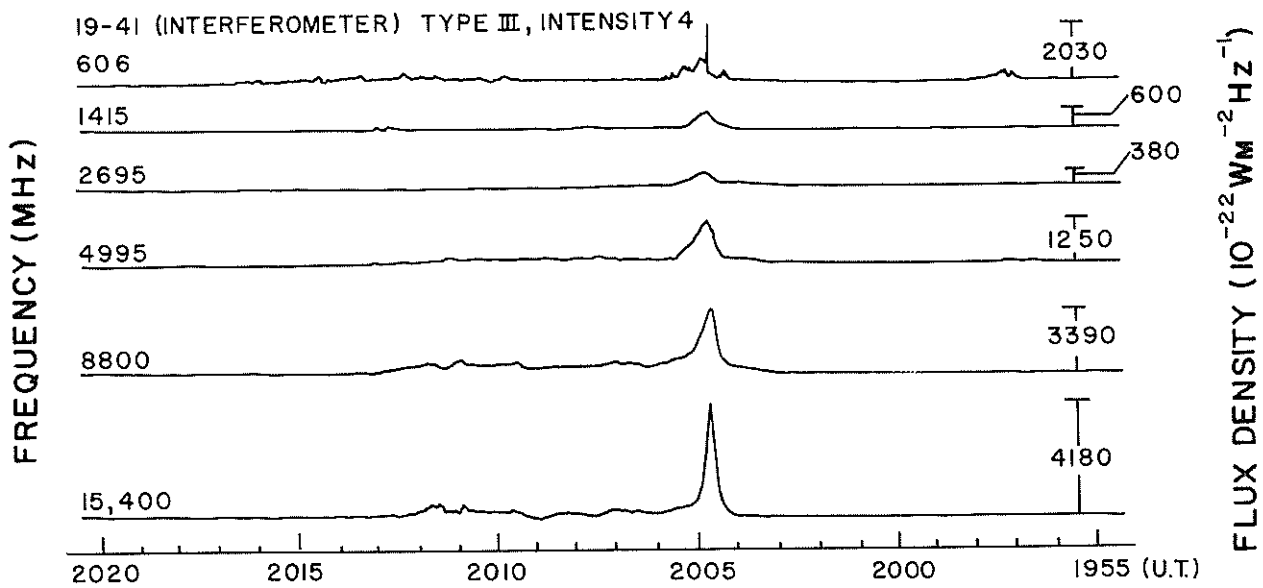


Fig. 9. Complex and simple 2F radio burst observed 1 November 1968 at Sagamore Hill Radio Observatory, Hamilton, Mass.

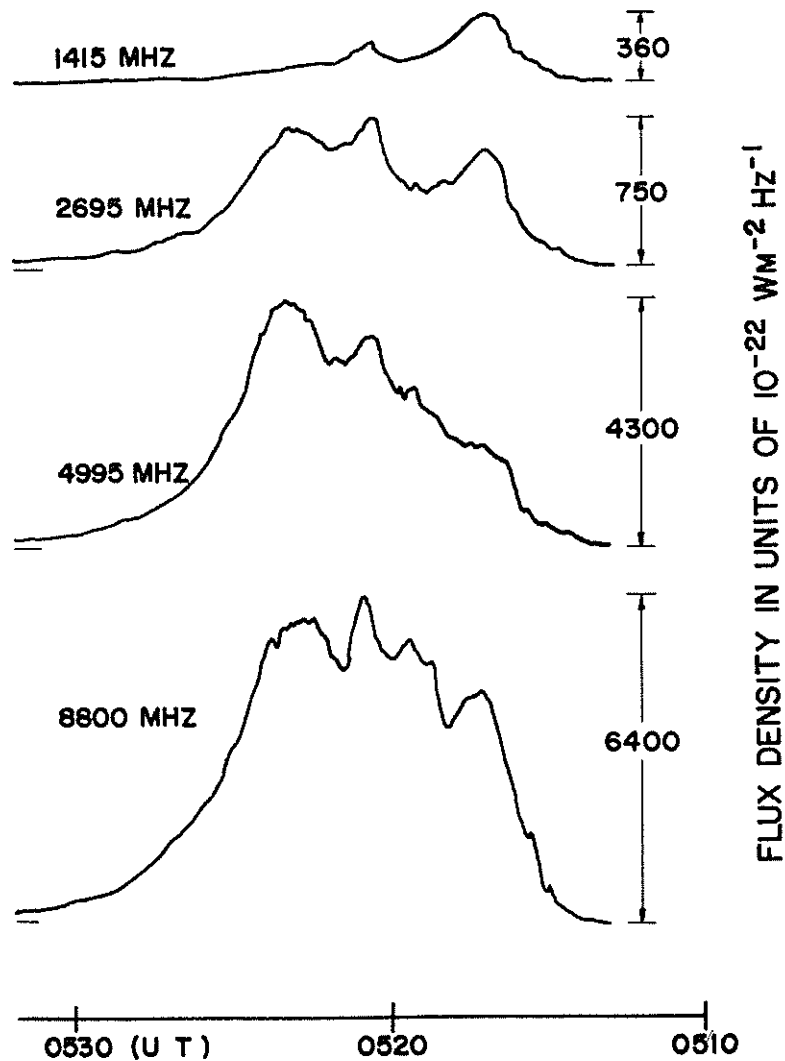


Fig. 10. Complex radio burst observed 4 November 1968 at Manila Radio Observatory.

productivity rate which has been recognized by the authors as typical of delta regions in general. It is apparent also that a high magnetic index (5) prevailed throughout significant parts of the entire period.

The sunspot configuration continuity was less consistent and its variation seems similar to the burst spectral history. For a few days before 30 October when there were bursts with intense low frequency emission, the sunspot configuration was essentially Zurich H according to Sacramento Peak Observatory reports. The H group is essentially unipolar. However, since flares and burst occur there, probably a small vestige of opposite magnetic polarity was also present. A consensus specifies that the region had a D configuration during these days. However, we are inclined to favor the Sacramento Peak classification in this period for certainly the average character of bursts then was different from that of later bursts. By 30 October, the configuration had changed to Zurich D, varying between C and D or D and E according to some observers for the next few days, during which important proton activity for the principal PCA's prevailed. It seems that the production of proton flares is somehow related to the sunspot configuration. The configuration also has a strong influence on the spectral type of bursts.

One must not be too rigorous in attempting to formulate this type association. Most sunspot and magnetic data available are recorded for a brief interval during each 24 hour period. Therefore, one cannot be sure what configuration prevailed at burst time. Also, all observatories' classifications do not agree with each other. Apart from that, it appears that proton flares may occur in several of the Zurich type sunspot configurations. In our evaluation of the 9 principal PCA's >2.0 dB absorption at 30 MHz) between 1966 and 1968, we had

4 events in Zurich D regions  
2 events in Zurich E regions  
3 events in Zurich F regions

Earlier association of proton flares with D sunspot areas seems to have good precedent.

The study of the correlation of radio burst spectra with optical and magnetic features was earlier undertaken by Castelli, et al. [1969] and is being continued.

#### Discussion

The radio bursts associated with proton events are characterized by spectra which exhibit a crossover frequency. Below the crossover frequency the burst intensity increases with decreasing frequency for some unspecified interval of bandwidth, while above the crossover frequency the intensity may increase monotonically with frequency up to 15,000 MHz and at times much higher. At times the intensity may peak somewhere in the 5,000-15,000 MHz range and decrease thereafter. This spectrum is not necessarily limited to proton events. However, bursts having these spectral characteristics with intensities higher than 1000 flux units near 3 cm wavelengths are found to be correlated with proton events.

Large radio bursts without direct or indirect particle detection possess spectra with maxima generally below 600 MHz and exhibit a steep drop of intensity on both high and low frequency ends.

Both particle associated radio bursts and those without particle association described earlier may conform to meter  $\lambda$  Type IV emission which can be explained by the synchrotron mechanism.

In the case of particle associated bursts, the spectral characteristics may be divided into two domains -- namely above and below the crossover frequency. The portion below the crossover frequency may be considered as a coronal event and that above it as a chromospheric phenomenon. It may be considered that in the flash phase of the flare occurring at the base of the corona (near 20,000 km.), electrons and protons are accelerated to high energy values. The accelerated particles travel in all directions. Those which travel toward the chromosphere are soon trapped in the sunspot magnetic field and give rise to synchrotron radiation in the dm-cm range of wavelengths. The distance travelled cannot be great as the radiation starts and peaks at about the same time as the optical flare. The characteristic spectrum of synchrotron radiation exhibits a peak owing to the absorption of gyro-radiation in the low frequency end and decrease of emissivity at higher harmonics of gyro-radiation and non-isotropic radiation due to pitch angle distribution.

The position of the peak depends on the value of the magnetic field at the level of synchrotron radiation. Flares may emit particles with a range of energies extending up to soft cosmic rays. If particles ejected during the flare are very energetic, they travel faster and farther before being trapped at lower levels in the chromosphere having higher values of magnetic field. As such, depending on the energy of the particles and the sunspot magnetic field, the peak burst emission may occur within a wide range of frequencies in the dm-cm range. However, for a magnetic field of given intensity, the position of the peak (within the spectrum) at the higher end of the frequency range is determined by the particle energy. Therefore, for very energetic particles, the peak intensity may occur beyond the highest frequency of observation, i.e. 15,400 MHz for the period under discus-

sion. A group of a dozen or more events observed in 1969 shows larger flux values at 35,000 MHz than below. For less energetic particles on the other hand, the peak may be discernible within the frequency range of observations available for the October-November 1968 period.

During the same event, the stream of protons and electrons travels outward through the corona. If the acceleration is high, the protons may escape the sunspot magnetic field and arrive at the earth to give rise to a GLE (ground level event of increase of neutrons) and fast PCA in less than an hour. The main plasma cloud travels outward behind a shock front and carries the "frozen" magnetic field to higher levels in the corona. The trapped electrons in the "frozen" magnetic field generate Type IV meter emission. If the magnetic field is transported to higher altitudes, the wide band synchrotron radiation can escape without being affected by the refractivity of the coronal electron density in front of it. Later with gradual weakening up of the transported magnetic field, the trapped protons may escape the solar atmosphere. Depending on the configuration of sun-earth magnetic field, these protons may subsequently cause slow PCA events. The delay between the onset of such PCA and the actual burst depends to a large extent on the interplanetary magnetic field. For instance, previous solar events might channel these particles into the earth's atmosphere easily with less delay. It may thus be concluded that the U-type or modified "U" type spectra with leveling off and decreasing at the highest frequencies in the dm-cm range of wavelengths indicates that very energetic electrons and protons have been released which may ultimately cause PCA events.

In addition to the spectral characteristics the intensity at the high frequency end is a very important criterion. The number of high energetic particles causing such type of spectra control the burst intensity. A high level of peak flux at the high frequency end signifies a large number of highly accelerated electrons and protons whose probability of escaping the solar atmosphere and ultimate arrival at the earth is very high. The mechanism of acceleration of particles in the solar atmosphere for causing such proton events must be linked to the magnetic field configuration and its instability. It is interesting to note that the particular spectral class of burst causing proton events is linked with bipolar groups with large gradients of magnetic field intensity.

The other type of large bursts in this period but without particle events possessed a peak around 500 MHz or lower and steep decrease of intensity towards both the high and low frequency ends. It may be considered that these bursts were caused by low energy particles which were mainly guided toward the corona and very few particles were ejected toward the chromosphere to generate cm bursts. The less energetic particles could not possibly move to very high levels in the corona.

If we consider that the level of emission is low in the corona, the refractive effects of ambient plasma could cause a sharp low-frequency cut-off which is known as the RAZIN effect [Ramaty and Lingenfelter, 1967]. The sharp cut-off at the high frequencies may be caused by the decreasing intensity of radiation at the higher harmonics of the gyrofrequency and anisotropic pitch angle distribution [Ramaty, 1969]. The low acceleration of particles is to be sought in the magnetic configuration corresponding to this class of bursts located above unipolar spot groups.

### Conclusion

The variation of flux of the undisturbed sun showed a pronounced peak at all the shorter wavelengths on 29 October as the coronal condensation associated with plage #9740 crossed the central meridian. Assuming that most of the variational excess flux was contributed by this one region, it is apparent that there is about a 1 to 1 ratio between 15400 and 8800 or 8800 and 4995 MHz. The contribution at 2695 MHz is definitely less. Therefore, the region was especially hot at the higher frequency. This is sometimes taken as a signature of proton flare regions. Most of the important burst activity, however, took place as the total flux was decreasing.

Throughout the whole period, a delta magnetic configuration prevailed. Statistically, this configuration forbodes important flare-burst activity. Strong proton flare activity occurred during periods when the associated sunspot group had a Zurich D, C or E classification. The peak flux spectra of bursts coming from this region, especially in the period 30 October - 4 November are the preferred ones for proton emission. Impressive m-dm bursts peaking near 600 MHz, even though associated with meter wavelength type IV events, have shown little tendency to have proton association.

The heliographic longitudes of flares in this region, 170° - 180° have not been recognized as preferred longitudes for southern hemisphere activity.

In view of the importance of plage #9740, investigation of microwave burst correlation with H $\alpha$  flare-intensity area profiles, X-ray and EUV bursts must ultimately be undertaken.

### Acknowledgement

The authors express their appreciation to MSgt Arthur Francis for data reduction of difficult events and associated graphics.

## REFERENCES

- BADILLO, V. L. and J. P. CASTELLI 1969 The Proton Flare of 9 June 1968, Astrophysical Letters, 4, No. 1, 5-9.
- CASTELLI, J. P., J. AARONS and G. A. MICHAEL 1967 Flux Density Measurements of Radio Bursts of Proton-Producing Flares and Non-Proton Flares, J. Geophys. Res., 72, 5491-5498.
- CASTELLI, J. P., J. AARONS, G. A. MICHAEL, C. JONES and H. C. KO 1969 Spectral Considerations of Microwave Solar Bursts, Solar Flares and Space Research, North Holland, Amsterdam, 194-201.
- CASTELLI, J. P. and J. AARONS 1969 Radio Burst Spectra and the Short Term prediction of Solar Proton Events (Paper 11), September 1969, to appear in Proceedings of AGARD Symposium on Ionospheric Forecasting.
- 1968 ESSA, Solar-Geophysical Data, IER-FB 291 and 292, November and December 1968.
- MASLEY, A. D. 1969 Private communications.
- O'BRIEN, W. E. In special study of proton flare-bursts in requirement for AFIT Graduate Thesis, to appear.
- PAULIKAS, G. A. 1969 Private communication.
- RAMATY, R. and R. E. LINGENFELTER 1967 The Influence of the Ionized Medium on Synchrotron Emission Spectra in the Solar Corona, J. Geophys. Res., 72, 879-883.
- RAMATY, R. 1969 On the Nature of the High Frequency Cutoffs of the Type IV Solar Radio Bursts, Astrophysical Letters, 4, 43-45.
- STRAKA, R. M. and W. R. BARRON 1969 Multi frequency Solar Radio Bursts as Predictors of Proton Events (Paper 10), September 1969, to appear in Proceedings of AGARD Symposium on Ionospheric Forecasting.

Appendix

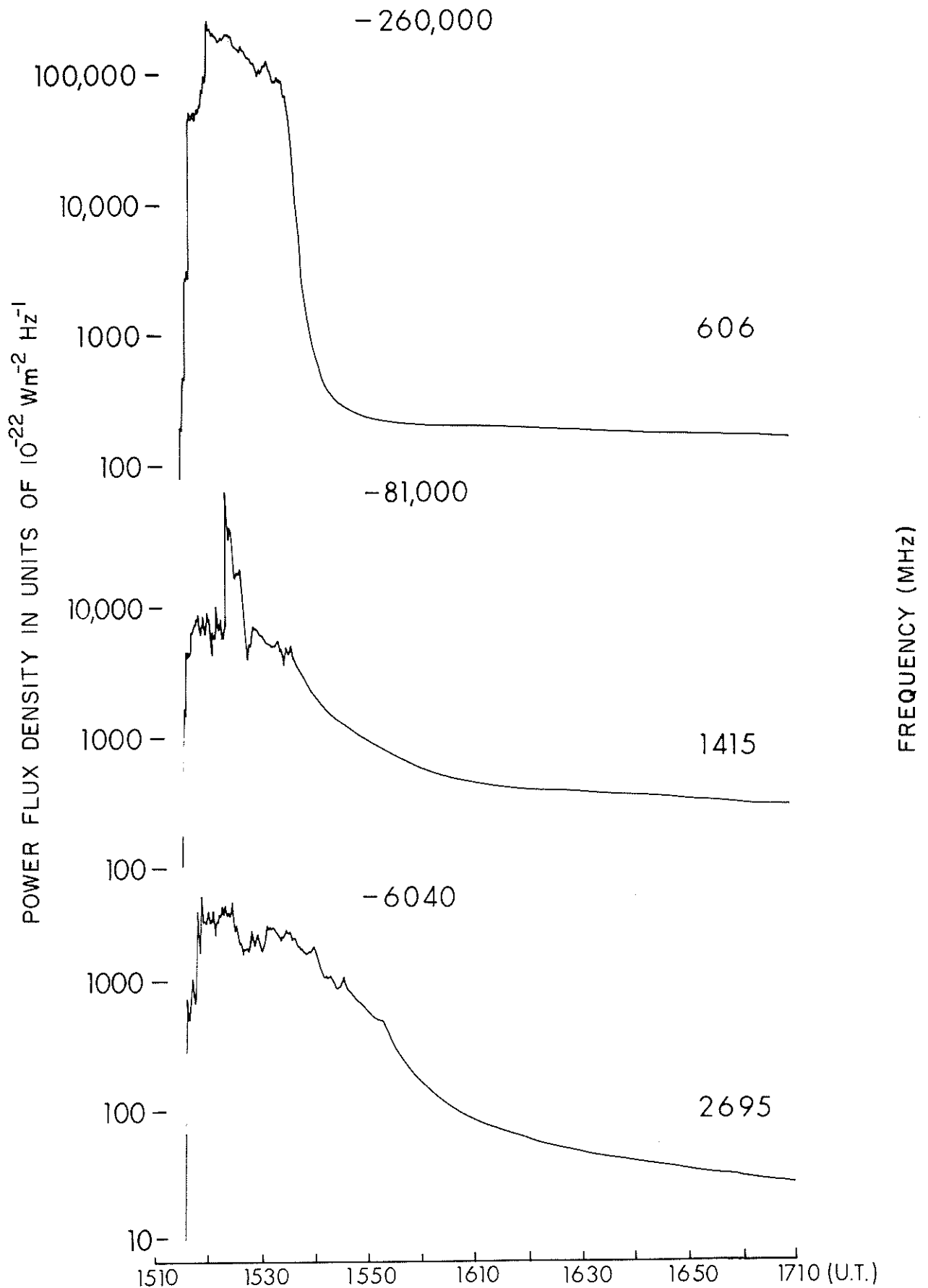
Castelli et al. list 13 important bursts from 22 October - 4 November 1968. These are at the following dates and times:

23 October	2359 UT
27 October	1234
27 October	1306
29 October	1218
29 October	1516
30 October	1331
30 October	2338
31 October	2239
1 November	0815
1 November	1209
1 November	2003
2 November	0924
4 November	0514

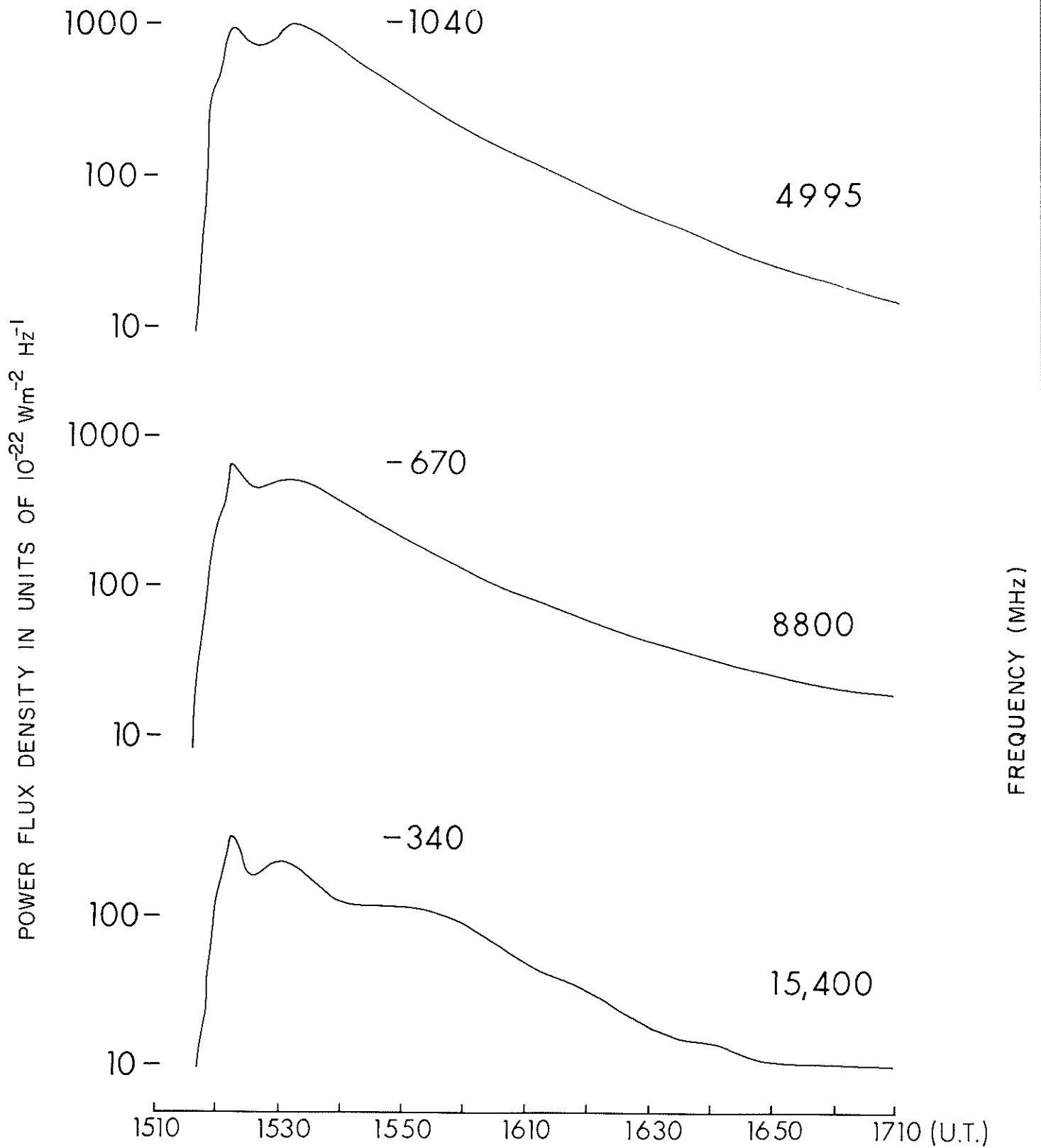
Details of all of these bursts can be found on pages 69 to 90 of this Report with the exception of the first one which is given below.

1968	Freq. MHz	Station	Type	Starting time UT	Time of maximum	Duration min.	Flux peak	Density Mean
23 October	8800	MANI	3	2359.6	0003.3	11.2	325.4	162.2
	4995	MANI	3	2358.9	0003.3	11.6	535.8	267.9
	2695	MANI	3	2358.8	0003.9	11.9	541.5	270

The burst profiles of the large event on 29 October 1968 are presented in the final figure.



Great burst observed on 29 October 1968 at Sagamore Hill Radio Observatory, Hamilton, Massachusetts.



Great burst observed on 29 October 1968 at Sagamore Hill Radio Observatory, Hamilton, Massachusetts.

"Solar Radio Bursts During the Period 27 October through 5 November 1968"

by

Fred L. Wefer  
The Pennsylvania State University  
Radio Astronomy Observatory  
University Park, Pennsylvania

The data presented in this paper are from observations made with fixed frequency radiometers operating at 10.7 GHz, 2.7 GHz, 960 MHz and 328 MHz. The observations were made at The Pennsylvania State University Radio Astronomy Observatory (PSURAO) 40° 50'N, 77° 53'W.

The radiometers are operated primarily as a burst patrol. The quiet sun flux densities, while they are computed daily, are not presently regularly published. The daily averages of the quiet sun flux densities for October and November 1968 at 10.7 GHz, 2.7 GHz and 960 MHz are shown in Figures 1 and 2. These values have not been corrected for atmospheric effects. The mean error of the relative values at a given frequency is about 10%. The uncertainties in the measured values of the gains of the antennas are quite large. An error in the gain of the antenna causes all flux densities at that frequency to be in error by the same factor.

The tabulated values for all distinct events observed during the period 27 October through 5 November, as reported to ESSA and included in IER-FB 291 and 292 can also be found in the tables of pages 69 to 90 of this Report under station PENN.

The profiles of all events in which the peak flux density was greater than 300 f.u. on at least one frequency, are shown in Figures 3 through 9. In these figures, blank areas in the burst profiles are either equipment failure, periods of automatic calibration or periods when the recorder was off scale. The latter are indicated by dashes at the tops of the profiles. For some of the bursts the observed profiles were not complete enough to be included. All of the profiles are linear in flux density, the relative scale being shown at the left of each profile in solar flux density units,  $10^{-22} \text{Wm}^{-2} \text{Hz}^{-1}$ . The Universal time is marked every five minutes.

Using a method similar to that of Parks and Winckler [1969], the Fourier spectra of ten of the larger bursts were computed. These bursts are those at 10.7 GHz, 2.7 GHz and 960 MHz October 27 at 1235 UT; at 10.7 GHz, 2.7 GHz and 328 MHz October 27 at 1306 UT; at 10.7 GHz, 2.7 GHz and 328 MHz October 29 at 1205 UT; and at 10.7 GHz October 29 at 1516 UT. Because most of the spectra are rather long and not easy to interpret, only three are presented. The Fourier spectra of the burst shown in Figure 3, are shown in Figure 10. In this figure the logarithm of the absolute magnitude of the Fourier amplitude is plotted against frequency. The data have been normalized so that the amplitudes of the components at  $7.2 \times 10^{-4}$  Hz,  $7.2 \times 10^{-4}$  Hz and  $8.3 \times 10^{-4}$  Hz for 10.7 GHz, 2.7 GHz and 960 MHz respectively, have value unity. The spectrum of the 10.7 GHz burst profile is the simplest of the ten that were computed.

REFERENCE

- |                                    |      |   |
|------------------------------------|------|---|
| PARKS, G. K. and<br>J. R. WINCKLER | 1969 | Simultaneous Observations of 5- to 15-Second Period Modulated Energetic Proton Fluxes at the Synchronous Altitude and the Auroral Zone, <u>J. Geophys. Res.</u> , <u>74</u> , 4003. |
|------------------------------------|------|---|

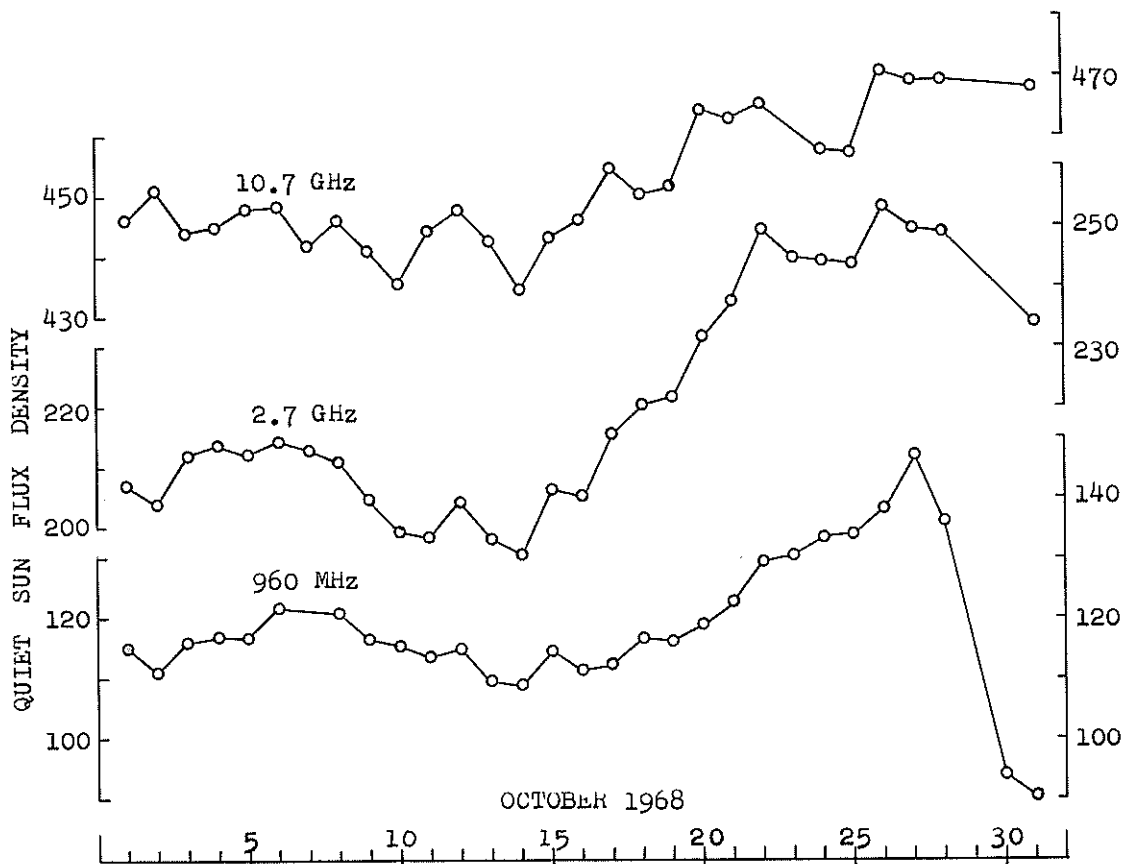


Fig. 1. The daily averages of the quiet sun flux densities at 10.7 GHz, 2.7 GHz and 960 MHz for October 1968. The unit of flux density is  $10^{-22} \text{Wm}^{-2} \text{Hz}^{-1}$ .

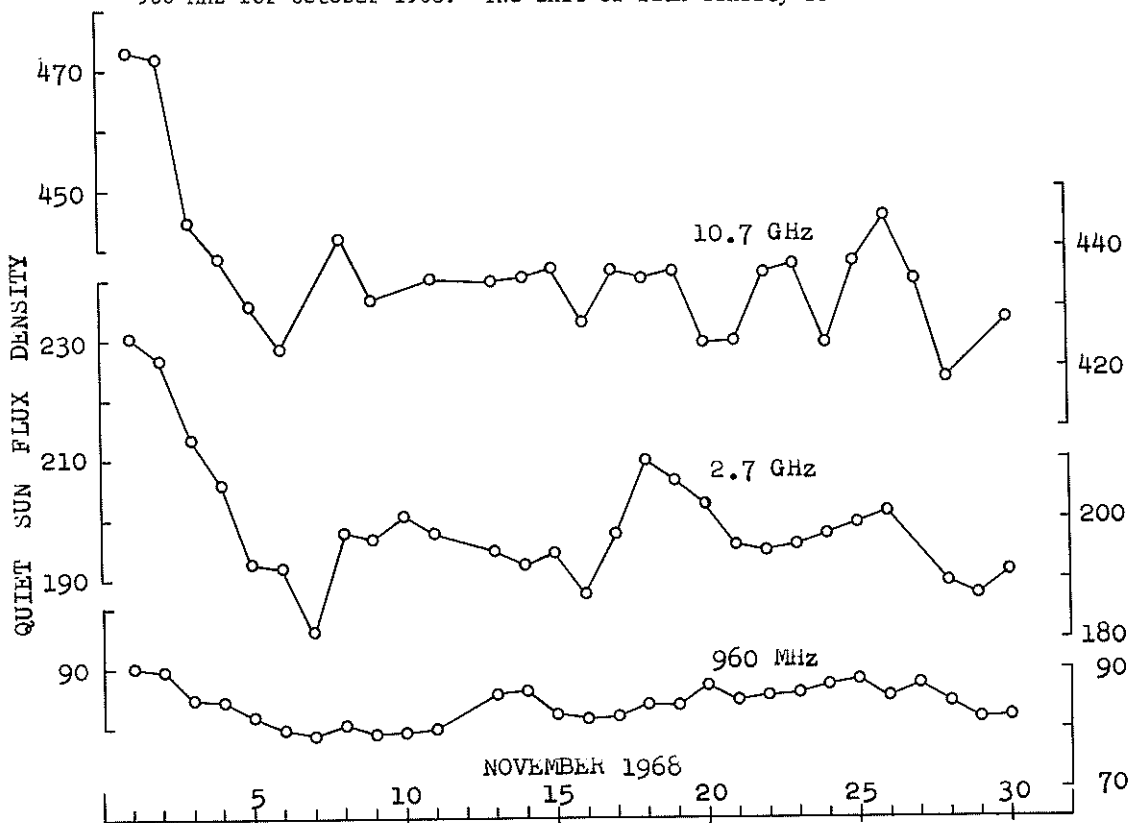


Fig. 2. The daily averages of the quiet sun flux densities at 10.7 GHz, 2.7 GHz and 960 MHz for November 1968. The unit of flux density is  $10^{-22} \text{Wm}^{-2} \text{Hz}^{-1}$ .

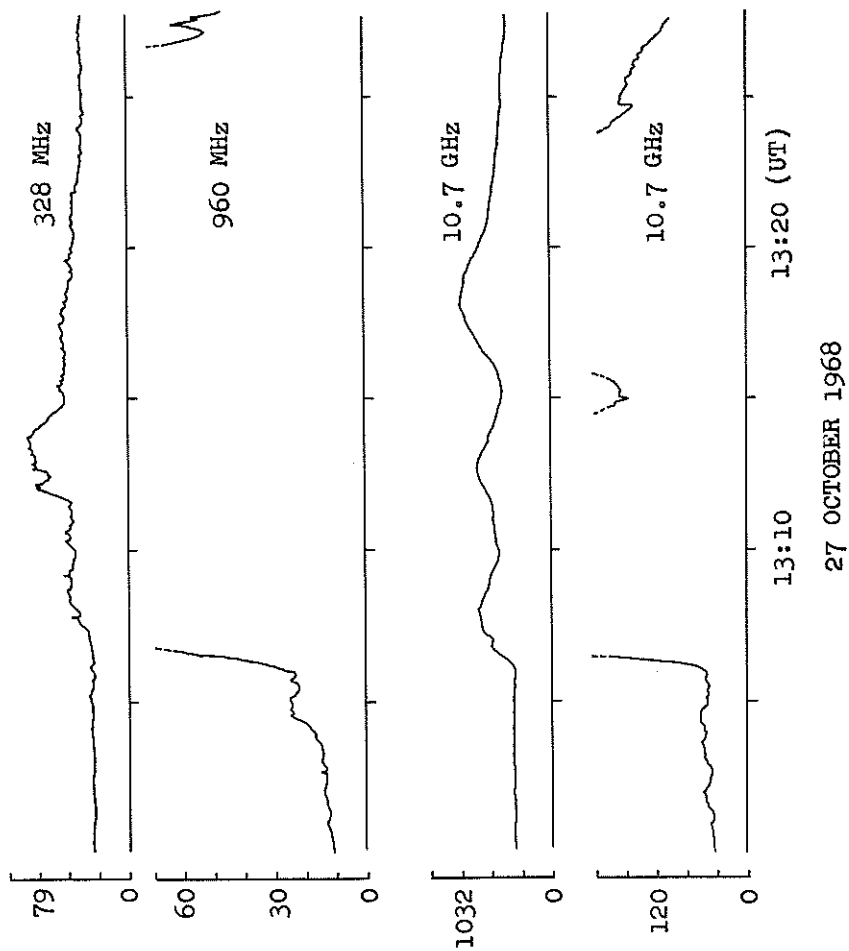


Fig. 3. Solar radio burst of 27 October 1968 at PSURAO. The 328 MHz radiometer was not operating at this time. The gap in the 2.7 GHz profile at 1247 UT was due to equipment failure. The burst began just as the antennas were pointed at the sun.

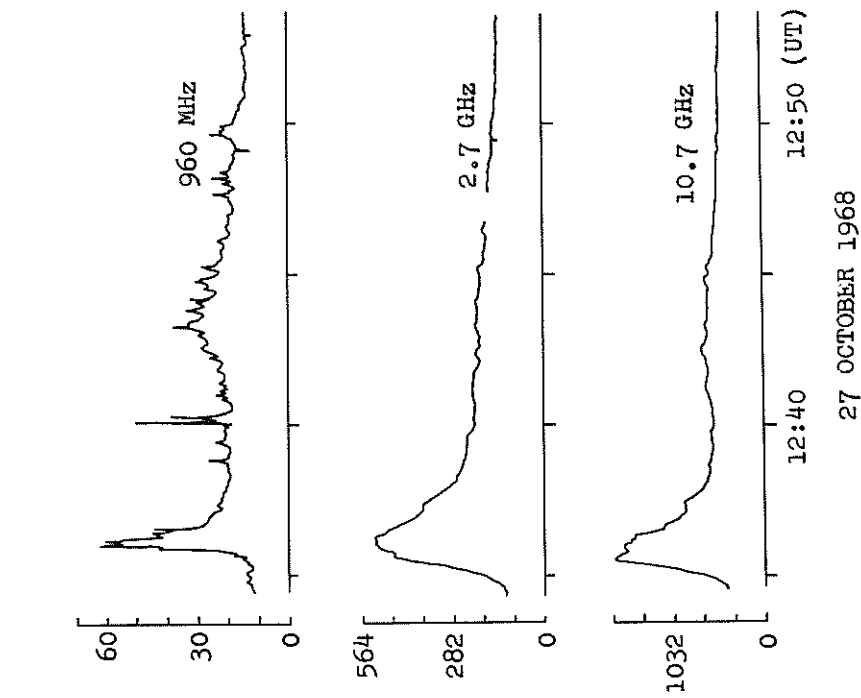


Fig. 4. Solar radio burst of 27 October 1968 at PSURAO.

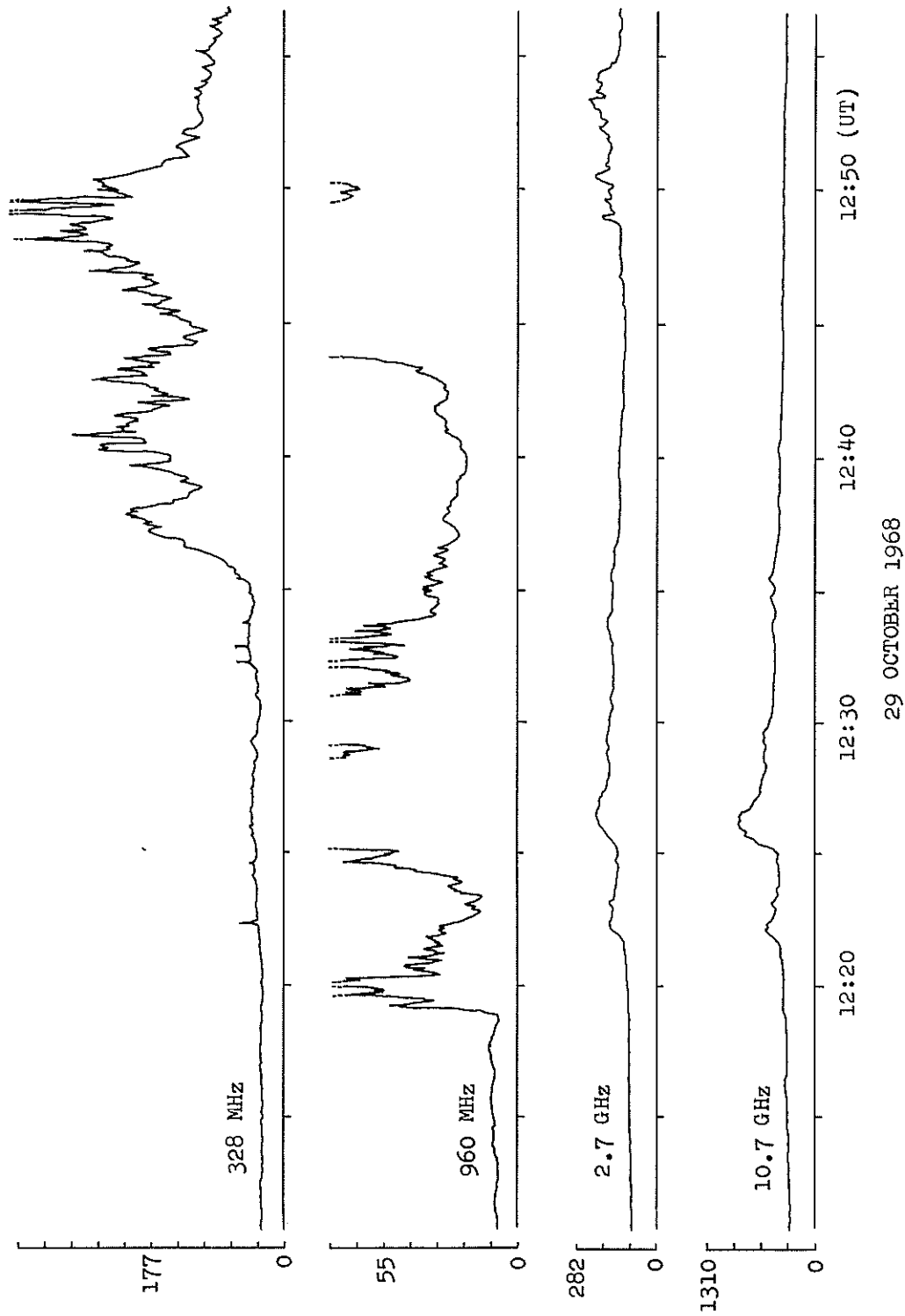


Fig. 5. Solar radio burst of 29 October 1968 at PSURAO. The high gain recorders at 10.7 GHz and 2.7 GHz were off scale during most of this time.

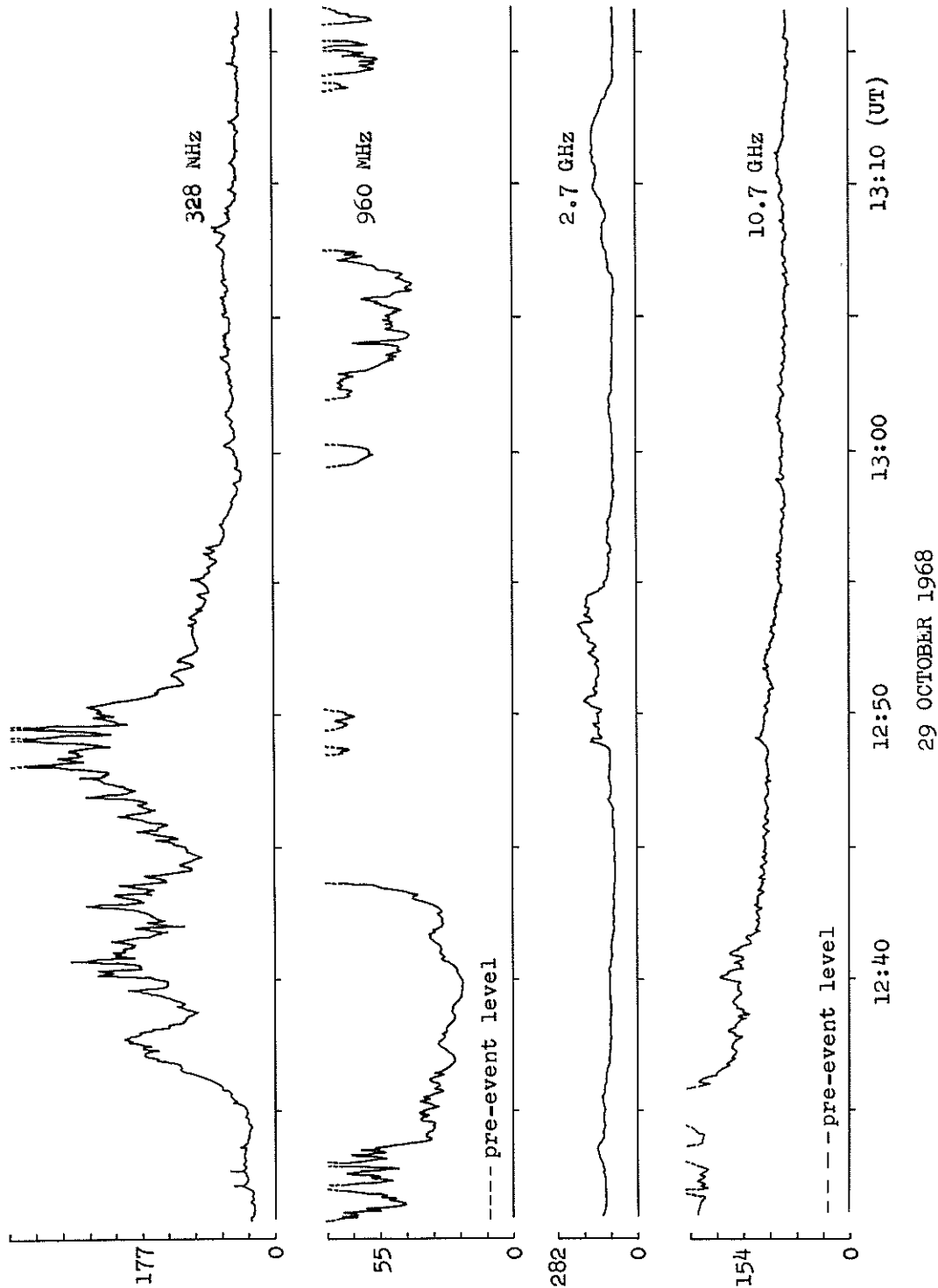
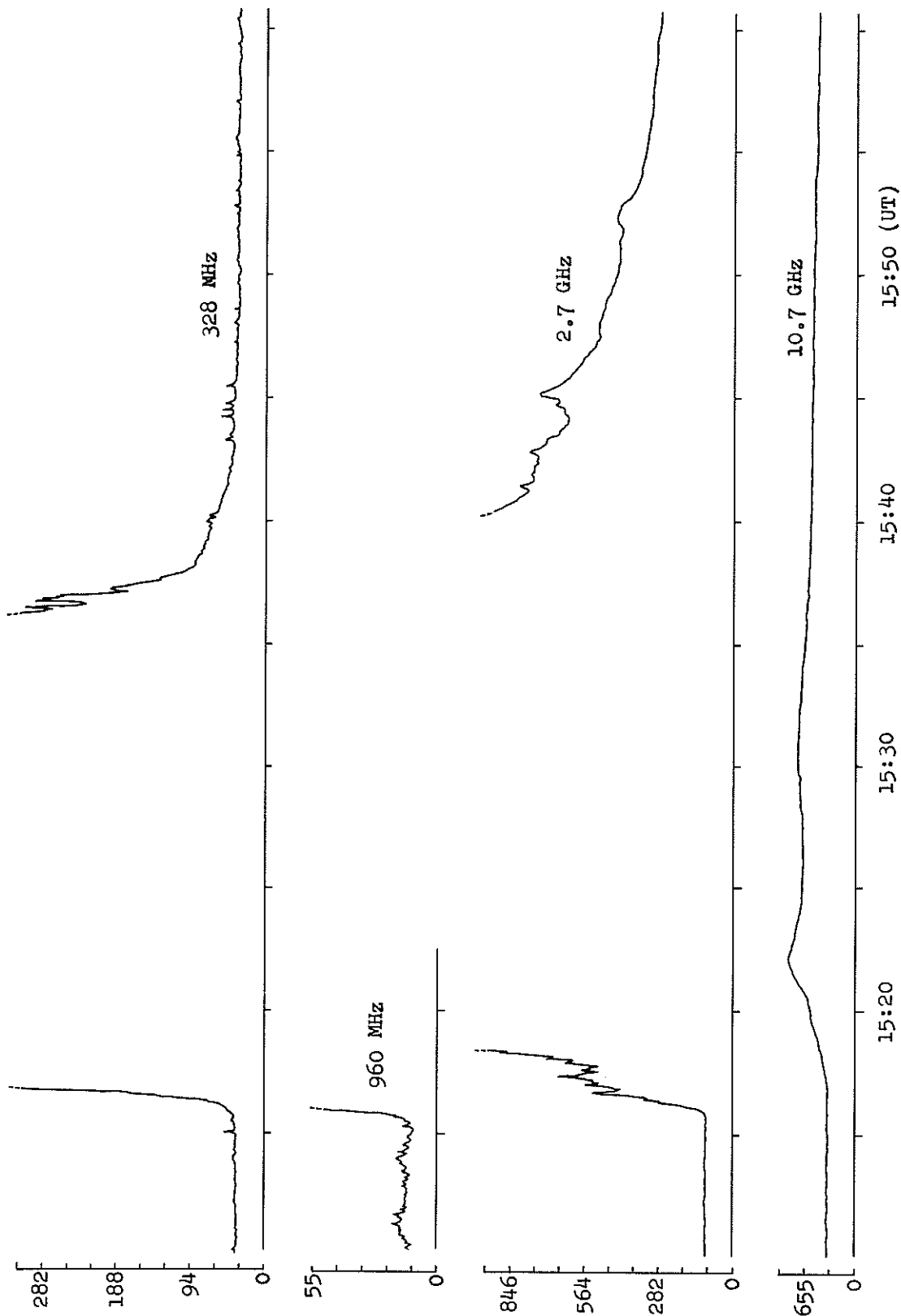


Fig. 6. Solar radio bursts of 29 October 1968 at PSURAO.



29 OCTOBER 1968

Fig. 7. Solar radio burst of 29 October 1968 at PSURAO. The 960 MHz recorder remained off scale until after the period shown here.

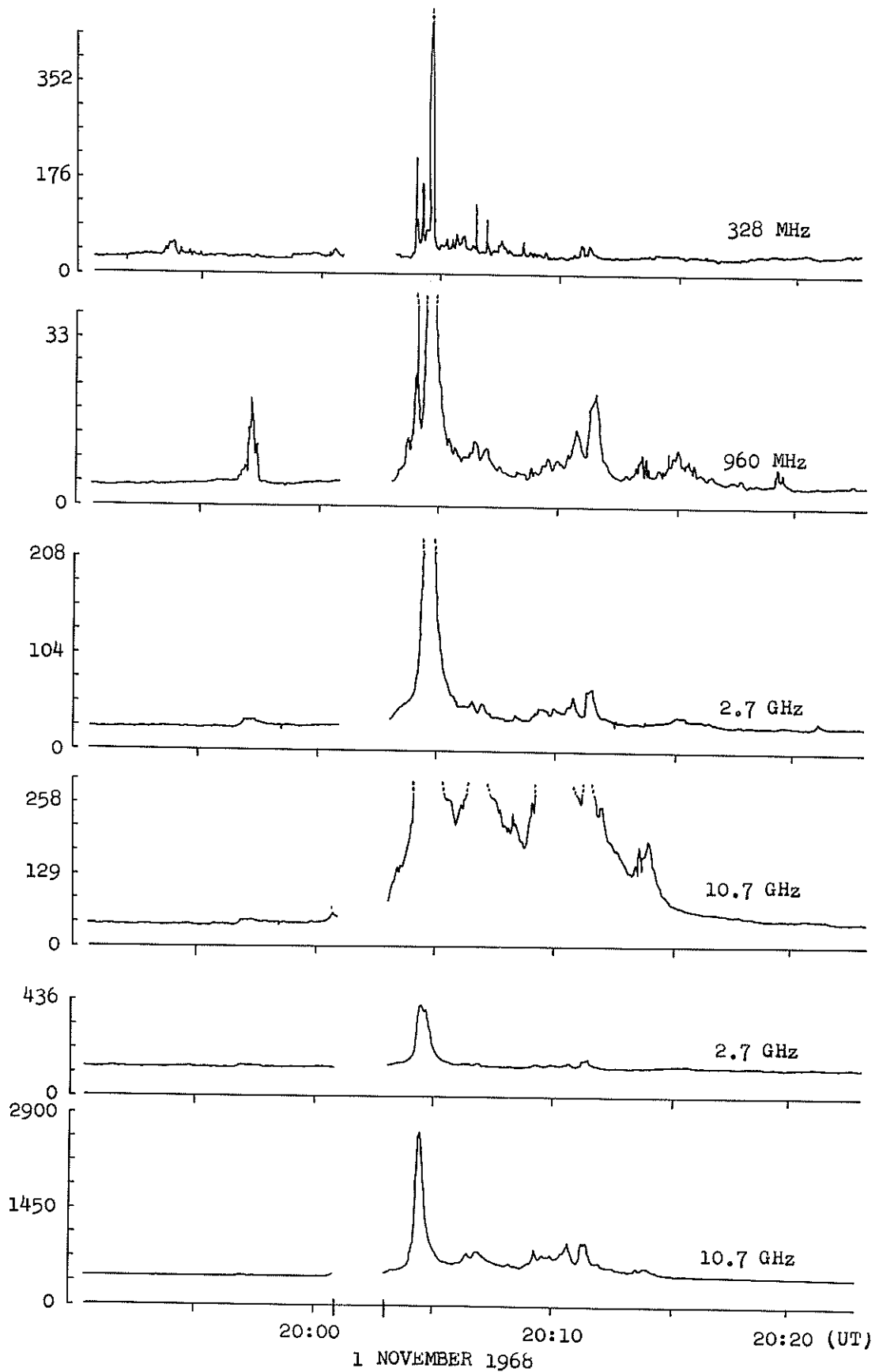


Fig. 8. Solar radio burst of 1 November 1968 at PSURAO. The gaps in the profiles at 2001 UT are due to automatic calibrations.

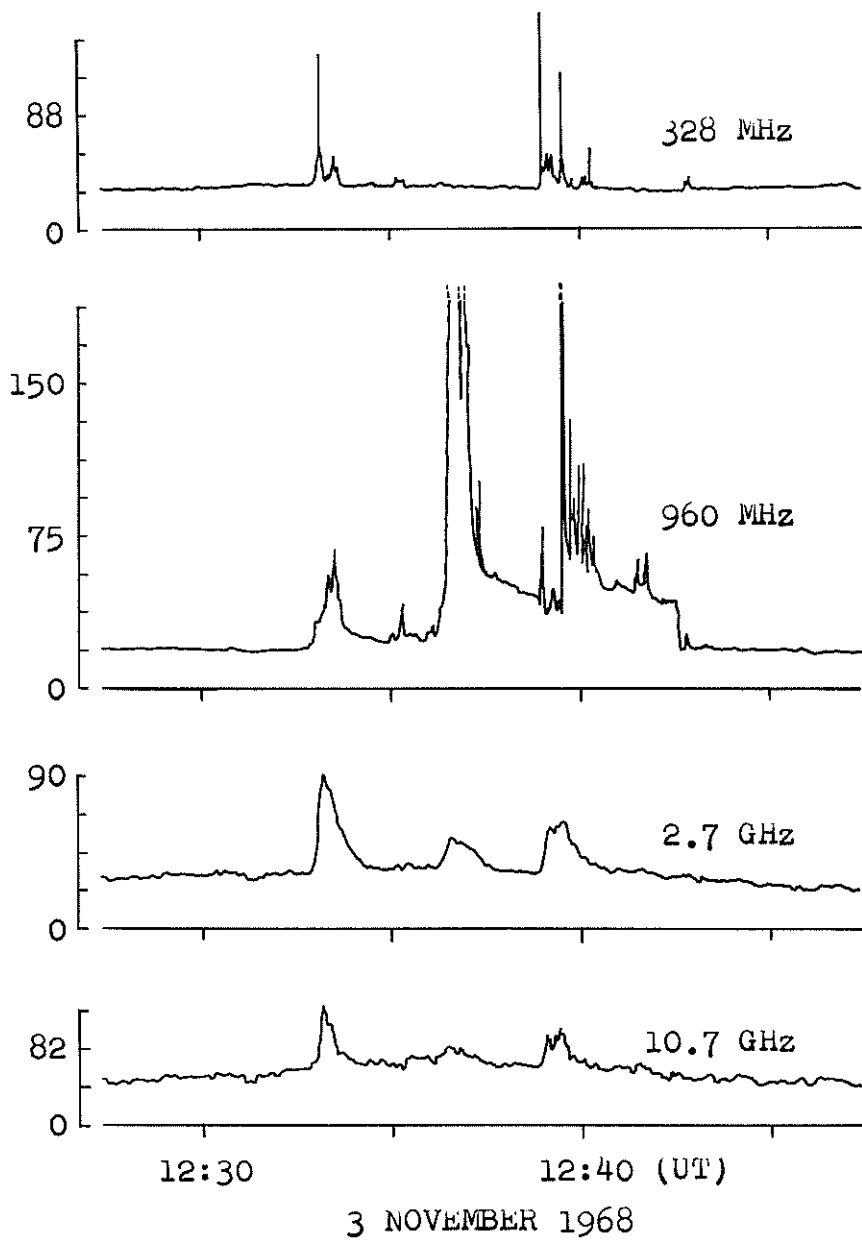


Fig. 9. Solar radio burst of 3 November 1968 at PSURAO.

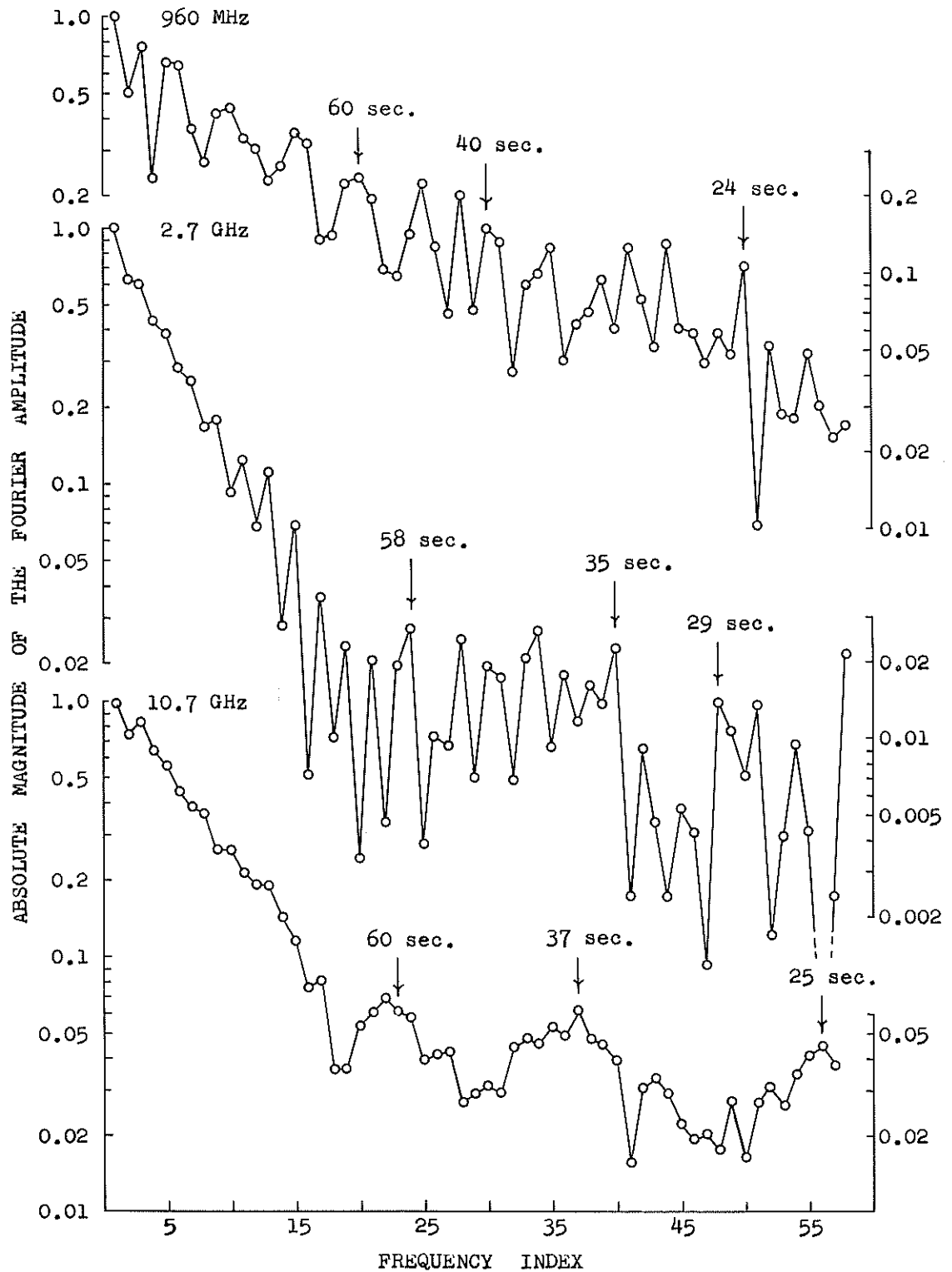


Fig. 10. Fourier spectra of the profiles of the burst of 27 October 1968 which was in progress at 1234.5 UT. The absolute magnitude of the Fourier amplitude is plotted against the frequency index. The frequencies corresponding to one unit of frequency index are  $7.2 \times 10^{-4}$  Hz,  $7.2 \times 10^{-4}$  Hz and  $8.3 \times 10^{-4}$  Hz at 10.7 GHz, 2.7 GHz and 960 MHz, respectively.

"Report on the Solar Radio Events of the period 1968 October 27 - November 4"

by

A. Böhme, F. Fürstenberg, and A. Krüger  
 Central Institute for Solar-Terrestrial Physics  
 Heinrich-Hertz-Institut (HHI)

The period of visibility of the solar active region belonging to the McMath plage region number 9740 was characterized by a series of at least 8 major Type IV bursts, some of them being associated with proton events. A rough compilation of these events is given in Table 1. In this table some other burst events extending from centimeter to dekameter wavelengths are also included under (b). The general activity of microwave bursts especially at 3 cm wavelength was remarkably strong, as is characteristic for proton-active regions. During the period from October 22 to November 4, 1968 at least 93 well flare-associated centimeter bursts could be detected from all stations around the earth. The number of cm-bursts which could not be correlated with observed flare events was even higher.

Table 1  
 Radio events belonging to McMath plage region No. 9740

a) Type IV bursts				
Date	Start UT	Max. 3cm-flux (Obs.)	Flare Position	Remarks
27 Oct 1968	1231	1600 (HHI)	S17 E16	PE >30 MeV
29 Oct 1968	1132	800 (HHI)	S16 W12	
30 Oct 1968	1230	80 (SAG)	S18 W25	
31 Oct 1968	2231	2300 (NAG)	S15 W49	
1 Nov 1968	0802	1850 (HHI)	S15 W47	PE >30 MeV
1 Nov 1968	1945	3400 (SAG)	S13 W57	
2 Nov 1968	0919	6600 (HHI)	S14 W66	PE >30 MeV
4 Nov 1968	0513	8000 (NAG)	S15 W90	
b) Other compound broad-band radio events				
23 Oct 1968	2354	>225 (NAG)	S12 E59	
24 Oct 1968	2045		S18 E52	
26 Oct 1968	0104		S20 E32	
31 Oct 1968	2223		S15 W49	
3 Nov 1968	1232	60 (HHI)	S19 W83	

The evolution of the ratio of the daily numbers of observed microwave bursts to flares in comparison with the occurrences of large radio events and the spectral characteristics of the s-component during the period under consideration is shown in Fig. 1. The period is reflected by a remarkable increase of the ratio of the microwave burst to flare production indicating an increasing exchange of higher energies in the flare process. The period of Type IV burst activity was also accompanied by a remarkable increase of the flux ratio of the whole-sun s-component between 9400 and 1500 MHz indicating an increased storage of energy in the active region. A brief maximum of these ratios was also present on October 23, 1968 but no great Type IV burst occurred on that day.

Records of the Type IV bursts observed at the HHI are given in Figs. 2 - 6.

In these figures the ordinate scale refers to solar units of flux density, i.e.  $10^{-22} \text{ Wm}^{-2} \text{ Hz}^{-1}$ . At the frequencies 9400 - 1500 MHz the horizontal zero line denotes the pre-burst level. Relative units expressed in fractions of the pre-burst level are additionally marked (e.g.  $\odot_{-1/4}$  means one fourth of the pre-burst level). The numerator of the fraction given in brackets indicates the absolute value of the pre-burst level. Broken lines denote changes of sensitivity. The scale of the high sensitivity record is given at the left edge of the drawing, the low sensitivity scale is at the right side, if the sensitivity is changed. In case that the intensity is off scale only for a short time, or only one sensitivity is used at some one frequency, the time of maximum is given by an arrow and the peak intensity derived from the photographic record is noted above the arrow.

The first observed Type IV event of this series on October 27, 1968 (1231 UT) already was well developed at centimeter-waves. At meter-waves, however, only the later phases of burst are clearly expressed whereas in the dekameter region most parts of the burst are missing.

Also the onsets of the next Type IV bursts on October 29, 1968 (1132 UT) and October 30, 1968 (1230 UT) were successively delayed and became less impulsive with increasing wavelengths. In both cases besides the Type IV components in the microwave region Type IVmB bursts were present.

Spectral diagrams of the Type IV bursts on November 1, 1968 (0802 UT) and November 2, 1968 (0919 UT) are shown in Figs. 7 and 8. In both events centimeter and meter components as well as decimeter components were present.

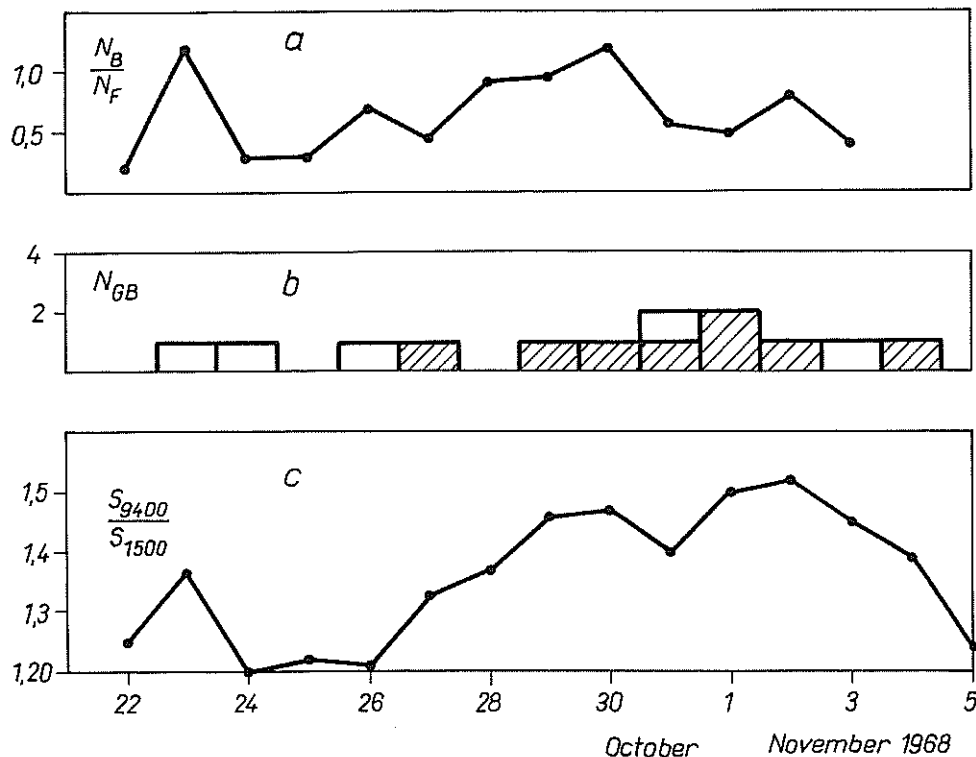


Fig. 1. (a) Ratio of numbers of microwave bursts to number of flares, (b) the number of broad band bursts (Type IV shadowed), (c) ratio of the fluxes of the s-component during the development of the active region belonging to McMath plage region No. 9740.

Concerning the association of proton-events one gets the impression, that the existence of both, strong Type IV cm-bursts and Type IVmA-like burst components, which do not necessarily contain a moving part, are specifically related to the ejection of fast protons [cf. Castelli *et. al.*, 1968; Krüger, 1968]. On the other hand, Type IVdm-bursts and to a certain extent also Type IVmB-bursts do not appear characteristically connected with proton events [cf. e. g. Böhme and Krüger, 1969].

Tables of burst data are contained in the HHI Solar Data, Vol. 19 (1968) Nos. 10 and 11 and are included in the tables on pages 69 to 90 of this Report.

#### REFERENCES

- |  |      |  |
|--|------|--|
| BÖHME, A. and<br>A. KRÜGER                         | 1969 | <u>HHI Supl. Ser. Solar Data</u> , <u>I</u> , No. 3. |
| CASTELLI, J. P.,<br>J. AARONS and<br>G. A. MICHAEL | 1968 | <u>Astrophys. J.</u> , <u>153</u> , 267-273          |
| KRÜGER, A.   | 1968 | <u>Habil-Schrift</u> , Rostock                       |

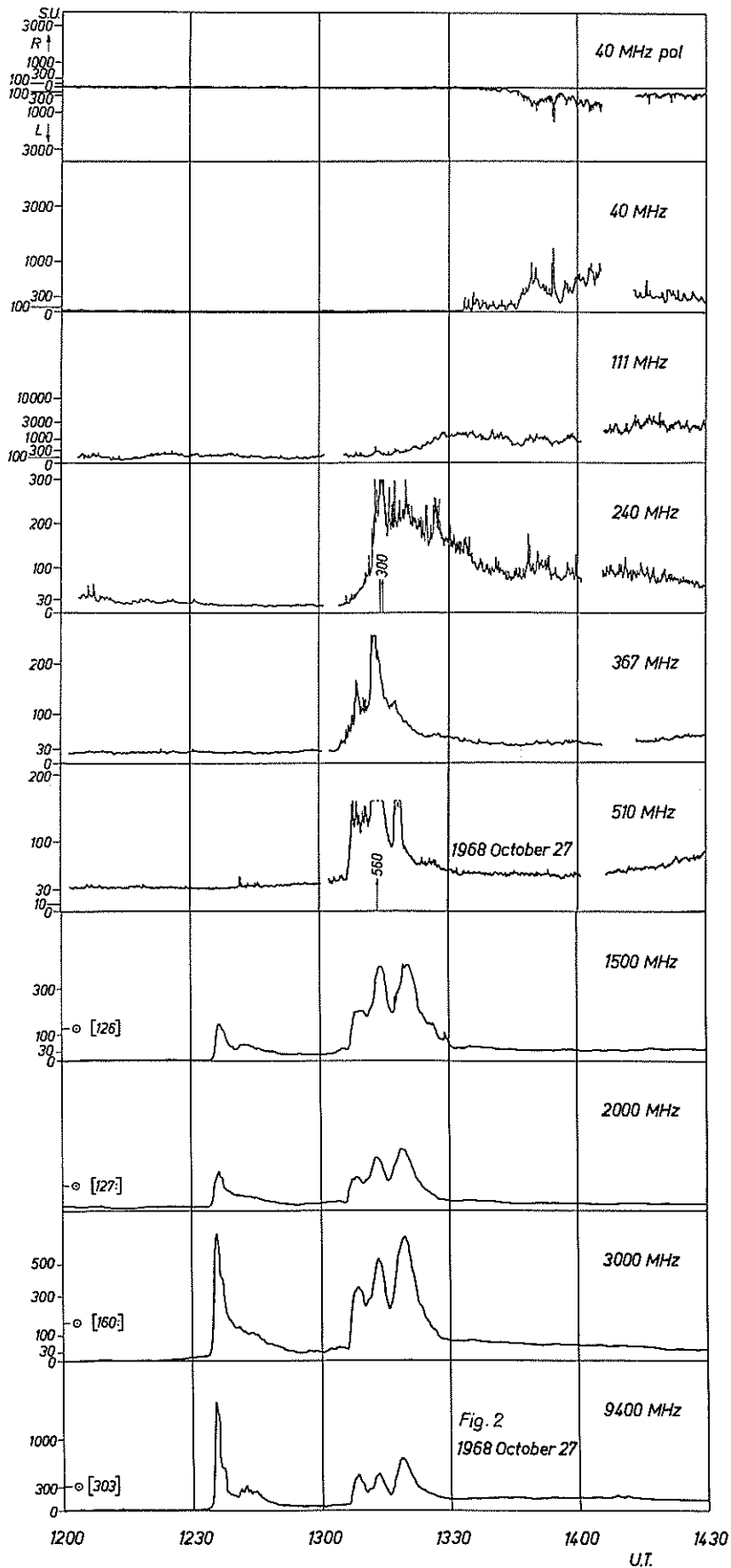


Fig. 2. Type IV burst observed at HHI October 27, 1968.

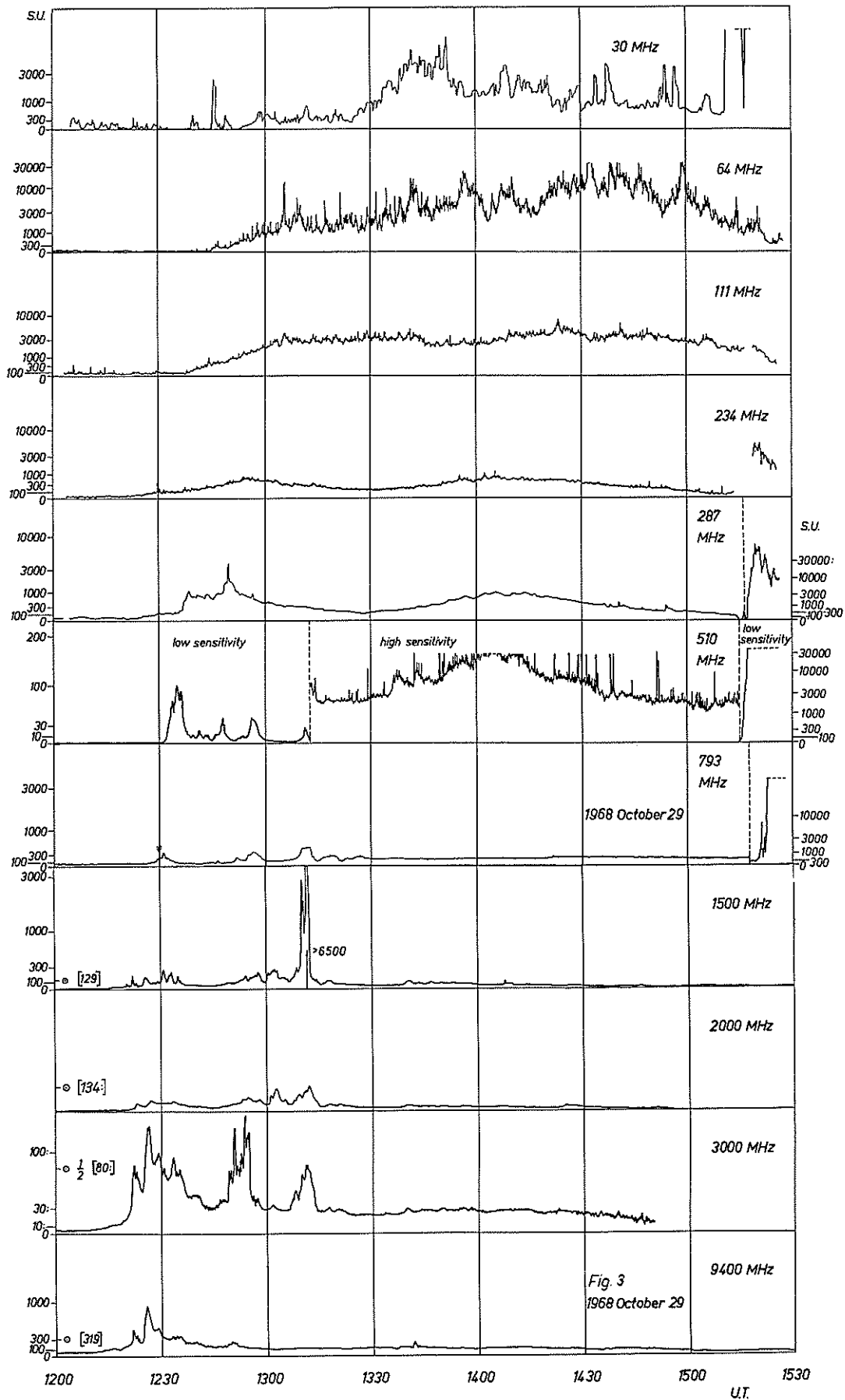


Fig. 3. Type IV burst observed at HHI October 29, 1968.

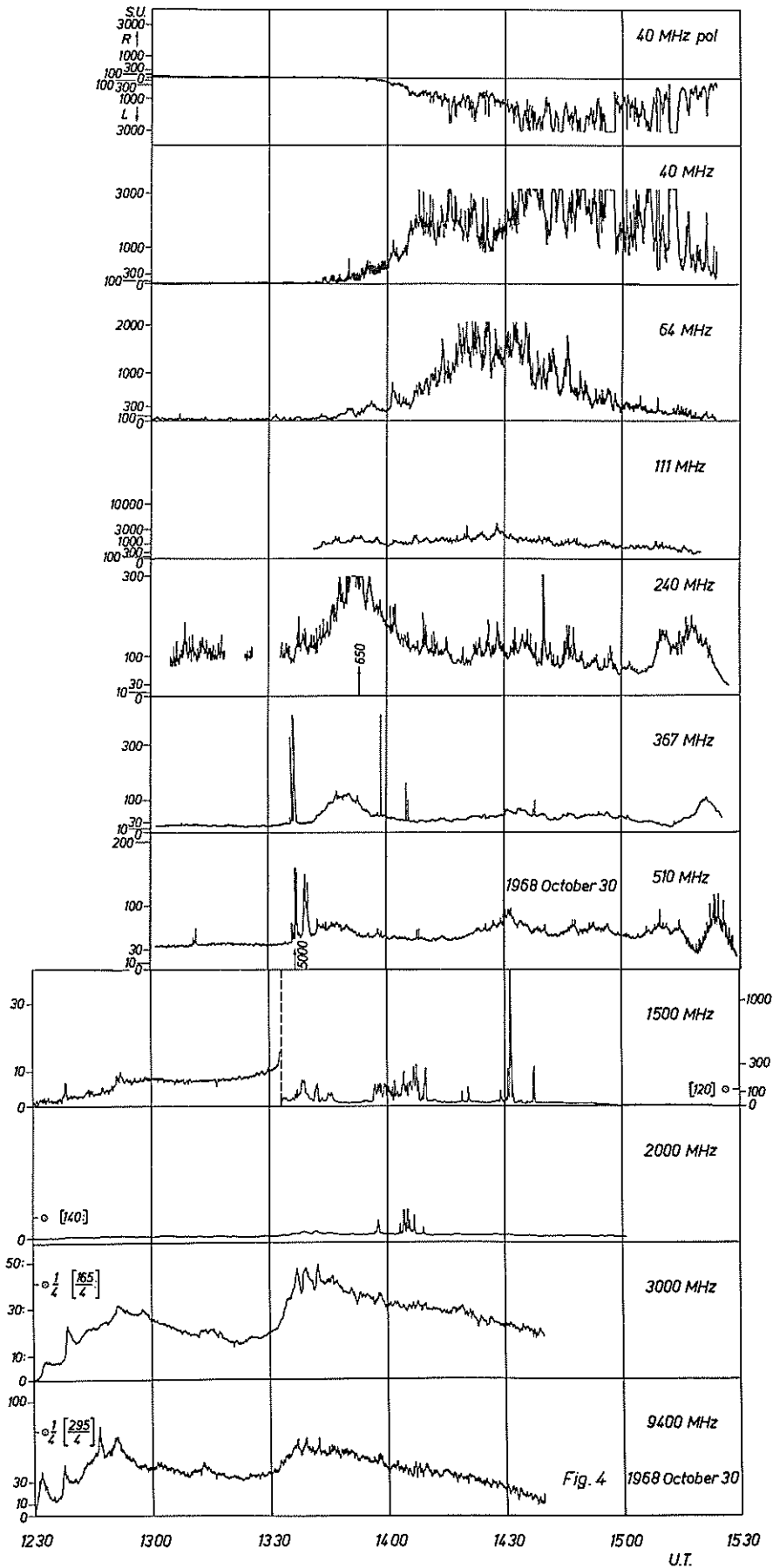


Fig. 4. Type IV burst observed at RHI October 30, 1968.

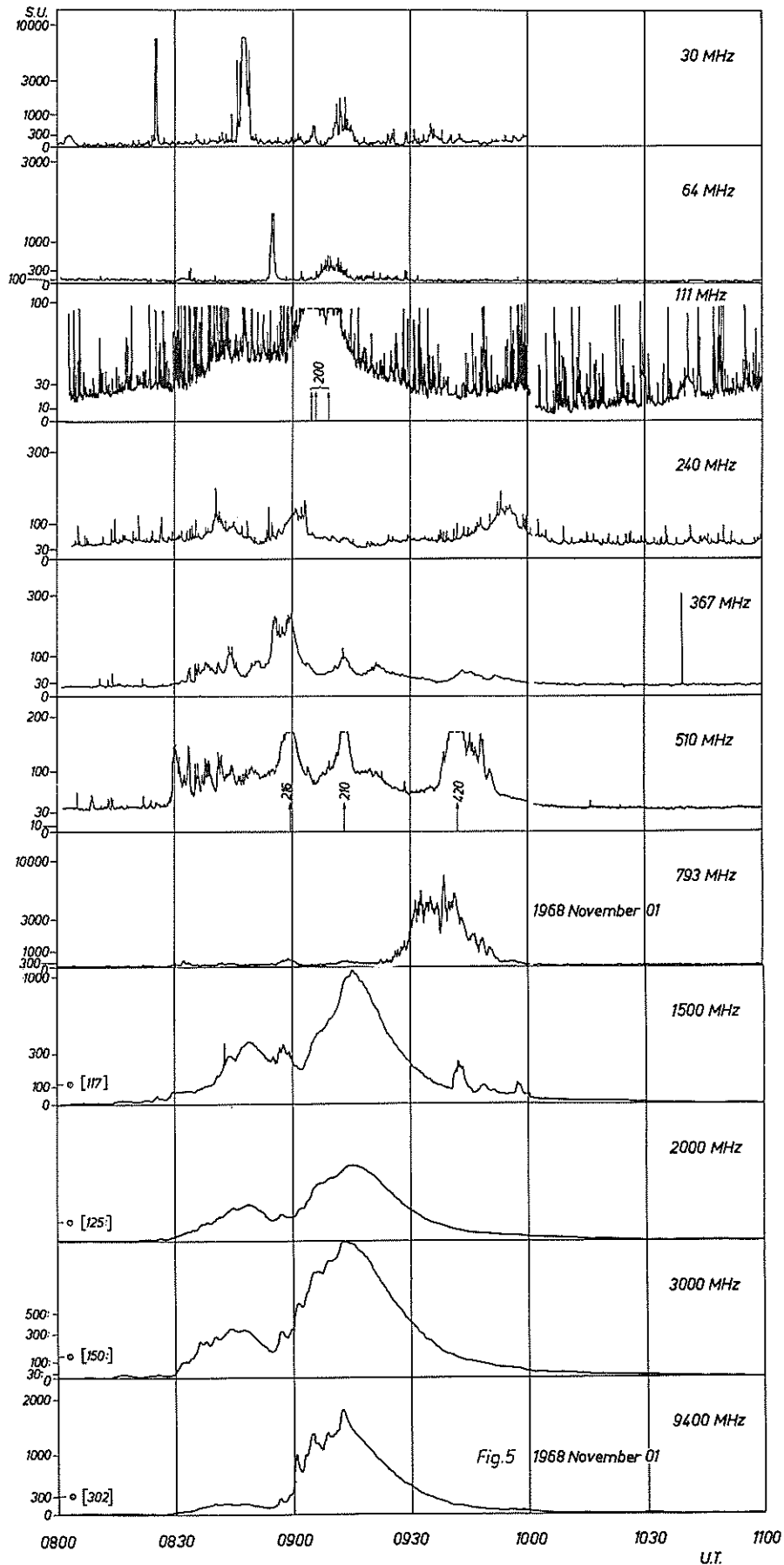


Fig. 5. Type IV burst observed at HHI November 1, 1968.

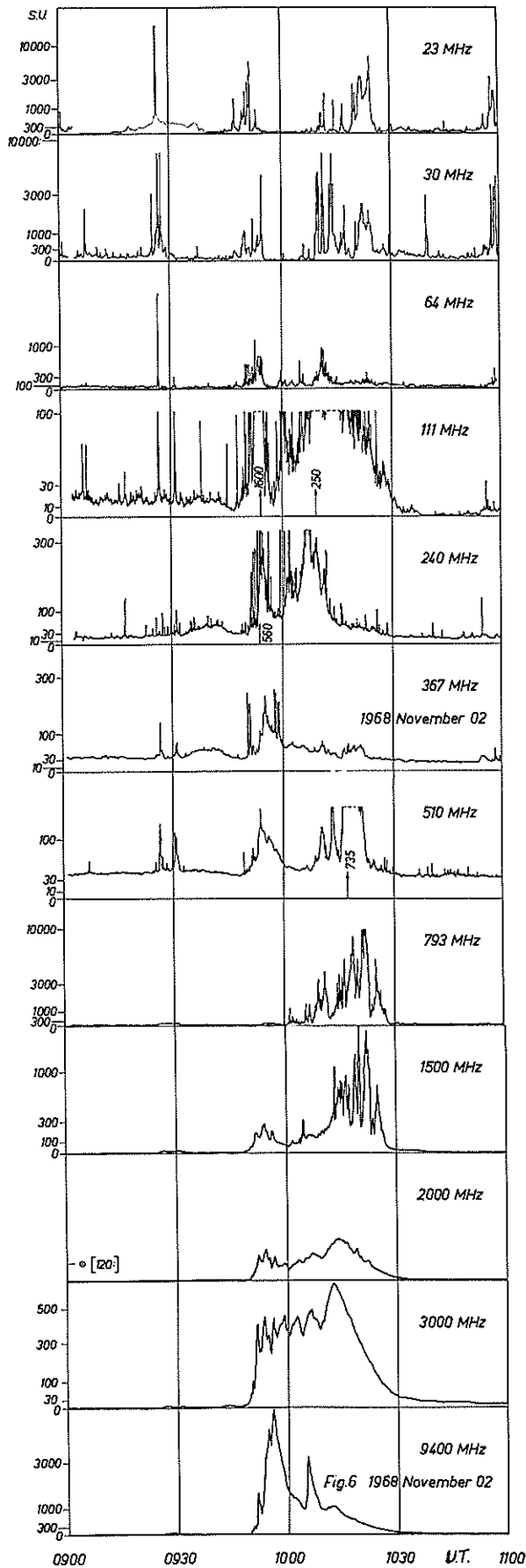


Fig. 6. Type IV burst observed at HHI November 2, 1968.

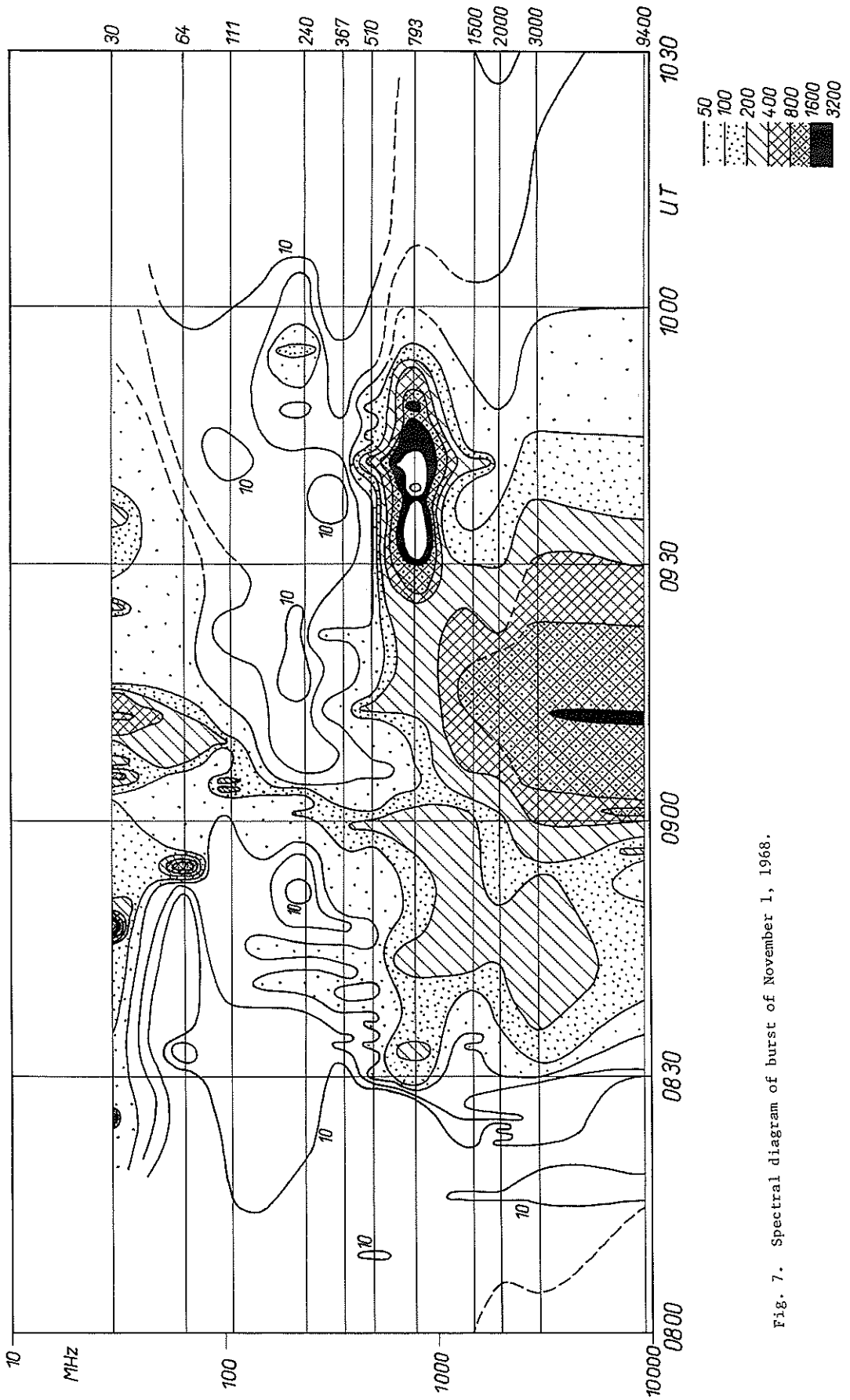


Fig. 7. Spectral diagram of burst of November 1, 1968.

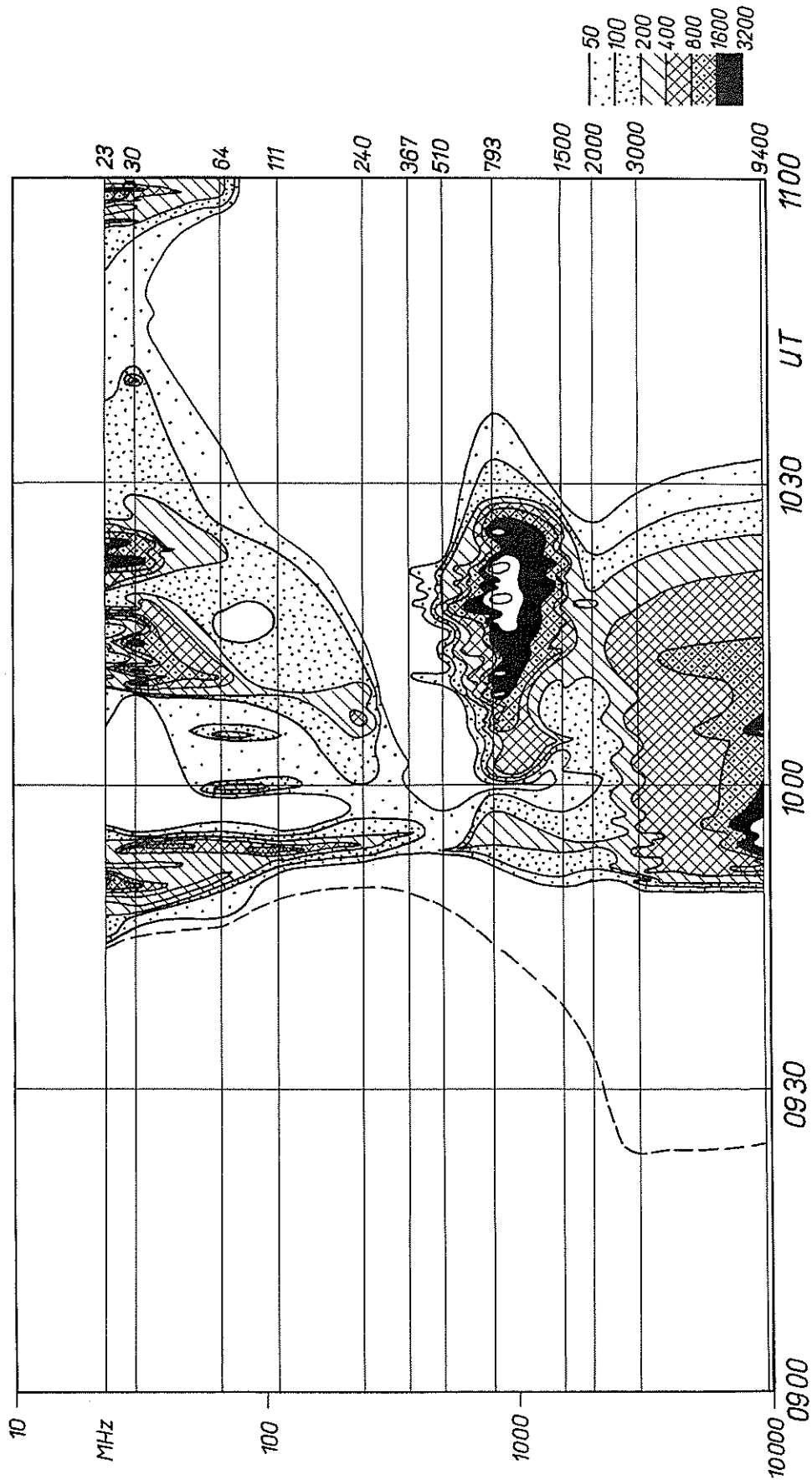


Fig. 8. Spectral diagram of burst of November 2, 1968.

"Solar Activity at  $\lambda = 1.6$  cm (19 GHz) During the Period  
27 October - 4 November 1968 and Its Relation to Proton Events"

by

D. L. Croom\* and R. J. Powell  
S.R.C. Radio and Space Research Station, Slough, Bucks., England

Introduction

The period from 27 October to 4 November 1968 was one of considerable activity in the southern hemisphere McMath plage 9740. The purpose of this note is to present and comment on the solar radio data obtained during this period at a wavelength of 1.6 cm at the Slough Solar Radio Observatory.

The 1.6 cm Events

The principal events at 1.6 cm were recorded on 29 October, 1 November and 2 November, and are shown in Figures 1-3. Two of these are particularly outstanding events. The 1 November burst is unusual because of its combination of relatively high intensity (1400 solar flux units peak increase,  $1 \text{ sfu} \equiv 10^{-22} \text{ Wm}^{-2} \text{ Hz}^{-1}$ ), extremely long duration (2-3 hours) and because at 1.6 cm it is extremely rare for a burst of this intensity to be non-impulsive, the time from start to maximum being about one hour.

On the other hand, the much more intense burst of 2 November (7400 sfu peak increase) reached its maximum within 7 minutes (a more usual value for large 1.6 cm bursts). Only once during the 2½ year period from July 1967 (when observations were started) until late 1969, has a more intense 1.6 cm burst been recorded at Slough, on 6 July 1968 [Croom and Powell, 1969].

Relation of the 1.6 cm Bursts to Solar Protons

One of the authors (DLC) is currently making an investigation of 1.6 cm solar radio bursts in relation to the occurrence of solar proton events. Whilst it is not the purpose of the current paper to discuss this work in detail it is already apparent that 1.6 cm bursts can be used as reasonably reliable indicators of the occurrence of such events provided that (a) the peak flux increase is >50% of the pre-burst solar flux level (the pre-burst level is usually the range 6-700 solar flux units), and (b) the burst enhancement is  $\geq 10\%$  of the pre-burst level for >5 minutes.

Table 1 lists the main cm-wavelength events for the period under discussion including all those which meet the above criteria, and all those which meet the multi-wavelength U-shaped spectra criteria developed by Castelli and Aarons [1969]. In order to get as complete coverage as possible it has been necessary in some cases to estimate the 1.6 cm data from 2.0 cm records made at the Sagamore Hill Observatory of the U. S. Air Force Cambridge Research Laboratories, Bedford, Mass., and from the 1.8 cm data of Tokyo Observatory.

Whether or not these radio criteria were accurate indicators of proton events or false alarms depends very much on the final analysis of this very complex sequence of solar events, since once one large proton event has begun it is often difficult to tell whether or not there were subsequent smaller proton events which were masked by the earlier one. However, in the final column an indication has been given of the main proton events as determined from the hourly-averaged particle data from the Explorer 34 satellite (1967-51A) as published in the U. S. Environmental Science Services Monthly "Solar-Geophysical Data".

It can be seen from Table 1 that there is only one difference between the "predictions" based on the two sets of radio criteria, namely the event of 29 October starting at about 1217. According to the multi-wavelength U-shaped spectra criteria this should not be a proton event, whereas according to the single wavelength 1.6 cm criteria it should be one. The Explorer 34 data shows that there was in fact a weak proton event starting at about 16-1700 hrs. UT. The flux in the 10-30 Mev range increased by a factor of about 6, but there was no detectable increase in the >30 Mev energy range.

Observations at 4.2 mm (71 GHz)

No events were recorded at 4.2 mm wavelength during this period. However, the radiometer klystron failed a few minutes before the largest 1.6 cm burst on 2 November.

\* Currently on leave of absence as NRC-OAR Senior Post-Doctoral Research Associate, AFCRL, L. G. Hanscom Field, Bedford, Mass. 01730.

TABLE 1 - List of the Main Events at Wavelengths Close to 1.6 cm  
for the Period 27 October - 4 November 1968

DATE	START (UT)	MAX (UT)	INTENSITY ( $10^{-22} \text{Wm}^{-2} \text{Hz}^{-1}$ )	MEETS U- CRITERIA FOR PROTON EVENT	MEETS 1.6 cm CRITERIA FOR PROTON EVENT	PROTON EVENTS
27 Oct	1234	1236	1400 (A)	YES	YES	?
27 Oct	1306	1318	415 (A)	NO	UNCERTAIN	?
29 Oct	1217	1227	466	NO	YES	10-30 Mev proton event (E)
29 Oct	1516	1522	262	NO	NO	?
30 Oct	2353	2411	940 (T)	YES	YES	10-30, 30-60 and >60 Mev proton event (E)
31 Oct	2239	2257	> 400 (T)	YES	YES	?
1 Nov	0800	0912	1400	YES	YES	10-30, 30-60 and >60 Mev proton event (E)
1 Nov	2003	2005	4180 (A)	YES	YES	?
2 Nov	0332	0333	370 (T)	NO	NO	?
2 Nov	0949	0956	7400	YES	YES	?
4 Nov	0514	0521	>2600 (T)	YES	YES	10-30, 30-60 and >60 Mev proton event (E)

Notes: (A) = AFCRL value for 15.4 GHz (2.0 cm)  
(T) = Tokyo Observatory value for 17 GHz (1.8 cm)  
(E) = Explorer 34 satellite data (ESSA "Solar-Geophysical Data")

REFERENCES

CROOM, D. L. and R. J. POWELL 1969

"Outstanding Solar Radio Burst at 4.2 mm", Nature, 221, 945.

CASTELLI, J. P. and J. AARONS

"Radio Burst Spectra and the Short Term Prediction of Solar Proton Events", to appear in Proceedings of AGARD Symposium on Ionospheric Forecasting, September 1969.

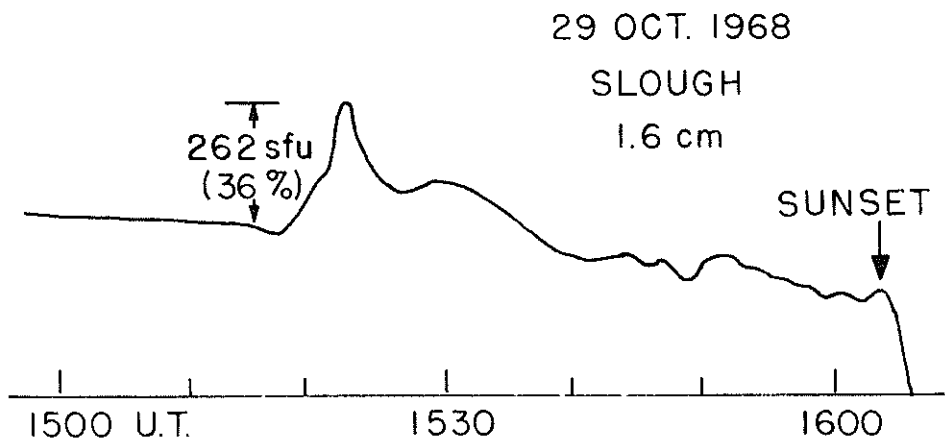
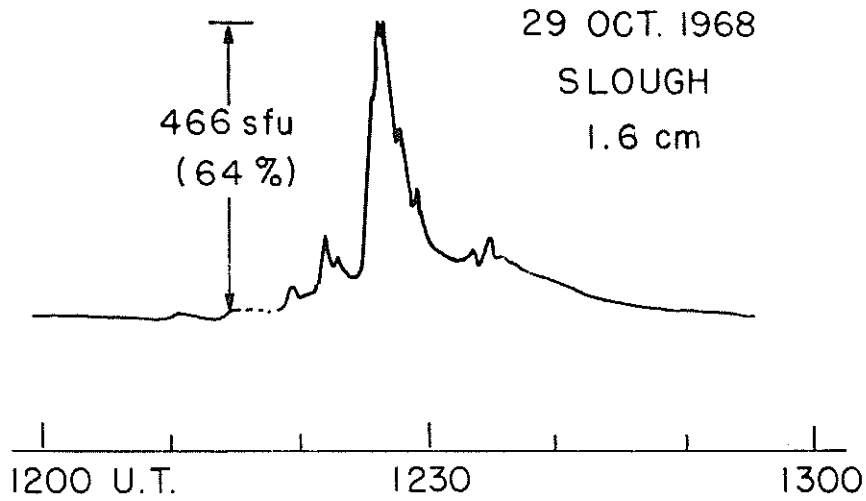


Fig. 1. 1.6 cm solar radio bursts of 29 October 1968.

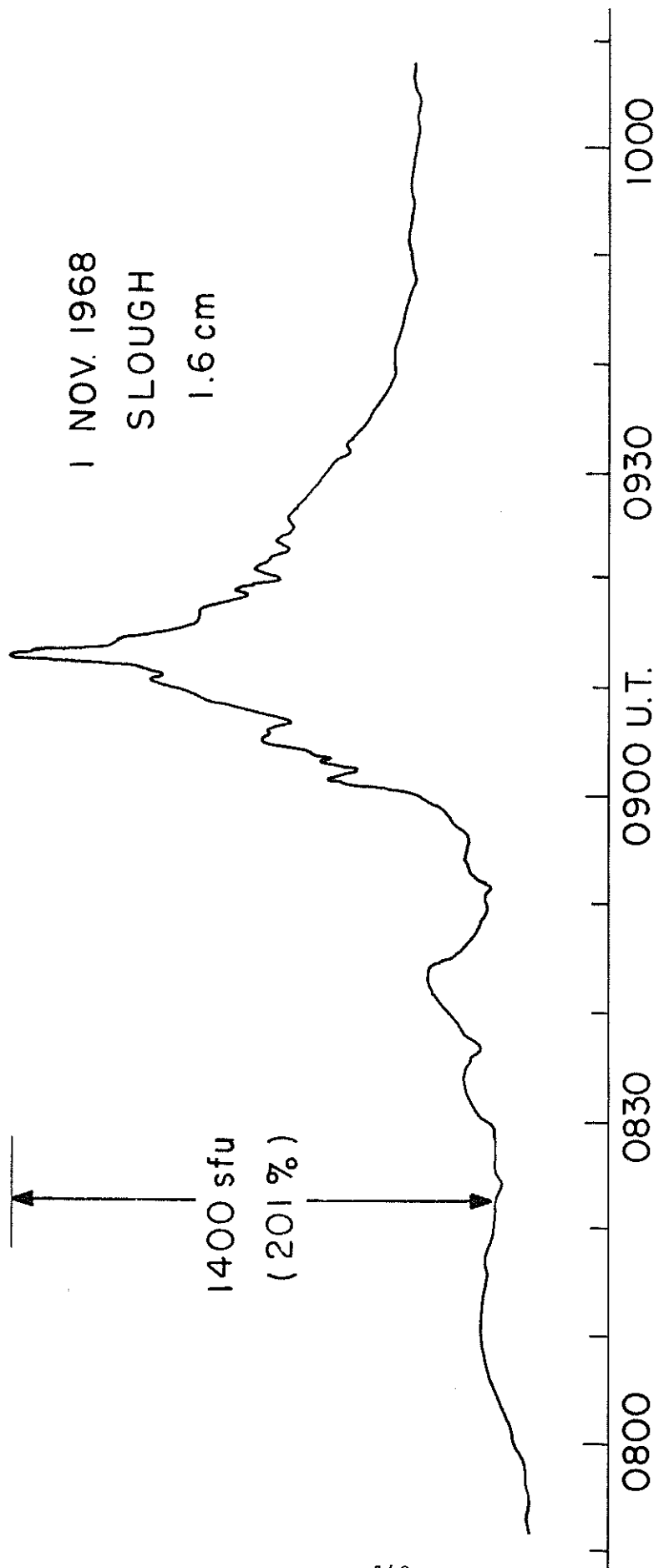


Fig. 2. The large 1.6 cm solar radio burst of 1 November 1968.

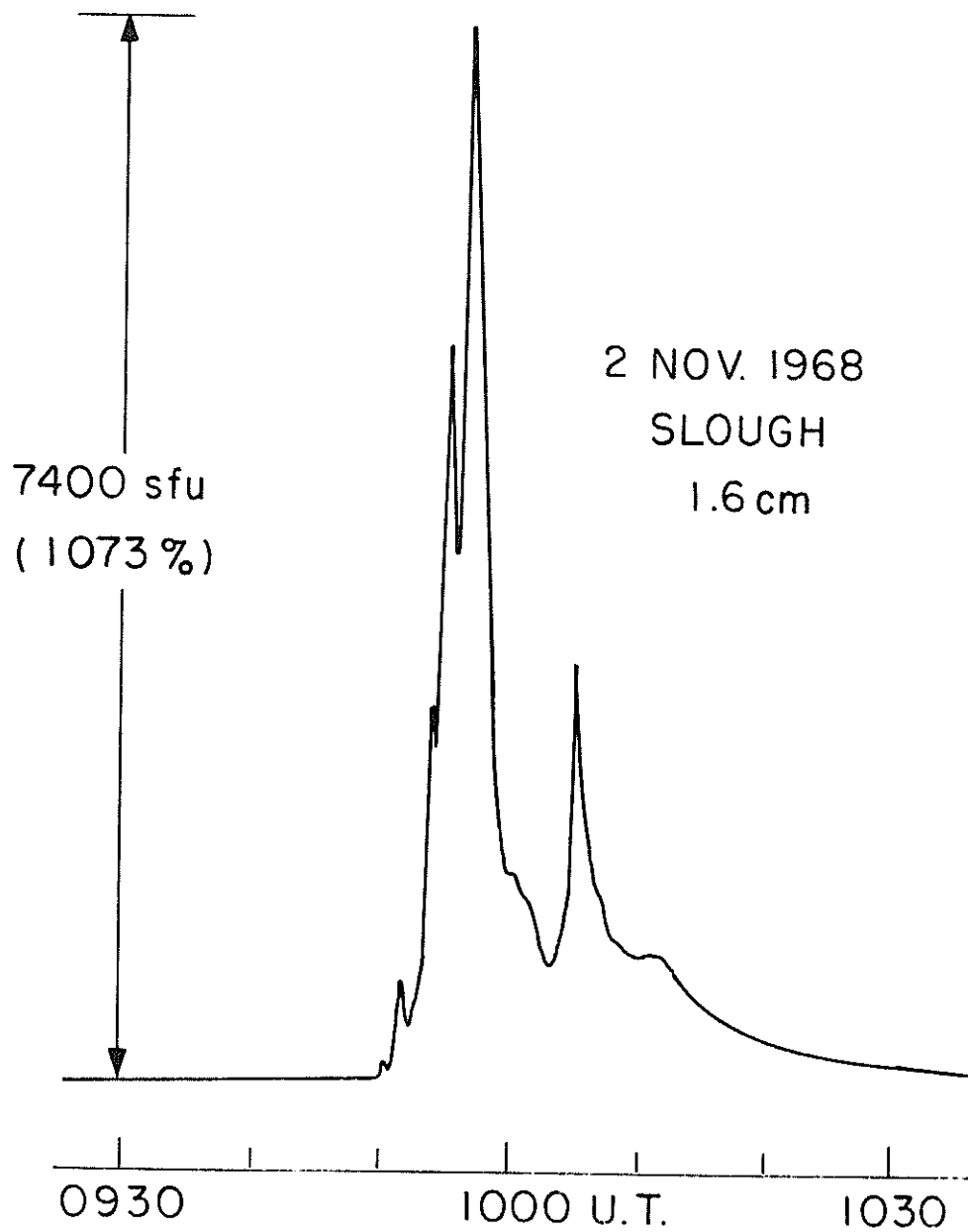


Fig. 3. The large 1.6 cm solar radio burst of 2 November 1968.

## UNUSUAL 1 TO 5 GHz SOLAR RADIO EMISSION OF 29 OCTOBER 1968

R. A. MENNELA AND J. H. REID  
Lockheed Electronics Company, Houston, Texas, U.S.A.

On 29 October 1968, solar activity produced one of the largest, if not the largest, burst of solar microwave radiation ever measured of 1.420 GHz. The activity occurred between 15:15-16:52 UT and provided peaks of  $379,000 \times 10^{-22} \text{ W m}^{-2} \text{ Hz}^{-1}$ ,  $5370 \times 10^{-22} \text{ W m}^{-2} \text{ Hz}^{-1}$ , and  $570 \text{ W m}^{-2} \text{ Hz}^{-1}$  at 1.420 GHz, 2.695 GHz, and 4.995 GHz, respectively. The solar radio emission appears to have originated from an active region which was just behind the west limb.

### INTRODUCTION

The radio telescope site located at the Manned Spacecraft Center in Houston is part of the Solar Particle Alert Network (SPAN) directed by NASA. The instrument uses crystal-mixer, Dicke-type radiometers with channels at 1.420 GHz, 2.695 GHz, and 4.995 GHz; the antenna is an eight-foot-diameter paraboloidal reflector equipped with a log-periodic feed. The IF amplifiers operate at 30 MHz, have a logarithmic response, and a bandwidth of 10 MHz. The entire system records a range of antenna temperatures from about 100 to about  $2 \times 10^6$  degrees. To extend the range further, the system employs a precision 3-dB attenuator in the feed-line from the antenna. While observing the undisturbed sun, the rms output fluctuations were approximately 15 °K, with a one-second integration time; this fluctuation level is equivalent to about 5 solar flux units. The response of the system permits measurement of changes in flux densities from about 5 to 450,000 solar flux units, without saturation of the receiver.

### CALIBRATION TECHNIQUES

Argon noise generators commonly used in radio astronomy as secondary reference sources for the calibration of radiometers provide temperatures of about 10,000 °K. Attenuators in series with an argon noise generator were used first to establish the response of the system up to the maximum capability of the noise generator. With a 3-dB attenuator in the antenna feed-line to reduce the received solar radiation by a factor of two, the upper limit of the argon noise generator calibration was established as approximately 5,000 solar flux

units, which was obviously quite inadequate for the range of expected solar radio activity. To extend the range further, without resorting to additional attenuators in the signal feed-line and without loss of sensitivity, a CW source and a new, solid-state, broad-band, microwave, noise source (Solitron RFN-30) were used as signal sources to establish the response of the receiver up to approximately 450,000 solar flux units. (The Solitron noise diode is a promising broad-band noise generator that may provide a satisfactory secondary source for solar microwave measurements. The device is small, simply constructed, requires only 28 volts to operate, and provides a noise temperature of over 300,000 °K, which is more than 30 times the temperature available from an argon noise source). The calibration of the extended receiver response was established by comparisons of the overlap between the outputs of the argon noise generator, the narrow-band continuous wave generators, and the Solitron noise source.

Precise measurements of absolute flux densities were not possible, due to uncertainties or unknowns in the antenna gain, losses in the radome, and losses in the RF front-end (feed covering, transmission lines, and coaxial switches, couplers, etc.). Uncertainties also exist in the precise determination of the argon generator output; furthermore, errors induced by possible argon noise generator mismatch in the fired condition (Pastori 1968) have not been determined. Total possible error, therefore, can be considerable so that the stated results must be considered as preliminary at this time. Estimates of total uncertainty are given as 1.5 dB at 1.420 GHz and 2.695 GHz and as much as 3 dB at 4.995 GHz.

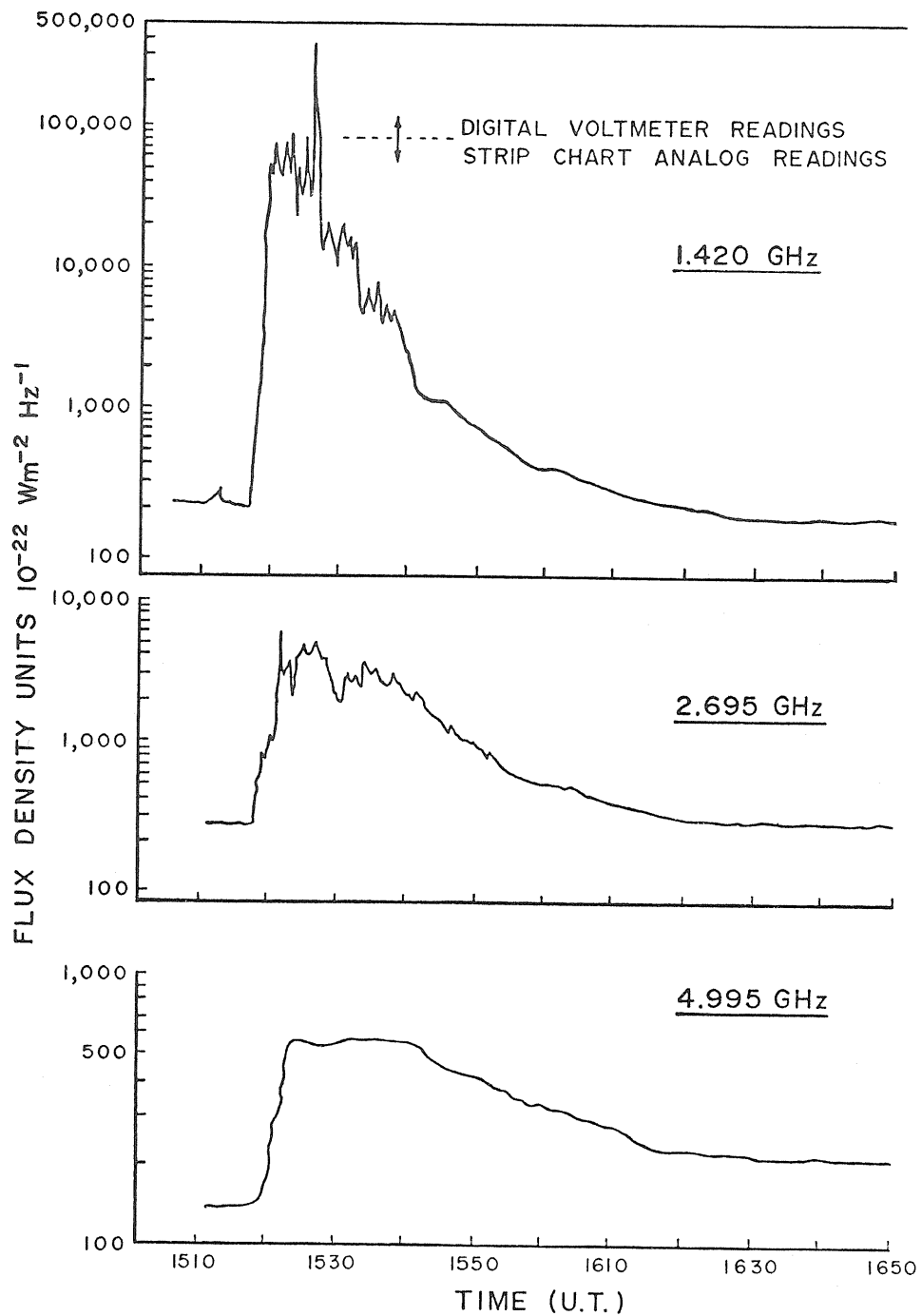


FIG. 1. Unusual solar radio burst of 29 October 1968

UNUSUAL 1 TO 5 GHz SOLAR RADIO EMISSION OF 29 OCTOBER 1968

OBSERVATIONS OF OCTOBER 29 1968

Table I and Figure 1 summarize the preliminary results of the observation of the significant solar burst that occurred between 15:15 and 16:50 UT of 29 October 1968. Unfortunately, the analog chart recorder was limited in range, so that the structure of the peak of the signal observed at 1.420 GHz was lost. However, digital voltmeter

readings of the radiometer output were read and tabulated during the event and were used to establish the peak values.

Great radio bursts have been reported previously by other observers that provided magnitudes of several thousands of flux units (Castelli *et al.* 1968). However, the larger magnitudes are generally associated with lower frequencies (600 MHz or

TABLE I  
Unusual Radio Burst of 29 October 1968

Frequency (GHz)	Start time (UT)	End time (UT)	Peak time (UT)	Maximum flux (Solar flux units)
1.420	15:15:00	16:31:30	15:25:00	379,000 $\pm$ 1.5 dB
2.695	15:16:30	16:37:00	15:20:30	5,370 $\pm$ 1.5 dB
4.995	15:17:00	16:52:00	15:23:00	570 $\pm$ 3 dB

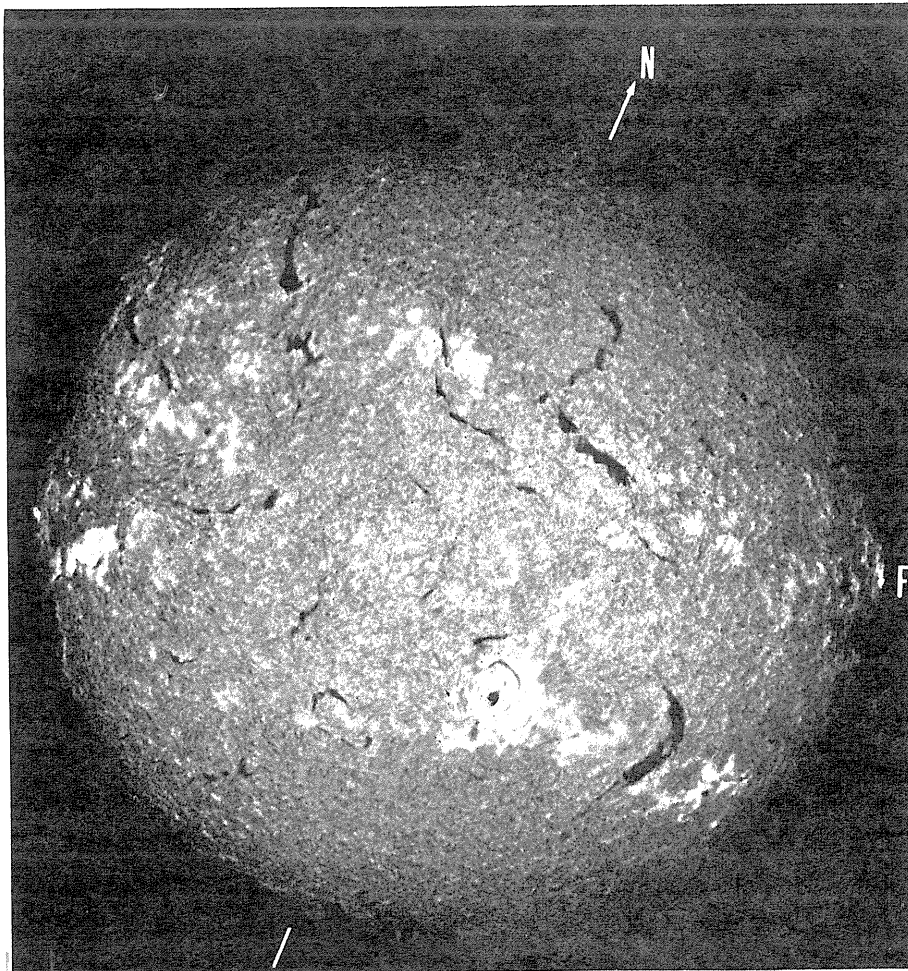


FIG. 2. H $\alpha$  photograph of the sun at 1518 UT on 29 October 1968 showing the Class SN flare, denoted by the letter F on the photograph at N15 W82.

below) and have obvious major solar activity associated with them. The burst reported here appears to be one of the largest, if not the largest, ever recorded at 1.420 GHz. The burst was also observed and recorded with an identical radio telescope at the SPAN site at the Canary Islands.

A large radio burst was observed earlier, from 13:07:00 to 13:15:00 UT on October 29, on the 1.420 GHz channel. This earlier burst yielded a maximum on the order of 10,000 flux units. However, the observation was degraded by multipath effects that are present when the elevation angle of the antenna is less than 15 degrees.

### OPTICAL OBSERVATIONS

Unfortunately, the optical telescope at Houston was being modified on the day of this radio burst, so that a local concurrent film record of solar H $\alpha$  activity was not available. However, the Boulder, Colorado, optical station of the SPAN system did have some observations at the time of the radio burst. These records show a small limb event at N15 W82, which started at 1515 UT and had a maximum at 1518 UT. Due to a film change there was no record between 1525 and 1545 UT. At the latter time, the region had returned to normal.

Figure 2 shows that on 29 October the solar disk was dominated by an extremely complex region at S14 W14, which was the site of considerable activity. At the time of the great radio burst, however, it showed little flare activity, and the limb event, mentioned previously, was the only time-

related optical event. Although small in size, with a measured area of 0.4 square degrees, it is probably only a portion of a major flare associated with the region that crossed the West limb on October 28 and which had a central meridian passage about October 23. This region also exhibited considerable activity during its passage across the disk and it is planned to study these two major regions and their radio emission in some detail.

The fact that the centimeter burst had a much lower flux provides further evidence for a behind-the-limb event, since the source would then be partially occulted by the sun itself. Another small limb-flare in the same position (N15 W82) occurred at 1704 UT with a maximum at 1706 UT, and the radio records show a spike only on the 1.420 GHz channel. The other major active region on the disk produced a Class 3 flare on October 30, but the radio spectrum was different from that on October 29. Preliminary data for the October 30 burst from the SPAN station at Carnarvon, Australia, indicate a maximum flux of 1787 flux units on the 2.695 GHz channel, with the lowest flux on the 1.420 GHz channel. At the time of writing, we have been unable to associate the burst at 1307 UT on October 29 with a specific flare event but will attempt to do so in the more detailed study.

### REFERENCES

- Castelli, J. P., Aarons, J., and Michaels, G. A., 1968, *Astrophys. J.*, 153, 272.  
 Pastori, W. E. 1968, *Microwaves*, 7, 58.

Received 17 March 1969

"Comments on Solar Circumstances at the Time of the  
Great Radio Frequency Burst, 1968 October 29, 1516 UT"

by

Helen W. Dodson and E. Ruth Hedeman  
McMath-Hulbert Observatory  
The University of Michigan

In the interval October 27 to early November 1968, two important centers of activity were crossing the solar disk. In the north, at latitude  $17^\circ$ , McMath plage 9735 (CMP, October 23.9) approached and traversed the west limb. In the south, at latitude  $15^\circ$ , McMath plage 9740 crossed the central meridian on October 28. Both of these regions were flare-rich, but in the northern region (9735) major flaring had stopped before October 27. Flaring in the southern region (9740) was at a maximum from October 27 - November 3.

Nine flares of importance  $\geq 2$  were observed between October 27 and November 3. Eight of them were in the southern center of activity (plage 9740). (The remaining flare at 1631 UT on November 2 was one of the rare major flares in a spotless plage.) All of the flares in plage 9740 were accompanied by major ionospheric disturbances and by enhancements at radio frequencies with time patterns in accord with past experience. (See Table 1.)

In addition to the phenomena clearly associated in time with observed major flares, Table 1 includes, at radio frequencies, another event of great magnitude. It was the strong, long-enduring burst that began on October 29 at 1516 UT and lasted for at least 80 minutes. This event included known enhancements in the radio spectrum from 184 to 15,400 MHz. According to the Ottawa records, the burst reached a peak flux of  $3900 \times 10^{-22} \text{ Wm}^{-2} \text{ Hz}^{-1}$  at 2800 MHz. At AFCRL, a maximum as great as 260,000 in the same units was attained at 606 MHz. It is of special interest that ionospheric disturbances have not been reported for the time of this major radio frequency burst.

With what solar phenomenon should this great radio frequency event at 1516 on October 29 be associated? Clouds at the time of the burst prevented observations at the McMath-Hulbert Observatory so we turn to the reports from other optical observers. Three reports cover the time in question.

- (a) San Miguel considered the flare that began at 1232 in Region 9740 still to be in progress at 1516 UT. Their time report for the flare reads <1230 - >1630 UT.
- (b) Sacramento Peak reported:  
Sn 1515 - 1558 S14 W19 (Region 9740)  
In 1558 - 1619 S14 W11 (Region 9740)
- (c) Boulder reported:  
Sn 1515 - >1525 N15 W82 (Region 9735)  
In 1558 - 1628 S13 W13 (Region 9740)

It is clear that the above reports are not in complete agreement. Nevertheless, they do show that flaring, albeit minor, was observed in both of the two important centers of activity (9735 and 9740) during the time of the great radio burst. Since region 9735 was traversing the west limb on October 29, a flare in that region could have been observed only partially and its importance underestimated.

In an attempt to gain insight into the event at 1516 on October 29, we have brought together in Table 2 solar and ionospheric data for all bursts at  $\sim 10$  cm. from 1947-1969 (October) for which the peak flux is known to have been  $\geq 3000 \times 10^{-22} \text{ Wm}^{-2} \text{ Hz}^{-1}$ . There were only 28 such cases in the 22-year interval. Except for the event on 1968 October 29, there is general accord in the phenomena and circumstances associated with these great 10 cm. bursts. Major short-wave fades (SWF's) accompanied the bursts. The associated H $\alpha$  flares, except when near the limb, were evaluated as important events. When the time information is adequate, it appears that the great 10 cm. bursts began during the early phases of the flares and SWF's.

Only the 1968 October 29 event introduces a conspicuous departure from the above patterns. If it is assumed that this great radio event is similar in kind to its predecessors then it probably should be associated with a flare in region 9735, then traversing the west limb. This identification already has been suggested by Mennella and Reid [1969]. If this is the case, the H $\alpha$  flare can be assumed to have been observed only in part and its importance therefore underestimated. An ionospheric disturbance was not in progress perhaps because the ionizing radiation that causes such effects was effectively occulted by the solar limb. The ionizing radiation presumably emitted during this event would have been confined to levels in the solar atmosphere that were lower than those associated with the great radio frequency emission. It should be noted that some flares beyond the limb are associated with ionospheric disturbances. See events No. 1 and 28 in Table 2, and the report by Badillo and Salcedo [1969].

TABLE 1

FLARES OF IMPORTANCE  $\geq 2$ , 1968 OCT. 27 - NOV. 3, AND ASSOCIATED IONOSPHERIC AND  $\sim 10$  Cm. EVENTS

Date 1968	H $\alpha$ Flare				Short Wave Fade			$\sim 10$ Cm. Emission				
	Start UT	Max. UT	Imp.	Position	Start UT	Duration	Type, Imp.	Start UT	Duration	Type <sup>(a)</sup>	Peak Flux <sup>(b)</sup>	Freq. <sup>(c)</sup> MHz
Oct. 27	<u>12<sup>h</sup>32<sup>m</sup></u>	{ 12 <sup>h</sup> 37 <sup>m</sup> 13 22	2n	S18 E17	12 <sup>h</sup> 36 <sup>m</sup>	-	S/3	12 <sup>h</sup> 32 <sup>m</sup> 12 32	4 <sup>h</sup> 50 <sup>m</sup> 20	S 3AF Gr.Burst	74 570	2800 "
Oct. 29	<12 22		{ 12 23 12 34	2b	S16 W12	12 18	1 <sup>h</sup> 10 <sup>m</sup>	S1/3-	12 19	1 03	C	215
	-	-	-	-	-	-	-	15 16	1 20	Gr.Burst	3900	2800
Oct. 30	<12 35	{ 12 52 13 46	2b	S18 W26	12 43	2 10	S/3	12 35 12 35 13 25	4 35 50 3 45	S 3AF Burst Burst	50 32 50	2800 " "
Oct. 30	<u>23 40</u>		{ 23 58 24 12	3b	S14 W37	23 43	3 18	S1/2+	23 43	*	C	75*
Oct. 31	<u>22 29</u>	{ 22 44 23 02	2b	S14 W49	22 46	$\sim 47$	S1/1+	22 23 22 47	>1 25 28	S 3AF Gr.Burst	3 890	2800 2695(P)
Nov. 1	<u>08 14</u>		{ 08 43 09 03	2n	S16 W47	08 28	1 44	G/2+	08 00 08 29 10 08	29 38 1 45	Precur. Gr.Burst p.b.i.	35 2325 70
Nov. 2	<u>09 40</u>	{ 09 57 10 12	2b	S15 W65	09 49	$\sim 1$	S1/3-	09 25 09 49 10 40	24 51 43	Precur. C p.b.i.	16 925 15	3000(N) " "
Nov. 2	<u>16 31</u>		{ 16 59 17 08	2n	N20 E26	-	-	-	16 30	3 25	S 3	12
Nov. 3	<u>12 33</u>	12 37	2b	S19 W82	12 37	13	S/1	12 33	8	C	77	2695(S)

(a) S = simple burst; C = complex burst; other designations follow conventions in reports from Ottawa and Penticton.

(b) In units of  $10^{-22} \text{Wm}^{-2} \text{Hz}^{-1}$

(c) (S) = Sagamore Hill; (P) = Penticton; (N) = Nera.

\* Observed in sunset.

The only other event that we know about for which the circumstances somewhat resemble those on October 29 at 1516 UT is the great radio frequency burst on 1967 February 5 at 1255 UT, and it too may have been associated with a flare beyond the limb. On this date, a burst at 606 MHz reached a peak value of  $80,000 \times 10^{-22} \text{Wm}^{-2} \text{Hz}^{-1}$  and again there was the unusual circumstance of no SWF in time association with a radio frequency burst of this magnitude. For the time of this burst, flare information is incomplete and no flare is known. However, on February 5, 1967, a region suspected of major activity on the invisible hemisphere [Dodson & Hedeman, 1969] was just one day beyond the east limb. It is known to have been the site of major flare-activity during its transit of the east limb in early February. Thus both the 1967 February 5 and 1968 October 29 bursts may represent radio frequency events with flares so far beyond the limb that associated ionizing radiation could not reach the earth.

If, on the other hand, it is thought that the great burst of 1516 UT on October 29, 1968 should be associated with phenomena in region 9740, the currently great flaring center at  $S16^\circ W12^\circ$ , it is probable that the burst, or the solar circumstances accompanying it, differed significantly from those at the times of all of the other great  $\sim 10$  centimeter bursts known to have occurred since 1947. (See Table 2.) The H $\alpha$  event in region 9740 at the beginning of the great October 29 burst was only a subflare. Towards the end of the burst, enhanced H $\alpha$  emission increased and the flare was then evaluated (by Sacramento Peak and Boulder) as of importance 1 according to the ESSA "Solar-Geophysical Data" Bulletins. The ionosphere was not disturbed and solar X-rays (2-12 Å) as great as 4 times the quiet sun were not observed.

TABLE 2

GREAT CENTIMETER BURSTS ( $\geq 3000 \times 10^{-22} \text{Wm}^{-2} \text{Hz}^{-1}$ ), 1947-1969, AND ASSOCIATED FLARE AND IONOSPHERIC DATA

No.	Date	$\sim 10 \text{cm. Burst}$				H $\alpha$ Flare				Short Wave Fade		
		Start U.T.	Duration	Peak(a) Flux	Freq. MHz	Start U.T.	Max. U.T.	Imp.	Position	Time (U.T.) Start	End	Type Imp.
1.	1947 Apr. 15	17 <sup>h</sup> 26 <sup>m</sup>	>3 <sup>h</sup> 50 <sup>m</sup>	>5,200	2800	<16 17	-	2	S37>W90	14 <sup>h</sup> 47 <sup>m</sup> - 22 <sup>h</sup> 30 <sup>m</sup>		S/3+ <sup>(b)</sup>
2.	1956 Feb. 23	03 33	50 <sup>m</sup>	>4,700	3000	<03 34	-	3	N23 W80	03 30 - 06 10		S/3+ <sup>(b)</sup>
3.	1957 Apr. 17	20 06	1 <sup>h</sup> 19 <sup>m</sup>	6,000	2800	<22 20	-	1+	N27 E69	19 37 - 22 20		S1/3+
4.	1957 Aug. 31	13 01	1 <sup>h</sup> 05 <sup>m</sup>	3,900	2800	12 57	13 12	3	N25 W03	13 03 - 16 47		S/3+
5.	1957 Oct. 20	16 44	51 <sup>m</sup>	4,000	2800	16 37	16 42	-	S26 W45	16 39 - 19 15		S/3+
						16 44	16 47	3+	S26 W35			
6.	1958 July 7	00 50	1 <sup>h</sup> 40 <sup>m</sup>	3,770	3000	00 20	01 10	3+	N25 W08	00 25 - 02 30		S1/3
7.	1958 Aug. 16	04 34	1 <sup>h</sup> 10 <sup>m</sup>	5,030	3000	04 33	04 40	3+	S14 W50	04 32 - 07 20		S/3+
8.	1958 Aug. 26	00 05	50 <sup>m</sup>	5,050	3750	00 05	00 27	3	N20 W54	00 10 - 04 10		S1/3+
9.	1959 July 10	02 06	$\sim 40^m$	6,300	3750	02 06	02 30	3+	N20 E60	02 00 - 05 10		S1/3+
10.	1959 July 14	03 30	1 <sup>h</sup> 40 <sup>m</sup>	6,000	3750	03 25	03 49	3+	N17 E04	03 28 - 06 28		S/3+
11.	1959 July 16	21 18	>3 <sup>h</sup>	6,500	2800	21 14	21 32	3+	N16 W31	21 18 - 24 15		S/3+
12.	1959 Sept. 3	04 20	2 <sup>m</sup>	6,850	3000	04 21	04 23	1	N25 W86	04 22 - 04 42		S/3
13.	1960 Mar. 29	06 55	52 <sup>m</sup>	8,250	3750	06 50	07 10	2+	N12 E30	06 52 - 08 53		S/3+
14.	1960 Apr. 5	01 40	1 <sup>h</sup> 30 <sup>m</sup>	6,000	3750	<02 15	02 45	2	N12 W63	01 40 - 04 47		S1/3+
15.	1960 May 13	05 17	1 <sup>h</sup> 45 <sup>m</sup>	3,750	3750	05 19	05 32	3	N30 W67	05 12 - 08 53		S/3+
16.	1960 June 1	08 31	60 <sup>m</sup>	3,100	2980	08 23	09 00	3+	N29 E46	08 37 - 09 57		S1/3
17.	1960 Sept. 3	00 39	1 <sup>h</sup> 25 <sup>m</sup>	12,000	3750	00 37	01 08	2+	N18 E88	00 45 - 02 51		S1/3+
18.	1960 Nov. 11	03 15	1 <sup>h</sup> 55 <sup>m</sup>	3,450	3750	03 05	03 40	2	N28 E12	03 11 - 06 16		S/3+
19.	1960 Nov. 12	13 20	5 <sup>h</sup> 40 <sup>m</sup>	5,500	2800	13 15	13 30	3+	N27 W04	13 26 - 16 00		S/3+
20.	1960 Nov. 14	02 58	2 <sup>h</sup> 20 <sup>m</sup>	4,300	3750	02 46	03 04	2+	N27 W20	03 00 - 05 00		S1/3
21.	1960 Nov. 15	02 19	1 <sup>h</sup> 20 <sup>m</sup>	11,600	3750	02 07	02 21	3	N25 W35	02 17 - 06 30		S/3+
22.	1961 July 12	10 18	1 <sup>h</sup> 27 <sup>m</sup>	4,100	2980	10 00	10 25	3	S07 E23	10 23 - 12 00		S/3
23.	1963 Sept. 15	00 15	1 <sup>h</sup> 30 <sup>m</sup>	8,080	3750	00 15	00 42	2	N15 E75	00 15 - 03 15		S/3+
24.	1963 Sept. 20 <sup>c)</sup>	25 00	45 <sup>m</sup>	5,350	3750	23 14	24 03	2	N10 W09	23 51 - 27 25		S/3
						23 51						
25.	1966 July 7	00 26	1 <sup>h</sup> 54 <sup>m</sup>	4,730	3750	00 25	00 40	2b	N35 W48	00 25 - 03 29		S/3
26.	1967 May 23	19 36	1 <sup>h</sup> 13 <sup>m</sup>	8,000	2800	18 35	18 44	2b	N28 E26	18 34 - 22 30		S/3+
						19 32	19 47	3b				
27.	1968 Oct. 29	15 16	1 <sup>h</sup> 20 <sup>m</sup>	3,900	2800	15 15 <sup>d)</sup>	-	Sn	S14 W19	No ionospheric disturbance reported.		
						15 15 <sup>d)</sup>	-	Sn	N15 W82			
28.	1969 Mar. 30	02 47	1 <sup>h</sup> 30 <sup>m</sup>	32,000	3750	>02 49(d)	?	-Sb	N09 E50	02 48 - 05 45		S/2-
						>03 32(d)(e)?		-In	N19 W90			

(a) In units of  $10^{-22} \text{Wm}^{-2} \text{Hz}^{-1}$ .

(b) Importance is evaluated on basis of reported residual intensity and duration.

(c) The observations cover September 20 and 21.

(d) Event reported by only one observatory.

(e) With great eruptive prominence.

For the radio burst itself, there is some evidence that it may have been "different" from other great bursts. Many great radio bursts are observed first at high frequencies and then, somewhat later, at lower frequencies. They thus represent outward-moving phenomena. If the reported starting times for the great burst on October 29, 1968 are taken literally, a reverse relationship is shown. For frequencies between 328 and 3000 MHz the burst began between 1515.6 and 1516.0 UT but for higher frequencies, the starting times were later, 1516.7 - 1517.5 UT. If these time differences are significant, they suggest a rapidly descending feature, perhaps a consequence of events that began earlier with a major flare at 1222 UT in region 9740.

It is possible that specialists in radio frequency phenomena can distinguish between the alternatives suggested by the ambiguous optical solar circumstances on October 29, 1968. On the other hand, the solar events on October 29 may have been very complex and may have involved both region 9735 and 9740, as is suggested by the concomitant optical events. Such solar complexity recently has been demonstrated by the radio heliograms obtained by Wild, *et al.* [1968] and Kai, *et al.* [1968] at CSIRO, Sydney and perhaps cannot be ruled out in this case.

## REFERENCES

- BADILLO, V. L. and  
J. E. SALCEDO 1969 Nature, 224, 503.
- DODSON, H. W. and  
E. R. HEDEMAN 1969 "Solar Circumstances at the Time of the Cosmic Ray  
Increase on January 28, 1967," Solar Physics, 9, 278-295.
- KAI, K.,  
D. J. McLEAN,  
W. J. PAYTEN,  
K. V. SHERIDAN and  
J. P. WILD 1968 Proceedings of the Astronomical Society of Australia,  
1, 79.
- MENNELLA, R. A. and  
J. H. REID 1969 Astrophysical Letters, 3, 129.
- WILD, J. P.,  
K. V. SHERIDAN AND  
K. KAI 1968' Nature, 218, 536.

Commonwealth of Australia  
 COMMONWEALTH SCIENTIFIC AND INDUSTRIAL RESEARCH ORGANIZATION  
 Reprinted from  
*Proceedings of the Astronomical Society of Australia*  
 Volume 1, Number 5, pages 191-192, March 1969

## Movement and Structure in a Complex Solar Outburst at 80 MHz

N. R. LABRUM

*Division of Radiophysics, CSIRO, Sydney*

On 1968 October 30 a large solar flare (importance 3B to 4B) began at approximately 23<sup>h</sup>42<sup>m</sup> U.T. We present here a preliminary account of the associated radio emission.

### OBSERVATIONS

Figure 1\* shows the dynamic spectrum in the range 10-200 MHz and the solar flux density at 80 MHz for the radio event, from about 4 min after the listed starting time of the optical flare. A strong noise storm, associated with the active region which produced the flare, had been in progress for some days; it began to increase rapidly in intensity and area at about 23<sup>h</sup>50<sup>m</sup>, and its radiation was the dominant component at 80 MHz for most of the period shown in Figure 1. A succession of rather weak fast-drift type III bursts began about 2 min after the optical flare; these were followed by a pair of type II bursts, apparently harmonically related, and both showing a split-band doublet structure. Only the second harmonic extended as high as 80 MHz in frequency. Finally, a

assume a height of about 0.6  $R_{\odot}$  above the photosphere—the usual 80 MHz plasma level over an active region). The later development of this source took place directly above the flare. Both the original noise storm and its later extension showed strong left-handed circular polarization; this corresponds to ordinary-mode propagation for the magnetic field of the leading sunspot. The type II and type III emission, on the other hand, had no detectable polarization.

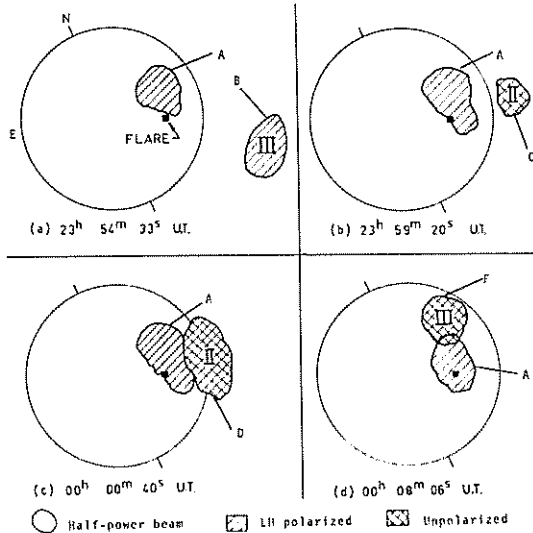


Figure 2. Positions of noise storm and sources of type II and type III bursts.

storm of some hundreds of very intense type III bursts began 25 min after the flare, at about 00<sup>h</sup>07<sup>m</sup>.

The positions of these sources are shown in Figure 2. The noise storm A was initially located over a part of the active region slightly to the north of the flare site (if we

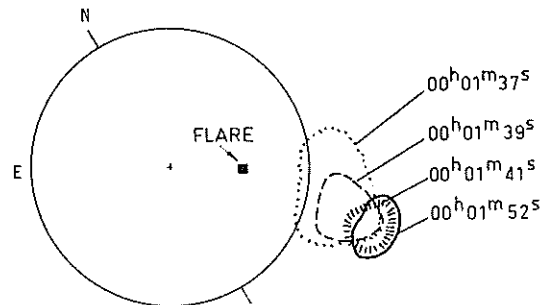


Figure 3. Example of rapid movement of a radio source in the flare region.

For about 5 min after the time of occurrence of the type II bursts there was evidence of rapid and chaotic movement in the corona above the flare. The spectrum contains a number of faint, rather diffuse fast-drift features, while the second-by-second heliograms reveal small sources moving or expanding, generally outwards from the solar limb. An example is the 'jet' shown in Figure 3. This spread outwards a distance of 70 000 to 100 000 km (the exact value depends on whether movement is assumed to be radial from the Sun or transverse to the line of sight) in about 4 s, then contracted to a stationary source which persisted for some minutes.

At about the same time a faint, very extended source began to develop near the west limb of the Sun. This was stationary in position and about 20' arc in diameter, and showed predominantly right-handed polarization. On several occasions its whole area brightened, simultaneously within 1s. These brightenings coincided in time with faint fast-drift bursts in the spectrum. Figure 4a† is a photograph of this source (in right-handed polarized radiation, so that the much brighter left-handed polarized source is suppressed). The configuration of sources at this period is also shown in Figure 4b, where the boundaries of the various components are their respective contours of half maximum brightness.

\*See Plate VII.

158 †See Plate VII.

## DISCUSSION

We consider first the noise-storm component A. On the basis of the spectral and total-flux data, the increase in continuum radiation from this source would be classified as a stationary type IV burst. Now, Weiss<sup>1</sup> suggested from an examination of two-aerial interferometer observations, that this phase of the type IV event may well be a separate phenomenon, not causally connected with the moving type IV burst. The radioheliograms support Weiss's opinion, since the stationary type IV burst is in the present instance seen to be essentially an extension of the noise storm, located close to the flare and at a considerable distance from the sources of the other concurrent radio events.

If the first group of type III bursts originated radially above the flare, then their height above the photosphere must have been about  $2 R_{\odot}$ . This would imply an abnormally high electron density in part of the corona. We cannot postulate a general raising of the plasma level over the whole flare region, since the height of the noise storm A was almost certainly near the usual value of  $0.6 R_{\odot}$  at 80 MHz; the position B of the type III bursts would seem to indicate that there was an upward bulge in the corona. Wild *et al.*<sup>2</sup> have suggested that such a situation may occur with an eruptive prominence; in the present case we unfortunately have no information on optical prominence activity.

Turning now to the extended source E (Figure 4), we notice that, although it showed no appreciable motion, it had most of the other characteristics of the 'moving type IV'

burst (temporal association with type II, extraordinary-mode polarization, and large angular size). The polarization is most readily explained on the generally-accepted synchrotron theory of emission in bursts of this type. However, the sudden brightening of the source on several occasions, which appears in the spectrum as a series of fast-drift bursts, suggests a plasma-wave mechanism. The height of this source is between  $1.5 R_{\odot}$  and  $2 R_{\odot}$ , the value depending on whether the source is considered to be over the flare or over the region of the type II bursts. These figures are not necessarily inconsistent with the plasma-wave hypothesis, since we have just seen that the type III observations suggest abnormally high coronal electron densities. Before forming a definite conclusion, we clearly need observations of some further examples of bursts of this type.

It has already been mentioned that only the second-harmonic part of the type II burst was detectable at 80 MHz; the fundamental began at a much lower frequency. The 80 MHz sources corresponding to the two split-band components of the harmonic occurred about 1 min apart at positions C and D respectively (Figure 2). The positions and times are compatible with the now well-established theory (Wild<sup>3</sup>) that these events are triggered by shock waves from the flare. The fact that the two components are emitted from different regions suggests that, at least in the present case, the spectral band-splitting represents the nearly-simultaneous excitation of type II radiation, either from different parts of the same shock wave (as proposed by McLean<sup>4</sup>) or from two separate shock waves.

<sup>1</sup> Weiss, A. A., *Aust. J. Phys.*, 16, 526 (1963).

<sup>2</sup> Wild, J. P., Sheridan, K. V. and Kai, K., *Nature*, 218, 536 (1968).

<sup>3</sup> Wild, J. P., *Proc. ASA*, 1, 181 (1969).

<sup>4</sup> McLean, D. J., *Proc. ASA*, 1, 47 (1967).

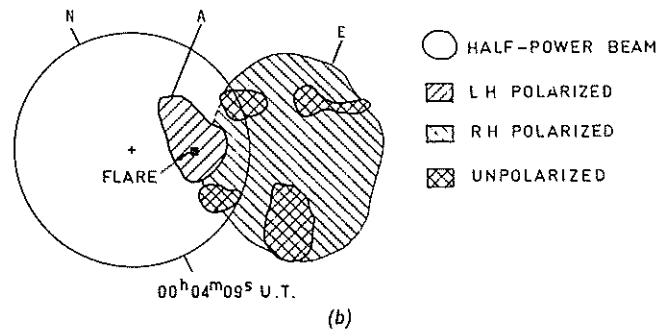
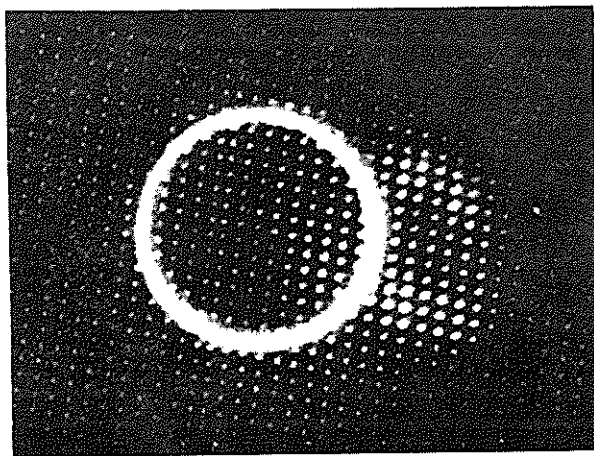
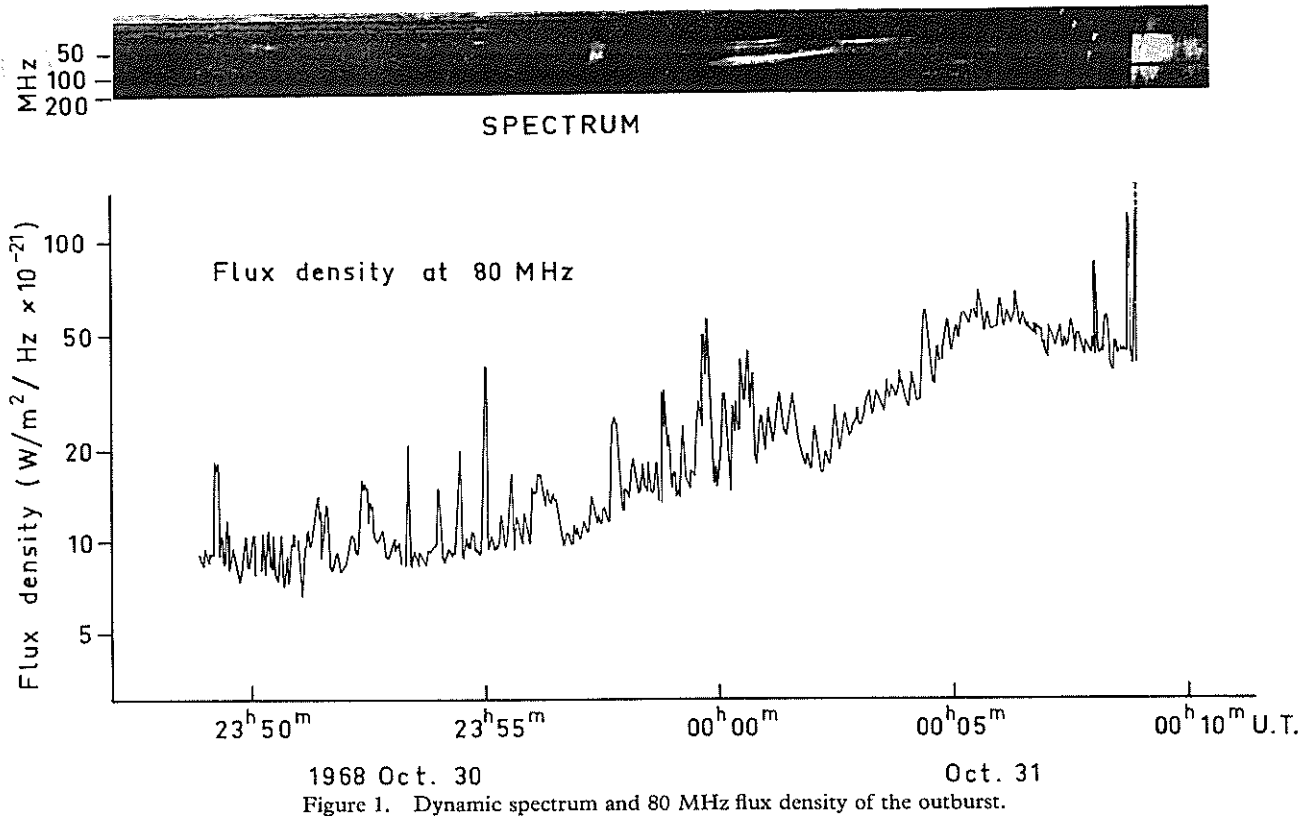
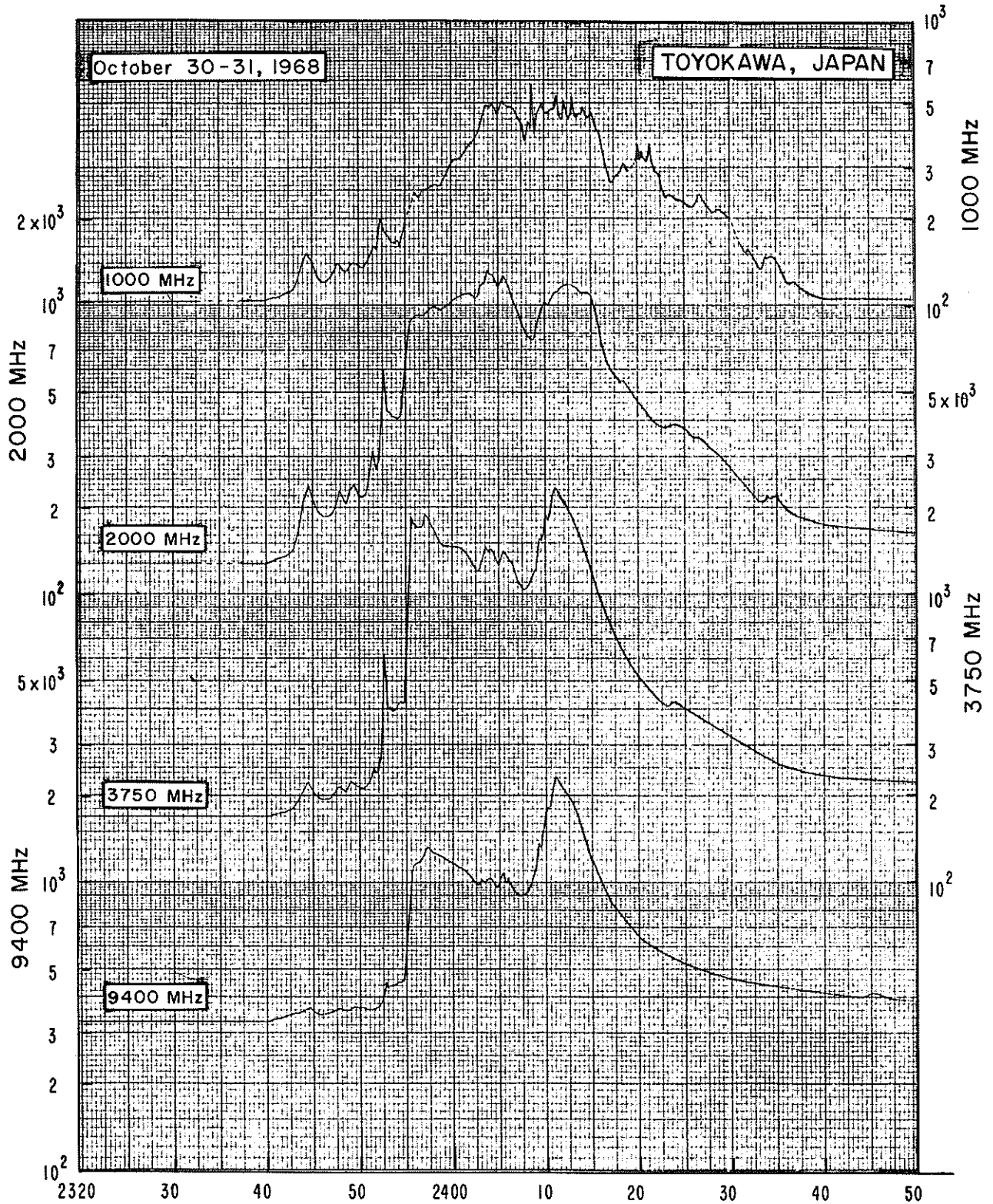
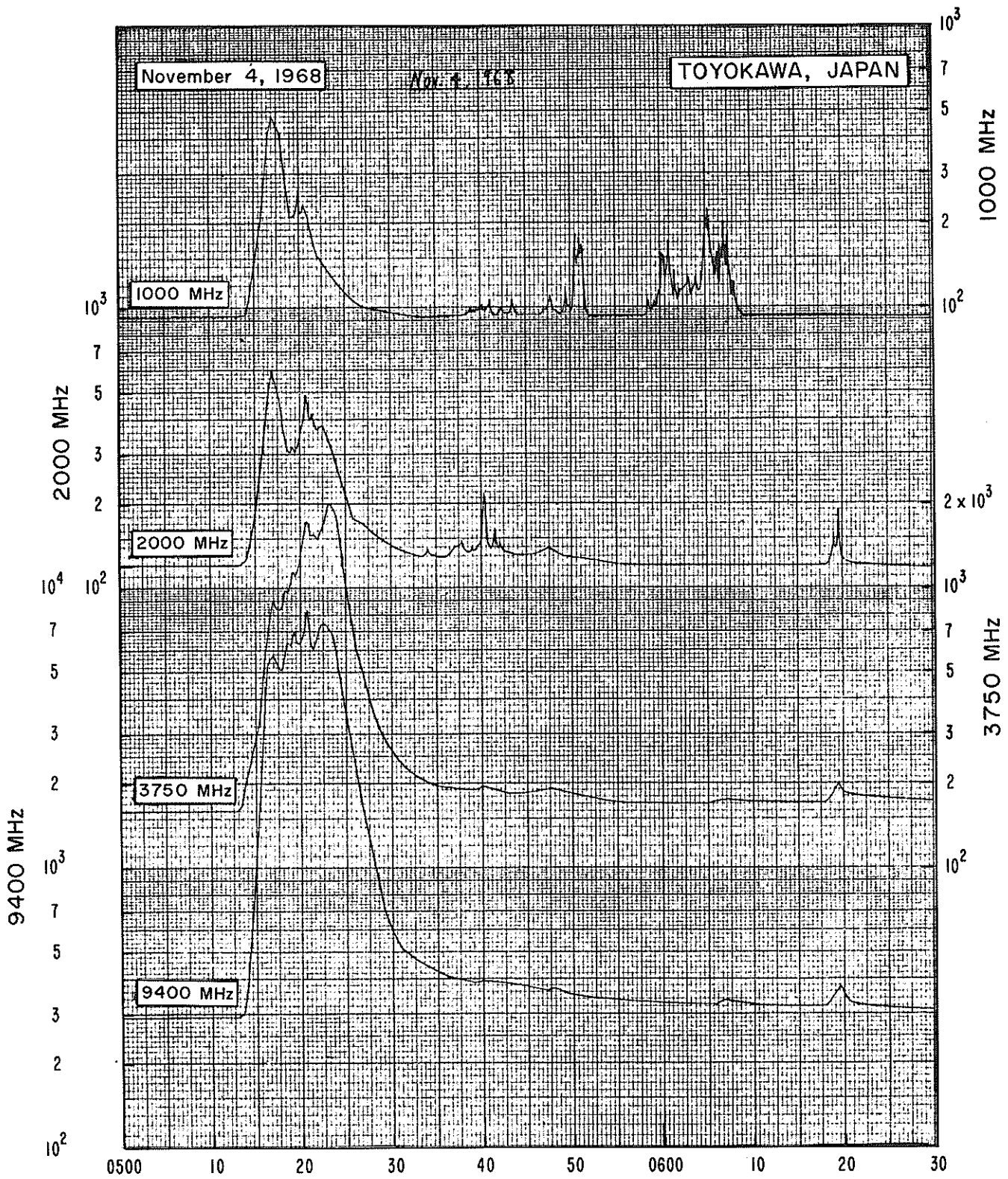


Figure 4. Extended type IV source: *a* Photograph of radioheliograph record (RH circular polarization—00<sup>h</sup>04<sup>m</sup>30<sup>s</sup> U.T.). *b* Configuration of sources at 00<sup>h</sup>04<sup>m</sup>09<sup>s</sup> U.T. The boundary shown for each source is its contour of half maximum brightness.

"Bursts of October 30-31 and November 4, 1968 at Toyokawa, Japan"

[The two figures are reproduced from data which are routinely submitted to World Data Center A by the Toyokawa, Japan, Observatory of the Radio Astronomy Section of the Research Institute of Atmospherics of Nagoya University.]





"Some Radio Bursts in the Period October 29 - November 3, 1968 Observed at Metric Waves with High Temporal Resolution"

by

A. Abrami  
Astronomical Observatory  
Trieste, Italy

Starting with August 1967 the observing facilities of the solar radiometric equipment at the Trieste Astronomical Observatory were improved in order to record the solar radio events on metric waves with high temporal resolution.

During the period October - November 1968 the radiometer, working at a frequency of 239 MHz, was still fed by the low gain meridian corner antenna [Abrami, Sedmak, 1967] located at the observing station at Basovizza (45°38'28" lat. North, 0h55m30s long. East, 398 m a.s.l.) of the Trieste Observatory. This fact restricted the observing time to two hours before and after the Sun transit but the low gain of the antenna more easily allowed recording of high intensity solar events without falling into receiver saturation. The solid state radiometric receiver was equipped with a square-law IF amplifier-detector in order to obtain records linearly related to input power, and the whole system was calibrated by means of accurate computation of the antenna gain and comparison with a noise source, taking in account the measured insertion losses of the transmission line. The regular flux density measurements agree very well with those of other stations working in the same frequency band.

The radiometric output drove a two channel high resolution Brush recorder with a response time ranging from three to twelve seconds, linearly related to the pen displacement [Abrami, 1967]. The sensitivity of the two channels was kept in a ratio of ten in order to permit the record of the high intensity emissions with a sufficient dynamic range and good detail. In order to catch the high intensity emissions which occurred suddenly, the recorder has been equipped with an automatic starting device driven by fast signals higher than a predetermined threshold level. The delay time, owing to motor inertia and rise time of the signal itself, is of the order of, or shorter than, a second.

The time profiles of some more important events occurred in the period October 29 - November 3, 1968 during our observing time interval (0900 - 1300 UT) and are presented in the Figs. They have been obtained from the original records by means of an electronic computer, taking in account: (i) the flux density scale obtained on the same day from the standard noise source; (ii) the saturation effect for very high intensity signals; (iii) the value of the antenna gain, variable with the hour angle of the Sun; and (iv) the value of the sky temperature for the time of each event. The flux densities are drawn on a logarithmic scale.

Table 1  
Data on the radio solar events

Date	Radio Burst					Optical Flare				Notes		
	Start Time	Time of maximum	Dura- tion	Flux density	Total Energy	GRP	Start Time	End Time	Import- ance			
Da.Mo.	UT	UT	Sec.	Type						Peak	Mean	No.
					$10^{-22} \text{Wm}^{-2} \text{Hz}^{-1}$	$10^{-18} \text{Jm}^{-2} \text{Hz}^{-1}$						
29 10	9 <sup>h</sup> 43 <sup>m</sup> 32 <sup>s</sup>	9 <sup>h</sup> 43 <sup>m</sup> 37 <sup>s</sup>	21	eC	860	155	0.325	18816	9 <sup>h</sup> 45 <sup>m</sup>	10 <sup>h</sup> 13 <sup>m</sup>	1n	
29 10	9 53 29	9 54 44	98	RF	110	69						
29 10	9 53 36	9 53 38	33	eC	490							
1 11	12 9 38	-	190	C+	200							
1 11	12 10 50	12 11 1	33	eC	>2680	>139	>2.635	18884	12 10	12 13	Sn	(1)
1 11	12 11 28	12 11 29	5	eC	2030							
2 11	9 50 24	9 53 2	>300	C+	750	-	-	18910	9 49	10 48	2b	(2)
2 11	10 54 59	10 55 5	20	C	240	30	0.060	18910	9 53	11 8	2b	
3 11	9 18 53	9 18 57	9	eC	125	49	0.046	-	-	-	-	
3 11	9 27 4	9 27 27	39	C	540	76	0.295	-	-	-	-	
3 11	9 31 35	9 32 9	50	C	660	69	0.347	-	-	-	-	
3 11	9 35 20	9 35 28	18	C	290	73	0.132	-	-	-	-	
3 11	12 23 48	12 23 54	18	C	280	73	0.131	(933)	12 16	12 27	1n	
3 11	12 33 1	12 33 6:	50	C	>5600	>566	>2.830	18934	12 33	12 59	1b	
3 11	12 38 56	12 39 34	88	eF	3960	170	1.497					

- (1) The main bursts were preceded and followed by some series of rapid fluctuations with characteristic periods of about 0.2 - 0.4 sec.  
 (2) The event reported here is the initial phase of a longer Type IV.

Table 1 above reports some interesting data which are obtained from these profiles, as (i) the starting time; (ii) the maximum emission time; (iii) the estimated duration of the emission; (iv) the type of burst on the International Astronomical Union scheme; (v) the maximum and mean flux density; (vi) the integrated energy emitted during each event for square meter and frequency interval unit; and (vii) the times and importance class of the correlated flares by group number as given in ESSA's "Solar-Geophysical Data", IER-FB 296 and 297.

#### REFERENCES

- |                              |      |  |
|------------------------------|------|--|
| ABRAMI, A., and<br>G. SEDMAK | 1967 | <u>Boll. "Osserv. solari" 1 - 2 (suppl.), 3.</u> |
| ABRAMI, A.                   | 1967 | <u>Atti XI Conv. S.A.It., 125.</u>               |

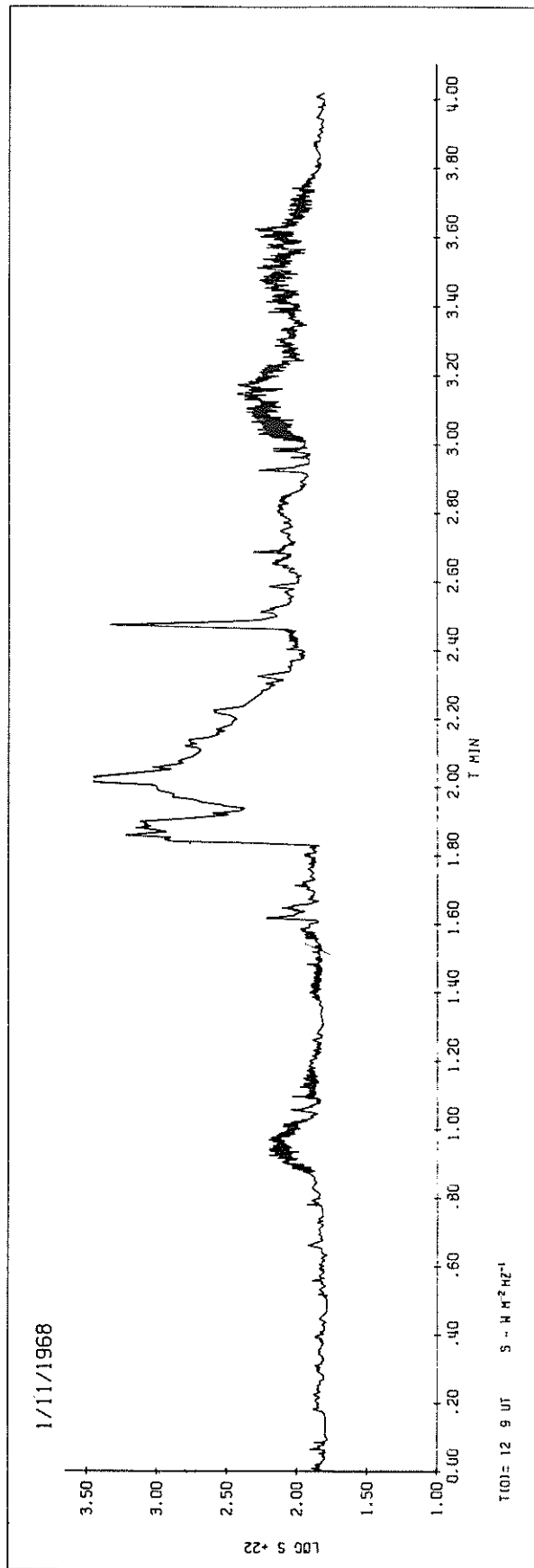
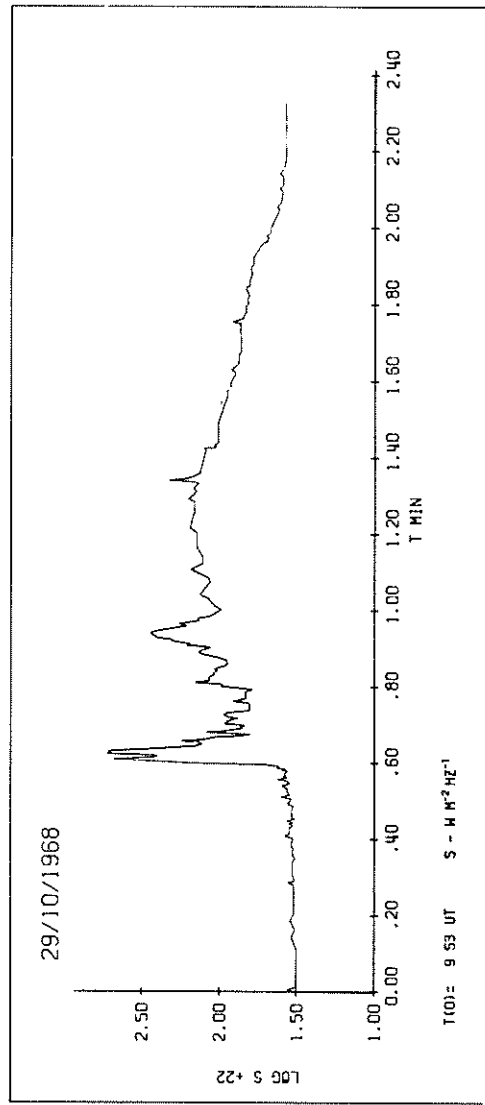
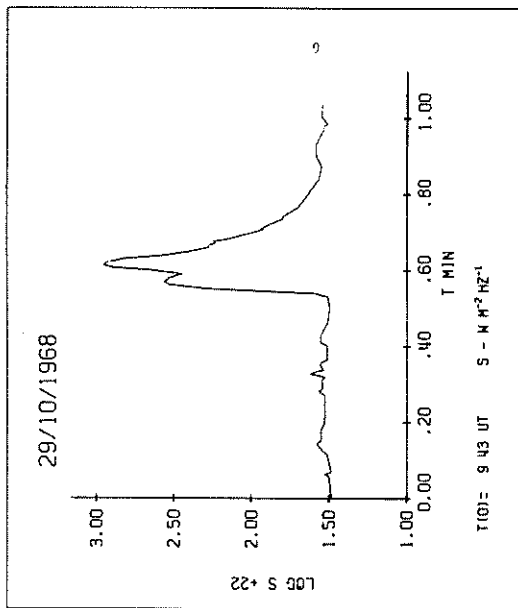


Fig. 1. Burst profiles at 239 MHz on October 29 and November 1, 1968 at Trieste Astronomical Observatory.

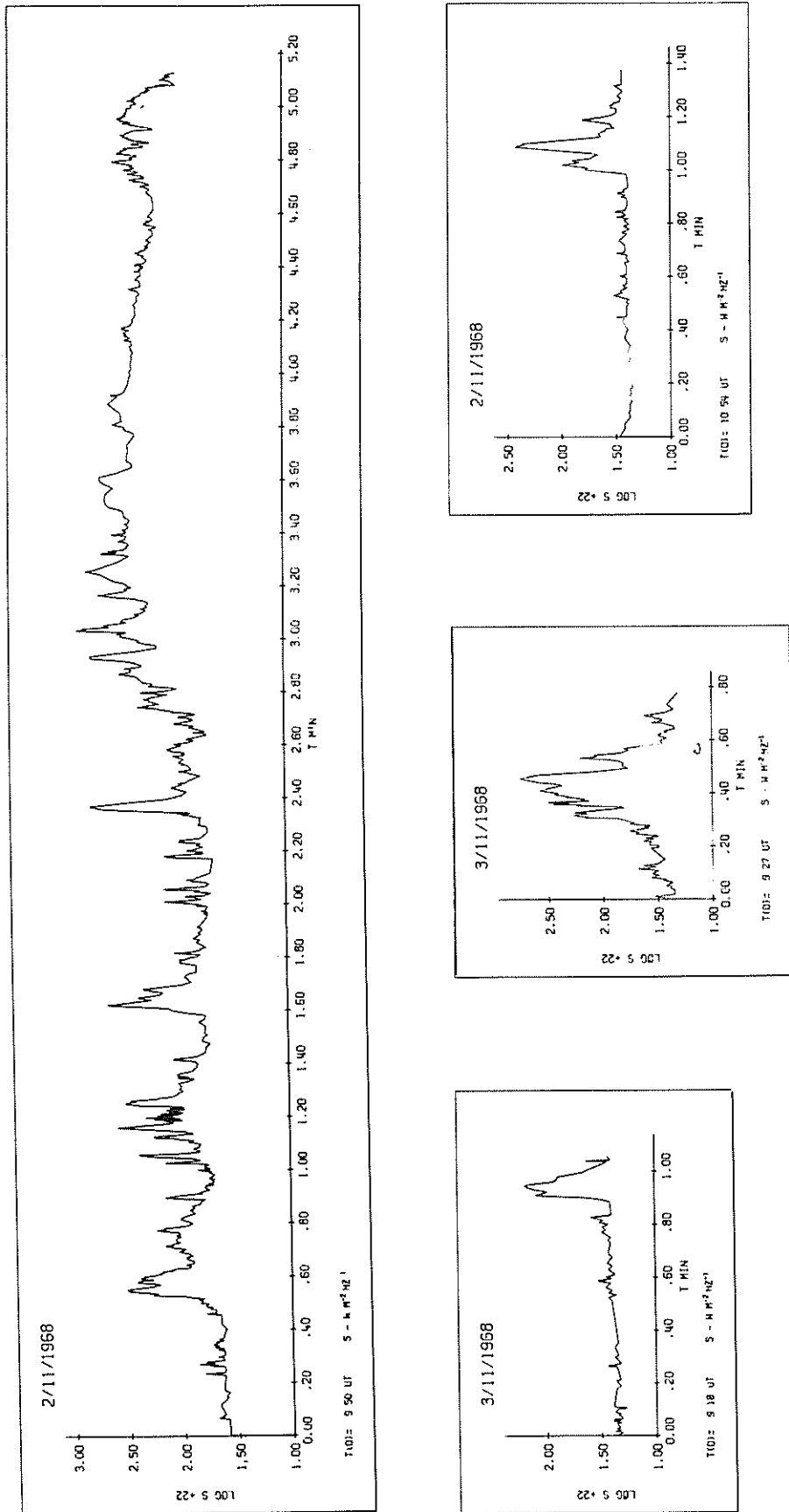
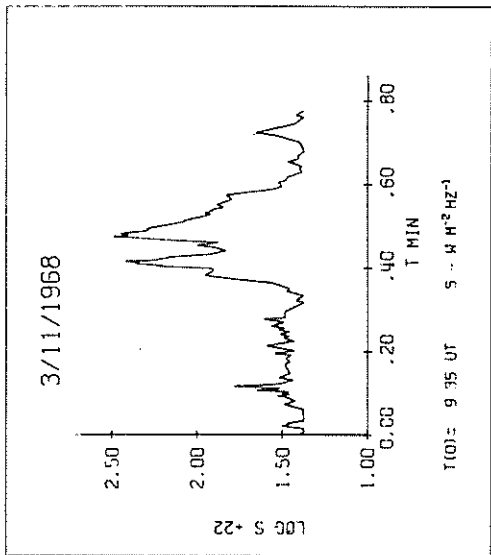
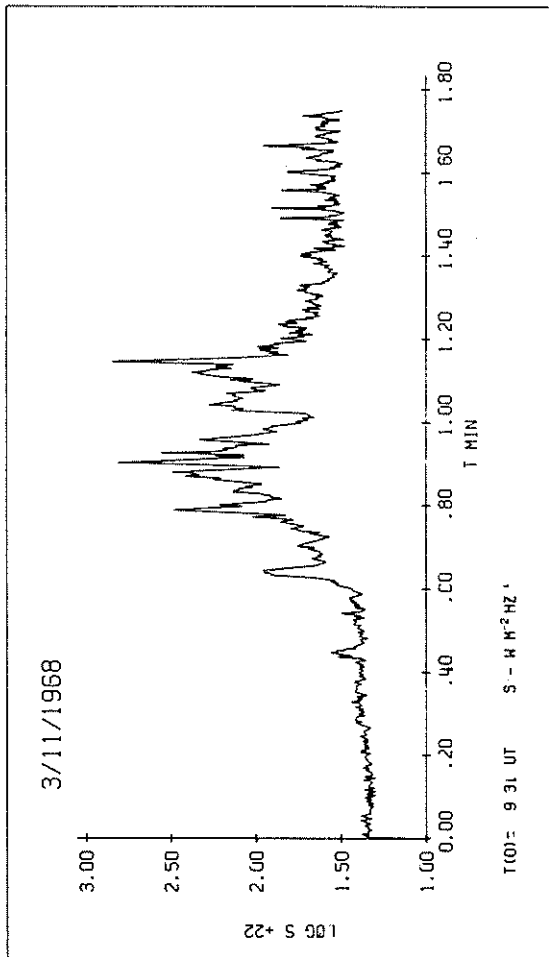


Fig. 2. Burst profiles at 239 MHz on November 2 and 3, 1968 at Trieste Astronomical Observatory.



167

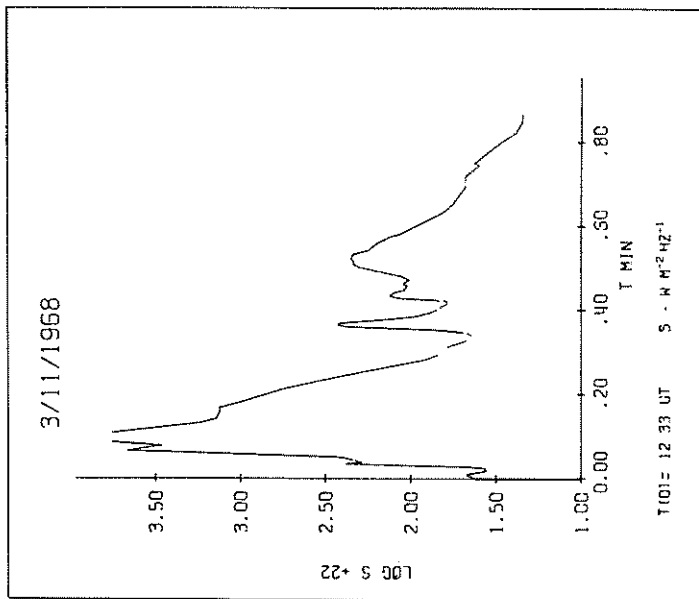
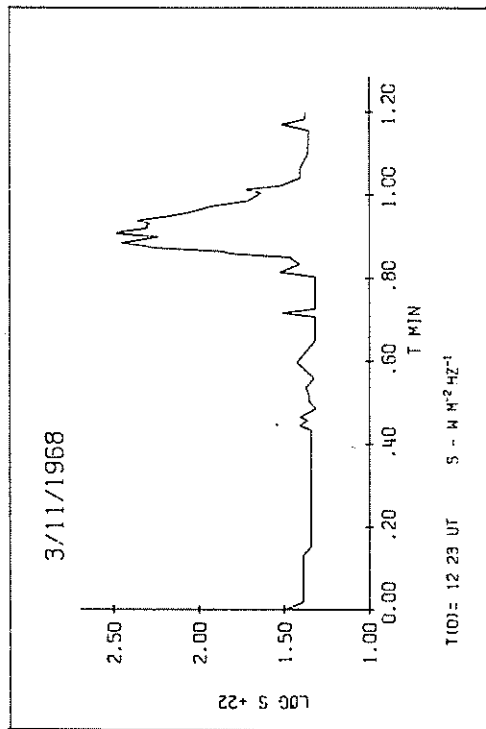
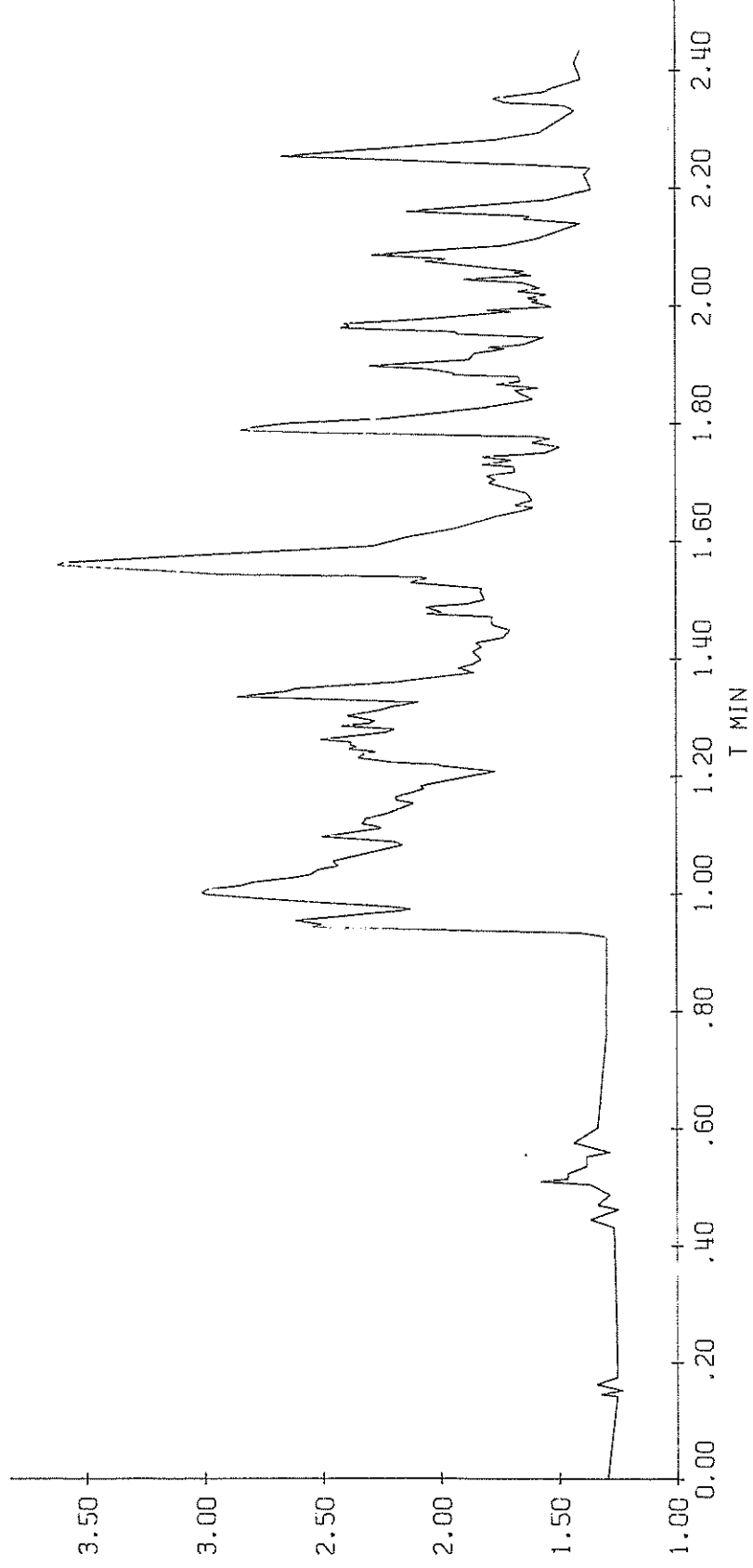


Fig. 3. Burst profiles at 239 MHz on November 3, 1968 at Trieste Astronomical Observatory.

3/11/1968



T(0) = 12 38 UT S -- W M<sup>-2</sup> HZ<sup>-1</sup>

Fig. 4. Burst profiles at 239 MHz on November 3, 1968 at Trieste Astronomical Observatory.

"Spectral Diagram of the Event of 1968 Nov. 2"

by

K. J. van den Heuvel Rijnders  
Observatory Sonnenborgh, Utrecht

[The figure and description has been reprinted with permission from "Information Bulletin of Solar Radio Observatories", No. 25, September 1969, published by the Utrecht Observatory "Sonnenborgh", Zonnenburg 2, Utrecht, the Netherlands.]

A spectral diagram of the type IV outburst of 1968 Nov. 2, 0950 UT is given below in Figure 1. This outburst was associated with a class 2b flare at S15 W65. It was the final major radio burst of a series of big radio events that occurred between October 27 and November 2.

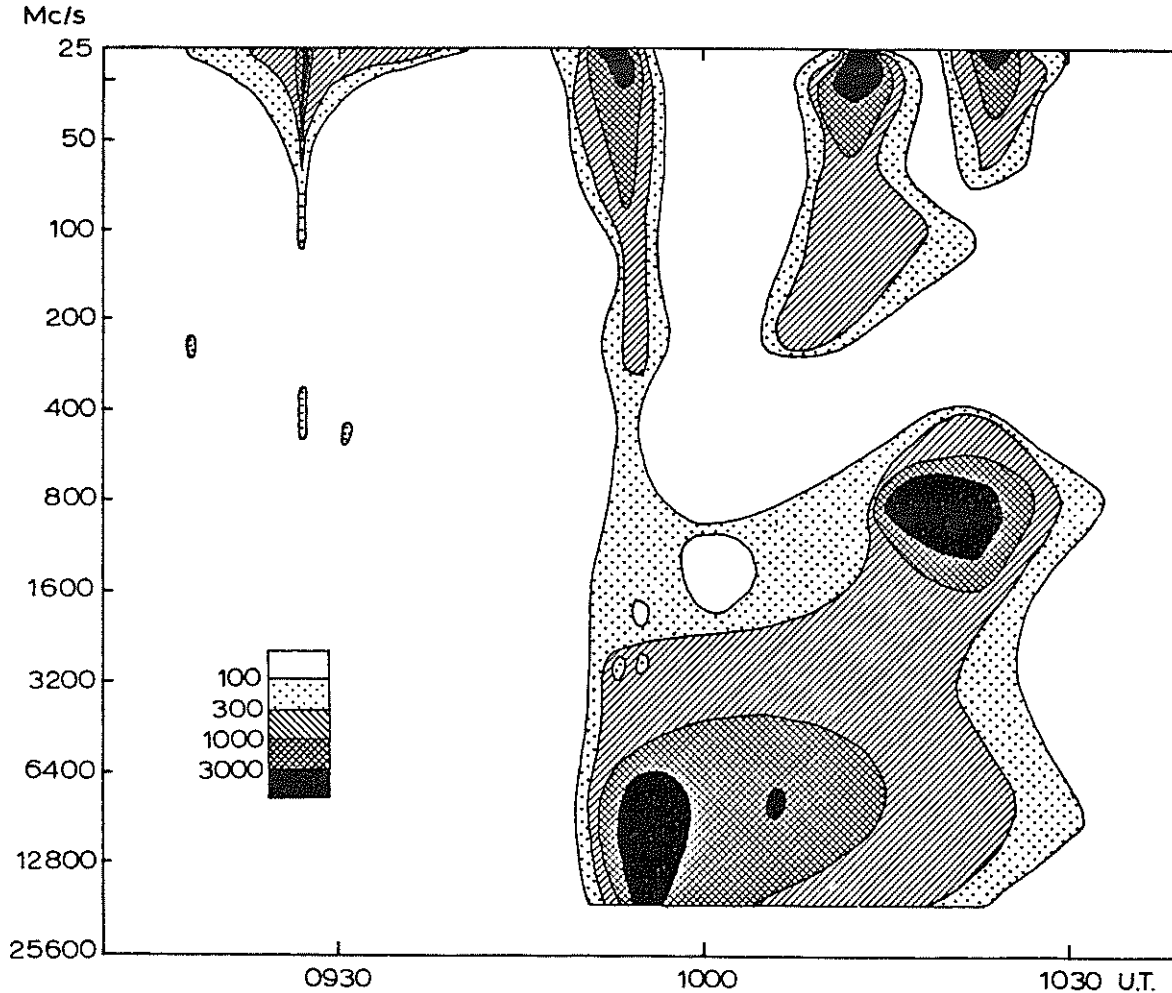


Fig. 1. The type IV event of November 2, 1968.

The reports used are given below in MHz where HHI = Heinrich-Hertz-Institut, Berlin-Adlershof; KIE = University of Kiel; WEI = Weissenau Observatory; NED = Netherlands PTT and Utrecht University Observatory; and SLG = Radio and Space Research Station, Slough, England.

30	} HHI	367	} HHI	1000	Wei	3000	Ned, HHI
64		510		1420	Kie	9400	HHI
111		610	1500	} HHI	9500	Ned	
240	Kie, HHI	793	2000		18750	Slg	

